Medizinische Fakultät der Martin-Luther-Universität Halle-Wittenberg

Spektrum von während der intraoperativen Hämofiltration entfernten Blutproteinen - Adsorption außer Zytokine

Dissertation
zur Erlangung des akademischen Grades
Doktor rerum medicarum (Dr. rer. medic.) für das Fachgebiet
Molekulare Medizin

vorgelegt
der Medizinischen Fakultät
der Martin-Luther-Universität Halle-Wittenberg

von Veronika Piskovatska
geboren am 28.4.1990 in Odesa

Betreuer: Prof. Dr. Andreas Simm

Gutachter:

Prof. Rüdiger Horstkorte

Prof. Lars-Oliver Klotz, Jena

06.10.2020

15.04.2021

Summary

Hemofiltration is a blood purification technique, widely used in intensive care to treat diseases driven by peaking concentrations of pro-inflammatory cytokines. CytoSorb hemofilter consusts of polysterene-divinylbenzene beads and has a wide range of clinical indications.

In current work we aimed to identify proteins that are retained on the CytoSorb matrix during intraoperative hemofiltration in patients undergoing valve surgery with cardiopulmonary bypass (CPB). Among 127 proteins, identified in all filters after intraoperative blood purification, the majority (64%) of the proteins had molecular weight below 60 kDa. The majority of the proteins, identified in all patient samples possessed hydrophilic properties at pH 7.4. Measurable concentrations of C-reactive protein and interleukins (IL-1β, IL-6, IL-8 and IL-10) were eluted form the filters, IL-8 had the highest concentration among all cytokines. Patients with infective endocarditis tended to have higher levels of cytokines in the eluted protein fractions.

Endothelial cells, treated with plasma proteins, eluted from the polymer beads demonstrate wide range of functional alterations. Endothelial cells subjected to treatment show reduction in viability, proliferation and lateral migration. Treatment with protein mixture, eluted from the adsorber resulted in massive transcriptional changes. Clusters of genes responsible for regulation of amino acid, folate, nucleic acid, lipid, and energy metabolism were up-regulated in the cells after 24-hour treatment. Phosphoserine aminotransferase (PSAT) and mitochondrial methyltetrahydrofolate reductase 2 (MTHFD2) were significantly up-regulated on protein level. Mitotic proteins kinesin superfamily protein 20A (KIF20A) and mitotic checkpoint kinase (BUB1) were significantly down-regulated on the protein level. Proteins extracted from the filter matrix also contribute to endothelial activation by increase in secretion of pro-coagulant factors: plasminogen activator inhibitor 1 and von Willebrand factor.

Our experimental results suggest that hemofiltration during heart surgery with CPB allows to remove broad spectrum of blood proteins from the circulation. Except cytokines, a battery of proteins triggering endothelial activation can be removed, potentially tackling the endothelial compound of systemic inflammation in patients undergoing heart surgery with CPB.

Piskovatska, Veronika: Spectrum of Blood Proteins Removed during Intraoperative Hemofiltration - Adsorption beyond Cytokines, Halle, Univ., Med. Fak., Diss., Pages – 80, Figures – 47, Tables – 17, 2020.

Referat

Die Hämofiltration ist eine Blutreinigungsmethode, die häufig auf Intensivstationen zur Behandlung von Krankheiten, die durch hohe Konzentrationen entzündungsfördernder Zytokine gekennzeichnet sind, eingesetzt wird. Die hier untersuchten CytoSorb-Hämofilter bestehen aus Polysteren-Divinylbenzol-Kügelchen und bieten eine breite Palette klinischer Indikationen.

In der vorliegenden Arbeit sollten die matrixbindenden Proteine identifiziert werden, die während der intraoperativen Hämofiltration bei Patienten vorkommen, die sich einer Klappenoperation mit kardiopulmonalem Bypass (CPB) unterziehen.

Die Mehrheit der insgesamt in allen Filtern identifizierten 127 Proteine hatte ein Molekulargewicht von unter 60 kDa (64%) und besaß bei dem pH-Wert von 7,4 hydrophile Eigenschaften. Dabei wurden aus den Filtern messbare Konzentrationen von CRP, IL-1β, IL-6, IL-8 und IL-10 eluiert. Die höchste Konzentration hatte unter allen Zytokinen IL-8. Bei Patienten mit infektiöser Endokarditis wurden in den eluierten Proteinfraktionen tendenziell höhere Zytokinspiegel nachgewiesen.

Des Weiteren wurde der Einfluss der aus den Filtern eluierten Proteine auf Endothelzellzen einer näheren Analyse unterzogen. Folgendes konnte ermittelt werden: behandelte Endothelzellen weisen eine Verringerung der Zellvitalität, der Proliferation und der lateralen Migration auf. Die Behandlung mit einer vom Adsorber eluierten Proteinmischung führte zu massiven Transkriptionsänderungen. Nach einer 24-stündigen Behandlung wurde in den Zellen ein Cluster von Genen, die für die Regulation des Aminosäure-, Folat-, Nukleinsäure-, Lipid- und Energiestoffwechsels verantwortlich sind, hochreguliert. Auf Proteinebene wurden Phosphoserinaminotransferase (PSAT) und mitochondriale Methyltetrahydrofolatreduktase 2 (MTHFD2) signifikant hochreguliert. Zu den auf der Proteinebene signifikant herunterregulierten Proteinen gehören Kinesin Superfamilie Protein 20A (KIF20A) und mitotische Checkpoint Kinase (BUB1). Darüber hinaus konnte festgehalten werden, dass aus der Filtermatrix extrahierte Proteine zur Endothelaktivierung betragen, indem sie die Produktion von gerinnungsfördernden Faktoren erhöhen Plasminogenaktivator-Inhibitor 1 und von-Willebrand-Faktor.

Die vorliegenden experimentellen Ergebnisse legen nahe, dass die Hämofiltration während einer Herzoperation unter Anwendung von CPB die Entfernung eines breiten Spektrums von Blutproteinen aus dem Kreislauf ermöglicht. Außer Zytokinen kann eine Reihe von Proteinen entfernt werden, die eine Endothelaktivierung auslösen, wodurch möglicherweise bei Patienten, die sich einer Herzoperation mit CPB unterziehen, die Endothel-Komponente einer systemischen Entzündung bekämpft werden kann.

Piskovatska, Veronika: Spektrum von während der intraoperativen Hämofiltration entfernten Blutproteinen - Adsorption außer Zytokine, Halle, Univ., Med. Fak., Diss., 80 Seiten, 2020.

Table of contents

List of abbreviations and clinical study acronyms

a.u. – arbitrary units

AA – amino acid

ACN – acetonitrile

AF – atrial fibrillation

AGEs – advanced glycation end products

AKI – acute kidney injury

ALB – human serum albumin

Arg-Pyr – argpyrimidine

ATF – activating transcription factor

BACE1 – beta-secretase 1

BCA – bicinchinonic acid

BrdU – bromodeoxyuridine

BSA – bovine serum albumin

BUB1 - budding uninhibited by benzimidazoles 1 kinase

CA1 – carbonic anhydrase 1

CABG – coronary artery bypass graft

CASHSP – Clinical study: Use of Extracorporeal Treatment With the Cytosorb-Adsorber for the Reduction of SIRS in Heart Surgery Patients

CAT – catalase

CBA – cytometric bead array

CCB – Coomassie colloidal blue staining

CCCC – Clinical study: Cytokine Clearance With Cytoabsorbant Device During Cardiac Bypass

CCKR – cholecystokinin receptor signaling

cDNA – complementary DNA

CEL – carboxyethyllysine

cfDNA – cell-free DNA

CID – collision induced dissociation

CML – carboxymethyllysine

Cofact – concentrate of coagulation factors II, VII, IX and X

CPB – cardiopulmonary bypass

CPD – citrate phosphate dextrose

CPK – creatine phosphokinase

CRP – C-reactive protein

CSTA – cystatin A

DAMPs – damage-associated molecular patterns

DC – deoxycytidine

DDA – data-dependent acquisition

ddH_2O – double-distilled water

DIA – data-independent acquisition

dsRNA – double-stranded RNA

DTT – dithiothreitol

EC – European Union medical device certification

ECC – extracorporeal circulation

ECGM2 – endothelial cell growth medium 2

ECM – extracellular matrix

EDTA – ethylenediaminetetraacetic acid

EK – erythrocyte concentrate

ELISA – enzyme-linked immunosorbent assay

ER – endoplasmatic reticulum

ET-1 – endothelin-1

EuroSCORE II – The European System for Cardiac Operative Risk Evaluation

Ex/Em – excitation/emission

FA – formic acid

FCS – fetal calf serum

FFP – fresh frozen plasma

FGF-2 – fibroblast growth factor-2

GAPDH – glyceraldehyde-3-phosphate dehydrogenase

GO – gene ontology

GRAVY – grand average of hydropathy

HACEK - **H**aemophilus species (Haemophilus parainfluenzae, Haemophilus aphrophilus and Haemophilus paraphrophilus), **A**ctinobacillus actinomycetemcomitans, **C**ardiobacterium hominis, **E**ikenella corrodens and **K**ingella kingae

HAECs – human aortic endothelial cells

HB – hemoglobin

HBB – hemoglobin subunit beta

HBD – hemoglobin subunit delta

HCD – higher collision induced dissociation

HF – hemofiltration

hs-CRP – high-sensitive C-reactive protein

HSP – heat shock proteins

HMGB1 – high-mobility group box 1

HSP – heat shock proteins

HPX – hemopexin

HRG – histidine-proline-rich glycoprotein

I.U. – international units

IB – immunoblotting

ICC - immunocytochemistry

ICU – intensive care unit

IE – infective endocarditis

IL-6 – interleukin-6

IL-8 – interleukin-8

IMEECCACS – Clinical study: Immunomodulatory Effect of Extracorporeal Cytokine Adsorption in Cardiac Surgery

IMHeS – Clinical study: Hemadsorption During and After Cardiopulmonary Bypass to Modulate the Inflammatory Response

LC-MS/MS – liquid chromatography-coupled mass-spectrometry

LTA – lipoteichoic acid

LFQ – label-free quantification

MG-H1 – methylglyoxal-derived hydroimidazolone-1

mRNA – messenger RNA

MVR – mitral valve replacement

MTHFD1L - methylentetrahydrofolate dehydrogenase 1-like

MTHFD2 – methylenetetrathydrofolatedehydrogenase 2

MW – molecular weight

MWCO – molecular weight cutoff

MyDeCCS – Clinical study: Myeloid-Derived Supressor Cells in Cardiac Surgery Patients

NAD/NADP+ - nicotinamide adenine dinucleotide, nicotinamide adenine dinucleotide phosphate

NO – nitric oxide

NP-40 – nonyl phenoxypolyethoxylethanol

Ox-LDL – oxidized low-density lipoproteins

Ox-phospholipids – oxidized phospholipids

PAF – platelet-activating factor

PAI-1 – plasminogen activation inhibitor, type 1

PAGE – polyacrylamide gel electrophoresis

PAMPs – pathogen-associated molecular patterns

PBS – phosphate buffered saline

PE – phycoerythrin

pfHb – plasma-free hemoglobin

pI – isoelectric point of the protein

PI – propidium iodide

PMSF – phenylmethylsulfonyl fluor

PPSB – prothrombine concentrate (contains coagulation factors II, VII, IX and X)

PSAT1 – phosphoserine aminotransferase

PSM – peptide spectrum match

PSDVB – polysterene-divinylbenzene

PTFE – polytetrafluoroethylene

PTIC – protein transport inhibitor cocktail

PTM – post-translational protein modification

RAGE – receptor to advanced glycated end products

RBC – red blood cells

RECCAS – Clinical study: REmoval of Cytokines during CArdiac Surgery

REMOVE – Clinical study: Hemoadsorption for Prevention of Vasodilatory Shock in Cardiac Surgery Patients with Infective Endocarditis

REMOTE – Clinical study: Removal of Cytokines in Patients Undergoing Cardiac Surgery with CPB

REFRESH – Clinical study: Reduction of Free Hemoglobin During Cardiac Surgery

REFRESHII-AKI - Clinical study: Reduction of FREe Hemoglobin/Acute Kidney Injury (AKI) During Cardiac Surgery

RIPA – radioimmunoprecipitation assay buffer

ROS – reactive oxygen species

RT – room temperature

SD – standard deviation

SDS – sodium dodecyl sulfate

SIRS – systemic inflammatory response syndrome

sFLT-1 – soluble thyrosine kinase

SFN – sulforaphane

SOFA-score – sequential organ failure assessment score

SPE – solid-phase extraction

SREBP - sterol regulatory element-binding proteins

ssRNA – single-stranded RNA

STC1 – stanniocalcin-1

THBS1, 2 – thrombospondin 1 and 2

TK – thrombocyte concentrate

TM - thrombomodulin

tPA – tissue type plasminogen-activation factor

TRIF – TIR-domain-containing adapter-inducing interferon-β

TrisHCl – tris(hydroxymethyl)aminomethane hydrochloride

tRNA – transfer RNA

TXN – thioredoxin

UPR – unfolded protein response

VEGF – vascular endothelial growth factor

VP – vasopressors

1. Introduction

1.1.1. Hemofiltration, description of the method, clinical indications

Hemofiltration (HF) has a wide range of indications, the majority of them being diseases and conditions that are supported as so-called “cytokine storm”, when peaking concentrations of pro-inflammatory substances enforce and instigate pathogenesis of critical illness (systemic inflammatory response syndrome (SIRS), sepsis, septic shock, massive trauma, burns) (Bonavia et al., 2018). One of the recent clinical indications, that is currently investigated in a clinical trial, is intraoperative use of HF in patients undergoing cardiac surgery with cardiopulmonary bypass (CPB) in order to reduce the amount of circulating inflammatory cytokines in high-risk patients (Frieseke et al., 2017). Setup for intraoperative hemofiltration is shown in suppl. fig. 1.

1.1.2. Properties of CytoSorb matrix, data from *in vitro* studies, current gaps in the research

CytoSorb HF system, the hemofiltration system used in this study, is filled with porous, polyvinylpyrrolidone-covered polystyrene divinylbenzene (PSDVB) beads, possessing surface area of around 40.000 m^2 (Honore et al., 2013) and binding blood proteins presumably by hydrophobic adsorption (Gruda et al., 2018; Malard et al., 2018).

Previous studies with CytoSorb adsorbent system were mainly concentrated on the removal of pro-inflammatory cytokines, like IL-1β, IL-6, IL-8, IL-10, and TNF-α (Malard et al., 2018; Houschyar et al. 2017). *In vitro* data suggest a vast spectrum of adsorption by CytoSorb, including cytokines, pathogen-associated molecular pattern molecules (PAMPs), damage-associated molecular pattern molecules (DAMPs), proteins, hormones (cortisol and T3), metabolic toxins, antibiotics and other drugs, including digoxin, valproate, carbamazepine, phenobarbital (Poli et al., 2019), see Fig. 1.

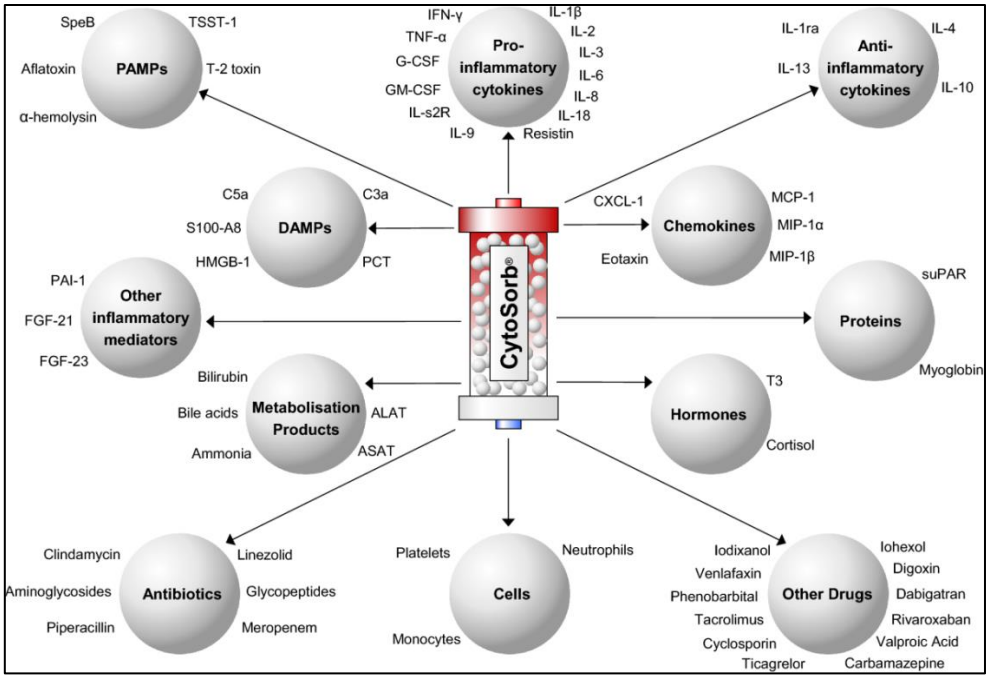

Figure 1: Spectrum of the molecules adsorbed by CytoSorb polymer matrix. Based on previous *in vitro* studies; from Poli et al., 2019).

1.1.3. Current evidence from clinical trials

Current evidence from clinical trials suggests that the use of this blood purification system allows to significantly reduce concentrations of pro-inflammatory cytokines (IL-1β, IL-2, IL-6, IL-8, TNF-α) and offers some benefits, reducing patients need in vasopressors, without changing other clinical and survival parameters significantly (Ankawi et al., 2019). A randomized controlled clinical study in sepsis patients has shown a significant reduction of IL-6, averaging between 5 and 18% per pass of blood through the device (Schädler et al., 2017). HF in 26 critically ill septic patients resulted in hemodynamic stabilization and increased survival (Kogelmann et al., 2017). A retrospective case series study, evaluating outcomes in critically ill patients, showed significant reduction of bilirubin, lactate and CPK (Calabro et al., 2018). Other small clinical trials, case reports and case series, describe elimination of other substances and metabolites, like bilirubin (Singh, 2019; Piwowarczyk et al., 2019; Calabrò et al., 2019), myoglobin (Wiegele et al., 2019), and free hemoglobin (Gleason et al., 2019). Another prospective study reported significant reduction of the cfDNA levels in plasma of patients, undergoing heart surgery with CPB (Braun et al., 2018). The adsorbent system was shown to efficiently remove rivaroxaban and ticagrelor from circulation of patients undergoing urgent cardiac surgery and thus reducing the rates of perioperative complications, associated with high risk of bleeding (Hassan et al. 2019). Removal of soluble urokinase-type plasminogen activator receptor, a molecular factor related to progression of focal segmental glomerulosclerosis was described in a case report (Schenk et al., 2017). Although the size range of adsorbed proteins seems to be within 5 - 60 kDa, moderate reduction in concentrations of plasma albumin (67 kDa), fibrinogen (340 kDa) and total protein have been previously described in clinical settings by Schädler et al., 2017 and Bernardi et al., 2016. Recent *in vitro* study by Harm et al., 2019, revealed significant total plasma protein and albumin reduction during experimental plasma perfusion for 8 hours. Reduction of total protein concentration was more than 30%. It is important to underline, that 1 L of human plasma was used for the hemoperfusion experiment with 300 mL volume cartridge, which does not correspond to the ratio between total perfused blood volume and volume of cartridge in clinical conditions. A recent study, evaluating cytokine clearance in patients undergoing cardiac surgery, discovered no significant difference in concentrations of the main coagulation factors, except antithrombin and factor II, that were significantly decreased after the HF (Poli et al., 2019). Another study shows reduced incidence of post-operative sepsis and sepsis-related mortality in patients with native mitral valve endocarditis, if they were allocated to hemoadsorption during valve surgery (Haidari et al., 2020). Patients, receiving HF treatment were also more hemodynamically stable and had faster recovery of inflammatory markers (procalcitonin, C-reactive protein and white blood cell count). Main clinical trials, addressing the use of CytoSorb filters in patients undergoing heart surgery are briefly summarized in supplementary table 1.

Other hemofiltration systems are also available on the European market and their spectrum of indications does include use in intraoperative and perioperative settings in cardiac surgery (Ankawi et al., 2019). The properties of these filters along with indications and peculiar characteristics are briefly described in supplementary table 2. Unfortunately, clinical studies including head-to-head comparison of different hemofiltration systems for different indications are missing, and studies evaluating spectrum of adsorbed blood proteins are scarce.

1.2.1. SIRS in patients undergoing heart surgery

Systemic inflammatory response syndrome (SIRS) is a complex clinical syndrome of dysregulated inflammatory response that might be or might not be accompanied by infection (Singer et al., 2016). SIRS has multiple underlying causes: infection, autoimmune disorders, pancreatitis, vasculitis, and thromboembolism (Hawlik et al., 2017). Surgery, particularly cardiovascular surgery is often complicated by sterile inflammation due to predisposing background of the patient and the trauma caused by surgical intervention (Somer, 2012). Key compounds of SIRS pathogenesis are summarized in Fig. 2: complement activation, endotoxemia and ischemia-reperfusion injury result in systemic activation of endothelial and immune cells, platelets, massive release of cytokines and mediators of inflammation. About one-third of patients undergoing heart surgery with CBP are developing systemic inflammatory reaction (Squiccimarro et al., 2019), in pediatric population this rate is similar (Boehne et al., 2016). According to the recent retrospective cohort study of 28513 patients undergoing heart surgery, the risk of SIRS is more pronounced in young patients, as in young patients in comparison to the advanced age patients the immune system reactivity does not decline. Additional risk factors of SIRS were identified in this study: high BMI (over 30 kg/m^2), diabetes mellitus, recent myocardial infarction, left ventricular dysfunction and intraoperative use of intra-aortic balloon pump (Dieleman et al., 2017).

SIRS is clinically defined by the presence of at least two of the following criteria (Singer et al., 2016):

- Temperature >38°C or <36°C
- Heart rate of more than 90 beats/minute
- Respiratory rate more than 20 beats/minute or $PaCO_2$ of less than 32 mm Hg
- Abnormal white blood cell count (>12.000/mm^3 or <4.000/mm^3)

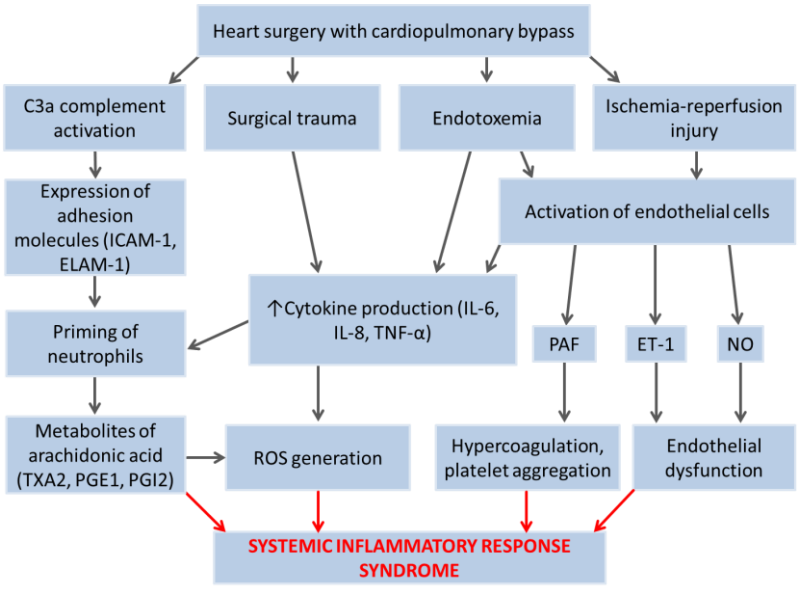

Figure 2: Pathophysiological changes during cardiac surgery with cardiopulmonary bypass, contributing to systemic inflammatory response. Adaptation from Karamlou & Ungerleider, 2014; Punjabi & Taylor, 2013.

Abbreviations: ICAM-1 - intercellular adhesion molecule 1; ELAM-1 - endothelial-leukocyte adhesion molecule; TXA2 – thromboxane A2; PGE1 – prostaglandin E1; PGI2 – prostacyclin; PAF – platelet-activating factor 1; ROS – reactive oxygen species; ET-1 – endotelin-1; TNF-α – tumor necrosis factor alpha; NO – nitric oxide.

SIRS significantly contributes to the development of postoperative complications: respiratory failure, renal dysfunction, bleeding disorders, liver failure and multi-organ dysfunction syndrome (Papparella et al., 2002). Small fraction of patients (about 2 to 10% according to the data from Day & Taylor, 2015; Warren et al., 2009) develops severe

complications with life-threatening multi-organ dysfunction and mortality rates of about 10% (Hoffmann, 2013). Together with high incidence of SIRS in patients undergoing heart surgery with CPB, rates of associated morbidity and mortality create an urge for timely and safe measures to prevent systemic dysregulation of inflammatory response. Methods, targeting several compounds of pathogenesis are highly preferable (Simoni, 2019).

1.2.1. Heart surgery in patients with infective endocarditis

Infective endocarditis (IE) is a life-threatening condition with mortality of about 30% within the first year of disease (Cahill et al., 2017). The incidence of IE is estimated between 30 and 100 episodes per 1 million of population each year (Hoen & Duval, 2013) and tends to grow due to increased incidence of intervention procedures creating favorable environment for interaction between blood and pathogenic microorganisms (Schirone et al., 2018). Caused by bacterial infection and orchestrated by plethora of complex physiological mechanisms, IE leads to systemic inflammation with local degradation of valvular tissues, formation of bacterial vegetations, valve dysfunction and congestive heart failure (Werdan et al., 2014).

Patients with IE are at high risk of thromboembolic events, including stroke. Surgery is a life-saving measure; it is required in 25-50% of cases during acute infection due to severe valve leakage and hemodynamic instability. About 20-40% of patients would require surgery after recovery of infection (Leone et al., 2012; Olmos et al., 2013).

Patients with IE, undergoing heart surgery have multiple risk factors predisposing them to SIRS and high risk of perioperative complications, including acute kidney injury, respiratory failure, cognitive dysfunction (Wang et al., 2019). Bacterial spread-out from the vegetation, exposure to CPB and surgical trauma can induce massive release of IL-6 and IL-8 with hemodynamic instability and shock (Träger et al., 2017), risk of complications increases with the increasing on-pump time (Kumar et al., 2019). Very often, patients undergoing urgent cardiac surgery are already having thromboembolic complications of IE (Fukuda et al., 2012).

1.2.2. Alterations in plasma composition, occurring due to cardiopulmonary bypass

Cardiopulmonary bypass initiates multiple changes in blood proteins and blood cells (Zakkar et al., 2015). CPB in heart surgery leads to reduction in total blood protein and particularly albumin. Studies report reduction in albumin concentration by 50 to 70%, primarily due to hemodilution (van Beek et al., 2018). Hemodilution and reduction of albumin concentration are independent predictors of kidney injury, increased major morbidity and mortality after heart surgery with CPB (Karas et al., 2015; Karkouti et al., 2005). Excessive hemodilution results in postoperative anemia with hematocrit (HCT) reduction and reduced oxygen transport capacity of the blood (Jameel et al., 2010). Sub-lethal damage of red blood cells (RBC) and hemolysis, occurring due to CPB is one of the important pathophysiological triggers for postoperative complications and mortality (Olia et al., 2016). Hemolysis is considered an inevitable complication of extracorporeal circulation and is linked to kidney damage, ischemia-reperfusion injury and induction of SIRS (Vermeulen Windsant et al., 2011). The site of operation wound becomes a massive source of IL-6 (Jawa et al., 2011) and contact with non-endothelial surface leads to the activation of complement system and coagulation cascade, Fig. 3 (Sato et al., 2015).

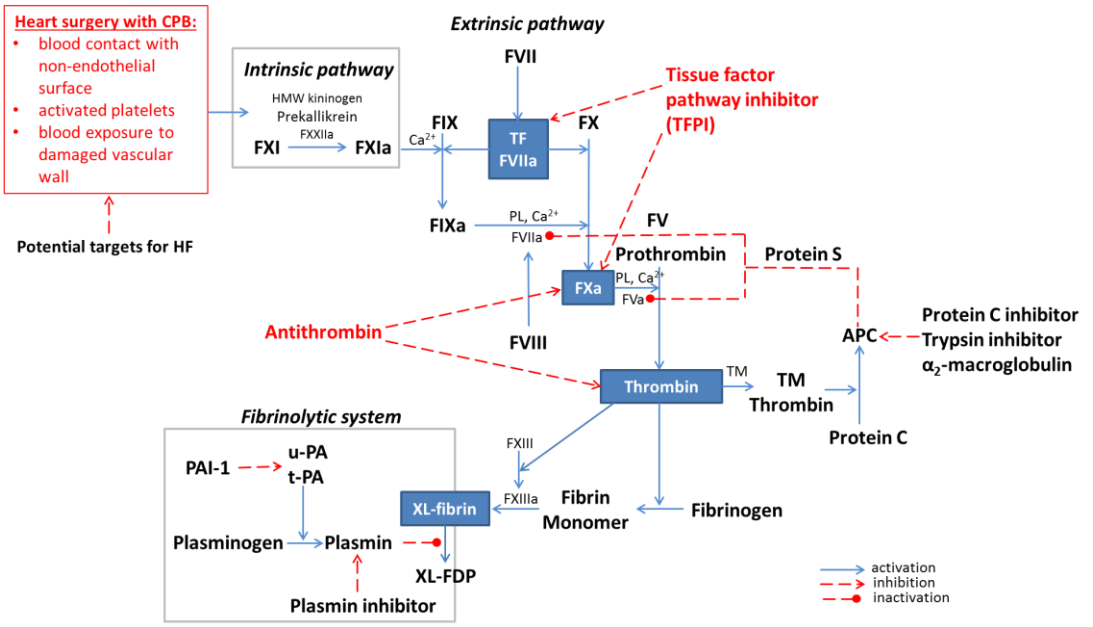

Figure 3: Cardiopulmonary bypass activates coagulation cascade. Factors, which can be potentially influenced by HF, are listed in the red box (adaptation from Day & Taylor, 2005).

Abbreviations: APC – activated protein C, CPB – cardiopulmonary bypass, HF – hemofiltration, HMW – high molecular weight, PAI-1 – plasminogen activator inhibitor 1, PL – plasminogen, t-PA – tissue plasminogen activator, TF – tissue factor, TM – thrombomodulin, u-PA – urokinase plasminogen activator, XL-fibrin – cross-linked fibrin, XL-FDP – cross-linked fibrin degradation products.

1.3. Endothelial dysfunction in SIRS

1.3.1. Endothelium as a target organ in SIRS and CPB

Endothelial cells (ECs) mediate the onset, amplification and resolution of the inflammatory response through their multidimensional structural and signaling properties (Aird, 2007; Xiao & Wang, 2014). Endothelium expresses multiple receptor types on their surface, being a vulnerable target for circulating DAMPs and PAMPs (Fig. 4).

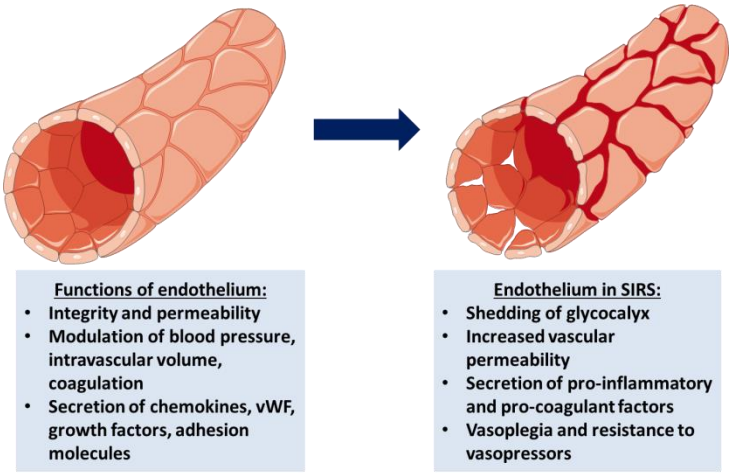

Figure 4: Role of endothelium in homeostasis and pathophysiological alterations in systemic inflammatory response syndrome (SIRS). Endothelium is an organ with large surface, and multiple regulatory functions, spanning from the fine regulation of blood coagulation and vascular tone to the production of molecules mediating inflammation and tissue damage. In SIRS, activation of endothelium by pro-inflammatory factors and immune cells leads to systemic dysregulation of vascular resistance and permeability, as well as secretion of the battery of pro-coagulant and pro-inflammatory factors. Figure produced by author, using Servier Smart Art vector graphics, distributed under Creative Commons Attribution Non Commercial CC BY-NC 4.0 license.

It is known that activation of pro-inflammatory signaling in ECs is mediated via diverse family of toll-like receptors (TLRs), interacting with plethora of SIRS-associated ligands (Table 1; Matsuda, 2016). Different types of TLRs are differently expressed in different vascular beds; evidence of expression and signaling in ECs exists for 10 types of these innate immune receptors. TLRs of endothelial cells, upon binding with their ligands activate pro-inflammatory intracellular signaling mediated through NF-κB and the MAP kinases. TLR agonists, including LPS and bacterial lipoproteins can directly up-regulate expression of pro-inflammatory cytokines in ECs (Khakpour et al., 2015).

ECs cells secrete a range of molecules, involved into angioneogenesis and promoting maintenamce of endothelial barrier. Vascular endothelial growth factor (VEGF), soluble tyrosine-kinase (sFLT-1), soluble VEGF receptor, angiopoietin-2 are mediators of vascular permeability and are associated with adverse outcomes in experimental and human sepsis (Yano et al., 2006). Thrombomodulin (TM), von Willebrand factor (vWF), tissue plasminogen activator (tPA) are regulators of coagulation cascade and are implicated in pro-coagulant changes and subsequent disturbances of microcirculation (Aird et al., 2003; Hou et al., 2017).

Activation of ECs in case of CPB occurs in generalized manner, resulting in systemic endothelial dysfunction, pathological disturbances of vascular tone, microcirculation, coagulation, and end-organ damage (Verrier & Morgan, 1998). Multiple factors, associated with surgery *per se* and external circuit of CPB are involved into systemic activation of ECs. Under physiological conditions, ECs express and secrete multiple factors (prostaglandin I_2, heparin-like factors, tPA, thrombomodulin), promoting anticoagulant phenotype and thus, efficiently preventing clot formation. In response to CPB, increased expression of tissue factor on the surface of ECs occurs. Tissue factor is binding to factor VIIa, initiating subsequent critical conversion of factor X into factor Xa and thrombin formation and massive deposition of fibrin in microvasculature. Pro-coagulant phenotype is also exaggerated by concomitant down-regulation of thrombomodulin. In contrast, dramatic increase of tissue plasminogen as a consequence of systemic EC activation leads to clotting disturbances and put certain individuals under risk of life-threatening bleedings (Verrier & Morgan, 1998).

Table 1: Subtypes of TLRs expressed in human endothelium and their ligands

TLR subtype	PAMPs	DAMPs
TLR1	(w/TLR2) triacyl lipoprotein	unknown
TLR2	Lipoproteins (w/TLR1), triacyl lipoprotein (w/TLR6), diacyl lipoprotein, LTA, zymosan	(w/TLR6) HMGB1, HSPs, ECM
TLR3	dsRNA	mRNA
TLR4	LPS, viral envelop proteins	HMGB1, HSPs, ECM, Ox-phospholipids, β-defensin 2 (w/TLR6), β-Amyloid, Ox-LDL
TLR5	Flagellin	unknown
TLR6	(w/TLR2) diacyl lipoprotein, LTA, zymosan	(w/TLR2) HMGB1, HSPs, ECM
TLR8	ssRNA	ssRNA (immune complex)
TLR9	DNA, hemozoin	DNA (immune complex)
TLR10	Unknown	Unknown

Abbreviations: ECM – extracellular matrix, HMGB1 – high-mobility group box 1, HSPs – heat shock proteins, LTA – lipoteichoic acid, LPS – lipopolysaccharide, Ox-LDL – oxidized low-density lipoprotein, ssRNA – single-stranded RNA.

1.3.2. Endothelium as a key player in inflammatory response

Endothelial cells, forming inner layer of blood vessels, cover approximately 4000-7000 m^2 of surface (Aird, 2005). Apart maintaining the integrity of the vessel wall, this cell type plays an important role in metabolism and homeostasis, controlling vessel permeability, angiogenesis, regulation of blood pressure, balance between thrombosis and fibrinolysis factors, trafficking of cells and biologically active substances (Félétou, 2011). Endothelium is an active secretory organ, producing variety of vasoactive substances and mediators of multiple biological functions, including interleukins and eicosanoids. ECs express plethora of chemokines and adhesion molecules, thereby influencing the extent, localization and duration of inflammatory response and regulating proper defense and tissue repair (Luscinskas et al., 1996). A multistep adhesion cascade leads to interaction between the endothelial surface and leukocyte, promotes leukocyte rolling and extravasation. P-selectin, E-selectin and receptor of advanced glycation end-products (RAGE) are engaging leukocyte and provide rolling; ICAM-1, VCAM-1, and MadCAM-1 provide firm adhesion to endothelial surface, whilst PECAM-1 ensures trans-endothelial migration of the activated leukocyte to the site of injury or inflammation (Granger & Senchenkova, 2010; Frommhold et al., 2010).

On the one hand, endothelium is an organ that undergoes injury in septic conditions, on the other hand, variety of bioactive substances, secreted by endothelial cells, drive inflammatory process further, inducing shock and organ failure (Ince et al., 2016; Boisrame-Helm et al., 2013). Endothelial cell signaling and endothelium-derived biomarkers were shown to be predictors of clinical outcomes in septic patients (Hendrickson et al., 2018; Fang et al., 2018). In particular, based on biomarker data from clinical trials, IL-6 and IL-8 are associated with acute respiratory distress syndrome in septic patients (Hendrickson et al., 2018). Furthermore, endothelial dysfunction in sepsis plays an important role in alteration of blood flow by massive production of endothelial and leukocyte adhesion factors. It promotes leukocyte activation, adhesion to endothelial cells and extravasation (Fabian-Jessing et al., 2018). Endothelial markers of permeability (sFLT-1 and Ang-2) and hemostasis (vWF, tPA, TM) were shown to be associated with mortality in septic patients (Hou et al., 2017).

1.3.3. Advanced glycation end-products and inflammation

Advanced glycation end-products (AGEs) result from non-enzymatic reaction between proteins, lipids, or DNA with sugars or reactive dicarbonyls (i.e., glyoxal, methylglyoxal). These products were shown to accumulate in tissues with aging and age-related diseases, supported by impaired glucose and lipid metabolism (Nowotny et al., 2014; Chaudhuri et al., 2018). Human body is exposed to dietary AGEs; about 10% of ingested AGE-modified amino acids can be absorbed from gastrointestinal tract and enter the circulation (Nowotny et al., 2018; Scheijen et al., 2018). AGEs can be also produced endogenously as a side product of glycolysis or due to sustained oxidative stress and hyperglycaemia (Moldogazieva et al., 2019). AGE-modification of amino-acid residues can alter binding sites of the proteins, alleviating their transport or receptor functions (Soudahome et al., 2018). In case of albumin, the major transport protein of human plasma, glycation at the binding sites imposes a serious issue for pharmacokinetics of many commonly used drugs, affecting drug distribution and concentration in tissues (Qiu et al., 2020). Accumulation of AGE-modified proteins and cross-linked proteins is especially pronounced in the proteins with slow turnover (collagen, crystalline). These cross-links disrupt elasticity and functional resistance

of these tissues, contributing to age-related functional decline and occurrence of certain diseases (skin aging, hypertension, diastolic heart failure, osteoarthritis, cataracts, etc.) (Nandi et al., 2020; Bejarano & Taylor, 2019).

Apart from their structure-disruptive role, AGEs can bind to RAGE-receptor subsequently inducing a cascade of down-stream signalling. RAGE receptor is a multi-ligand receptor having affinity to AGE-modified proteins, as well as damage-associated molecular pattern molecules (β-amyloid, HMGB1, proteins of S100-superfamily, β2-integrin Mac-1, DNA) (Tobon-Velasco et al., 2014). RAGE is also an innate immunity sensor for bacterial endotoxin, respiratory viruses, and microbial DNA (Hudson & Lippman, 2018). RAGE mediates acute and chronic vascular inflammation playing role in pathogenesis of atherosclerosis and diabetic vasculopathy (Lin, 2009). Increased RAGE-signaling results in the overexpression of RAGE-receptors on the cell surface; RAGE-overexpression tunes the cell towards further RAGE-activation and thus, completes pro-inflammatory vicious circle (Yan et al., 2010). AGE/RAGE signaling plays an important role in regulating the production/expression of TNF-alpha, oxidative stress, and endothelial dysfunction in diabetes (Kierdorf & Fritz, 2013). Apart from increased production of inflammatory cytokines, RAGE-activation results in over-expression of pro-fibrotic molecules, instigating cardiac and vascular remodeling (Zhao, 2014). RAGE-receptors on ECs, mononuclear phagocytes, and lymphocytes interact with protein S100A12, triggering cellular activation, production and release of pro-inflammatory mediators (Jin et al., 2015; Kierdorf & Fritz, 2013; Bierhaus & Nawroth, 2009; Ding et al., 2007).

The definite role of AGE-RAGE axis in the onset and progression of systemic inflammation is yet to be elucidated. Small observational studies provide limited and controversial data on the prognostic value of plasma AGE levels. Previous systematic review and meta-analysis of studies, exploring interventions in animal models of bacterial sepsis suggest that RAGE-inhibition could serve as potential therapeutic intervention. In case of Gram-positive bacterial infections, RAGE-inhibition alleviated bacterial growth and disseminatioin, having favourable effect on plasma cytokine levels and pulmonary injury (Zhao et al., 2018). Rather small observational study has shown that plasma levels of CML and CEL were decreased in patients with severe sepsis; plasma levels of these AGEs supposedly were associated with renal dysfunction compound of SOFA-score (Andrades et al., 2012). In another study, CML and CEL levels of critically ill patients were strongly correlated with SOFA-score. High baseline levels of CML were associated with increased mortality risk (Meertens et al., 2016).

Expression of RAGE in leukocytes and plasma sRAGE levels were significantly increased in patients with septic shock, compared to healthy controls and post-operative patients without sepsis. This study also emphasized that increase in immunologic RAGE-ligands, particularly S100A8 and S100A9 was associated with the severity of sepsis, rather than AGE-ligands of RAGE (Hofer et al., 2016). Soluble isoform of RAGE (sRAGE) is another unknown compound of the inflammatory equation. It can potentially act as a trap to neutralize RAGE-ligands and alleviate RAGE signalling (Prasad et al., 2018). However, sRAGE is also known to interact with leukocyte CD11b receptor, boosting inflammatory mediator production (Wang et al., 2010). In a study by Hamasaki et al. (2014) patients with septic shock, having elevated serum levels of sRAGE had worse outcomes, accompanied by increased production of IL-1α, IFN-γ and TNF-α.

In general, research in patients with sepsis and systemic inflammation has a slant towards DAMPs and PAMPs-ligands of RAGE, addressing possible role of sRAGE as a prognostic biomarker for septic patients (Denning et al., 2019; Pregernig et al., 2019).

2. Aims of the study

Hemofiltration (HF) is a perspective treatment method with a variety of indications, including life-threatening conditions, i.e. sepsis, septic shock, massive trauma, burns, acute liver failure and drug poisoning. To date, clinical trials have demonstrated several benefits of HF treatment, including reduction in levels of pro-inflammatory mediators, reduced stay in intensive care unit and reduced need to use vasopressors. However, it remains unclear what is the spectrum of the bound molecules, including many of the plasma proteins and the extent. Furthermore the mechanism of binding remains largely unknown. Therefore the aims of the current work are:

1. To establish a technique allowing efficient isolation of the proteins bound on the polymer matrix. The isolation method should be compatible with further LC-MS/MS identification of the proteins in the sample and testing in cultured human cells.
2. Identification of plasma proteins, bound to the polymer beads after intraoperative hemofiltration in patients undergoing cardiac surgery with cardiopulmonary bypass (CPB) via LC-MS/MS.
3. Broad characterization of the properties of the proteins, retained on the filter polymer matrix, including molecular weight, size, charge, hydrophobicity and isoelectric point.
4. Identification of AGE-modified proteins, bound on the polymer of the CytoSorb filters in clinical settings.
5. Comparison of plasma samples, derived from the patients before and after intraoperative hemofiltration, using LC-MS/MS with label-free quantification.
6. Establishing potential connections between clinical outcomes in patients undergoing intraoperative HF and changes in blood plasma composition.
7. Investigating changes in plasma protein concentrations and AGE-modified protein content via *in vitro* adsorption system, resembling HF in clinical settings.
8. Investigating effects of the isolated plasma proteins in cultured human endothelial cells (ECs) to show potential cytotoxicity, functional and morphological alterations in ECs, as well as changes in gene transcription, and validation on the protein level.

3. Patients, materials, and methods

3.1.1. Patients

Patients undergoing cardiac surgery have been enrolled in 2018-2019 into a clinical study REMOVE in the heart surgery department of the University Hospital Halle (ClinicalTrials.gov Identifier: NCT03266302; Diab et al., 2020). Study design was approved by local ethical committee. Inclusion criteria for REMOVE study were the following: patients with infective endocarditis (according to Duke Criteria, see table 2) undergoing cardiac surgery; signed informed consent; age ≥18 years. Patients with EuroSCORE II ≤ 3, or currently participating in another interventional trial, pregnant women, patients on immunosuppressive or

immunomodulatory therapy (with dosing of glucocorticoids over Cushing threshold) or former participants of the REMOVE study were not included into the study. Clinical characteristics of patients, including age, BMI, renal function, type of surgical procedure performed and on-pump time are presented in Table 3.

Table 2: Modified Duke Criteria for diagnosis of infective endocarditis (Holland et al., 2016)

Major clinical criteria	Minor clinical criteria
Positive blood culture for either of the following: • Typical microorganism (*S.viridans*, *S. gallolyticus*, HACEK organisms, *S. aureus*, community-acquired enterococci in the absence of a primary focus) from 2 separate blood cultures • Persistent bacteremia (two positive cultures >12 hours apart or three positive cultures or a majority of ≥4 culture positive results >1 hour apart)	**Predisposing condition:** Intravenous drug use Use of venous catheter Predisposing cardiac condition
Evidence of the involvement of endocardium, either of the following: • Echocardiographic findings of mobile mass attached to valve or valve apparatus, abscess, or new partial dehiscence of prosthetic valve • New valvular regurgitation	**Vascular phenomena:** Arterial embolism Septic pulmonary emboli Mycotic aneurysm Intracranial hemorrhage Conjunctival hemorrhages Janeway's lesions
Serological findings: • Single positive blood culture for *C. burnetii* or antiphase 1 IgG antibody titer of ≥1:800	
Definite diagnosis of IE can be defined by the fulfilment of clinical criteria: either two major criteria, one major and three minor criteria or five minor criteria	

Another subgroup of enrolled patients was comprised of subjects undergoing elective aortic valve surgery, having no history of IE (clinical characteristics of the patients are shown in table 4 (Ethical committee approval: Amendment to the REMOVE study, Bearbeitungsnummer 2018-121). CytoSorb filters, as well as plasma samples before and after intervention were collected in this subgroup.

Table 3: Baseline clinical characteristics of the REMOVE-study population

Patient number	Age, years	Gender, m/f	BMI, kg/m^2	IE, y/n	eGFR, ml/min	LVEF, %	Procedure performed	CPB time, min.
1	37	m	24	y	34	44	TVR	199
2	67	m	24.5	y	22	-	MVR	153
3	36	f	18.4	y	55	18	MVR+TVR	288
4	53	m	24.1	y	90	45	MVR	128
5	75	f	40.5	y	40	-	MVR	185
6	79	m	21.3	y	18	-	AVR	92
12	37	m	22.3	y	90	-	MVR	161

Abbreviations: BMI – body mass index; eGFR – estimated glomerular filtration rate; IE – infective andocarditis; LVEF – ejection fraction of the left ventricle; TVR – tricuspid valve replacement; MVR – mitral valve replacement; AVR – aortic valve replacement.

Table 4: Baseline clinical characteristics of the patients undergoing elective valve surgery

Patient number	Age, years	Gender, m/f	BMI, kg/m^2	IE, y/n	eGFR, ml/min	LVEF, %	Procedure performed	CPB time, min.
7	77	f	34.2	n	47	70	AVR	94
8	60	m	33.5	n	40	50	AVR	211
9	70	f	33.1	n	64	40	AVR	105
10	43	f	25.5	n	71	60	AVR	83
11	52	m	27.3	n	89	45	AVR	84

Abbreviations: BMI – body mass index; eGFR – estimated glomerular filtration rate; IE – infective andocarditis; LVEF – ejection fraction of the left ventricle; AVR – aortic valve replacement.

3.1.2. Polymer material acquisition

CytoSorb 300 ml filters (CytoSorbents Inc., Monmouth Junction, NJ, USA) were used for intraoperative HF combined with roller-pump cardiopulmonary bypass machine HLM S5 (Sorin/LivaNova). Filters were integrated into the circuit with CytoSorb PVC-adaptors (Hemotronic s.p.a.). Each filter was washed through with 500 ml of 0.9% saline in order to remove remaining blood cells, debris and blood proteins that are not adsorbed at the surface of the beads. After being disconnected from CPB circuit, each filter was stored at 4°C; filter acquisition was performed within 2 hours of storage at 4°C. Afterwards, each device was dismantled, and polymer material was stored in 5.0 ml Eppendorf tubes at -20°C until further protein extraction.

3.1.3. Plasma samples

Blood plasma samples were collected at the start of the operation (skin incision) and at the end of CPB into 5.0 ml K2-EDTA vaccutainers. Blood samples were centrifuged at 2000×g for 15 min., at room temperature (RT). Resulting supernatants were carefully separated from cell pellets without disturbing the buffy coat and leaving the remaining ≈200 µl of plasma, covering the cell pellet, untouched. Plasma samples were collected into 0,5 ml Eppendorf tubes and stored as 200 µl aliquots at -80°C until further analysis, all the procedures of plasma handling for further proteomics preparation are described elsewhere (Geyer et al., 2018; Greening & Simpson, 2019).

3.2.1. Isolation of proteins, adsorbed on polymer matrix

Elution of the proteins adsorbed on the surface and inside the pores of PSDVB matrix appeared to be a challenging task. Using buffer systems with acidic and basic pH, salt solution, and acetonitrile (all listed in table 5) did not provide elution of the proteins in sufficient amounts. Applying SDS in different concentrations and heating in denaturing sample buffer for 5 min. (thermo mixer with shaking at 95°C) allowed isolating and identifying considerable amount of plasma proteins. However, due to harsh conditions used, this method did not allow precise protein concentration measurements and limited the use of the eluted fractions in cell culture experiments.

Table 5: Buffers used to elute proteins from the polymer matrix

Buffer	Composition
Acidic glycine buffer	100 mM glycine (Roth) in ddH_2O, pH adjusted with HCl (pH=2)
Acetonitrile	Acetonitrile (Roth)
Basic glycine buffer	Glycine (Roth) in ddH_2O, pH adjusted with NaOH (pH=11)
Salt solution	1M NaCl
SDS	20% SDS-solution (Roth), diluted to 2% and 10% with ddH_2O
5×Denaturing sample buffer	0.3 M Tris-HCl (Boehringer Mannheim), pH 6.8; 25% β-mercaptoethanol (Sigma); 10% SDS (Roth); 50% glycerol (Merck Millipore); 0.5 % bromphenol blue (Merck Millipore)

Using grinding with porcelain pestle and mortar with subsequent filtration with syringe filter (Whatman FP 13/0,2 RC-S, 0,2 µm cellulose acetate membrane) (Fig. 5, A) allowed the isolation of considerable amounts of plasma proteins with a prevalent band at MW of 70 kDa (Fig. 5, B). This method was beneficial, as it did not require addition of any solvents or detergents and resulted in a transparent, uncolored elution sample. However, this method was incompatible with broader identification of protein fractions via LC-MS/MS due to potential contamination with small fragments of polymer matrix; for this reason it was also not taken into consideration for further biological testing.

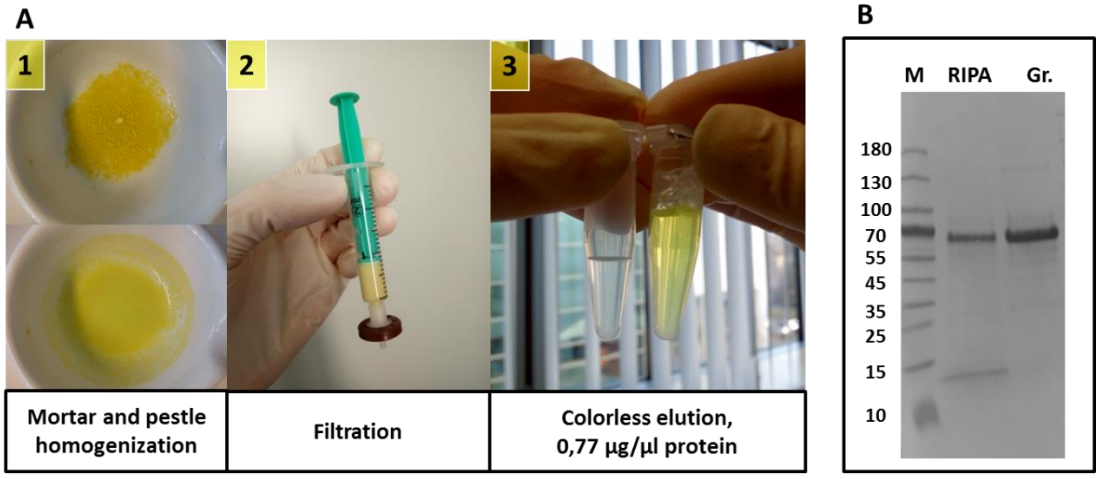

Figure 5: Development of optimal elution system. A. Steps to obtain proteins from polymer matrix, involving extraction of intact beads from the filter (1, upper picture) and mechanical disruption of the bead structure (1, lower picture) with subsequent filtration of the sample (2). Colorless elution was a result of grinding procedure (3, left). B. Amido Black staining of different elution samples, transferred on 0.45 mm nitrocellulose membrane. M – PAGE-Ruler, pre-stained molecular weight marker (Thermo Fisher); Lane 1 (RIPA) – Elution sample, obtained with RIPA-buffer; Lane 2 (Gr.) – elution sample obtained via grinding of PSDVB-beads with subsequent filtration of the sample.

The best result in protein isolation was achieved by addition of 1×RIPA-buffer (0.5 M Tris-HCl, pH 7.4, 1.5 M NaCl, 2.5% deoxycholic acid, 10% NP-40, 10 mM EDTA (Merck Millipore)) to the beads, that were taken from 300 mL device that was used in clinical settings. For that, beads from the column were loaded into 0.8 ml centrifuge columns (Thermo Scientific), material was rinsed twice with 1×PBS (pH 7.4) to remove blood cells, cellular debris and

proteins that could have remained unbound on the surface of the polymer. Prepared beads were rinsed with 500 µl of 1×RIPA and centrifuged at 11800×g for 1 min. at RT.
Obtained elutions were transparent and yellow-colored (Fig. 5, panel A3, probably due to the presence of bilirubin and other blood pigments on the matrix (after the cartridge had been used in the clinical settings, the polymer beads lose their initial white color and acquire yellow coloring). To purify protein samples from detergents and prepare them for further analysis, dialysis was performed in 0.5 ml Slide-A-Lyzer cassette (Thermo Scientific) with 10 kDa molecular weight cutoff towards 500 ml of deionized water for 48 hours. Finally, to concentrate and desalt the samples, Amicon-Ultra 0.5 ml centrifugal filter units with 10 kDa molecular weight cutoff (Merck Millipore) membrane were used at 14000×g for 30 min. at 4°C.
Protein concentration was determined with the BCA-assay, using a commercially available kit (Thermo Scientific), transparent flat bottom 96-well plate (TPP) and Tecan M1000 i-Control plate reader with standard BCA-protocol.

3.2.2. Preliminary characterization of protein fractions

Denatured protein samples were loaded into 12-well Criterion TGX pre-casted 4-20% gel (Bio-Rad) and run at 200 V. Afterwards, gel was rinsed for 15 minutes in deionized water, and subsequently stained with Colloidal Coomassie Blue (CCB), containing: 0,02% Colloidal Coomassie Blue G250 (BioRad), 5% aluminum sulfate (Applichem), 10% ethanol (Sigma-Aldrich), 2% ortophosphoric acid (Merck Millipore); for 3 hours at RT with gentle shaking, destained overnight in water. Protein bands were visualized using 700 nm wavelength detection in an Odyssey Clx reader (Li-Cor).

3.2.3. Mass-spectrometry methods used for elution samples

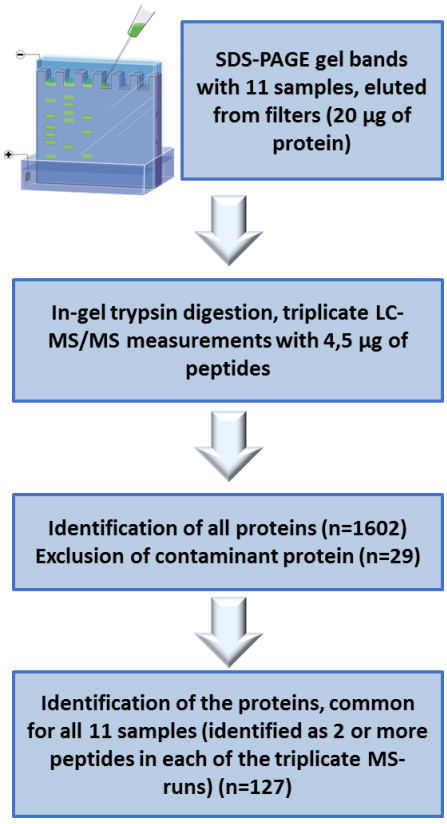

Denatured protein samples (20 µg of each sample) were loaded into Protean TGX pre-casted 4-20% gel (Bio-Rad) and run as described above. To avoid cross-contamination of the samples, loading of the gel was performed in an alternating manner, leaving each second pocket empty. After running, the gel was washed for 15 minutes in ddH_2O, subsequently stained with CCB for 3 hours at RT with gentle shaking and destained overnight in water.

Figure 6: Workflow used to identify the most abundant proteins in the elution samples. Figure produced by author, using Servier Smart Art vector graphics, distributed under CC BY-NC 4.0 license.

Protein bands were excised, gel pieces were washed with 100 mM ammonium bicarbonate, pH = 7.8 (PanReac AppliChem ITW reagents) and dehydrated with acetonitrile (Biosolve Chemie SARL) twice and then dried in a Speed Vacuum Concentrator at RT for 5 minutes. Reduction was performed using 5 mM tris-

(2-carboxyethyl)-phosphin (Thermo Fisher Scientific) in 100 mM ammonium bicarbonate, pH = 7.8, for 15 minutes at 37°C.

Gel pieces were washed with acetonitrile twice and then dried for 10 minutes in a speed vacuum concentrator. Alkylation was performed with 55 mM iodoacetamide (Sigma Aldrich) in 100 mM ammonium bicarbonate, pH = 7.8, for 20 minutes in the dark. Gel pieces were then washed with ammonium bicarbonate twice and thereafter with a solution of 50 mM ammonium bicarbonate and 50% acetonitrile at 37°C twice for 30 minutes. In the next step the gel pieces were dehydrated with acetonitrile twice and dried in a speed vacuum concentrator at RT for 5 minutes. Trypsin (Promega) was used to digest obtained proteins. For this gel pieces were rehydrated with a solution containing 260 ng trypsin in 200 µl of 50 mM ammonium bicarbonate (pH 7.8) at 4°C for 20 minutes. After that digestion was performed overnight at 37°C. The supernatant was taken off and peptides subsequently extracted with 50 mM ammonium bicarbonate (pH = 7.8), with 50% acetonitrile, 0.1% formic acid (Biosolve Chemie SARL) and 75% acetonitrile, 0.1% formic acid. The obtained peptide solutions were frozen at -80°C and dried in a speed vacuum concentrator at RT overnight.

Samples were analyzed by LC-MS/MS using the EASY-nLCTM 1000 system coupled to an Orbitrap Fusion™ Tribrid™ Mass Spectrometer (both Thermo Scientific) by the company Proteome Sciences R&D GmbH & Co. KG (Frankfurt-am-Main). Dried peptides were re-suspended in 2% ACN with 0.1% FA and a solid-phase purification step was performed using ZipTips (Millipore) according to manufacturer instructions. After that, re-suspended peptides were loaded onto a nanoViper C18 Acclaim PepMap 100 pre-column (Thermo Scientific) and resolved using an increasing gradient of ACN in 0.1% formic acid through an analytical column (Thermo Scientific) at a flow rate of 200 nL/min during the first 40 minutes and 300 nL/min over the last 20 minutes. LC gradient started with 10% ACN up to 30% ACN over the first 40 minutes, and then 90% ACN over the last 20 minutes. Peptide mass spectra were acquired throughout the entire chromatographic run (60 minutes) using a top speed collision induced dissociation (CID) combined with higher collision induced dissociation (HCD) method.

Table 6: Mass-spectrometry acquisition parameters

Acquisition parameter	**Value**
Acquisition time, min.	60
Cycle time, sec.	3
MSn level	2
Isolation window	1.6 / 1.2
Activation type	CID / HCD
Collision energy	30
Detector type	Ion Trap / Orbitrap
Orbitrap resolution	NA / 30000
Maximum Injection time, ms	40 / 100
AGC target	10000

Each Fourier-transform mass spectrometry (FTMS) scan was acquired in the Orbitrap with a resolving power of 120K. Corresponding MS2 scans were acquired at a resolving power 30,000 @400m/z by data dependent acquisition (DDA) mode (mass-spectrometry acquisition parameters are listed in table 6). MS spectra were generated from ~4.5 µg injected peptides. A commercial mixture of BSA peptides (MassPREP™ BSA Digestion Standard, Waters) has been run before and after the samples in order to check the analytical reproducibility of the MS performance.

3.2.4. Analysis of LC-MS/MS data

Raw mass spectrometry data files were submitted to Proteome Discoverer (PD) v2.1 (Thermo Scientific) using the Spectrum Files node. The Precursor Ions Area Detector node was included in the workflow to enable extraction of MS1 peak area (intensity) values suitable for use in Label Free quantification studies. Contaminant FASTA database (version June 2018) was used in order to identify and exclude common skin or laboratory contaminant proteins.

3.2.5. GO-annotation and annotation of protein properties (sequence length, molecular weight, isoelectric point, charge and hydrophobicity)

Annotations of protein function and attribution to classes and cellular compartments was performed with the expanded classification system PANTHER, version 11 (Ashburner et al., 2000; Mi et al., 2017). Network analysis with functional enrichment was performed with the use of STRING-database (Szklarczyk et al., 2019).

Sequence length and molecular weight of the proteins were retrieved from UniProt database. Isoelectric point and charge of the proteins were calculated with an on-line bioinformatics calculator Prot-Pi (https://www.protpi.ch/Calculator/ProteinTool/). Grand average hydrophobicity (GRAVY) was calculated with a GRAVY-calculator tool (http://www.gravy-calculator.de/), as a sum of hydropathy values for each amino acid in the protein, divided by the length of the sequence retrieved from UniProt. Multiple regression analysis was used to explore linear relationship between variables and was performed with MedCalc software (version 12.7.5).

3.3. Enzyme-linked immunosorbent assay (ELISA)

Concentrations of C-reactive protein and IL-6 were measured in the samples eluted from the polymer matrix. Plasma samples and elution samples were analyzed with commercially available high-sensitive CRP (hs-CRP) ELISA-kit and high-sensitive IL-6 ELISA kit (both IBL International) according to the manufacturer's protocol. Sensitivity of IL-6 ELISA was significantly flawed by the presence of hemolysis in large fraction of plasma samples (described further in section 4.2.2.).

3.4. Measurements of inflammatory cytokines in plasma and elution samples with cytometric bead array (CBA)

CBA Human Inflammatory Cytokine Kit (BD Biosciences) was used to measure IL-8, IL-1β, IL-6, IL-10, TNF, and IL-12p70 in plasma samples obtained from the patients before and after the surgery, as well in the protein samples eluted from the CytoSorb filters. The principle of method is based on capture beads conjugated with one of the cytokine-specific antibodies. The detection reagent is an antibody conjugated to phycoerythrin (PE), producing fluorescent signal proportional to the quantity of the bound cytokine. Upon incubation of capture beads and detection reagent with cytokine-containing solution a sandwich consisting of antibody-coupled bead, cytokine of interest and detection reagent is formed. These particles are further measured with flow cytometer, allowing identification of particles according to the fluorescence properties of the bead (identifies cytokine of interest) and detector (quantitative identification).

Wash buffer, assay diluent, cytometer setup beads, serum enhancement buffer, cytokine capture beads, and cytokine PE detection reagent were all compounds of the kit. 96-well

filter plate with the semi-permeable membrane bottom (PALL Corporation) was used to mix the samples and the reagents. All measurements were performed in duplicate. Plasma samples were diluted 1:10 and elution samples were diluted 1:2 with Assay Diluent (BD Biosciences) prior to measurements. Capture beads were pre-incubated with serum enhancement buffer to reduce the false-positive signals stemming from other plasma proteins. The plate was pre-washed with 100 µl of wash buffer per each well and placed on the vacuum manifold to remove the liquid. Each sample and pre-mixed cytokine standard was pipetted into the plate, followed by addition of 50 µl of capture beads; the plate was covered and placed on shaker for 5 minutes at 1100 rpm. The plate was then incubated at RT for 1.5 hours on a dry, non-adsorbent surface. After the incubation the plate was placed on the vacuum manifold to remove the liquid, well were washed 2 times by with 200 µl of wash buffer, followed by shaking for 2 minutes at 1100 rpm and aspiration of the liquid on the manifold. Content of the each well was reconstituted with 120 µl of wash buffer; beads were re-suspended in the liquid by shaking at 1100 rpm for 2 minutes. Acquisition of the samples was performed with BD Fortessa (BD Biosciences) after calibration of the cytometer with cytometer setup beads. Data analysis was performed with FCAP array software (BD Biosciences).

3.5. *In vitro* adsorption of proteins from human plasma

Current protocol was adjusted to mimic proportions between circulating volume and the volume of adsorbent, corresponding to real clinical situation (ratio between volume of liquid and volume of adsorbent ≈16.67). Compounds used for *in vitro* filtration setup are shown in Fig. 7. A 25 ml of CPD-stabilized FFP from healthy donor was thawed and supplemented with 1000 IU of heparin-sodium. A 1.5 ml experimental CytoSorb column was connected to two Tygon LMT-55 tubes, free ends of tubes placed into 50 ml tube (Saarstedt), containing plasma and 3×6 mm PTFE stir bar (Roth). The tube with plasma was placed on IKAMAG Reo magnet mixer to ensure steady stirring of the plasma at the bottom of the tube. An empty Rezorian tube (Sigma-Aldrich) with O-rings (McMaster-Carr) and 200 µm filter mesh (Sefar) was used as a control filtering condition, to evaluate potential reduction of protein concentration due to protein degradation and binding to the tubing, and other polymer compounds of the system. Filtration was performed for 2 hours with ISMATEC Reglo peristaltic pump at flow rate 2.5 ml/min. Aliquots of plasma (100 µl each) were taken before beginning of filtration and after 2 hours of continuous pumping through the circuit. Protein concentration measurements were performed using BCA-kit (Thermo Fisher).

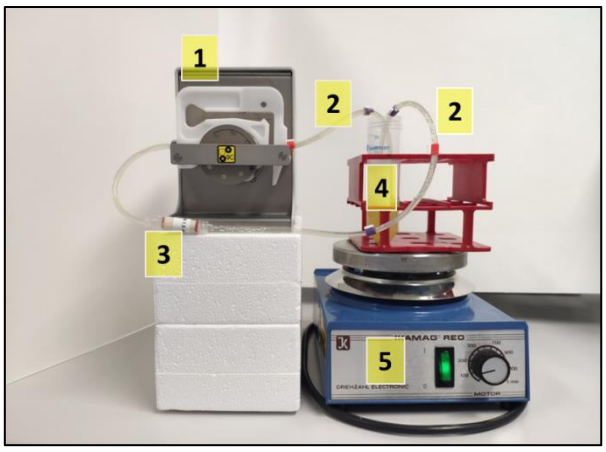

Figure 7: Setup for *in vitro* plasma filtration. Compounds: Peristaltic pump (1), connecting tubes with stoppers (2), 1.5ml experimental column filled with CytoSorb matrix (3), 50 ml tube with aliquot of plasma and stir bar (4), magnet mixer (5).

3.6. *In vitro* filtration of plasma, supplemented with AGE-modified proteins with subsequent LC-MS/MS quantification of relative content of CML and CEL

In order to show whether there is a preferential binding of the AGE-modified proteins to the polymer matrix, an experiment similar to in vitro plasma filtration was performed (described in section 3.5). Plasma from a healthy donor was supplemented with 5% AGE-modified plasma. AGE-modified plasma was prepared by incubating 200 ml of plasma from a healthy donor with 50 mM glucose and ribose, 10 µM of glyoxal and methylglyoxal at 37°C for 2 weeks in the dark. To remove active dicarbonyls and reactive sugars from the plasma, modified samples were dialyzed towards ddH_2O for 2 days at 4°C in the dark. Plasma samples were carefully mixed together and filtered through 1.5 ml CytoSorb experimental column in parallel with an empty control column as described above. Aliquots of plasma (200 µl) were taken before the beginning of filtration and directly after the end of 2 hour-cycle. Samples for further semi-quantitative LC-MS/MS identification were precipitated from 120 µl plasma aliquots with ice-cold acetone at -20°C and dried out at RT under the hood. Acetic hydrolysis and subsequent LC-MS/MS identification of modified amino acids was performed by Christoph Hohmann (Institute of Chemistry, working group of Prof. Dr. M. Glomb) as described elsewhere (Glomb & Pfahler, 2001; Baldensperger et al., 2020). CML and CEL content was normalized towards leucine content, as this amino acid is stable during the hydrolysis and represents total protein content of the sample. Up to 90% of arginine-derived modifications (MGH1, Arg-Pyr) can be degraded due to incubation at high temperatures and low pH, therefore only relative quantification of CML and CEL was performed (Ahmed et al., 2002).

3.7. Cell culture

Human aortic endothelial cells (HAECs) (Cell Applications Inc.) were used as a model for testing cytotoxic effects of plasma proteins, isolated from the matrix of adsorber. Cells were cultured with complete ECGM2 growth medium (PromoCell) containing 10% fetal calf serum (FCS) (Zellbiologische Produkte GmbH) and 1% penicillin-streptomycin (Sigma) in an incubator at 37°C and 5% CO_2. HAECs used for the experiments were between passages 6 and 10 to avoid growth and division retardation due to cellular senescence.

3.7.1. Proteins for cell culture treatment

A pool of four different elution samples, obtained from four patients, undergoing heart surgery with CPB, was used to treat endothelial cells across all the experiments. Obtained elutions were dialyzed in 0.5 ml Slide-A-Lyzer cassette (Thermo Scientific) with 10 kDa molecular weight cutoff towards 500 ml of deionized water for 48 hours. Dialyzed elution samples were filtered through 0.45 µm sterile Whatman SPARTAN 13/0.45 RC filter and pipetted into 0.5 ml Amicon-Ultra centrifugal filter units with 10 kDa molecular weight cutoff membrane under sterile conditions in laminar flow. Last step was performed to concentrate the samples at 14000×g for 30 min. at 4°C. Protein concentration of the obtained protein extract pool was determined with BCA-kit (Thermo Fisher).

3.7.2. Cell growth assay

HAECs were seeded on 96-well plate (black, flat transparent bottom, Eppendorf). To ensure that the cells are at the phase of exponential growth, a seeding density 1×10^4 cells per well was used. The HAECs were cultivated in complete ECGM2 medium with 10% FCS overnight.

Next day either cells were treated with proteins eluted from the hemofilter matrix (0.125 µg/ml; 0.25 µg/ml; 0.5 µg/ml) and corresponding concentrations of human serum (Sigma), 2 mM hydrogen peroxide (Uni-Apotheke, UKH) was used as a reference cytotoxicant. All treatment and control agents were dissolved in ECGM2 without FCS. After 24 hours stimulation, 20 µl of Cell Titer Blue (CTB, Promega) was added to each well. CTB is a fluorigenic dye, which is reduced by metabolically active cells with formation of resorufin, having specific spectrum of excitation and emission. Cells were incubated with CTB for 4 hours at 37°C, afterwards microplate reader Tecan M1000 i-Control was used to perform fluorescence measurements at Ex/Em=560/590 nm.

3.7.3. Cell viability assay

Same seeding density and treatment conditions as described in 3.6.2 were applied for viability assay. 2 mM hydrogen peroxide was used as known cytotoxicant. Sapphire700 dye (Li-Cor) was used to perform the assay. This dye is accumulating in cells with compromised membranes or dead cells; dye becomes fluorescent in near-infrared spectrum after binding to cytosolic proteins (Posimo et al., 2014). After 24 hours stimulation, 50 µl of Sapphire700, diluted 1:50 in FCS-free ECGM2 was added to each well, incubated at 37°C for 30 minutes and visualized with Odyssey Clx reader (Li-Cor) at 700 nm (red channel) with the following microplate settings: 3 mm focus distance, signal intensity 5, resolution 169 µm.

3.7.4. Cell proliferation assay based on Hoechst-BrdU quenching

HAECs were seeded on 6-well plates (TPP) with seeding density 0.3×10^6 cells per well and were incubated until confluence. Then, medium was changed to ECGM2 with 1% FCS to provide starvation and synchronize the cell cycles. After 2 days, medium was removed and substituted to ECGM2 with 10% FCS containing 100 µM of BrdU (Sigma-Aldrich) and 100 µM DC (Sigma-Aldrich) according to the protocol described by Kubbies, 1992. Cells were incubated with 0,125 µg/ml elution, serum, combination of elution and serum, medium without any additives and addition of 5 or 15 ng/ml human VEGF (PromoKine). After 48 hours of incubation with stimulants, controls, BrdU and DC, medium was removed, cells washed with PBS, trypsinized and placed into FACS-tubes and centrifuged at 200×g for 5 minutes at RT. Obtained pellets were incubated with 1 ml staining solution (1.2 µg/ml Hoechst 33258 in 100 mM Tris, pH 7.4; 154 mM NaCl; 1 mM $CaCl_2$; 0.5 mM $MgCl_2$; 0.1% NP40; 0.2% BSA) at 4°C in the dark for 15 minutes. Staining was followed by addition of 2 µg/ml of propidium iodide (PI) to each sample with subsequent incubation at 4°C in the dark for 15 minutes.

Flow cytometry was performed by Dr. Alexander Navarrete Santos in Core Facility "Flow Cytometry" of the Center of Basic Medical Research. For the excitation of the Hoechst 33258 dye, the UV laser (355 nm) was used. PI was excited using the yellow-green laser (561 nm). The emissions of Hoechst 33258 and PI were detected using the filters 450/50 nm and 610/20 nm respectively. The plot Hoechst-Area (A) versus PI-Area (A) was used for the analysis of the cells. For discrimination between single and duplet (cells), the dot plot Hoechst-A versus Hoechst-Height (H) and Hoechst-A versus the ratio Hoechst-A/Hoechst-H were used. All the parameters were measured on a linear scale. For the flow cytometric analysis $1x10^4$ events (single cells) were recorded. The strategy used for the analysis of the cell proliferation is shown in Fig. 8.

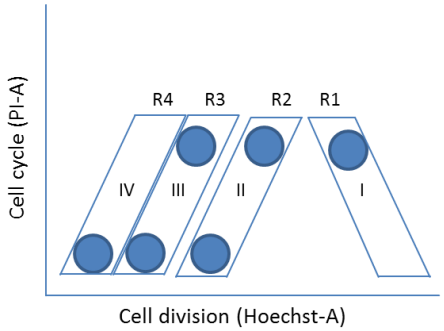

R1: no division
R2: 1st division
R3: 2nd division
R4: 3rd division

Figure 8: Schematic representation of the cell proliferation analysis based on Hochst BrdU fluorescence quenching. Numbers I-IV denote the cell cycle number. For the calculation, the percentage of cells in the regions (R) was used.

Percentage of fast growing cells was defined according to the following formula:

$$x = \frac{cell\ cycle\ III/_4 + cell\ cycle\ IV/_8}{cell\ cycle\ I + cell\ cycle\ II/_2 + cell\ cycle\ III/_4 + cell\ cycle\ IV/_8} \times 100\%$$

3.7.5. Cell attachment assay

HAECs were plated on 6-well plates with seeding density 0.3×10^6 cells per well, in 3 ml FCS-free ECGM2 medium with addition of elution proteins or corresponding amount of serum. Cells were incubated for 4 hours at 37°C and 10% CO_2, afterwards the medium with remained unattached cells was removed, cells were washed twice with PBS. Nuclear staining was performed with 2 µg/ml solution of Hoechst 33342 (Sigma) in ECGM2 for 10 min. at 37°C in the dark. Cells were fixed with 3.7% formaldehyde in PBS for 15 minutes in the dark at RT, washed with PBS and conserved in 50% glycerol at 4°C for further visualization.

3.7.6. Wound healing assay

HAECs were seeded on 10 cm dish (TPP) and cultivated till confluence. Next, cells were detached with trypsin-EDTA (Thermo Scientific) and seeded onto Nunclon 24-well plate (Thermo Scientific). After overnight cultivation, cells were confluent and ready for migration assay. Confluent cell surface were scratched using sterile SPLScratcher (SPL Life Sciences) with 24-well pattern. After this, cells were washed and plasma proteins from elution and human serum were added to each well in FCS-free ECGM2. Cell migration was visualized and recorded with Biotek Cytation for 24 hours with image recording every 30 minutes. Every image was evaluated with Biotek software; area of the scratch, cell density and cell area were automatically calculated at each time point.

3.7.7. Tube formation assay

Apart from lateral migration, endothelial cells are capable to form three-dimensional vessel-like structures when seeded on an extracellular matrix protein bed. Within 24 hours, they align, form polygonal networks, vessel-like structures with lumen and eventually, detach and degrade (DeCicco-Skinner et al., 2014). Normal dynamics of tube formation is shown in the table 7.

Table 7: Dynamics of the tube formation on the matrix gel

Timepoint	Stage of the tube formation
1 hour	Attachment and alignment of the cells
2 hours	Elongation and migration
4 hours	Formation of polygonal network
6 hours	Formation of stable honeycomb-like structures
16 hours	Network with lumen
24 hours	Degradation and detachment of the network

HAECs were seeded on 10 cm dish (TPP) and cultivated till 70% confluence. Meanwhile extracellular matrix gel (Abcam) was thawed at 4°C overnight and Nunclon 96-well plate (Thermo Scientific) was coated. Prior to seeding onto matrix-covered plate, cells were trypsinized and re-suspended in ECGM-2 (5% FCS, 1% penicillin-streptomycin) with addition of stimulants and growth factors (listed in table 8). Cells cultivated with 5% FCS ECGM2 served as an untreated control.

Table 8: Concentrations of stimulants and controls used for the tube formation assay

Stimulant/control	Concentration
VEGF (PromoKine)	15 ng/ml
Elution	0.125 µg/ml
Serum (Sigma)	0.125 µg/ml
Sulforaphane (Sigma)	2µM

Cells were seeded onto the coated plate with density of 10^4 cells per well. Tube formation was visualized and recorded with Biotek Cytation for 24 hours with image recording every 30 minutes. Tube formation, including the number of tubes in the network, nodes and meshes in each given image was quantified with Angiogenesis Analyzer, a plug-in for ImageJ software.

3.7.8. Transcriptomics

HAECs were cultivated on 10 cm cell culture dishes (TPP) until confluence, then cells underwent 24 hours treatment with 0.125 µg/ml elution, 0.125 µg/ml serum or FCS-free ECGM2 as described above.

Total RNA was isolated from HAECs by the TRIzol-method. For this purpose cells were washed with 1×PBS solution (Gibco) and harvested with TRIzol Reagent (Life Technologies, 1 ml per 6-well). After adding 200 µl of chloroform (Sigma Aldrich), mixing and centrifugation (2000×g, 5 min.) upper phase was gently agitated with isopropanol (Sigma Aldrich, 1:1 v/v) and incubated one hour at room temperature. RNA was pelletized by centrifugation (14.000×g, 10 min, 4 °C) and pellet was washed three times with 80% ethanol. After pellet drying nuclease free water was added and RNA was stored at -20°C. Additional purification step was included by using RNeasy MinElute Cleanup Kit, Quiagen) according to manufacturer instructions. To ensure quality and integrity for subsequent array analyses, RNA was dissected by Bioanalyzer. Only RNA with RIN values ≥8 was used for further array analysis. Array analysis was performed by Dr. Vesselin Christov in the Core Facility "Analysis" of the Center of Basic Medical Research.

Quantification of mRNA was performed with gene array method. Biotin-labeled cRNA was synthesized from total RNA with Ambion® WT Expression kit (Applied Biosystems, Carlsbad, CA) with subsequent GeneChip hybridization procedure using Clarion D human arrays (Affymetrix) and GeneChip Fluidics station 450 (Affymetrix, Santa Clara, CA). Hybridized mRNA chips were scanned with the Affymetrix GeneChip Scanner 7G with GeneChip Command Console 3.1 software. Data calculation was performed with the Robin software. Gene onthology annotation and overrepresenation test were performed with an on-line

bioinformatics platform ConsensusPathDB-human, release 34 (Herwig et al., 2016). Network analysis for the subsets of up-regulated and down-regulated genes was performed with STRING-database (Szklarczyk et al., 2019).

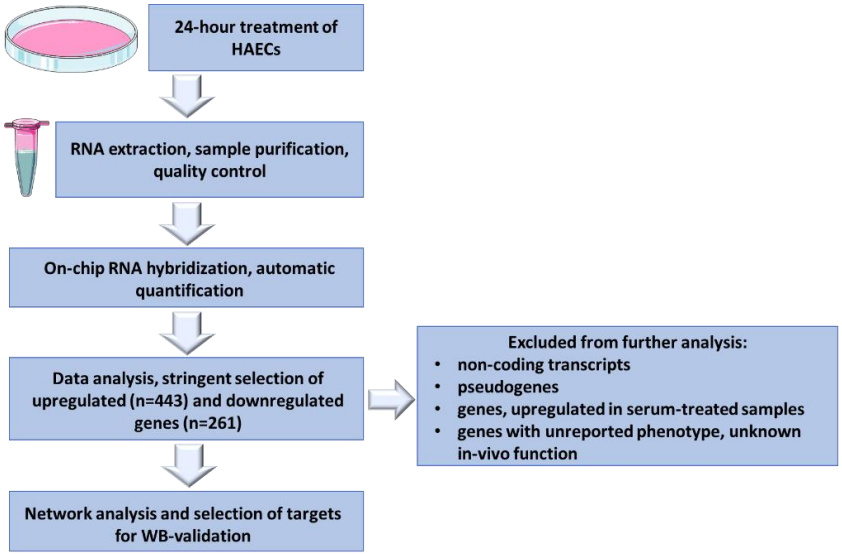

Figure 9: Description of the workflow used to identify upregulated and downregulated genes in HAECs, treated with proteins, isolated from the CytoSorb polymer matrix. Figure produced by author, using Servier Smart Art vector graphics, distributed under CC BY-NC 4.0 license.

3.7.9. Immunoblotting

HAECs were cultivated on 10 cm cell culture dishes (TPP) until confluency, then cells underwent 24 hours treatment with 0.125 µg/ml elution, 0.125 µg/ml serum or FCS-free ECGM2 as described above. Afterwards, cell were washed with PBS and lysed with 100µl of 1×RIPA buffer (Merck Millipore) with addition of 0,5µl of Benzonase (Novagen), 2 µl protease inhibitor cocktail (Sigma-Aldrich), 1 µl of 100 mM PMSF (Applichem), 1 µl of sodium orthovanadate 100 mM (Sigma Aldrich) as a phosphatase inhibitor. Protein concentration in obtained lysates was determined with BCA-kit (Thermo Scientific). Further, lysates were mixed with 5×denaturing sample buffer and cooked at 95°C for 5 minutes. Obtained samples were frozen and stored at -20°C until further use.

Cell lysates were loaded onto 10-well TGX pre-casted 4-20% gel (Bio-Rad), 20 µg of protein per lane, and run at 120 V for 60 minutes. The gel was transferred onto 0.45 µm nitrocellulose membrane in a transfer buffer at 150 mA for 1 hour, using BioRad chamber and BioRad Power-Pack 300. Composition of the buffers for SDS-PAGE, transfer, membrane incubation and blocking are shown in the table 9.

Membranes were blocked for 1 hour at RT, afterwards solution of primary antibody in 5% BSA-TBS-T was added to the membrane, incubation lasted overnight at 4°C on the rocking platform. After the incubation with primary antibody, membrane was washed with TBS-T three times (each wash 5 min.) and incubated with secondary antibodies (Li-Cor Biosciences) for 1 hour at RT on the rocking platform. Antibodies, dilutions and incubation times are described in table 10.

Table 9: Composition of the buffers used for SDS-PAGE and immunoblotting

Buffer	Composition
SDS-PAGE running buffer	23 mM Tris (Sigma Aldrich), 190 mM Glycine (Roth), 0,2% SDS (Roth) in ddH_2O
Transfer buffer	25 mM Tris (Sigma Aldrich), 150 mM Glycine (Roth), 10% methanol (Sigma) in ddH_2O
Blocking buffer (5% BSA in TBS)	5% BSA (Applichem) in TBS (Roth)
Antibody diluent (5% BSA in TBS-T)	5% BSA (Applichem) in TBS (Roth) with 0,1% Tween-20 (PanReac Applichem)
Washing buffer (TBS-T)	TBS (Roth) with 0,1% Tween-20 (PanReac Applichem)

Finally, the membrane was washed with TBS-T three times (each wash 5 min.) and visualized with Odyssey Li-Cor scanner. Images from the scanner were quantified with Odyssey Imaging system. Signal intensities from protein targets were normalized to signal intensities from β-actin. Normalized signal intensity from untreated control was taken for 100%; 2-tailed, paired T-test was used to determine the level of significance for the difference between normalized signal intensities.

Table 10: Antibodies, dilutions and incubation conditions used for immunoblotting

Antibody against (target)	1°Ab /2°Ab	Species	Manufacturer	Dilution	Incubation conditions
β-actin	1°Ab	Rabbit	Cell Signalling Technology	1:1000	1 hour, RT
β-actin (AC-15)	1°Ab	Mouse	Sigma Aldrich	1:1000	Overnight, 4°C
Checkpoint mitotic kinase (BUB1)	1°Ab	Rabbit	Abcam	1:1000	Overnight, 4°C
Goat anti-rabbit green	2°Ab	Goat	Li-Cor	1:20000	1 hour, RT, dark
Goat anti-mouse red	2°Ab	Goat	Li-Cor	1:20000	1 hour, RT, dark
Kinesin superfamily protein 20 (KIF20A)	1°Ab	Rabbit	Abcam	1:1000	Overnight, 4°C
Methylene-tetrahydrofolate reductase 2, mitochondrial (MTHFD2)	1°Ab	Rabbit	Abcam	1:1000	Overnight, 4°C
Plasminogen activator inhibitor 1 (PAI-1)	1°Ab	Mouse	Santa-Cruz (C9)	1:500	Overnight, 4°C
Phosphoserine aminotransferase- 1 (PSAT1)	1°Ab	Rabbit	Abcam	1:1000	Overnight, 4°C
Stanniocalcin-1 (STC1)	1°Ab	Rabbit	Abcam	1:5000	1 hour, RT, dark
Tissue plasminogen activator (tPA)	1°Ab	Rabbit	Boster Immunnoleader	1:1000	Overnight, 4°C

1°Ab – primary antibody; 2°Ab – secondary antibody

3.7.9.1. Experimental inhibition of intracellular protein secretory and transport pathway

To elucidate the reason for discrepancies between mRNA-array data and validation of secreted proteins on the protein level, experiments with inhibition of intracellular protein transport were done. For that Protein Transport Inhibitor (PTIC, Thermo Scientific) was used. PTIC is a mix of two compounds – Brefeldin A (5.3 mM) and Monensin (1 mM). Addition of this mixture to the cells leads to inhibition of intracellular transport and secretion of the proteins with subsequent accumulation of the synthesized proteins in the lumen of ER and Golgi apparatus (Fig. 10 B).

Table 11: Concentrations of Brefeldin A and Monensin in commercially available PTIC used for blockage of intracellular protein transport

PTIC concentration	Brefeldin A	Monensin
0.1x	1 µM	0.2 µM
0.05x	0.5 µM	0.1 µM
0.025x	0.25 µM	0.05 µM

HAECs were cultivated in 10% FCS medium on a 6-well plate, at confluence the cells were treated first with eluted proteins and 10 hours later PTIC was added (Fig. 10 A). Several concentrations of PTIC (0.1×, 0.05×, 0.025×) were employed to adjust the experimental conditions ensuring maximal cell viability. Molar concentrations of Brefeldin A and Monensin used for the treatment are shown in the table 11. After 24 hours incubation, cells were harvested and lysed as described above. Protein concentrations in obtained cell lysates were determined with BCA-kit (Thermo Scientific). Lysates were mixed with denaturing sample buffer and cooked at 95°C for 5 minutes. Cell lysates were further used for immunoblotting as described above.

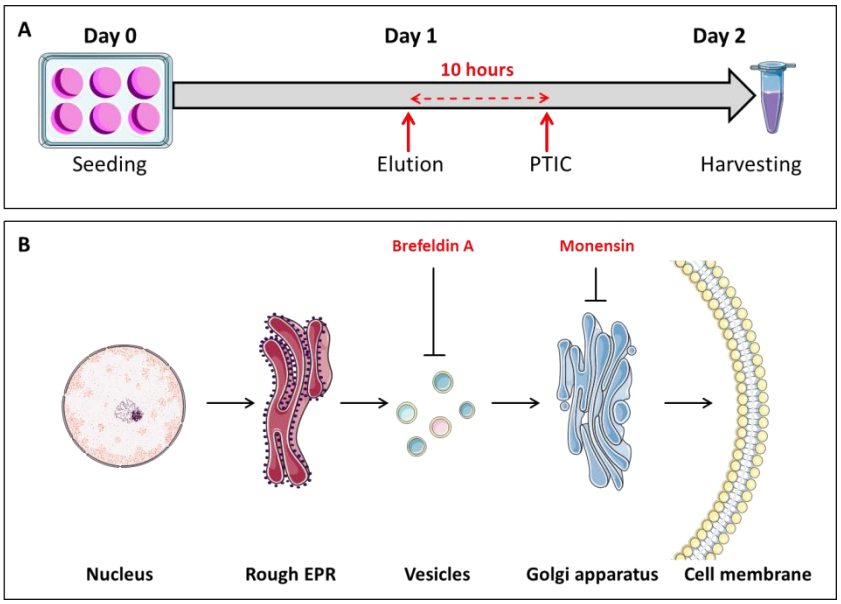

Figure 10: Schema of the experiment with intracellular protein transport blocker (A). Schematic representation of intracellular protein transport blockage (B). Brefeldin A and Monensin are lactone antibiotics of fungal origin disrupting protein trafficking from EPR to Golgi, causing accumulation of normally secreted proteins in the cytoplasmic organelles of the cell. Figures produced by author, using Servier Smart Art vector graphics, distributed under CC BY-NC 4.0 license.

3.7.10. Immunocytochemistry (ICC)

For immunocytochemical staining, the cells were seeded on round glass (⌀ 12 mm) cover slips (Marienfeld GmbH) in Primaria 24-well plate (Becton Dickinson Labware) and cultivated with 10% FCS ECGM2 *vide supra*.

After 24-hour treatment with stimulants and controls, culture medium was aspirated; cells were washed with PBS, fixed with formaldehyde for 15 min. at RT. Afterwards cells were permeabilized for 15 minutes at RT with subsequent blocking of unspecific binding for 1 hour at 37°C. After blocking cells were incubated with primary antibody solution overnight at 4°C. Secondary antibody solution was added to cells and incubation at RT for 1 hour took place. Incubation with secondary antibodies was followed by short DAPI-staining and thorough washing with PBS. After final wash, cover slips were removed from the multiwell plate, dehydrated, dried out and mounted with ProLong mounting medium (Thermo Scientific) on the 76 × 26 × 1 mm microscope slide (Süsse Labortechnik). Composition of buffers for cell fixation, permeabilization, blocking, and antibody dilution are listed in table 12. Concentrations of primary and secondary antibodies used for ICC are shown in table 13.

Table 12: Solutions used for cell fixation, permeabilization, blocking and dehydration

Buffer	Composition
Fixation buffer	3.7% formaldehyde (Merck Millipore) in 1×PBS (Gibco)
Washing buffer	1×PBS (Gibco)
Permebilizing buffer	0.5% Triton-X100 (Sigma-Aldrich) v/v in 1×PBS (Gibco)
Blocking buffer	1% BSA (Applichem), 0.3M Glycine (Roth) in PBS-T (0.1% Tween-20, Applichem)
Dehydrating solution	96% Ethanol (Roth)

Table 13: Antibodies, fluorescent dyes, dilutions and incubation conditions used for ICC

Antibody	1°Ab /2°Ab	Species	Manufacturer	Dilution	Incubation conditions
Alexa Fluor 488 anti-mouse	2°Ab	Donkey	Dianova	1:500	1 hour, RT, dark
Activating transcription factor 4 (ATF4)	1°Ab	Rabbit	Abcam	1:1000	Overnight, 4°C
Cy3 anti-rabbit	2°Ab	Donkey	Jackson Laboratories	1:500	1 hour, RT, dark
Cy3 anti-mouse	2°Ab	Donkey	Jackson Laboratories	1:500	1 hour, RT, dark
Cytochrome oxidase IV, mitochondrial (COXIV)	1°Ab	Mouse	Abcam	1:1000	Overnight, 4°C
DAPI	-	-	Applichem	300 nM	5 min., RT, dark
Histone H3	1°Ab	Mouse	Cell Signalling Technology	1:500	Overnight, 4°C
Methylene-tetrahydrofolate reductase 2, mitochondrial (MTHFD2)	1°Ab	Rabbit	Abcam	1:200	Overnight, 4°C
Plasminogen activator inhibitor 1 (PAI-1)	1°Ab	Mouse	Boster Immunnoleader	10 µg/ml	Overnight, 4°C
Phalloidin 488 Alexa Fluor	-	-	Thermo Scientific	1:40	1 hour, RT, dark
Von Willebrand factor (vWF)	1°Ab	Rabbit	Abcam	1:400	Overnight, 4°C

1°Ab – primary antibody; 2°Ab – secondary antibody

Fluorescent microscopy was performed with Zeiss fluorescent microscope using AxioCam software. Images were quantified with ImageJ software, applying corrected total fluorescence (CTCF) formula as described elsewhere (Gavet & Pines, 2010; Potapova et al., 2011):

$$CTCF = Integrated\ Density - (Area\ of\ selected\ cell \times Mean\ fluorescence\ of\ background\ readings)$$

4. Results

4.1. Identification of the broad spectrum of blood proteins, adsorbed by the filter during intraoperative hemofiltration

4.1.1. Preliminary characterization of the protein fractions on the gel

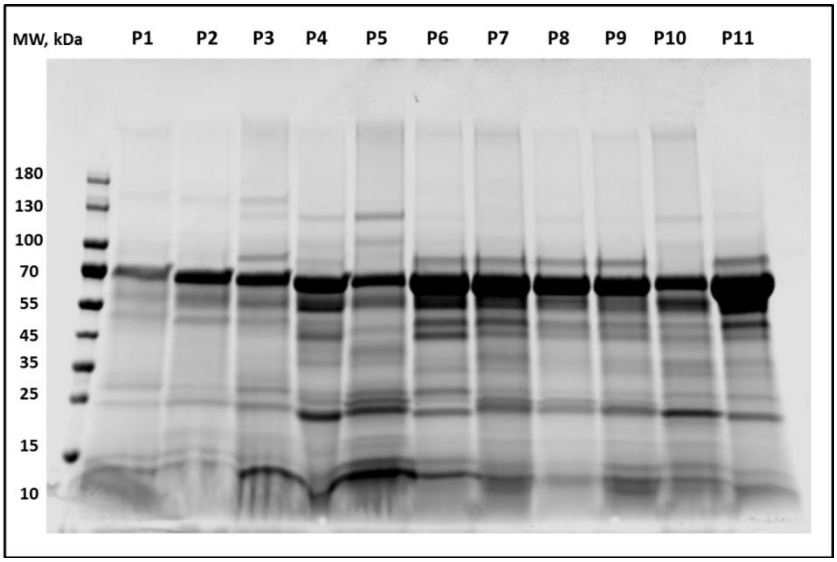

Figure 11: SDS-PAGE analysis of the eluted material, derived from filters used for intraoperative hemofiltration. P1-P6 represent patient samples derived from the filters used for IE surgery, P7-P11 – samples eluted from the filters used during elective valve surgery. Each lane contains 20 µg of protein, gel stained with CCB and visualized with Li-Cor Odyssey scanner at 700 nm wavelength.

Protein concentration in the eluted samples ranged between 1.78 and 6.52 µg/µl, on average 3.93 µg/µl. When characterized by SDS-PAGE, samples were rich in different proteins with a dominant band in the MW range of about 70 kDa. Each sample has an individual protein pattern with variable bands in the 25-35 kDa MW range and between 100 and 130 kDa (see Fig. 11).

4.1.2. LC-MS/MS identification of the proteins isolated from the filter matrix

As a result of triplicate LC-MS/MS measurements, 1602 proteins were identified in the material eluted from the CytoSorb filter matrix. From 1602 identified proteins, 29 proteins were identified as contaminant. Major contaminants stemmed from sample preparation and LC-MS/MS quality control (trypsin, used for protein digestion and BSA, serving as an internal standard for LC-MS/MS). Other major group of contaminants was comprised of keratins, common dust and laboratory contaminants, originating in the sample during different stages

of sample preparation. In general, the level of contamination was considered acceptable and did not majorly flaw LFQ of eluted proteins. Contaminant proteins excluded from further analysis are listed in suppl. table 3.

4.1.3. Comparison of the proteins, isolated from the matrix in the different subgroups of the patients

The quantity of proteins, identified via LC/MS-MS with 2 or more peptides was higher among patients undergoing elective valve surgery (n=166), see Fig. 12. Exclusive proteins, identified only in one of the subgroups are listed in the suppl. tables 4 and 5. The overlap between both subgroups was further analyzed in more detail, including protein properties and functional annotation (n=127). Full list of the 127 proteins identified in all elution samples with their molecular weight and GO-annotation can be found in suppl. table 6.

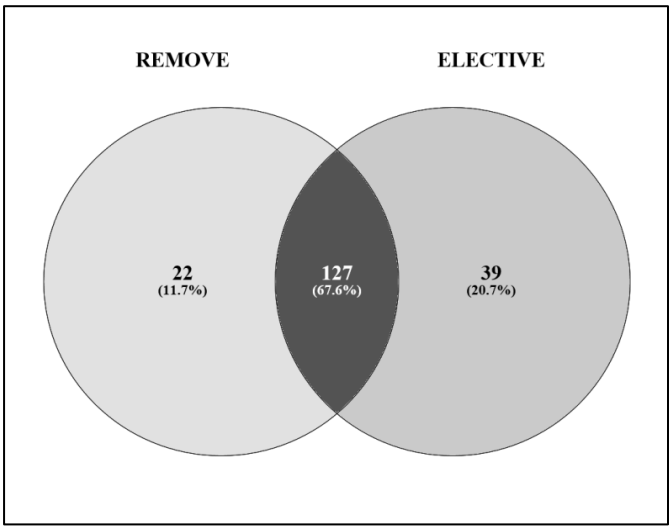

Figure 12: Venn diagram, demonstrating an overlap between proteins isolated from the filters used for the surgery in patients with infective endocarditis (REMOVE study) and patients undergoing elective valve surgery. Image generated with Venny 2.1.0 tool (Oliveros, 2015).

4.1.4. Properties of the isolated proteins

The majority of the isolated proteins were, as expected, in the molecular weight range below 60 kDa, however considerable number of proteins had high molecular weight, particularly 15 (12%) of 127 identified proteins had MW above 100 kDa (Fig. 13).

Predominant amount of isolated proteins were hydrophilic, with only small number of proteins (15; 11.8%) exhibiting hydrophobic properties (Fig. 14). Hydrophobic proteins identified in all 11 CytoSorb filters are listed in suppl. table 7. Hydrophobicity of these proteins is defined by their subcellular localization and specific functions that they exert. Among hydrophobic proteins, surface receptors and membrane proteins were dominant subgroups.

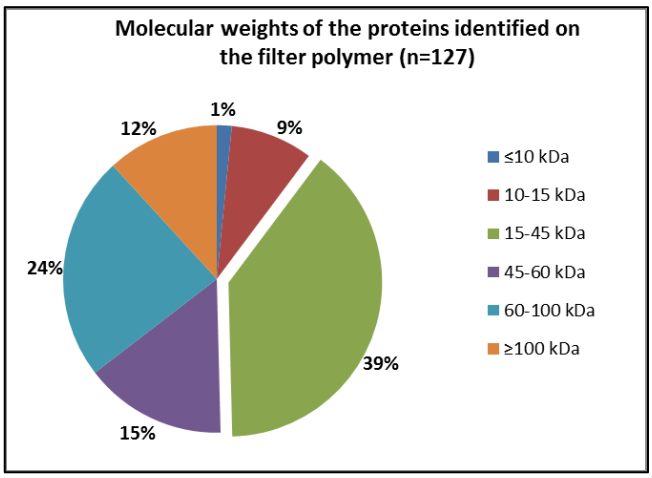

Figure 13: Molecular weight distribution of the proteins identified in all 11 elution samples. Proteins in the size range between 15 and 45 kDa were the most abundant group of identified proteins. The majority of the isolated proteins (83; 65.4%) had MW below 60 kDa.

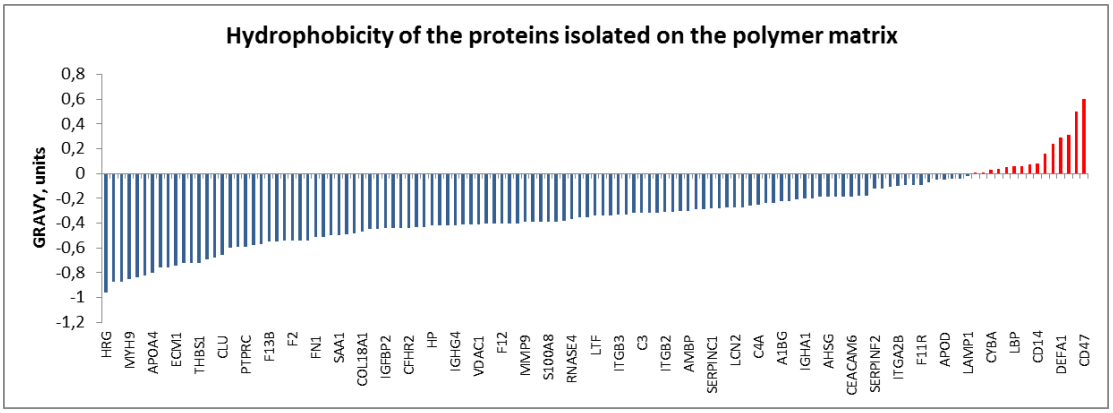

Figure 14: Hydrophobicity of the proteins (n=127) isolated from the polymer matrix of all 11 filters used for intraoperative HF. The majority of isolated proteins have GRAVY-values below 0, corresponding to hydrophilic properties at pH 7.4.

The GO-annotation of the isolated proteins revealed the diversity of protein classes. Unsurprisingly, the majority of isolated proteins belonged to classic residential plasma proteins, namely enzyme inhibitors, hydrolases and transport proteins (Fig. 15, A). Subcellular localization of the characterized proteins was also consistent with secreted plasma proteins with substantial fractions of intracellular proteins (12.5%) and cell membrane proteins (10.9%) (Fig. 15, B). Predominant number of proteins was implicated in blood coagulation pathway (12.5%), integrin signaling (9.4%), plasminogen activating cascade and inflammation mediated by cytokines and chemokines (4.7% and 4.7%, correspondingly) (Fig. 15, C). Molecular function annotation (Fig. 15, D) shows the majority of proteins identified as having binding function (33.6%) and catalytic activity (25.8%), other abundant molecular functions include regulators of molecular function (11.7%), molecular transducer activity (3.9%) and structural molecule activity (3.9%). Annotation of biological processes by PANTHER classification system identified almost half of the proteins as involved into cellular process (46.1%) followed by response to stimulus (22.7%), localization (21.9%), biological regulation (15.6%), metabolic process (14.8%), and immune system process (10,2%).

4.1.5. Identification of AGE-modified proteins in the elutions

Out of 1602 identified proteins, 24 proteins with AGE-modifications were identified in the elutions (suppl. table 8). Out of 24 glycated proteins, 21 were among those 127, identified in all 11 patient samples. None of the modifications was identified in all 11 samples. Albumin was the most modified protein among all AGE-modified proteins identified, having 21 modifications on lysine (CML and CEL together), and 8 modifications on arginine (MG-H1 and Arg-Pyr) (suppl. table 8). CML was the most abundant modification among all identified, followed by CEL. AGE-modifications on arginine were identified only on albumin (MG-H1: R105, R141, R361, R372, R434, R452, R509, Arg-Pyr: R34), neutrophil defensin 1 (MG-H1: R88), and paired amphipatic helix protein (Arg-Pyr: R932, R935).

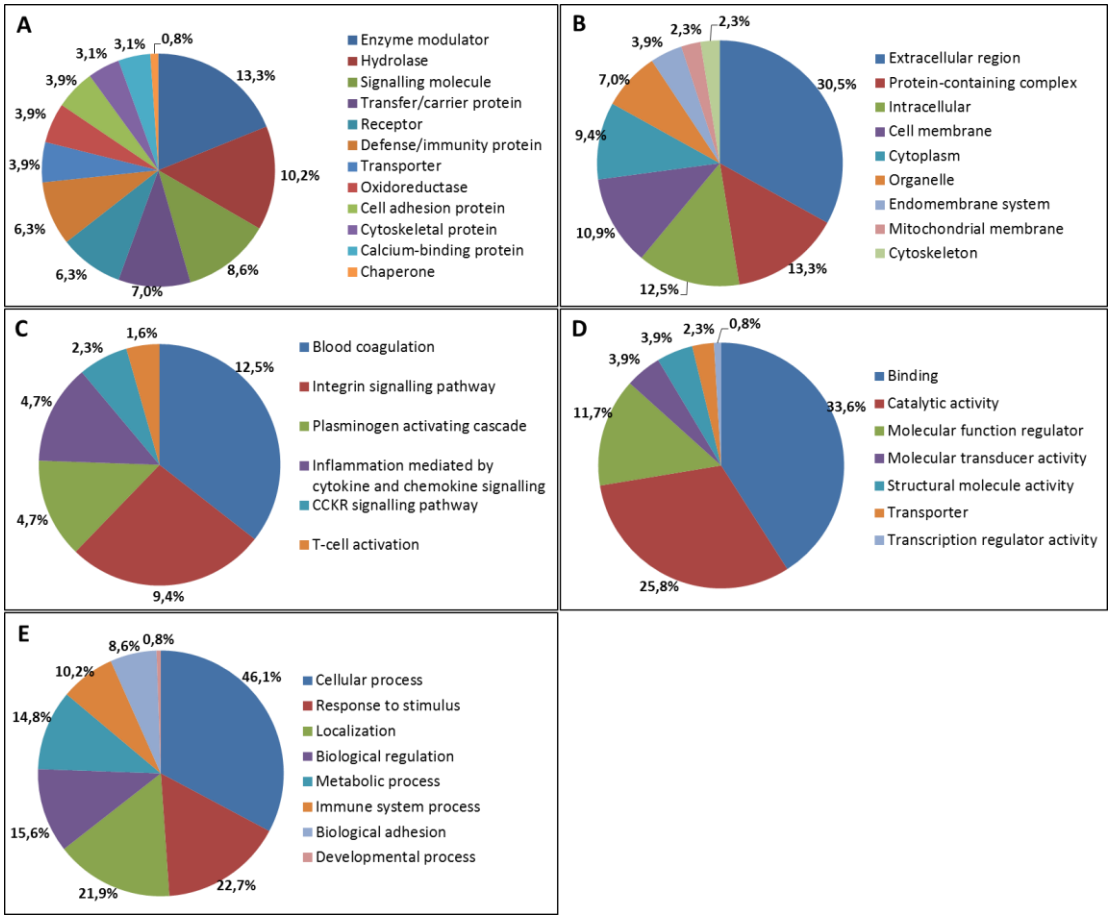

Figure 15: GO-annotation of the proteins isolated from CytoSorb polymer matrix (PANTHER classification system). Pie charts show predominant protein classes (A), annotation to cellular compartment (B), pathway (C), molecular function (D) and biological process (E).

4.1.6. Correlation between protein properties and abundance in the sample eluted from the matrix

A weak negative correlation was observed between isoelectric point of the protein ($p=0.02$), hydrophobicity ($p=0.002$) and relative abundance of the protein in the elution sample (Fig. 16 C, E). MW and charge of protein had correlation coefficient close to 0, suggesting absence of correlation (Fig. 16 A, D). Among all the properties, annotated to the identified proteins with available bioinformatic tools, protein length seemed to having weak yet significant correlation with protein abundance in the elution sample with $r=0.38$; $p<0.0001$ (Fig. 16, B).

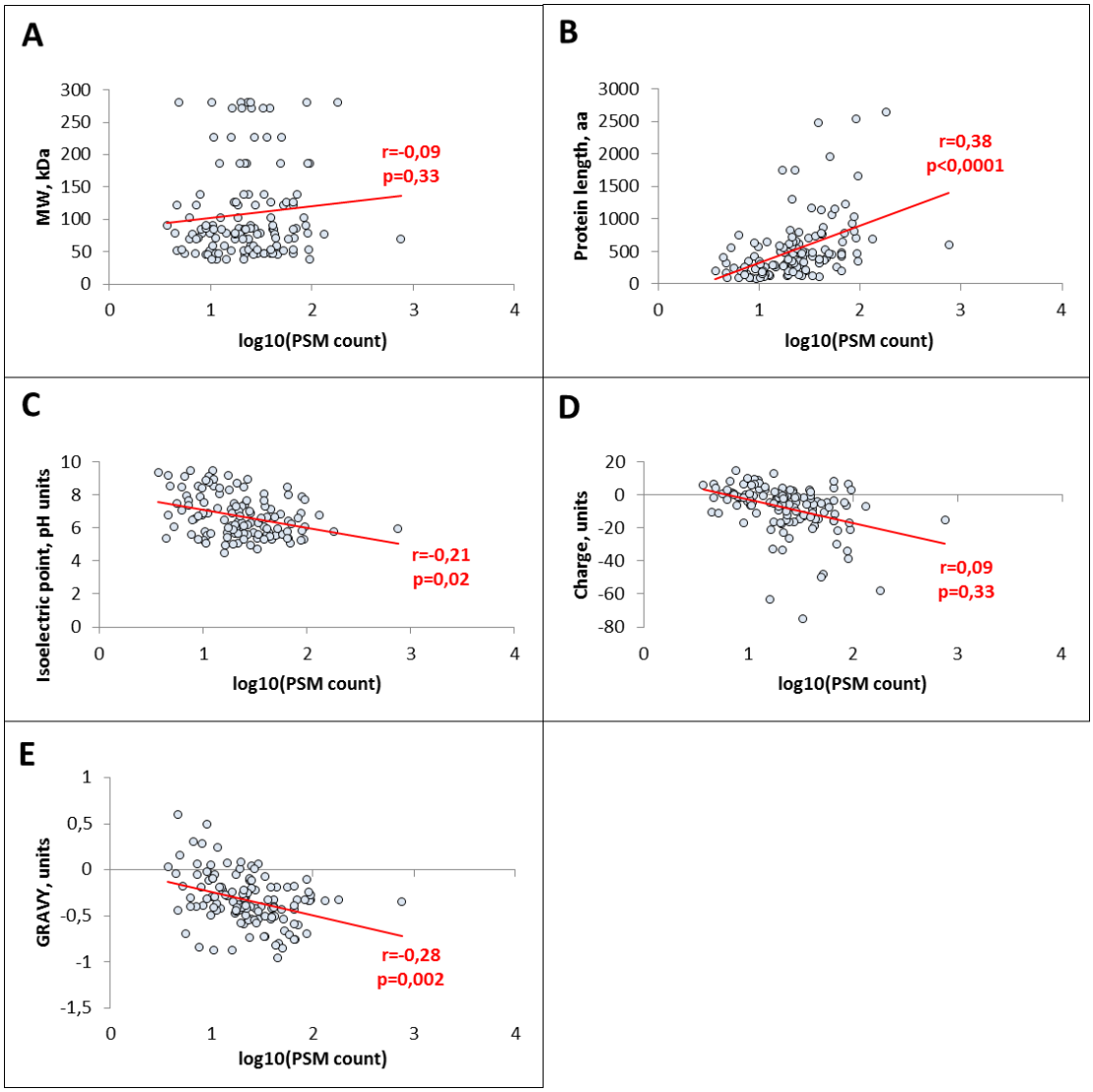

Figure 17: Correlation between protein abundance in the elution and protein properties: molecular weight (A), protein length (B), isoelectric point of the protein (C), protein charge (D) and hydrophobicity (E).

Abbreviations: aa – amino acids, GRAVY – grand average hydrophobicity, MW – molecular weight, r – coefficient of correlation.

4.1.7. ELISA-measurements of CRP in elution samples

Among less abundant proteins with known *in vitro* binding, only PAI-1, resistin, C3a and S100-A8 were identified in the eluted samples by our LC-MS/MS approach (data not shown). Since this method of protein identification did not allow detection or quantification of less abundant proteins due to general sensitivity problem and stochastic nature of acquisition (see section 5.1.), eluted material was also analyzed with more sensitive methods for cytokines and pro-inflammatory factors with small abundance (concentration ranges µg/ml – pg/ml). CRP was not identified by LC-MS/MS. ELISA-measurements demonstrated presence of detectable levels of CRP in all 11 elution samples. Levels of CRP were ranging from 0.16 to 0.53 µg/ml with mean value for all elution samples of 0.28 µg/ml. Even though CRP concentrations tended to be higher in material eluted from filters used within REMOVE-study, there was no significant difference between CRP levels in elutions obtained in different patient subgroups (Fig. 17).

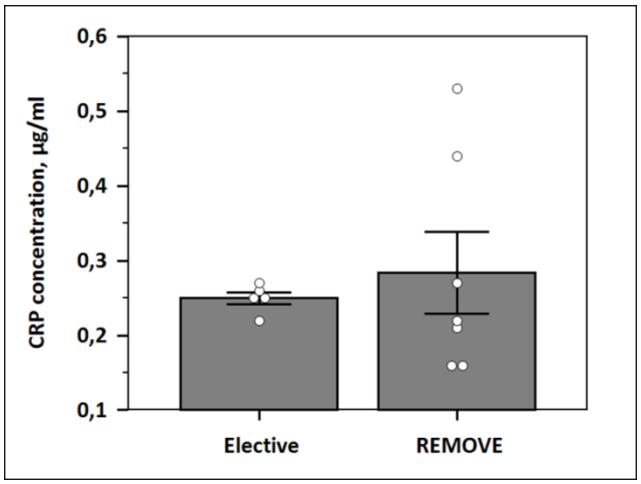

Figure 17: CRP concentrations in the elution samples obtained from CytoSorb cartridges used for intraoperative HF. No significant differences were observed between CRP concentrations within two patient groups. Data presented as mean ± SEM, each data point is shown as an individual dot, Mann-Whitney test was used to compare values from different patient groups.

4.1.8. Cytokine concentrations in the elution

Among the 6 cytokines available for measurement with Human Inflammatory Cytokines kit (BD Biosciences) TNF-α and IL-12p70 were not detected in any of the samples. Detectable amounts of IL-8 were observed in all samples eluted from the polymer matrix. IL-6 was the second most abundant cytokine isolated from the filter polymer.

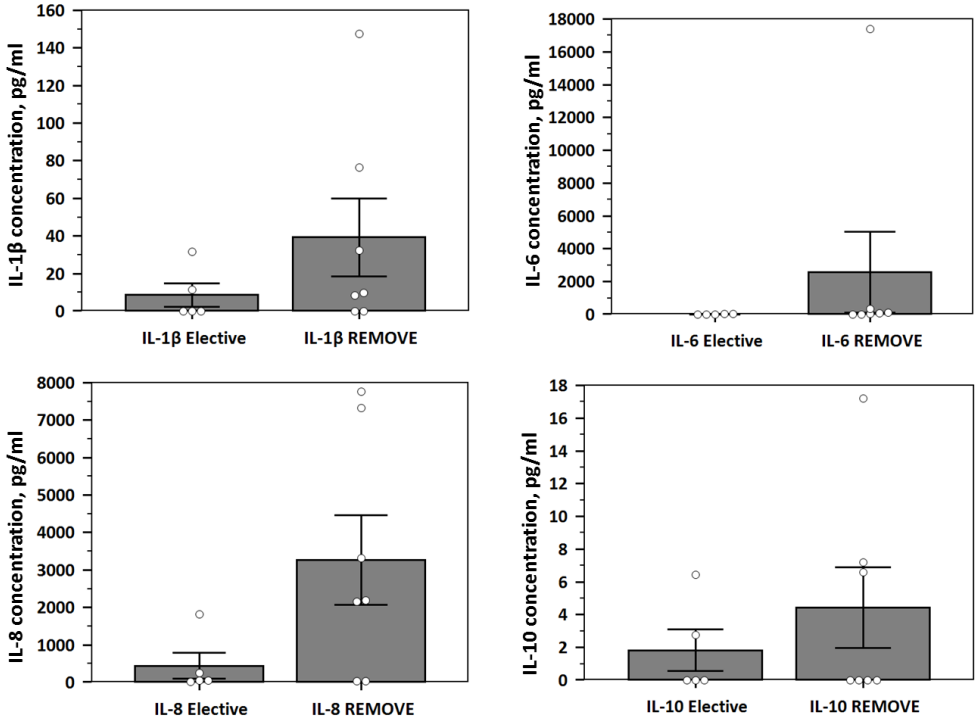

Figure 18: Comparison of cytokine concentrations in the material eluted from CytoSorb polymer matrix in patient subgroups. Data are presented as mean ± SEM, each individual data point is shown as a dot. Due to high inter-individual variability and relatively small sizes of the compared groups there was no significant difference between cytokine levels in the REMOVE-study participants and patients undergoing elective surgery. Mann-Whitney test was used to determine significance of the differences between the two independent groups.

Upon comparison of patient subgroups, patients undergoing elective surgery demonstrated, as expected, lower concentrations of cytokines in the eluted material (Fig. 18). These

differences were insignificant due to small number of observations and high inter-individual variability.

4.2. Changes in plasma samples of the patients, undergoing hemofiltration during cardiac surgery with cardiopulmonary bypass

4.2.1. Changes in plasma protein concentration

All plasma samples obtained from the patients undergoing heart surgery with CPB and concomitant hemofiltration have demonstrated marked reduction of total protein content. Average reduction of total protein concentration was about 38% (Fig. 19).

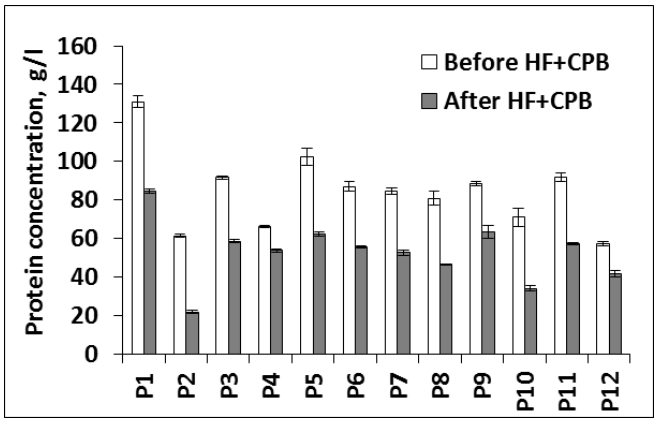

Figure 19: Changes in plasma protein concentrations after heart surgery with CPB and hemofiltration. Protein concentrations were measured with BCA-kit (Thermo Scientific), results are shown as mean ± SEM of 3 measurements.

Since multiple factors are potentially contributing to changes in plasma protein concentration in patients undergoing this type of surgery (including hemodilution, bleeding, adsorption of plasma proteins to CPB tubing, transfusion of FFP and other blood compounds), an *in vitro* experiment was performed to determine the role of HF in protein loss. *In vitro* filtration of plasma from healthy donor for 120 min. did not demonstrate any significant difference between protein concentration reduction in samples filtered through 1.5 ml experimental column (average protein concentration reduction was 5.1%, see Fig. 20) and through the empty column, that does not contain adsorbing matrix (average reduction represented 3.8%). This experiment suggests that reduction in protein concentration in intraoperative settings are mainly explained by hemodilution, bleeding and not by significant loss due to adsorption to the polymer matrix.

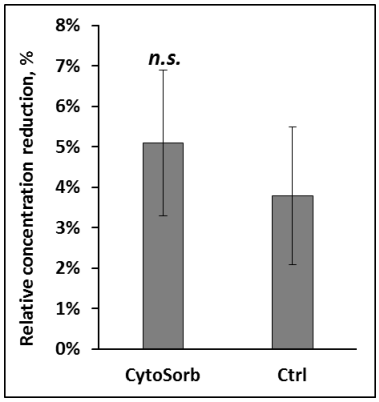

Figure 20: Relative reduction of the plasma protein concentrations after filtration *in vitro* (n=3). A 1.5ml experimental column, filled with CytoSorb beads was used for filtration of heparinized plasma from a healthy donor for 120 min.; empty Rezorian tube (Sigma-Aldrich) with O-rings and 200 µm filter mesh, not filled with PSDVB-beads was used as a control. Data presented as mean ± SEM, n.s. – no significant difference.

4.2.2. Removal of AGE-modified proteins from plasma via *in vitro* filtration

Experimental approach involving 2 hours of *in vitro* filtration through both 1.5 ml experimental CytoSorb column (shown as CytoSorb in Fig. 21 A, B) and an empty control column, consisting of empty Rezorian tube shell (Sigma-Aldrich) with O-rings and 200 µm

filter mesh (indicated as Ctrl in Fig. 21 A, B) did not demonstrate any reduction of CML and CEL in the sample of plasma from healthy donor, supplemented with 5% of AGE-modified plasma. Furthermore, relative amounts of CML and CEL, identified via LC-MS/MS and normalized towards total leucine content of the sample, were insignificantly increased in samples after *in vitro* filtration (Fig. 21 A, B).

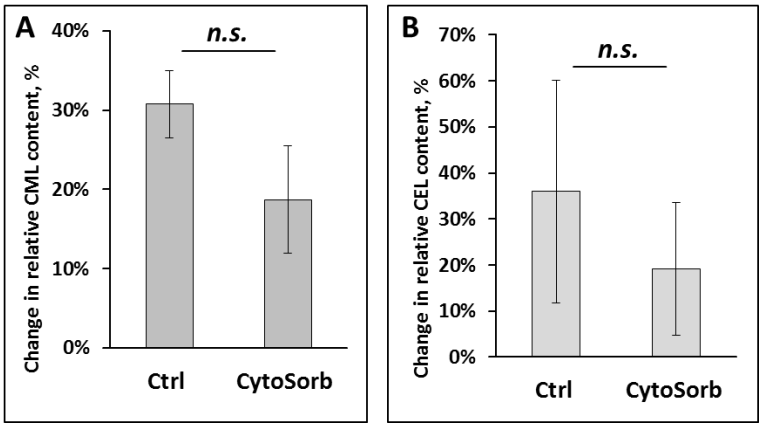

Figure 21: Relative changes in CML and CEL content after *in vitro* plasma filtration. Relative amounts of CML and CEL were determined via LC-MS/MS and normalized to total leucine content of the sample (n=3). Relative increase in CML- (A) and CEL content (B) was not significantly different comparing samples after CytoSorb 1.5 ml experimental column and empty control column (n.s. – no significant differences).

4.2.3. Characterization of plasma samples before and after intraoperative hemofiltration with mass-spectrometry

Plasma samples obtained before and after the surgery from patients with infective endocarditis (REMOVE-study participants) were analyzed with LC-MS/MS using data-dependent acquisition; this method allows comparing the samples before and after procedure, identifying protein groups that were affected as a result of intervention. As shown in the correlation matrix (Fig. 22), samples obtained from the same patients before and after the surgery did not differ dramatically. Major differences were observed between the individuals. Exceptional high similarity pattern was observed for REMOVE-study samples obtained from patient 1 (P1), patient 5 (P5) and sample from the patient 3 collected after the surgery (P3 after) (delineated in red, Fig. 22 A). Possible explanation of these similarities might be the supplementation with different blood products in the REMOVE-study participants (described in Table 14). Patients 1, 3 and 5 received transfusion of erythrocyte concentrate (EC), as well as platelets (TC) and fibrinogen supplementation.

Label-free quantification of the samples before and after intraoperative HF was performed by Dr. Alessandro Ori (Leibniz Institute on Aging – Fritz Lipmann Institute (FLI), Jena; cooperation withing RTG 2155 “Protein Modifications in Aging). Significant changes in the relative amount of several protein groups were revealed (Suppl. fig. 2). These changes were reproducible in both subgroups of the patients, undergoing valve surgery with CPB. Hemoglobin (HBB), carbonic anhydrase 1 (CA1), catalase (CAT), cystatin-A (CSTA), peroxiredoxin-6 (PRDX6), thioredoxin (TXN) were proteins, significantly up-regulated in both patient subgroups (Suppl. fig. 2 A, B, Suppl. tables 9 and 10). Myoglobin (MB), peroxiredoxin-2 (PRDX2), lactotransferrin (LTF), peroxiredoxin-1 (PRDX1), nucleobindin-1 (NUCB1), biliverdin reductase B (BLVRB), neutrophil gelatinase-associated lipocalin (LCN2) and flavin reductase (ALDOA) were significantly up-regulated and exclusive for the samples stemming from the REMOVE-study participants (Suppl. fig. 2 A). Hemoglobins (HBD, HBG1, HBG2),

glyceraldehyde-3-phosphate dehydrogenase (GAPDH), protein-S100A7, matrix metalloproteinase 9 (MMP9), moesin (MSN), elongation factors (EEF1A1; EEF1A2) were exclusively up-regulated in plasma samples of the patients undergoing elective valve surgery (Suppl. fig. 2 B). Down-regulated proteins are described in detail in the section 4.2.4.

Table 14: Intraoperative transfusion of blood compounds in the study population

Patient	EC, units	TC, units	FFP, units	PPSB, I.U.	Cofact, I.U.	Fibrinogen, g
1	8	2	4	-	-	4
2	4	-	-	-	-	-
3	6	1	4	3600	-	4
4	-	-	-	-	-	-
5	4	1	-	1200	-	2
6	6	-	-	-	4500	-
7	2	-	-	-	-	-
8	2	2	-	-	-	-
9	2	-	-	-	-	-
10	2	-	-	-	-	-
11	2	-	-	-	-	-
12	2	-	7	-	-	-

Abbreviations: Cofact, PPSB – concentrates of coagulation factors II, VII, IX, X; EC – erythrocyte concentrate; FFP – fresh frozen plasma; TC – thrombocyte concentrate.

Proteins affected the most were specific for certain tissues and cell types. Myoglobin (MB) was one of the most up-regulated proteins in plasma samples of the REMOVE-study participants. It is a typical cytoplasmic protein of striated muscles and is widely used in clinical settings as a biomarker of muscle tissue damage known as rhabdomyolysis. Red blood cell-specific proteins (hemoglobins, catalase, carbonic anhydrases 1 and 2, peroxiredoxins, thioredoxine, glyceraldehyde-3-phosphate dehydrogenase, biliverdin reductase B) were up-regulated in post-intervention plasma samples of both patient subgroups. Majority of other identified proteins were either highly enriched in immune cells or were difficult to attribute to certain type of tissues due to universal expression in multiple types of tissues.

These results were in line with our pre-analytical observations: some plasma samples presented visual signs of hemolysis (Fig. 23 A). These changes also caused significant problems with ELISA-measurement. Sulfuric acid as a reagent in the stop-solution, producing intense green coloring and false-positive results in one of the assays (Fig. 23 B). Conspicuously alteration in colorimetric reaction was obtained in the samples from patients after the operation (Fig. 23 B, plate area delineated in red).

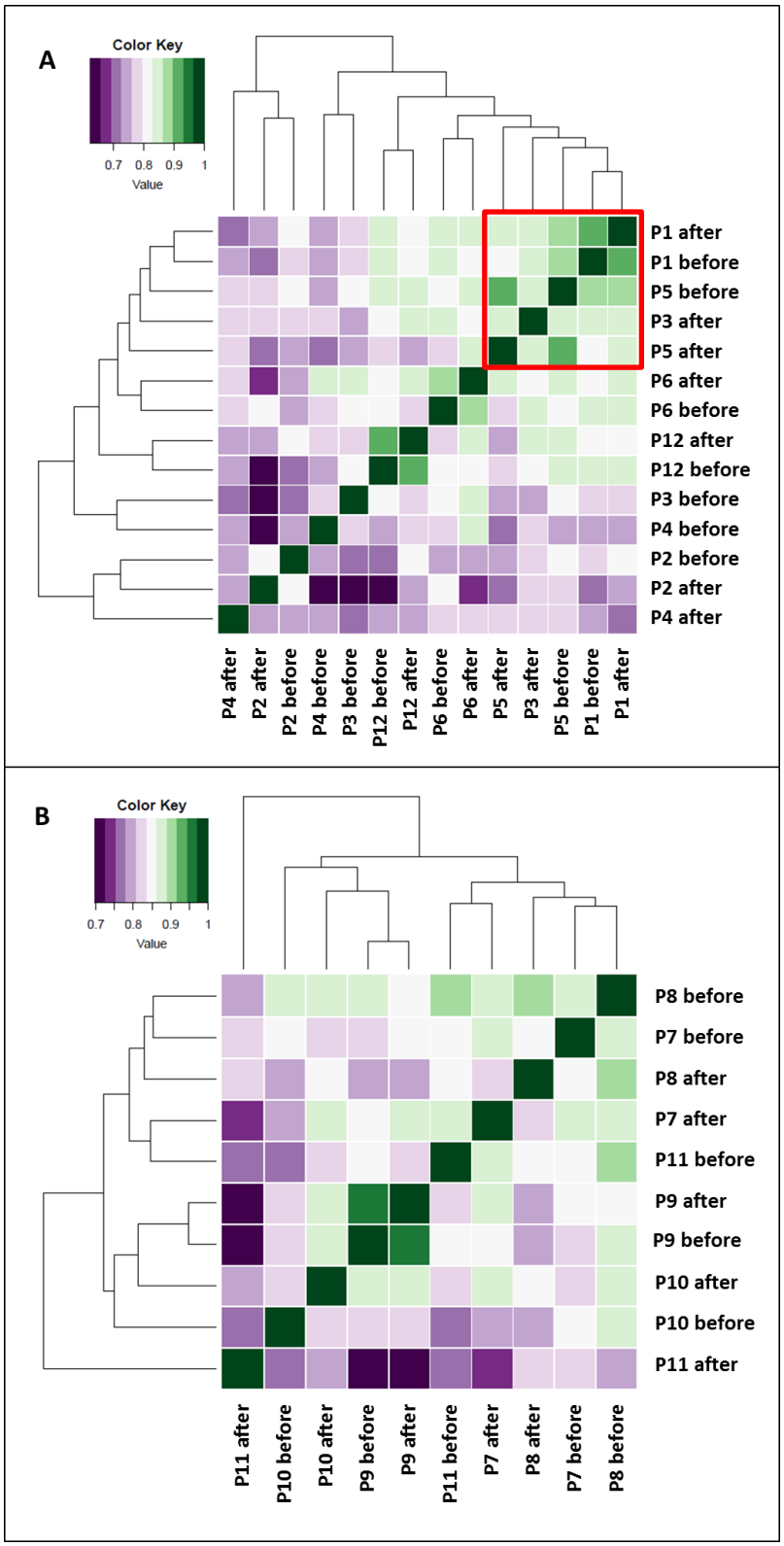

Figure 22: Correlation matrices demonstrating similarities between the samples before and after the intraoperative HF. Inter-individual differences seem to be more significant than differences between the samples before and after the intervention, this pattern was similar for the samples obtained from the REMOVE-study participants (A) and patients, undergoing elective surgery (B). Samples with high similarity pattern are delineated in red.

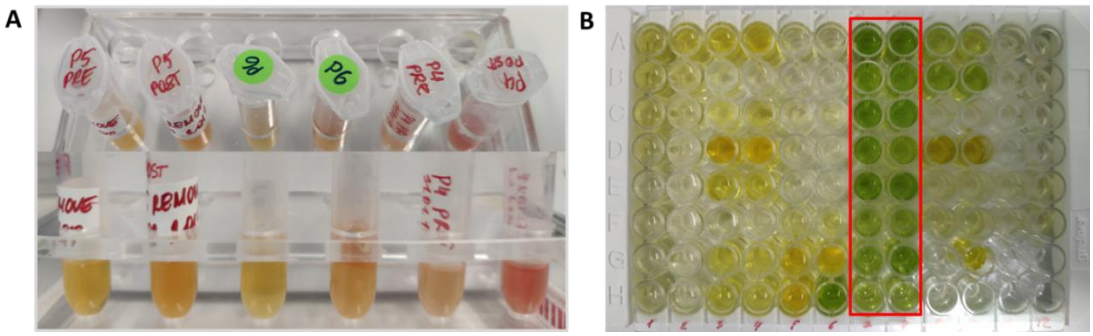

Figure 23: Hemolysis in plasma samples of REMOVE-study participants obtained after the surgery. A. Considerable amount of samples derived from the patients after the surgery presented with the change of the color attributed to RBC damage and release of free hemoglobin into biological sample. B. Hindered colorimetric reaction in IL-6 ELISA (IBL). All samples, derived from the patients after the surgery had altered color and produced falsely high signal (highlighted in red).

4.2.4. Overlap between the proteins identified on the filters (elutions) and the proteins down-regulated in the plasma samples after hemofiltration

To elucidate potential influence of intraoperative hemofiltration on the composition of plasma, an overlap between down-regulated proteins in plasma samples after CPB and the proteins, isolated on the polymer matrix was carefully studied. In the central part of Venn diagram (Fig. 24), an overlap between all four datasets can be seen, comprised of 22 proteins, described in detail in Suppl. table 11.

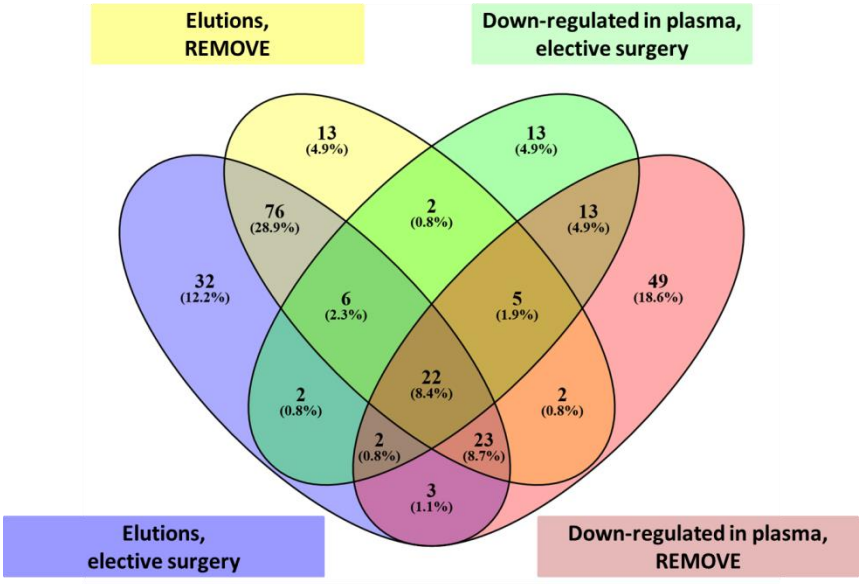

Figure 24: Overlap between proteins, eluted from the filters and proteins down-regulated in plasma samples after CPB with HF. Image generated with Venny 2.1.0 tool (Oliveros, 2015).

This overlap subgroup mainly consisted of carrier proteins (apoliportoteins A-IV, CI, CIII, D, serotransferrin, retinol binding protein 4), enzyme inhibitors (inter-alpha-trypsin inhibitor heavy chain H4, alpha-1-antitrypsin, histidine-rich glycoprotein, cystatin-C, alpha-2-antiplasmin), coagulation factors and anticoagulants (fibrinogen alpha, kininogen-1, alpha-2-antiplasmin, beta-2-glycoprotein, plasminogen). The chemoattractant and acute phase response protein serum amyloid A-2 protein was accompanied by two other acute phase reactants - inter-alpha-trypsin inhibitor heavy chain H4 and alpha-1-acid glycoprotein 2.

Proteins down-regulated in plasma samples of REMOVE-study patients, obtained after the intraoperative HF, had several peculiarities (Suppl. table 12). 17 out of 49 proteins, affected exclusively in REMOVE-study subgroup were annotated as immunoglobulins. Another group of proteins (n=5), down-regulated in plasma samples after the intraoperative HF were implicated in complement activation (complement component C8A, ficolin-2, C1q complement subcomponent, plectin and C1r complement subcomponent-like protein). Several proteins (n=4), mediating immune response to bacterial infection were also identified as down-regulated exclusively in the samples from patients with IE (attractin, S100A12-protein, leucine-rich α-2-glycoprotein, nucleolin).

4.2.5. Changes in plasma concentrations of pro-inflammatory cytokines

Proteins that are less abundant in plasma and cannot be identified and quantified with mass-spectrometry had to be measured separately with commercially available ELISA-methods or with cytometric bead array (CBA). CBA was chosen for the measurements of cytokines in plasma samples as it allowed overcoming false-positive signals inflicted by high content of free hemoglobin and other plasma proteins, often obscuring colorimetric reaction (as described above, see Fig. 23 B).

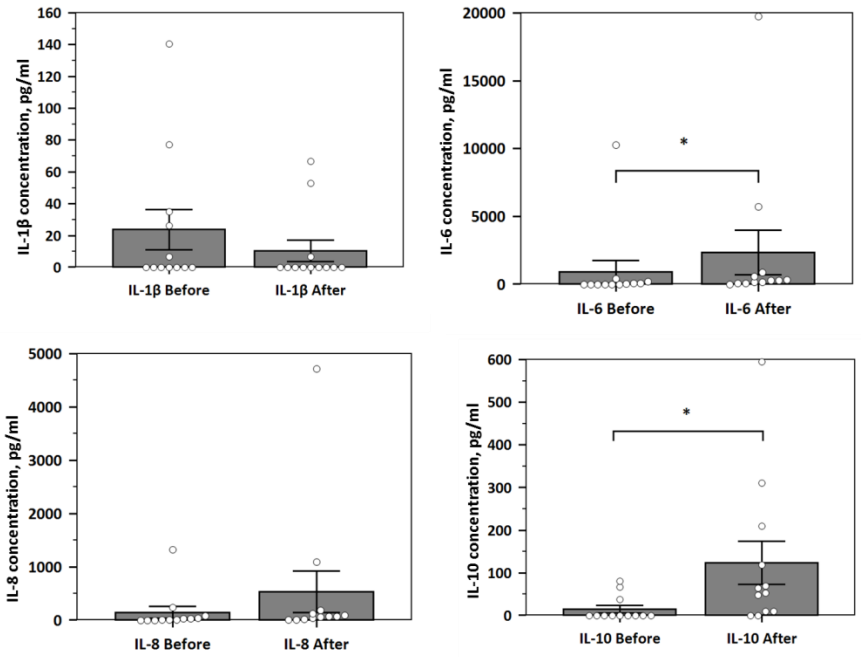

Figure 25: Plasma cytokine levels in the samples before and after cardiopulmonary bypass with HF (n=3). Data presented as mean ± SEM, each individual data point is shown as a dot, * $p \leq 0.05$, Wilcoxon rank test was used to compare variables before and after HF. Levels of IL-6, IL-8, and IL-10 were increased in all samples obtained after CPB, whilst concentration of IL-1β was reduced.

After the CPB, cytokine concentrations were increased in plasma samples of all patients. Particularly, levels of IL-6 and IL-10 were increased significantly after the CPB when compared to samples obtained directly after the initiation of the operation. There was no significant difference between plasma levels of IL-1β and IL-8 before and after CPB (Fig. 25). Comparison between the increase of plasma cytokine level (Δ) in the samples obtained from the REMOVE-study participants and patients undergoing elective heart surgery did not show significant differences between the patient groups. Only increase in IL-6 concentration

among REMOVE-study participants was higher (p=0.07) than among patients undergoing elective surgery (Fig. 26).

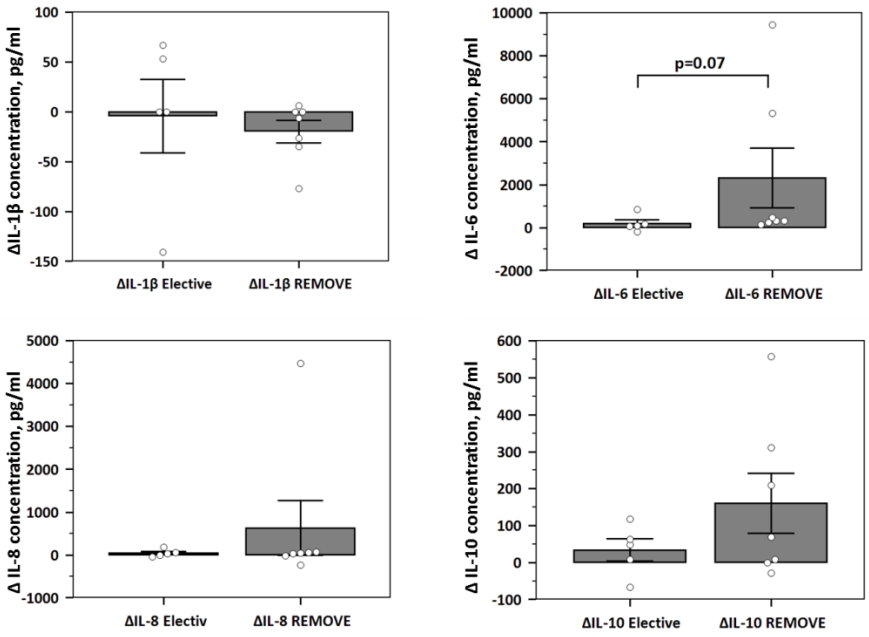

Figure 26: Differences between plasma cytokine levels in the samples obtained from the REMOVE-study participants and patients undergoing elective heart surgery (n=3). Data presented as mean ± SEM, each individual data point is shown as a dot. Mann-Whitney test was used to determine significance of the differences between the groups.

4.3. Effects of the proteins eluted from the filter matrix in cultured human endothelial cells

4.3.1. Changes in cell growth and viability

HAECs cultured with protein mixture eluted from 4 filter devices demonstrated severe alterations in cell viability. Percentage of viable cells was determined via CTB-assay based on their metabolic activity (reduction of resazurin by metabolically active cell) and expressed as percentage of viable cells, compared to untreated control (Ctrl, Fig. 27).

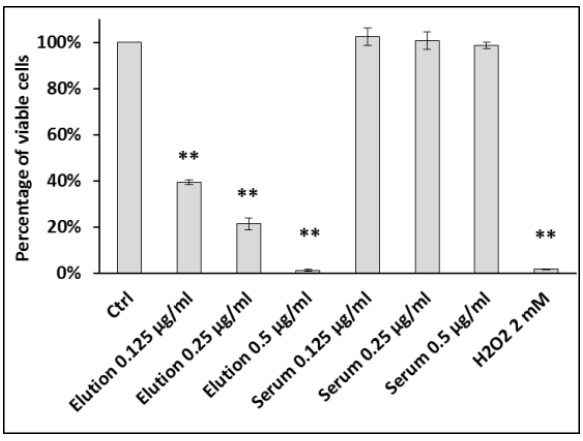

Figure 27: Changes in cell viability of HAECs treated with different concentrations of proteins isolated from polymer matrix (CTB-assay) (n=3). Cells treated with increasing concentrations of eluted proteins (0.125 µg/ml, 0.25 µg/ml, 0.5 µg/ml) for 24 hours, have demonstrated dramatic drop in the rate of metabolism compared to untreated control (** $p < 0.001$, t-test). Equivalent concentrations of serum did not produce significant changes in cell viability compared to untreated control.

Cell viability was reduced in concentration-dependent manner (by 60.45% and 78.51% in wells, treated with 0.125 µg/ml and 0.25 µg/ml of eluted proteins, correspondingly) after 24-

hour exposure. In wells exposed to 0.5 µg/ml of eluted proteins, reduction of cell metabolic activity was comparable to addition of 2 mM hydrogen peroxide (Fig. 27). No significant cell viability alterations in cells treated with corresponding concentrations of commercially available serum were observed.

Another viability test determining percentage of cells with permeable or compromised cell membrane showed an increase in the number of dead cells or cells with disrupted membrane integrity after 24-hour exposure to proteins eluted from the polymer matrix. The extent of cell viability reduction was different when compared to cell metabolism-based viability assay; we assume these differences are solely explained by the assay methodology. Fluorigenic dye Sapphire700 (Li-Cor) can penetrate only dead cells or cells with damaged cell membranes, after binding to cytoplasmic proteins becomes fluorescent in the near-IR spectrum; the higher the amount of dead cells in the well, the stronger is the signal intensity in 700 nm channel (Fig. 28 B). Percentage of dead or permeable cells in the wells treated with low and moderate concentrations of eluted proteins (0.125 and 0.25 µg/ml, correspondingly) was about 25%, whilst maximal dose of eluted proteins (0.5 µg/ml) resulted in the increase of dead cells count by 36% (Fig. 28 A).

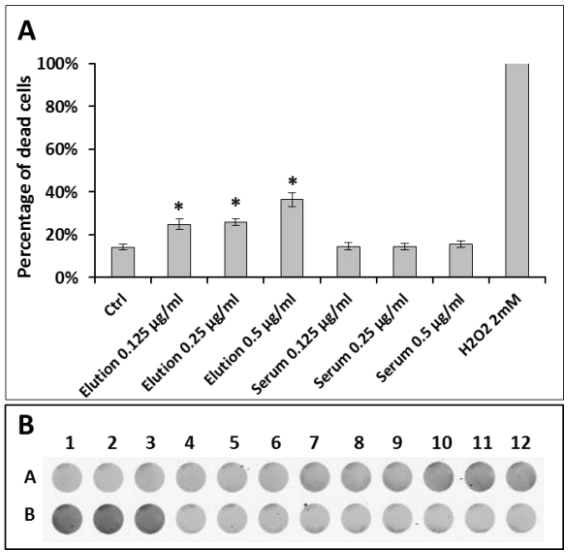

Figure 28: A. Number of dead cells or cells with compromised cell membrane after 24-hour treatment (n=3). Percentage of dead cells or cells with compromised cell membrane was calculated from H_2O_2-treated control. Data are represented as mean ± SEM, *p≤0.05 (t-test) compared to untreated control. B. Representative image of near-IR fluorescence at 700 nm wavelength in treated cells, incubated with Sapphire700 dye. Wells A 1 – 3 represent untreated HAECs; A 4 – 5: elution 0.125 µg/ml; A 6 – 9: elution 0. 25 µg/ml; A 10 – 12: elution 0. 5 µg/ml; B 1 – 3: 2 mM H_2O_2; B 4 – 5: serum 0.125 µg/ml; B 6 – 9: serum 0. 25 µg/ml; B 10 – 12: serum 0. 5 µg/ml.

4.3.2. Changes in cell cycle

Cells treated with the lowest concentrations of eluted proteins showed signs of cell cycle retardation and cell cycle arrest in the BrdU-assay. After 48 hours of cultivation with BrdU and DC, four divisions could be registered with flow-cytometry. Cells, treated with 0.125 µg/ml of eluted proteins stopped to divide after two cell divisions, when compared to control, cultivated with 10% FCS ECGM2 (further described as control, Ctrl in Fig. 29), $p<0.001$), at the same time the number of cells that underwent one or two divisions was significantly higher compared to control ($p<0.05$ and $p<0.001$, correspondingly, Fig. 29 A).

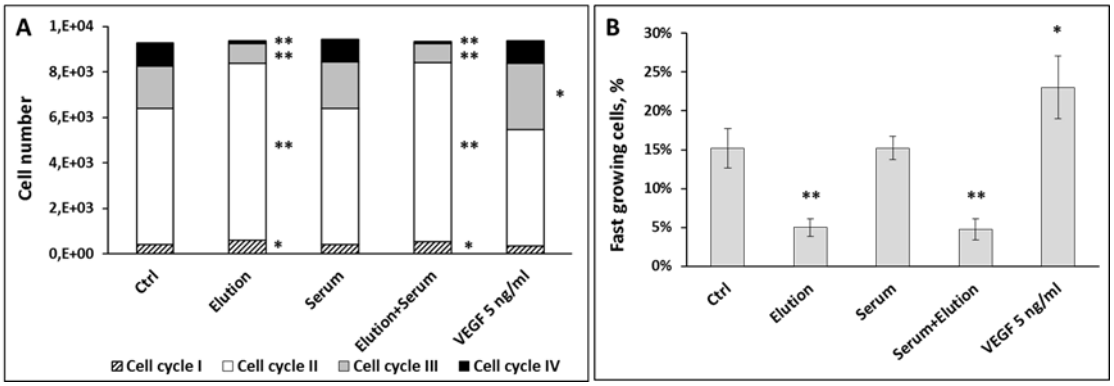

Figure 29: Cell cycle delay in endothelial cells treated with material, eluted from the filter (BrdU-assay). A. Cell cycle distribution in BrdU-assay (n=3). Absolute number of cells undergoing 3rd and 4th divisions was significantly lower in elution-treated HAECs compared to untreated controls, *p<0.05 (t-test) compared to untreated control, **p<0.001 compared to untreated control. B. Percentage of fast growing cells, defined as ratio of sum of cells in 3rd and 4th divisions to the sum of all viable cells identified in all cell cycles. Data are presented as mean ± SEM.

Addition of normal human serum to elution did not abolish the effects of eluted proteins, cells treated with this combination (shown as Elution+Serum, Fig. 29 A) demonstrated the same cell cycle distribution pattern as cells treated with elution alone. Addition of growth factors caused a significant increase in subpopulation of cells undergoing 3rddivision, time of the experiment was however too short to see significant differences in 4th division. Population of fast proliferating cells (cells in 3rd and 4th divisions) was significantly depleted in HAECs, exposed to elution or the combination of elution with serum when compared to control; VEGF-treated cells had the highest number of fast growing cells (Fig. 29 B).

4.3.3. Eluted proteins affect cell attachment

HAECs seeded into medium with eluted proteins showed an impaired attachment. Four hours after seeding, the number of cells attached to the plate bottom in the elution-treated wells was reduced by more than half compared to untreated controls. The effect was not dose-dependent within the tested concentrations. The control cells (addition of serum to the medium) attached to the wells not depending on the amount of serum (Fig. 30).

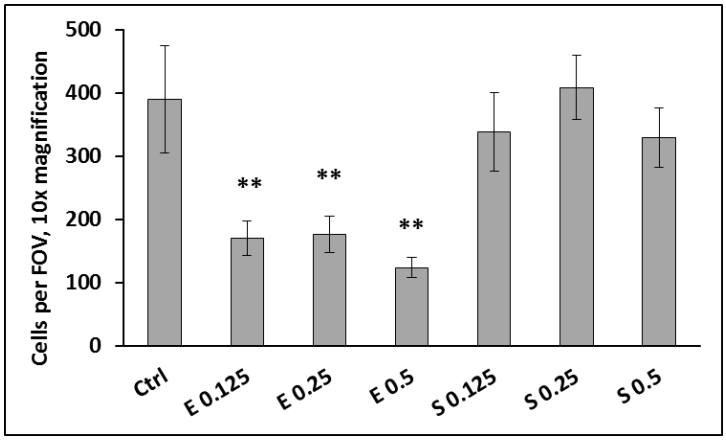

Figure 30: Number of the cells remaining adherent 4 hours after seeding into the medium with addition of eluted proteins (shown as E 0.125, E 0.25, E 0.5 with the numbers corresponding to protein concentration in µg/ml), or equivalent amount of human serum (shown as S 0.125, S 0.25, S 0.5 with the numbers corresponding to protein concentration in µg/ml) (n=3). Data are presented as mean number of cells per field of view (FOV) ± SEM, ** p≤0.001 (t-test) compared to untreated control.

4.3.4. Changes in lateral migration of endothelial cells

Complete closure of the scratch with lateral dimension of approximately 100 µm normally succeeds after 16-18 hours. This can be clearly seen in the panel of microphotographs (Suppl. fig. 3). Cells treated with proteins eluted from the CytoSorb filters used for intraoperative HF demonstrated dose-dependent retardation in lateral migration even after 8 hours (Fig. 31 A). Complete closure of the scratch did not take place even with the lowest concentration of eluted proteins added to cultivation medium (Suppl. fig. 3). Scratch area in the cells treated with 0.25 µg/ml and 0.5 µg/ml of eluted proteins was significantly increased, compared to untreated control after 24 hours (Fig. 31 B) and for the cells treated with the highest dose, scratch area was changed by only 20% from initial scratch area surface after 24 hours of observation. There was no significant difference in scratch closure between the serum-treated (S) and untreated controls (Suppl. fig. 3, also Fig. 31 A, B).

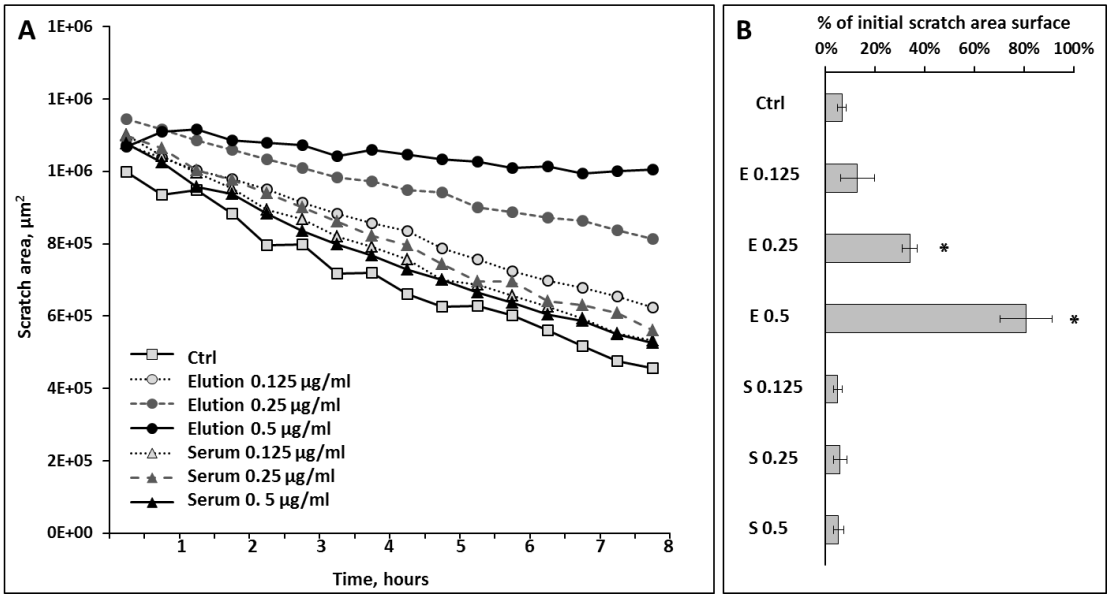

Figure 31: Migration assay in HAECs treated with different concentration of proteins, eluted from the matrix of the filter (E) and corresponding concentrations of human serum (S) (n=3). A. Dynamics of scratch area changes during 8 hours. B. Percentage of initial scratch area surface after 24 hours. Data are presented as mean ± SEM, * $p<0.05$ (t-test) compared to untreated control.

4.3.5. Tube formation assay

Surprisingly, small dose of eluted proteins (0.125 µg/ml) did not lead to significant alterations of tube network formation, when compared to untreated HAEC cells and serum-treated controls. Eight hours after the seeding onto the ECM-gel, number of network elements did not significantly differ among control conditions (cells, seeded into ECGM2 with 1% FCS and 0.125 µg/ml human serum) and 0.125 µg/ml concentrations of proteins eluted from the polymer matrix (Fig. 32 B). Treatment with VEGF resulted in significant increase in the number of network elements compared to untreated control ($p<0.05$), while addition of sulforaphane (SFN), an inhibitor of angiogenesis, resulted in severe inhibition of the network formation (Fig. 33 A) with significant reduction in the number of tubes ($p<0.05$), nodes and meshes ($p<0.001$) (Fig. 32 B).

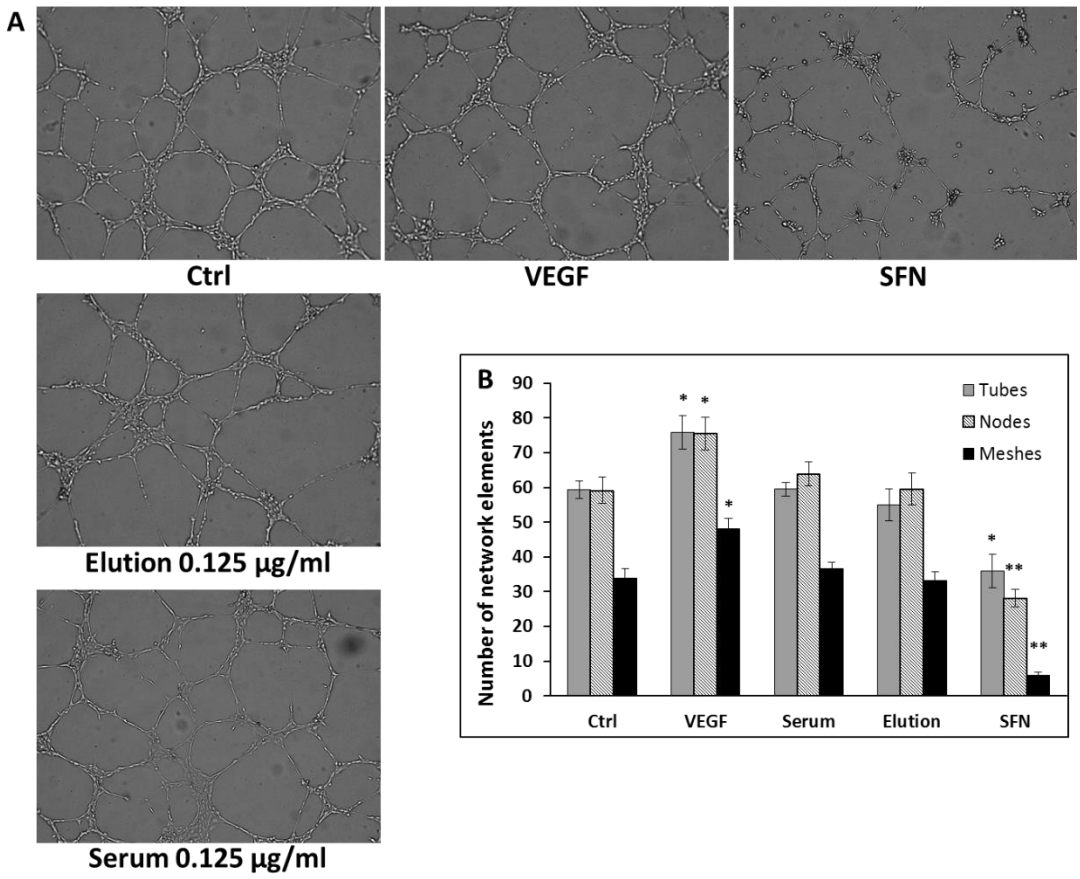

Figure 32: Tube formation assay (n=3). A. Representative microphotographs of the endothelial cell network 8 hours after seeding onto extracellular matrix with corresponding stimulants/controls. B. Quantification of network elements 8 hours after seeding on extracellular matrix gel, when a stable polygonal network of endothelial tubes was formed. Vascular endothelial growth factor (VEGF) and sulforaphane (SFN) were used as known stimulator and inhibitor of angiogenesis, correspondingly. Data are presented as mean ± SEM, * $p < 0.05$, ** $p < 0.001$ (t-test) compared to untreated control.

4.3.6. Cell transcriptomics

4.3.6.1. Up-regulated genes

Several heterogeneous groups of genes were up-regulated in HAECs as a result of 24-hour treatment with proteins eluted from the CytoSorb polymer matrix. Major groups, demonstrating significant enrichment in the set of up-regulated genes included genes involved into regulation of tRNA aminoacylation and translation. Another major cluster of up-regulated genes was comprised of metabolic controllers, particularly regulators of amino acid, cholesterol and pyruvate metabolism. Genes, responsible for the transport of amino acid across the cell membrane were also overrepresented among up-regulated genes, as well as proteins involved into ferroptosis, a specific type of programmed cell death (Fig. 33). Among the 20 most up-regulated genes, clusters of genes encoding enzymes catalyzing amino acid biosynthesis, transcriptional regulators, factors of growth and differentiation could be identified (Suppl. Table 15). To avoid erroneous interpretation of mRNA-array data, some of the targets were further validated with IB and IHC to prove changes on the protein level.

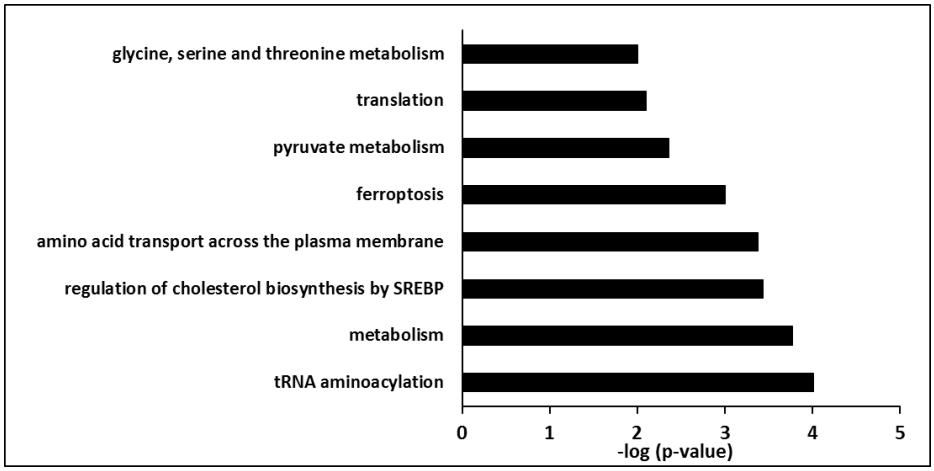

Abbreviations: SREBP - sterol regulatory element-binding proteins; tRNA – transfer RNA.

Figure 33: Biological process categories overrepresented in 201 up-regulated genes in HAECs after 24-hour treatment with eluted proteins. Significance generated with ConsensusPathDB-human (release 34, Herwig et al., 2016) is presented on the x-axis as negative logarithmized p-value.

4.3.6.1.1. Genes controlling cell metabolism

Among validated protein targets, several key metabolism regulators were significantly up-regulated after 24-hour treatment with proteins eluted from the polymer matrix. Protein levels of phosphoserine aminotransferase (PSAT), mitochondrial methylene tetrahydrofolate dehydrogenase 2 (MTHFD2) were significantly increased compared to untreated control (Fig. 34 A, B).

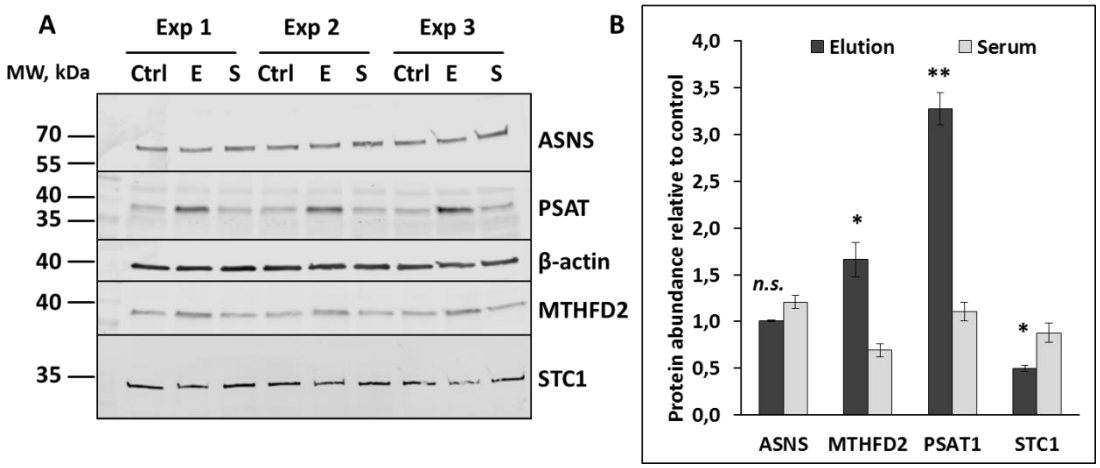

Abbreviations: ASNS – asparagine aminotransferase, PSAT – phosphoserine aminotransferase, MTHFD2 - methylene tetrahydrofolate dehydrogenase 2, STC1 – stanniocalcin 1.

Figure 34: Targets involved into metabolism regulators, up-regulated in HAECs after 24-hour treatment. A. Validation of up-regulated protein targets with immunoblotting. Proteins of interest were detected in cell lysates obtained from untreated HAECs (Ctrl), HAECs treated with 0.125 µg/ml of elution (E), 0.125 µg/ml of serum-control (S). Samples from three independent experiments are marked as Exp 1, Exp 2, Exp 3. B. Signal intensities from protein targets were normalized to signal intensities from β-actin, signals from treated cells are expressed as percent from untreated control. Data presented in arbitrary units (a.u.) as mean ± SEM, * $p \leq 0.05$; ** $p \leq 0.001$; n.s. – no significant difference compared to untreated control.

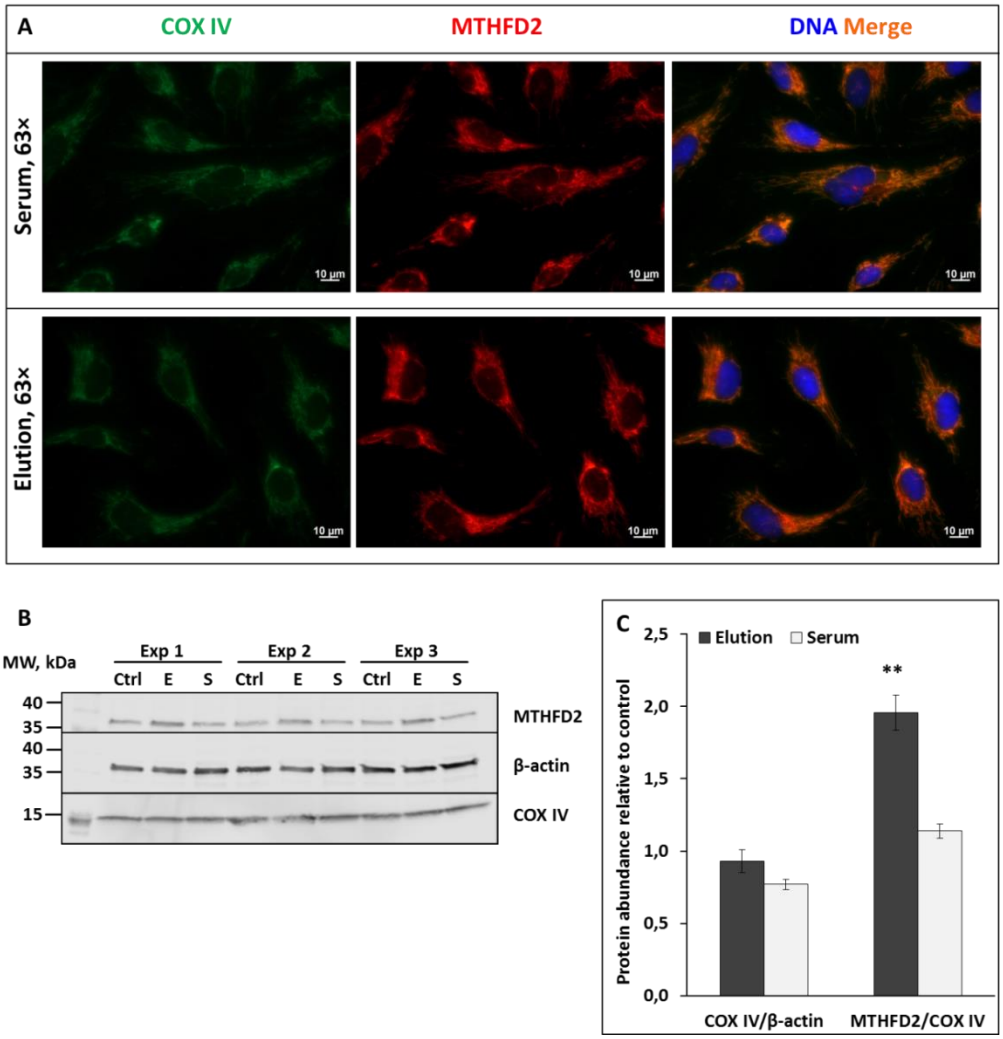

Abbreviations: COXIV – cytochrome oxidase IV, MTHFD2 - methylene tetrahydrofolate dehydrogenase 2.

Figure 35: Mitochondrial enzyme MTHFHD2 in HAECs subjected to 24-hour treatment with elution fraction. A. IHC of MTHFD2 (red) with mitochondria-specific enzyme COXIV (green), resulting in yellow color in perinuclear area of the cells, microphotograph with 63 × magnification. DAPI is used as nuclear counterstaining. B. Immunodetection of COXIV, MTHFD2 and β-actin in cell lysates obtained from untreated HAECs (Ctrl), HAECs treated with 0.125 µg/ml of elution (E), 0.125 µg/ml of serum (S). Samples from three independent experiments are marked as Exp 1, Exp 2, Exp 3. C. Signal intensities from COXIV normalized to β-actin; MTHFD2 normalized to COXIV, data presented in arbitrary units (a.u.) as mean ± SEM, ** $p \leq 0.001$ compared to untreated control.

MTHFD2 is a mitochondria-specific protein, as can be seen in IHC-images, showing co-localization of this enzyme with cytochrome oxidase IV (COXIV), a mitochondria-specific marker protein (Fig. 35 A). A WB normalization of MTHFD2 towards COXIV in cell lysates showed that there was no significant change in protein levels for COXIV, when normalized to β-actin (Fig. 35 C, D), while MTHFD2/COXIV ratio was significantly increased in elution-treated cells (Fig. 35 C, D).

Despite high protein expression levels (suppl. table 15) of asparagine aminotransferase (ASNS), protein levels of ASNS were not significantly different in elution-treated cells. Protein levels of stanniocalcin 1 (STC1), a hormone substance with exocrine and autocrine properties were significantly decreased in elution-treated cells compared to untreated

control (Fig. 34 A, B). Since STC1 is a secreted protein we have assumed that it can be produced and rapidly excreted outside of the cells.

Our suggestion was partially confirmed after experiments with addition of protein transport inhibitor cocktail (PTIC), allowing accumulation of STC1 inside the cells. Addition of PTIC in concentration 0.1 ×, corresponding to 1 µM of Brefeldin-A and 0.2 µM of Monensin resulted in significantly increased levels of STC1 in elution-treated cells (Fig. 36 A, B). This accumulation of STC1 was seen with a low concentration of PTIC (0.05 ×, 0.5 µM of Brefeldin-A and 0.1 µM of Monensin), however was not statistically significant. It is necessary to mention that addition of PTIC severely affected cell viability, morphology (data not shown), as well as potentially affected production of multiple proteins that are downstream targets of UPR-pathway, activated in response to ER-stress induced by protein transport inhibitors.

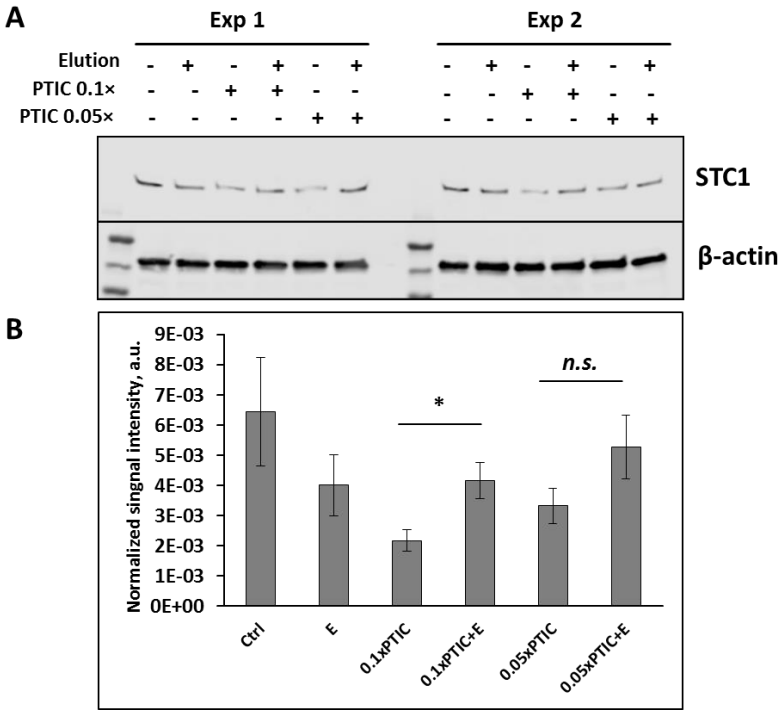

Figure 36: STC1 accumulation in HAECs, subjected to 16-hour treatment with protein transport inhibitor cocktail (PTIC). A. Representative immunoblot of HAEC cell lysates obtained in 2 independent experiments (Exp 1, Exp 2). Cells without treatment (Ctrl) or treated with 0.125 µg/ml eluted proteins (E) alone or in combination with 0.1 × and 0.05 × of protein transport inhibitor cocktail (PTIC). B. Normalized signal intensity (STC1/β-actin), results from 3 independent experiments. Data presented in arbitrary units (a.u.) as mean ± SEM, *p ≤ 0.05; n.s. – no significant difference.

Activating transcription factor 4 (ATF4) is a crucial controller of metabolism, activated in case of exogenous amino acid deficiency and as a part of UPR-pathway. Expression of ATF4 controls the expression of enzymes responsible for biosynthesis of amino acids, including ASNS and PSAT. Array data suggested an insignificant increase in ATF4 transcripts in elution-treated cells. We could detect a non-significant increase in ATF4 with IHC, normalizing signal from ATF4 to histone H3 as a nuclear loading control (Fig. 37 A, B).

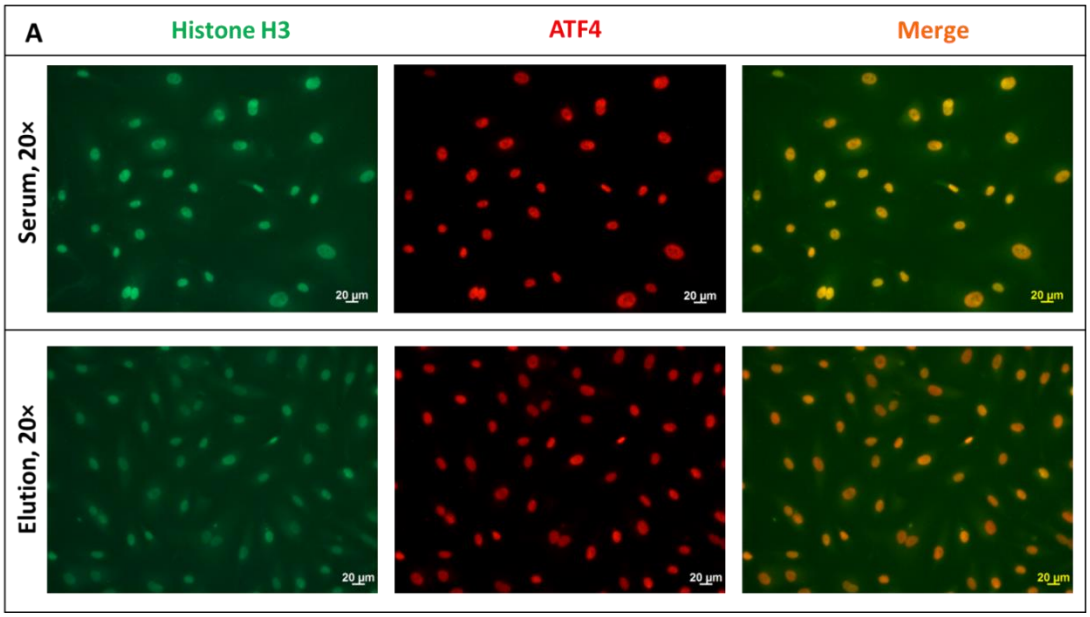

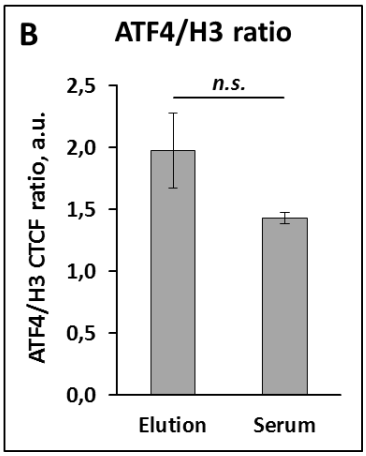

Figure 37: Detection of ATF4 by immunocytochemistry. A. Nuclear co-localization of ATF4 (red) with histone H3 (green), resulting in yellow color. ICC microphotographs captured with 20 × magnifications. B. Signal intensity ratios, quantified with Image J. Fluorescent signal from H3 and ATF4 was calculated as corrected total cell fluorescence (CTCF), including background subtraction for each individual cell, quantification performed in 100 cells from 3 independent experiments. Data presented in arbitrary units (a.u.) as mean ± SEM.

4.3.6.1.2. Genes controlling secretion of pro-coagulant factors

Plasminogen activator inhibitor-1 (PAI-1) is the key inhibitor of fibrinolysis, blocking tissue plasminogen activator (tPA). Protein levels of PAI-1 and tPA secreted by endothelial cells could be potential markers representing pro-coagulant changes in EC metabolism in response to treatment with proteins retained on the polymer matrix during intraoperative HF. Immunoblotting confirmed array data, suggesting an increase in PAI-1 levels in HAECs after exposure to proteins eluted from the filters (Fig. 38 A, B). Protein expression of tPA did not significantly increase in response to 24-hour treatment (Fig. 38 A, B), we also could not detect presence of tPA/PAI-1 complexes in cell lysates. IHC-detection of PAI-1 has confirmed cytoplasmic localization of the protein (Fig. 38, C), proving that increased PAI-1 protein levels do not stem from remnants of medium with added protein mixture, or presence of PAI-1 on the cell membrane of HAECs.

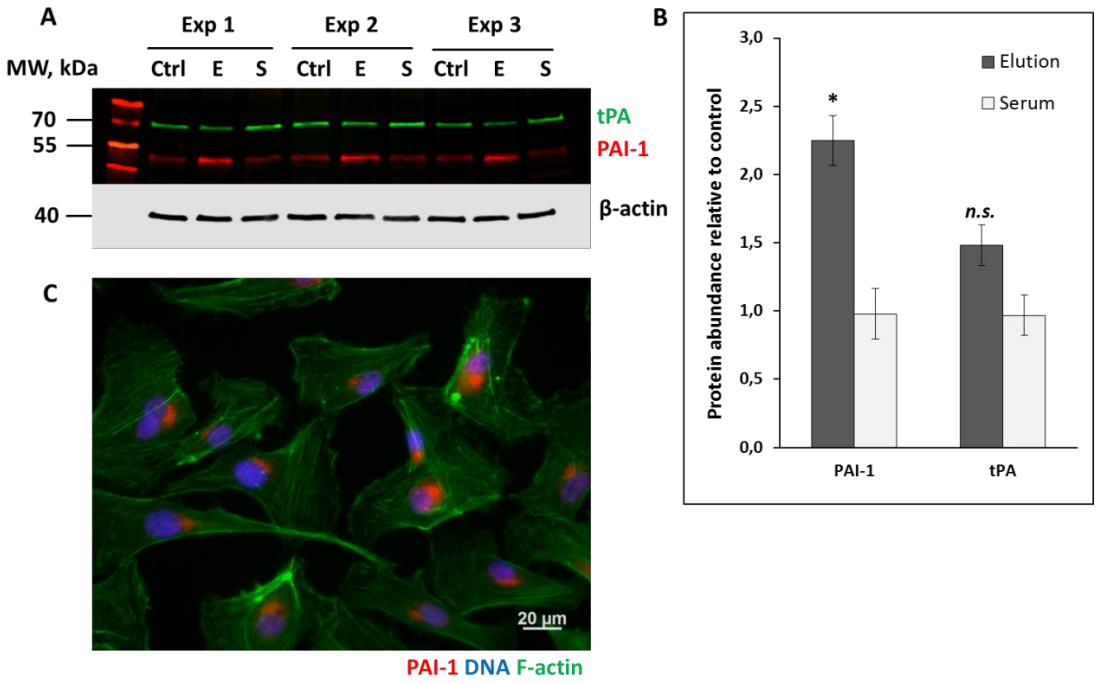

Figure 38: Increased production of PAI-1 in HAECs, treated with proteins eluted from CytoSorb filter matrix (n=3). A. Immunodetection of tPA and PAI-1 in cell lysates obtained from untreated HAECs (Ctrl), HAECs treated with 0.125 µg/ml of elution (E), 0.125 µg/ml of serum (S). Samples from three independent experiments are marked as Exp 1, Exp 2, Exp 3. B. Signal intensities from PAI-1 and tPA, normalized to β-actin and expressed as fold signal intensity of an untreated control. Data is presented in arbitrary units (a.u.) as mean ± SEM, *p ≤ 0.05, n.s. – no significant difference compared to controls. C. Intracellular localization of PAI-1 (red) in the treated HAECs (IHC), microphotograph with 40 × magnification. DAPI was used to stain the nuclei and Phalloidin Alexa Fluor 488 was used for F-actin staining.

Another pro-coagulant substance secreted by ECs in response to damage or inflammation is von Willebrand factor (vWF), a glycoprotein that participates in recruitment of platelets to the endothelial surface and facilitates clot formation. This large polymerized glycoprotein has multiple glycosylated isoforms, which is why identification of this protein could not be performed in whole cell lysates or in the supernatants of treated cells. IHC detection has demonstrated presence of vWF in cytoplasmic rod-like granular structures, corresponding to the morphology of Weibel-Palade bodies (WPB). WPB co-secrete multiple vasoactive substances in response to variety of stimuli, including exposure to pro-inflammatory mediators. Cells exposed to the proteins eluted from CytoSorb matrix have demonstrated increased accumulation of WPB (identified by presence of vWF), compared to the cells exposed to the corresponding concentrations of serum proteins (Fig 39 A, B).

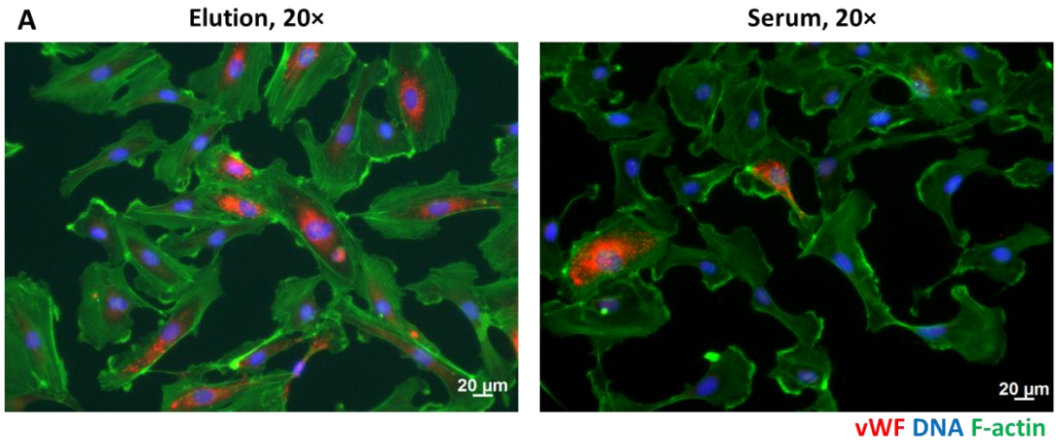

Figure 39: Representative microscopic images of von-Willebrand factor localized in cytoplasmic Weibel-Palade bodies of HAECs (n=3). Cells treated with 0.125 µg/ml of the proteins eluted from the CytoSorb filter in comparison with cells treated with the equivalent concentration of serum proteins. Microscopic images were performed with 20 × magnification; DAPI was used to stain the nuclei and Phalloidin Alexa Fluor 488 was used for F-actin staining. Ratio of vWF-positive cells to total cell number was significantly higher in elution-treated cells (C, data presented as mean ± SEM, *p≤0.05)

4.3.6.2. Down-regulated genes

Among 119 genes down-regulated in HAECs after 24-hour treatment with 0.125 µg/ml of proteins eluted from CytoSorb polymer matrix, numerous genes were annotated as involved into regulation of cell cycle (Fig. 40), biological network analysis also demonstrated that genes responsible for cell cycle regulation were highly enriched in the network (suppl. fig. 5, genes highlighted in red). Among cell cycle regulators genes involved into M-phase of mitosis, cell cycle checkpoints, RHO GTPase effectors, proteins of mitotic prometaphase and G2/M phase transition, factors affecting condensation of prometaphase chromosomes were significantly overrepresented in the dataset of down-regulated genes (Fig. 40). Twenty of the most affected genes are listed in suppl. table 16.

The most down-regulated target according to mRNA-array data, kinesin family member 20A (KIF20A) was also validated on protein level. However, the main obstacle in validation was the specificity of commercially available antibodies.

KIF20A, a mitotic protein essential for cell division is a key compound of cytokinetic bridge, formed in the process of cell division into two daughter cells. KIF20A is phosphorylated by polo-like kinase 1 (PLK-1) and is recruited into formation of the central spindle. KIF20A protein levels were significantly decreased in HAECs, treated with proteins eluted from the polymer matrix (Fig. 41 A (shown with arrow), Fig. 41 B). Phosphorylated form of this protein, modified at the position Ser528 (phosphorylation site specific for PLK-1 phosphorylation) was also correspondingly reduced in cell lysates obtained from the cells treated with proteins recovered from hemofilters (Fig. 41 A).

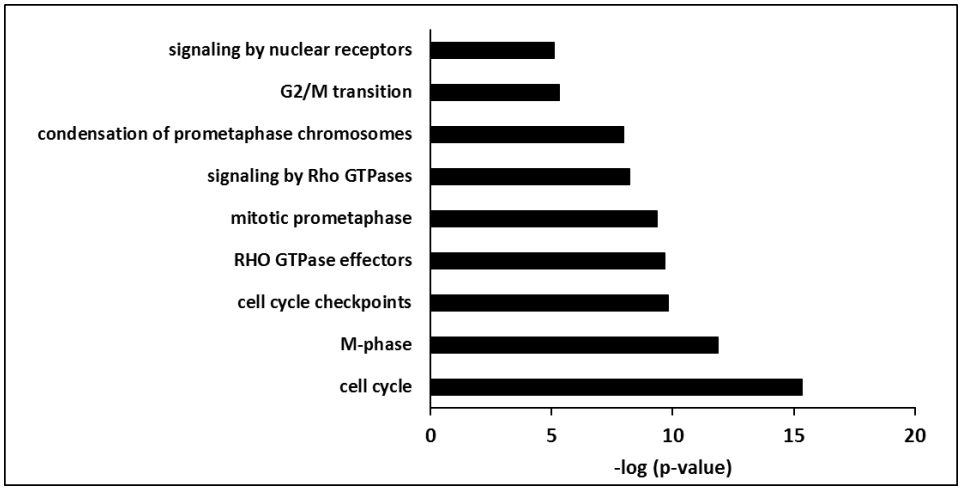

Figure 40: Biological process categories overrepresented in 119 down-regulated genes in HAECs after 24-hour treatment with eluted proteins. Significance generated with ConsensusPathDB-human (release 34, Herwig et al., 2016) is presented on the x-axis as negative logarithmized p-value.

Mitotic checkpoint kinase budding uninhibited by benzimidazoles 1 (BUB1) is another strongly down-regulated target upon treatment with protein mixture isolated from the polymer matrix identified by mRNA array. BUB1 is a serine/threonine protein kinase playing a key role in organization of mitotic spindle and chromosome alignment during the cell division. Protein levels of BUB1 were significantly reduced in cell lysates derived from HAECs treated eluted proteins (Fig. 42 A, B).

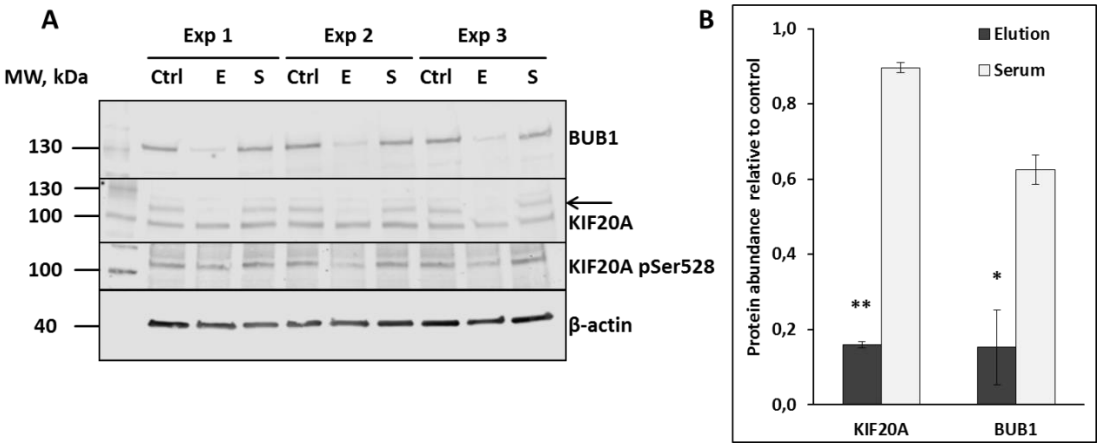

Figure 41: Targets involved into regulation of cell cycle, down-regulated in HAECs after 24-hour treatment with elution fraction (n=3). A. Validation of down-regulated protein targets with immunoblotting. Proteins of interest were detected in cell lysates obtained from untreated HAECs (Ctrl), HAECs treated with 0.125 µg/ml of elution (E), 0.125 µg/ml of serum (S). Samples from three independent experiments are marked as Exp 1, Exp 2, Exp 3. KIF20A band is shown with the arrow. B. Signal intensities from protein targets were normalized to signal intensity from β-actin, signals from treated cells are expressed as percent from untreated control. Data presented in arbitrary units (a.u.) as mean ± SEM, * $p \leq 0.05$; ** $p \leq 0.001$.

4.3.6.3. Establishing potential interactions between proteins eluted from the hemofilters and functional changes in endothelial cells

Two major phenotypical changes were observed and further dissected after the treatment with protein mixtures eluted from the polymer matrix: dose-dependent reduction in cell viability and inhibition of lateral migration.

STRING biological network analysis allowed identification of certain protein groups with common GO-annotations, overrepresented in the dataset of the proteins isolated from the filters applied during cardiac surgery with CPB. Relevant annotations included biological processes mediating migration, growth and apoptosis of ECs. Data summary from Table 15 shows identified proteins with potential effects on EC proliferation and migration. Regarding migration two groups could be identified: migration enhancers and migration inhibitors. Migration enhancers included factors stimulating angiogenesis (angiogenin, ANG), several integrins (ITGAM, ITGB1, ITGB3) and extracellular matrix proteins (extracellular matrix protein 1, ECM1; non-muscle myosin, MYH9; vitronectin, VTN).

Potential migration inhibitors were presented with a diverse group of proteins. For example β-2-glycoprotein (APOH) was shown to inhibit VEGF-mediated growth and migration in HAECs by suppression of VEGFR2, ERK1/2 and Akt phosphorylation (Chiu et al., 2013). N-terminal fragment of type XVII collagen, endostatin (COL18A1) is an extracellular matrix protein with signaling properties, alleviating EC migration via interaction with multiple integrins, nucleolin and various VEGF receptors (Sparding et al., 2019). Thrombospondin-1 (THBS1) and histidine-proline-rich glycoprotein (HRG) play a major role in cell-cell and cell-matrix interactions and are both inhibiting migration of ECs. HRG has a multidomain structure and acts as an adapter protein; this protein modulates cell adhesion, chemotaxis, angiogenesis, coagulation, and fibrinolysis (Poon et al., 2011). THBS1 is a ligand for CD36-receptors of ECs, and it inhibits growth factor signaling (Chu et al., 2013; Klenotic et al., 2013).

Table 15: Proteins identified in the elutions from the CytoSorb polymer matrix potentially influencing proliferation and migration of endothelial cells (LC-MS/MS data)

GO-term	Biological process description	Proteins eluted from the polymer matrix
GO:0043542	endothelial cell migration	APOA1, ITGB1, ITGAM, ITGB2, MYH9
GO:2000351	regulation of endothelial cell apoptotic process	COL18A1, FGA, FGB, FGG, THBS1
GO:0001938	positive regulation of endothelial cell proliferation	ANG, CYBA, ECM1, ITGB3
GO:0010594	regulation of endothelial cell migration	APOH, HRG, ITGB3, PLG, THBS1
GO:2001027	negative regulation of endothelial cell chemotaxis	HRG, THBS1
GO:0010596	negative regulation of endothelial cell migration	APOH, HRG, THBS1
GO:0030949	positive regulation of vascular endothelial growth factor receptor signaling pathway	ITGB3, VTN
GO:2000353	positive regulation of endothelial cell apoptotic process	COL18A1, THBS1
GO:0048010	vascular endothelial growth factor receptor signaling pathway	CYBA, CYBB, ITGB3

Members of NADPH oxidase superfamily (CYBA and CYBB proteins) unlikely can interact with ECs directly, exerting their pro-inflammatory effects and promoting endothelial dysfunction and apoptosis; in our experimental conditions they rather serve as markers of cell activation, most probably neutrophils and ECs. Fibrinogens (FGA, FGB and FGG) exert functions of both migration enhancers via several mechanisms. Addition of fibrinogen to cultured ECs affects

expression and production of pro-coagulant PAI-1 (Sahni et al., 2004), induces the expression of ICAM-1 and P-selectin (Shcheglovitova et al., 2006), increases ERK-phosphorylation-mediated permeability of ECs (Tyagi et al., 2008). Fibrinogen can also play a role of matrix, binding VEGF as well as fibroblast growth factor 2 (FGF-2) subsequently inducing proliferation and migration of ECs (Sahni et al., 1999; Sahni et al., 2000).

C-reactive protein (CRP) is another protein that was not elucidated in this current bioinformatic analysis. However, it was recovered from the elutions in detectable amounts (refer to section 4.1.7, Fig. 18). It was shown that CRP induces PAI-1 expression and activity in HAECs (Deveraj et al., 2003).

Plethora of genes, mediating processes of cell migration via different mechanisms, were also identified in mRNA array data from HAECs exposed to 24-hour treatment with protein mixture eluted from the hemofilters. Both up-regulated and down-regulated genes, influencing cell migration were identified (Table 16, mRNA-data, up-regulated genes are marked with "↑", down-regulated with "↓", correspondingly). A huge cluster of down-regulated genes is involved into cytoskeleton reorganization and cell polarity regulation. It is well-known that polarity factors are crucial for cell orientation, proper cell-cell interactions and lateral migration in ECs (Michaelis et al., 2013).

It is important to highlight, that some of the genes annotated in table 16 are not specific for migration of ECs exclusively. Some of the up-regulated genes (i.e. STC1, SERPINE1) mediate recruitment of leukocytes and platelets to the surface of ECs, thereby regulating complex cell-cell interactions during tissue damage and inflammation.

Table 16: Targets involved in regulation of cell migration upregulated or downregulated after treatment with eluted proteins identified by mRNA-array

GO-term	Biological process description	Genes affected in HAECs	mRNA data
GO:0030334	regulation of cell migration	ANXA3, CD274, CDH13, CXCL8, DOCK5, JUN, IGFBP3, FRMD5, NAV3, LAMB1, SERPINE1, NR2F2, STC1, SMAD3, MYADM, P2RX4, RAC2, VEGFA	↑
GO:0030335	positive regulation of cell migration	ANXA3, CD274, CXCL8, DOCK5, FRMD5, JUN, LAMB1, MYADM, P2RX4, RAC2, SERPINE1, SMAD3, VEGFA	↑
GO:0016477	cell migration	ARPC5L, ASPM, CD34, CDK1, CFL1, CTNNB1, EFNB2, FAM83D, GAB1, PDE4B, PHACTR4, PODXL, MEF2C	↓
GO:0007010	cytoskeleton organization	ABLIM1, ASPM, ARPC5L, AURKB, CALR, CCNB1, CDK1, CFL1, CTNNB1, DIAPH3, GAB1, KIF20A, KIFC1, LIMCH1, NDC80, PHACTR4, PRC1, TPX2, RACGAP1, TPX2, TUBB4B, TUBD1	↓

5. Discussion

5.1. Spectrum and properties of the proteins identified on the CytoSorb polymer matrix

Previous *in vitro* experiments refer to CytoSorb polymer as a resin with hydrophobic mechanism of binding, preferentially eliminating small hydrophobic molecules from circulation (Gruda et al., 2016; Malard et al., 2018). However, our results indicate that the majority of isolated proteins possess hydrophilic properties. Furthermore, GRAVY of the predominant number of blood proteins with known *in vitro* binding is below zero, indicating their hydrophilic properties (Fig. 42).

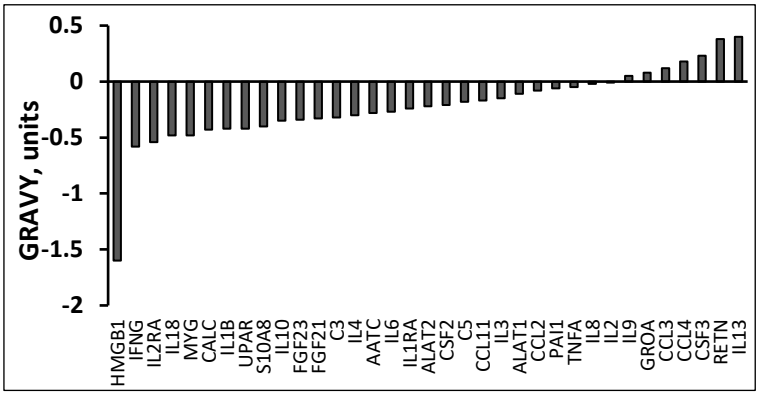

Figure 42: Grand average hydrophobicity (GRAVY) of the plasma proteins known to be adsorbed by CytoSorb matrix (*in vitro* studies, according to Poli et al., 2019). GRAVY-values below 0 indicate hydrophilic properties of the native protein at physiological pH 7.4.

According to our results, obtained through LC-MS/MS protein identification and bioinformatics annotation of the protein properties, Vroman effect (Slack and Horbett, 1995) could be the likely mechanism of protein binding to the polymer matrix. Proteins adsorbed at first are possibly later competitively replaced by larger proteins with stronger binding affinities (schematically depicted in Fig. 43). This is a largely dynamic process (Hirsch et al., 2013) that can potentially modulate the effects of the treatment by transient complex formation and auto-activation of certain proteins upon contact with polymer surface (Brewster et al., 2014). High MW plasma proteins, including albumin, immunoglobulins, fibrinogen, factor XII and high MW kininogen were previously shown to be sequentially adsorbed to the surface of the membranes used in hemodialysis, competitively replacing each other (Fumagall and Vincenzo, 2019). It is important to mention critically, that previous *in vitro* adsorption studies were often performed under suboptimal conditions. For example Volumes of filtrate, filtration times and concentrations of cytokines were chosen sub-optimally; substances of interest were dissolved in an inappropriate carrier (plasma or saline) which is not quite comparable to filtration of whole blood, as it occurs in the clinical settings (Feri, 2019). It is important to highlight that filters used for our studies were applied during a relatively short time period (average CPB time for patients in the REMOVE-study 172.3 min.), while there are clinical applications utilizing filtration times up to 24 hours (Ankawi et al., 2019; Brouwer et al., 2019). Further studies with larger number of observations, could help to establish the ratio between different plasma protein classes depending on the duration of HF treatment.
It is crucial to underline, that protein charge, MW, length, pI and GRAVY are predicted values, measured or calculated with consideration of perfect physiological conditions (pH =

7.4, t = 37°C). This model does not reflect *status quo in vivo*, where proteins change their properties dynamically according to physiological fluctuations.
In our bottom-up proteomic approach to protein identification, only a fraction of peptides was generated for each protein, creating a gap in knowledge about presence of potential proteoforms and post-translational modifications (PTMs). This partial protein sequence coverage imposes potential study limitation, underrepresenting potential influence of PTMs on the efficiency of protein binding and retention on the filter.

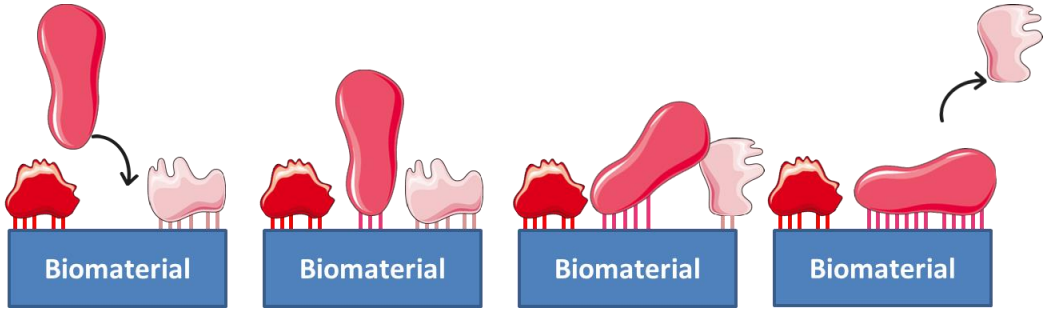

Figure 43: Schematic representation of Vroman effect (adaptation from Felgueiras et al., 2018). Proteins of a larger size, having a more complex conformation can strongly bind to the material due to their ability to develop more contact points. Figure produced by author, using Servier Smart Art vector graphics, distributed under CC BY-NC 4.0 license.

Further potential study limitation is the lack of quantitative data about protein binding on the column. This occurs due to several reasons. First, we do not know whether elution with RIPA-buffer ensures efficient extraction of all proteins from the porous structure of the polymer bead. Second, the obtained protein fraction undergoes numerous purification steps, peptide preparation and purification for LC-MS/MS, which causes protein loss at each stage (Klont et al., 2018). Furthermore, tryptic digestion of the proteins can be incomplete or hindered by protein modifications, providing insufficient peptide yield for further reliable identification of the protein (Tsiatsiani & Heck, 2015). Additionally, proteins with size below 10 kDa will be lost during the dialysis of the samples. Finally, mass-spectrometry method has a range of limitations, including stochastic nature of data acquisition with very limited opportunity to perform absolute quantification of the protein amounts. In addition, presence of certain large proteins in the elution might be explained by their presence in form of peptide fragments in the circulation. Certain proteins can form complexes with each other, potentially explaining their co-presence on the matrix.
It was not possible to identify cytokines, majority of DAMPs via LC-MS/MS, which can be due to their relative low abundance in the blood, when compared to residential blood transport proteins, immunoglobulins, protease inhibitors and enzymes (Anderson & Anderson, 2002; Hortin et al., 2008). Inability to identify small pro-inflammatory molecules (cytokines, chemokines, inflammatory mediators) previously described to be adsorbed *in vitro* is also explained by potential loss during extraction and purification of protein samples.
The majority of the identified plasma proteins is comprised of abundant transport proteins, antibodies, proteases and protease inhibitors. Albumin was the most abundant protein in all samples. Binding of albumin to the polymer matrix was previously shown in several clinical studies (Schädler et al., 2017; Bernardi et al., 2016), as well as in *in vitro* (Harm et al., 2019).

Alpha-1-acid glycoprotein (ORM1) and alpha 1B-glycoprotein (A1BG) were isolated universally in all elution samples. They were previously described to be associated with bloodstream infection in proteomic study by Kuusela et al., 2017, showing differential expression in sepsis survivors vs. non-survivors (Raju et al., 2016). Proteins of S100 superfamily (calgranulins) are DAMP-molecules, with a multifaceted role in the regulation of inflammatory response, apoptosis and cell metabolism (Xia et al., 2018; Timmermans et al., 2016). Being a ligand of RAGE-receptors, S100 proteins instigate inflammation via activation of downstream targets of RAGE signaling, including NF-kB and resulting in an increase of pro-inflammatory cytokine secretion (Chuah et al., 2013; Roh and Sohn, 2018).

A big fraction of the isolated proteins can be identified and annotated as acute phase reactants, which are specific molecules with a particularly important role in the pathogenesis of inflammation and modulation of pro-inflammatory cytokine secretion. Indeed, in line with our results, cardiac surgery with CPB leads to generation of DAMPs and can trigger systemic inflammatory response, similar to sepsis (Gleason et al., 2019; Baumann et al. 2016). The exact molecular mechanisms, causing systemic deterioration of homeostasis remain precisely unknown (Evora et al., 2016). Factors including surgical tissue damage, contact of blood with non-endothelial surfaces, reperfusion injury and endotoxemia contribute to activation of coagulation pathways, complement factors and cellular immune response (Kraft et al., 2015). Previous studies have shown that CPB is followed by the release of numerous DAMPs and inflammatory mediators, including mitochondrial DNA (Sandler et al., 2018), adenosine (Kerbaul et al., 2008), pentraxine 3 and other acute phase reactants (Holubcova et al., 2014). Putative trigger mechanisms of SIRS following CPB involve increased expression of IL-6 in neutrophils (Sandler et al., 2018), decreased toll-like receptor expression and decreased responsiveness of monocytes to TLR ligands (Flier et al., 2015), release of alarmins with subsequent induction of IL-10-, STAT-3- and BCL-3-dependent hypo-responsiveness of monocytes (Friese et al., 2019). All these pathophysiological changes potentially lead to vasoplegia, shock and multi-organ dysfunction. Removal of certain proteins involved in the pathogenesis of inflammatory response in SIRS can be beneficial for the prevention of systemic adverse events after complex cardiac surgery. HF, along with minimally invasive surgery and off-pump procedures potentially offers benefits in prevention of CPB-associated SIRS. Recent systematic review, pooling data from clinical trials underlines that the current evidence remains scarce to recommend this procedure for the routine use (Hawlik et al., 2017). Revision of data from currently completed (NCT02775123, NCT02566525, NCT02265419, NCT02297334, DRKS00007928) and ongoing clinical trials (NCT02312024, NCT03266302) with broader characterization of adsorbing capacities of the polymer matrix could potentially identify the place of HF in prevention of post-operative SIRS. Previous attempts to target and eliminate single chains of inflammatory cascade have failed to demonstrate clinical efficacy, which is why simultaneous elimination of several compounds mediating SIRS seems more perspective (Landis et al., 2014; Simoni, 2019).

As discussed by Geyer et al. (2019), filamin-A (FLNA), vinculin (VCL), talin (TLN1), and platelet basic protein precursor (PPBP) and non-muscle myosin (MYH9) are becoming increasingly abundant in plasma samples in presence of platelet contamination. High abundance of these proteins in the fraction eluted from the polymer could be an indirect evidence of platelet or platelet debris binding to the adsorbent.

Identification of non-protein blood compounds and metabolites is another important aspect that was not addressed in the current study. Certain substances, potentially removed from the matrix along with identified proteins, are further discussed in section 5.5.

5.2. Changes in plasma samples after surgery with cardiopulmonary bypass and CytoSorb hemofiltration

LC-MS/MS-based proteomics and interpretation of the obtained results has a range of pitfalls and discussible points. Plasma is superior in comparison to serum for the protein abundance analysis (Stenemo et al., 2016) due to absence of pro-inflammatory cytokines and coagulation factors secreted by activated cells during plasma clotting (Lee et al., 2015). However, enormous concentration range differences (10 orders of magnitude for certain proteins) lead to selective quantification of the most abundant proteins and completely blurs out the proteins with low abundance (Anderson & Anderson, 2002).

Changes in plasma protein concentrations in REMOVE-study originate from plethora of factors like surgical trauma and bleeding, transfusion of blood products, dead volume of CPB machine, adsorption of proteins to CPB tubing and finally, hemofiltration itself (Table 17). Priming volumes for adult CPB machines are usually ranging between 1400 and 2000 ml of crystalloid or colloid solution (Georgiou et al., 2015; Cooper and Giesecke, 2015). Certain patients in the REMOVE-study have received four portions of FFP, corresponding to total volume of ≈1200 ml (refer to section 4.2.3, table 14). Compared to hemodilution, transfusion of FFP and other blood products, adsorption to polymer matrix produces rather negligible effects. Unfortunately, drawing conclusions about individual contribution of one of the above-mentioned interventions on plasma protein concentrations and changes in abundance of particular protein fractions is not possible.

Table 17: Factors associated with heart surgery and CPB, which are contributing to changes in protein concentration and composition of plasma

Factors, increasing plasma protein concentration (increasing content of certain proteins)	Factors, reducing plasma protein concentration
• Supplementation with FFP, coagulation factors and other blood products • Surgical trauma, tissue damage, release of intracellular constituents • Hemolysis	• Hemodilution • Bleeding • Adsorption of blood proteins to PVC-tubing of CPB-contour • Adsorption of the proteins to hemofilter

Significantly increased abundance of certain proteins like myoglobin is probably a result of the surgery *per se*, including massive surgical tissue damage and CPB-associated blood cell damage. Sub-lethal damage to RBCs and subsequent leakage of intracellular erythrocyte compounds into the plasma samples impose confounding potential for further proteomic characterization of the samples. Previously this was demonstrated for proteins linked to oxidative stress in certain studies (Liu et al., 2018). Particularly, increased amounts of proteins from hemoglobin superfamily (HBA, HBB, HBD, HBG1 and HBG2), catalase (CAT), carbonic anhydrases (CA1, CA2), fructose-bisphospate aldolase (ALDOA), biliverdin reductase B (BLVRB), peroxiredoxins (PRDX2, PRDX6), superoxide dismutase (SOD1), thioredoxin (TXN), glyceraldehyde-3-phosphate dehydrogenase (GAPDH) are identified as cytoplasmic proteins

of red blood cells and are rather an evidence of the sample contamination resulting from hemolysis (Geyer et al., 2019; Kakhniashvili et al., 2004). In our study, excessive hemolysis and sub-lethal erythrocyte damage produced significant increase of the abundance of the proteins listed above in the samples after the surgery. Massive presence of erythrocyte and platelet proteins in plasma proteome was recently discussed by Ignjatovic et al., 2019, suggesting standard operational pre-analytical procedures to ensure prevention of blood cell degradation and protein leakage into the sample. However, considering quite a large overlap between proteins isolated on the polymer matrix and the proteins identified as up- or down-regulated in plasma samples after the operation, we assume significant presence of the intracellular platelet and RBC compounds in circulation of the patients due to blood cell damage for example in the heart-lung machine.

Massive increase in abundance of myoglobin (MB), according to the quantification of LC-MS/MS is probably surgery-related. This small (17 kDa) protein is ubiquitous in skeletal and cardiac muscle and accounts for around 5-10% of all cytoplasmic proteins in these cells (Berridge et al., 2013). MB has a short half-life of 2-3 hours in human plasma, undergoing rapid renal clearance (Chung & Brown, 2019) and is non-specific to muscle type, that is why it is not possible to determine the origin of this protein in plasma samples of the patients (Dasgupta & Wahed, 2014). MB is one of the biomarkers of acute myocardial infarction, however, can also be an evidence of rhabdomiolysis or skeletal muscle damage due to trauma or exercise (Sekhon & Peacock, 2019). Some studies have previously identified that myoglobinemia is associated with CPB surgery and is a predictor of AKI and mortality (Billings et al., 2011; Leaf et al., 2015). Thus, transitory elevation of MB in plasma could be attributed to surgical trauma, cardiac ischemia-reperfusion, muscle tissue damage and transient renal dysfunction. Follow-up post-operative measurements of MB in plasma and urine of the patients were not performed, making it hard to rule out further assumptions about clinical relevance of our finding.

Another up-regulated protein, lactotransferin (LTF) is presumably a product of degranulation of secondary neutrophil granules (Passov et al., 2019). This protein is concomitantly synthesized in the granules and produced along with neutrophil gelatinase-associated lipocalin (LCN2). LTF was also highly abundant among the proteins eluted from the CytoSorb polymer beads, it is concomitant partner LCN2 was also isolated on the polymer beads, but not identified as up- or down-regulated in plasma samples. LCN2 is an iron-scavenging protein and urinary levels are known to be increased during CPB surgery (Leaf et al., 2015), providing a compensatory sequestration of the cell-free iron from hemolysed RBCs and muscle cells.

Several clusters of proteins, up-regulated after the surgery with CPB and concomitant hemofiltration can be identified. Further, we have attempted to group them according to the origin of their increase, possible pathophysiological role and presence on the filter.

Hemolysis during cardiac surgery is a well-known factor contributing to systemic alterations of coagulation, platelet dysfunction, promoting erythrocyte aggregation, tubular kidney damage and increased mortality (Vercaemst, 2008). Mechanical forces of CPB can cause damage of RBCs with subsequent release of free hemoglobin and other RBC-constituents into the circulation. Sub-lethal damage of RBC can cause further problems like tissue hypoxia (Olia et al., 2016). Compromised membranes of RBC create a possibility of cell lysis and release of intracellular RBC compounds into the biological sample. Many of the samples

acquired within this clinical study were exposed to hemolysis, considerable number of samples after surgery with CPB were hemolytic. As indicated previously, high abundant free hemoglobin was obscuring the results of certain tests (Section 4.2.3, Fig. 23 A, B).

Label-free quantification of the plasma proteins before and after intraoperative HF in the REMOVE-study participants has shown down-regulation of S100A12 protein, significant and reproducible within the patient subgroup (Section 4.2.4, Suppl. Table 17). S100A12 protein is calgranulin produced by neutrophils and is implicated in the pathogenesis of inflammatory, autoimmune, metabolic diseases, cancer and neurodegeneration (Pietzsch & Hoppmann, 2009; Däbritz et al., 2013; Hofmann et al., 2011). *In vitro* data suggests that S100A12 exposure increases an expression of ICAM-1 and VCAM-1 in endothelium (Foell et al., 2007). Pro-inflammatory effects of S100A12 are mediated via DAMPs/PAMPs-receptors: TLRs and RAGE (Dubois et al., 2019). Intravenous administration of LPS to healthy volunteers led to increased circulating levels of S100A12, suggesting that S100A12 acts as potential mediator of bacterial infection. In patients with pneumonia, peritonitis, or urinary tract infection elevated plasma levels of S100A12 were observed compared to healthy subjects (Achouiti et al., 2013). Clinical studies suggest that S100A12 is a promising biomarker to diagnose sepsis (Tosson et al., 2018) and stratify high-risk patients with septic shock (Dubois et al., 2019). Further investigations involving sample analysis from properly matched controls and prolonged follow-up should shed some light on whether S100A12 reduction is exclusively attributed to HF and has an impact on prognosis in patients with IE, undergoing surgery with CPB.

Previously published data from pilot RCT of HF in elective cardiac surgery confirms that there was no significant reduction in cytokine concentration before and after the procedure. The authors hypothesize, that this might be explained by low inflammatory response at the baseline and a relatively small duration of HF, limited to the time when the CPB was used and mean bypass duration 145 min (Poli et al., 2019). We have observed results in the similar direction when analyzed plasma samples of the patients from REMOVE-study. Furthermore, we have observed a significant increase in plasma concentrations of IL-6 and IL-10 (as described in section 4.2.5, Fig. 25). An increase in cytokine production is an expected result of cell activation and tissue damage, arising from the surgery and CPB (Al-Fares et al., 2019; Jaffer et al., 2010). These observations were in line with an observed post-operative increase in plasma levels of the main biomarkers of inflammatory response – C-reactive protein and procalcitonin (Suppl. table 22). Absence of noticeable cytokine-clearing benefit of HF cannot be proven in this group without control arm, undergoing the same surgical intervention, but without CytoSorb hemofiltration.

5.3. Adsorption of AGE-modified proteins

We have identified a number of AGE-modified proteins in the material, eluted from the 11 filters used for intraoperative HF. Identified proteins were abundant plasma proteins, with albumin being the protein that had the largest amount of modifications on lysine and arginine. However, these results do not represent the real abundance of modified proteins in the elution, since the most abundant and large proteins are going to be identified first, superseding less abundant proteins, which can be modified as well. Furthermore, abundance of AGE-modified proteins can be less representative in terms of global protein glycation rate, since identified plasma proteins usually possess short half-life and are rapidly undergoing *de*

novo synthesis and replacement (Li et al., 2012). Correct quantification of AGE-modified proteins imposes another serious scientific challenge due to limited proteome coverage: glycation of lysine would interfere with tryptic digestion of proteins creating discordance between modified and non-modified peptides used as a reference for quantification (Rabbani et al., 2016). To provide better understanding of possible selective binding of AGE-modified proteins, LC-MS/MS strategies with peptide labelling (i.e. multiple reaction monitoring) could be a better choice for precise quantification of AGE-modified peptides in biological samples (Thornalley et al., 2014). Considering lack of precise quantification for AGE-modified peptides in our study, as well as small sample size, data about plasma protein glycation and removal of these proteins by CytoSorb filter material is inconclusive.

Glycation of transport proteins might affect their binding capacity and imposes risk of unwanted pharmacokinetic and pharmacodynamics deviations. Albumin (ALB) and α-1-acid glycoprotein (ORM1) are two main transport proteins, engaged into drug binding, storage and transport in the circulation (Lehman-McKeeman, 2013; Fanali et al., 2012). Albumin accounts for about 60% of total plasma protein amount (Lewitt & Lewitt, 2016) and possesses 7 binding sites for fatty acids and 2 binding sites with high affinity to a number of drugs (Bteich et al., 2019). Albumin molecule is highly affected by glycation, as it is rich in both lysine (60 a.a., 9.85% of ALB molecule) and arginine (27 a.a., 4.43% of ALB molecule) (calculated with https://www.protpi.ch/Calculator/ProteinTool). We have identified 21 AGE-modifications on lysine and 8 – on arginine. In the samples retrieved form the CytoSorb polymer matrix, AGE-modifications on albumin CEL-K199 and CML-K438, identified in the elutions are localized in Sudlow's sites I and II, correspondingly. These modifications can have potential influence on drug binding (Anguizola et al., 2013; Qui et al., 2020). Previous studies suggest that in healthy subjects, about 6 to 13% of all circulating albumin pool can be glycated (Anguizola et al., 2013). Paradela-Dobarro et al. (2019) have identified multiple lysine and arginine AGE-modifications of albumin from blood of healthy subjects; interestingly, number of glycation sites and their localization did not majorly depend on the plasma concentration of AGEs.

ORM1 possesses only one main binding site, demonstrating high affinity to basic drugs (Huang & Ung, 2013). We have identified solitary modification with LC-MS/MS in the samples eluted from the filters was K128, located outside the drug binding site of ORM1 (Suppl. table 13).

Plasma with AGE-supplementation is a suboptimal model for investigation of the possible preferential AGE-modified protein binding. Conditions applied for modification of plasma proteins are very harsh and drastically deviate from physiological or diabetic conditions. *In vitro* glycation can cause coarse alterations to the structure of the plasma proteins, inducing formation of high MW cross-links (Khan et al., 2011). These aggregated and cross-linked proteins might retain in the solution, contrary to the unmodified proteins, which would be more susceptible to binding and would be more likely removed from the plasma mixture, serving as a possible explanation of the increase in relative concentration of CML and CEL in plasma samples after *in vitro* filtration.

5.4. Limitations of the clinical study

One of the major limitations of our study is the lack of properly matched control group, either comprised of patients with similar clinical background, but undergoing heart surgery

without CPB with intraoperative HF, or patients undergoing heart surgery with CPB without intraoperative HF. Under given conditions it is quite difficult to distinguish effects of CPB, transfusion of crystalloid priming solution, and blood loss from exclusive effects of HA with CytoSorb matrix. It was also impossible to draw any conclusions about clinical outcomes in the investigated group of individuals due to relatively small sample size. Measurement of plasma biomarkers in the patient groups encounters challenges and critique due to proportional decrease in plasma protein and hematocrit (Suppl. table 23), corresponding to hemodilution (Dasgupta & Sepulveda, 2013). It imposes a serious pre-analytical problem and variety of protein biomarkers cannot be measured accurately directly after CPB; gaining importance only in perioperative period (Aĝirbaşli et al., 2010; Aĝirbaşli et al., 2014). Chronologically, peaking concentrations of IL-6 and other inflammatory biomarkers are observed by the end of the first post-operative day (Karu et al., 2010). We could assess concentrations of these biomarkers only at two specific timepoints that do not represent the extent of changes over the first 48-72 postoperative hours.

5.5. Pharmacological agents and non-protein substances potentially contributing to the observed functional and metabolic changes in endothelial cells

Some of the effects, described above might be partially explained by the presence of aggregated, oxidized, fragmented and denatured proteins in the eluted protein fractions. A number of scavenger receptors towards modified and denatured proteins were previously described in endothelial cells (Merlot et al., 2014; Apostolov et al., 2016). These receptors are responsible for the uptake and metabolism of dysfunctional proteins, their interaction with specific ligands (i.e. modified albumin) initiates endocytosis of target proteins and changes cell permeability for proteins (Bito et al., 2005; Malik, 2009).

Furthermore, certain carrier and adaptor proteins identified in the elutions and discussed previously in section 4.3.6.3 possess direct or indirect anti-angiogenic properties, inhibiting proliferation and migration of ECs (Fig. 44). Effects observed in ECs could be partially explained by the presence of non-dissociated cargoes on the transport proteins, isolated from the polymer matrices. Some of the pharmacological agents, introduced to the patients in pre- and perioperative settings can also be retained by the filter beads (antibiotics, anticoagulants, vasopressors) (Poli et al., 2019). We cannot exclude possible presence of these factors in the eluted protein fractions. In addition, plasma proteins like albumin and α-1-acid glycoprotein act as transport molecules for various endogenous metabolites, hormones, xenobiotic substances and pharmacological agents (Varshney et al., 2010; Israili & Dayton, 2011).

Major plasma transport proteins identified in the elutions from the CytoSorb polymer beads and their known ligands are briefly summarized in Fig. 44. From the case histories of the patients it is known that all of them are exposed to vasopressors, noradrenalin and dopamine. These vasopressors can be bound and transported by albumin and other transport proteins (de Vera et al., 1988; Khalid et al., 2019). It was previously shown, that both noradrenaline and dopamine can alter metabolism, induce apoptosis and inhibit angiogenesis in cultured ECs (Chignalia et al., 2020; Sarkar et al., 2017; Nickel et al., 2009; Fu et al., 2006; Fu et al., 2004). We rather believe that the majority of the substances bound to plasma protein carriers would dissociate from the transport protein during dialysis of the

eluted sample (described in detail in section 3.7.1). However, residual presence of the transport protein ligands with distinct influence on ECs cannot be completely excluded.

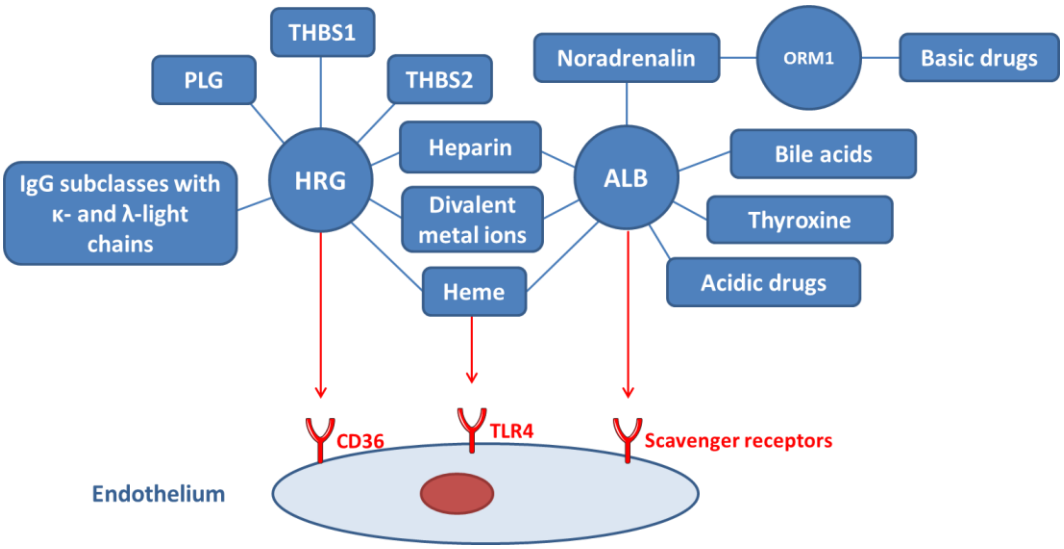

Figure 44: Plasma transport and adaptor proteins and their ligands. Multiple substances can be transported on the transport proteins, identified on the filter matrix. Albumin (ALB), being the most abundant protein among isolated in the eluted protein fractions, has three binding sites and ability to carry multiple pharmacological agents. Histidine-proline-rich glycoprotein (HRG) acts as an adaptor protein, tethering other molecules to the cell surface. Figure produced by author, using Servier Smart Art vector graphics, distributed under CC BY-NC 4.0 license.

Abbreviations: ALB – albumin, HRG – histidine-proline-rich glycoprotein, IgG – class G immunoglobulins, ORM1 – orosumucoid 1, α-1-acid glycoprotein, PLG – plasminogen, THBS1, 2 – thrombospondine 1 and 2, TLR4 – toll-like receptor type 4.

Apart from proteins, other substances with cytotoxic and pro-inflammatory properties are adsorbed on polymer beads. In-vitro experiments have shown that the beads efficiently disrupt the complex between albumin and bilirubin, removing bile pigment and other bile acids from circulation (Gemelli et al., 2019; Chen et al., 2016). Several case reports have also described effective bilirubin removal in intraoperative settings or in critically ill patients with hyperbilirubinemia (Singh, 2019; Piwowarczyk et al., 2019; Calabro et al., 2019). Bilirubin and bile acids possessing detergent properties are factors, possibly contributing to functional alterations in cultured endothelial cells, described in sections 4.3.1-4.3.4. Previous *in vitro* studies confirmed that addition of bile acids to cultured endothelial cells activates ROS, NF-κB and p38 signaling pathways and induces expression of adhesion molecules (Qin et al., 2006).

Furthermore, free hemoglobin (HB) and heme could potentially contribute to endothelial dysfunction (Frimat et al., 2019; Petrillo et al., 2018; Vinchi & Tolosano, 2013). Since HB can be bound to the CytoSorb filter matrix (Gleason et al., 2019), we cannot exclude presence of cell-free HB and HB metabolites in the elution fractions used to treat ECs. Heme can be potentially protein-bound in the elutions due to presence of protein carriers like ALB, HBB, HBD, HRG, and HPX (recovered in all samples obtained from filter used during cardiac surgery with CPB; Suppl. table 11). It was previously shown that protein-associated heme does not trigger inflammation in cultured human endothelial cells compared to free heme

(Vallelian et al., 2018). In different types of primary ECs culture in the presence of free HB caused strong inflammatory response. Free HB and HB denaturation products can induce oxidative transformation of other molecules (i.e., LDL) inflicting additional cell damage (Schaer et al., 2013).

Exposure to oxidized phospholipids can also result in the activation of amino acid and folate metabolism with distinct overexpression of MTHFD2 (Hitzel et al., 2018). Treatment with fraction, eluted from CytoSorb matrix led to increase in mRNA levels of cystatione synthase (CBS), an enzyme converting homocysteine into cystatione, with subsequent enzymatic transformation into cysteine (Fig. 45). Homocysteine is a known modulator of endothelial dysfunction and one of the key players in pathogenesis of atherothrombosis (Lai & Kan, 2015; Pushpakumar et al., 2014). Exposure of ECs to this metabolite *in vitro* was shown to have anti-angiogenic (Rodríguez-Nieto et al., 2002) and pro-inflammatory effects (Esse et al., 2019), triggering ER stress and activation of the UPR (Austin et al., 2004). Homocysteine might be bound to the polymer matrix and can be subsequently eluted from it, being another candidate substance, potentially contributing to the functional and metabolic changes in ECs that were observed.

5.6. Changes observed in endothelial cells upon exposure to protein mixture eluted from CytoSorb matrix

5.6.1. Discrepancies between cell transcriptomics and protein abundance in the treated endothelial cells

Several targets were not proven to be up-regulated on protein level accordingly to mRNA-array data. One of the proteins demonstrating such a discrepancy is stanniocalcin 1 (STC1), a glycoprotein secreted by a number of human tissues and primarily exerting regulation of calcium and phosphate metabolism (Guo et al., 2013). Experiments with cultured ECs confirm that STC1 mediates monolayer permeability and trans-endothelial migration of leukocytes (Chen et al., 2008; Chakraborty et al., 2007). STC1 is hypothesized to be a natural endogenous anti-inflammatory agent, limiting the site of tissue injury by preventing excessive migration of immune cells (Mohammadipoor et al., 2016). STC1 has pleiotropic effects in different tissues. A growing body of evidence connects STC1 expression to tumor angiogenesis, identifying this gene as one of multiple hypoxia-induced genes, playing role in hypoxia-induced angiogenesis (Ho et al., 2005; Klein et al., 2009). In endothelial cells, STC1 regulates gene expression and has multiple metabolic and cytoprotective effects, including ROS inhibition (Sheikh-Hamad, 2009; Huang et al., 2012), maintaining glycolysis, mitochondrial bioenergetics, and mitochondrial calcium levels (Zhang et al., 2019).

Contrary to the array data, protein levels of STC1 were significantly lower in elution-treated cells (shown in the section 4.3.6.1.1). Since STC1 is a secreted protein, we assumed that levels of STC1 in whole cell lysate could be reduced due to rapid secretion, and our experiment with intracellular protein transport blockage partially proves it (Fig. 36, section 4.3.6.1.1). Initial attempts to use protein transport inhibitor (PTIC) in 1× and 0.5× concentrations for 24 hours led to severe reduction in cell viability, altered morphology and detachment of the cells. However, adjustment of PTIC concentration to 0.1× (corresponding to 1 µM Brefeldin A and 0.2 µM Monensin), and reduced time of exposure (14 hours) led to accumulation of STC1 in the cells resulting in significant differences detected with immunoblotting in 3 independent experiments. Results of this experiment have to be taken

into consideration with a grain of salt, since Brefeldin A and Monensin have multiple off-target effects on endothelial cells. Both agents cause ER stress and can initiate unfolded protein response (UPR) pathway (Iurlaro & Muñoz-Pinedo, 2015), involving phosphorylation of eIF2a and up-regulation of downstream transcription factors, i.e., ATF4 subsequently tackling downstream metabolic regulators.

Asparagine synthetase (ASNS) was another protein which was not up-regulated on the protein level when validated via immunobloting (section 4.3.6.1.1), contrary to the mRNA-array data. There are several possible reasons for such a discrepancy between mRNA data and protein levels. Posttranslational mRNA regulation can be one of the reasons for these dicrepancies. For example, synthesized mRNA can be regulated by micro-RNAs and thereby degraded before translation into the protein (Liu et al., 2016). It was described that ASNS mRNA has a half-life of 9 hours and periodic circadian up-regulation in cell culture experiments (Lorenzi et al., 2008). Little is known about the enzymatic activity of ASNS in human cells, perhaps the protein half-life is too short and protein degradation takes place quite quickly after the protein synthesis, thus detection of increased cellular levels of this enzyme is technically difficult and requires additional experimental approaches to control the rate of protein synthesis or turnover. In addition, up-regulation of the above-mentioned enzyme might take place in a cascade-like manner: excessive expression of one leads to increased mRNA levels of others, however protein synthesis might not keep up with increased demands. Previous studies have identified that ASNS can be localized on the outer cytoplasmatic membrane of the cells and can be secreted (He et al., 2011). Potential secretion of ASNS could not be investigated by introducing inhibitor of intracellular protein transport, due UPR-activating properties of Brefeldin A and Monensin (*vide supra*, Iurlaro & Muñoz-Pinedo, 2015), actively up-regulating ATF4 and ASNS, correspondingly.

Massive down-regulation of key mitotic processes also explains low mRNA and protein levels of all targets, involved into regulation of cell cycle, described in section 4.3.6.2. In contrast, targets like KIF20A and BUB1 tend to accumulate during G1 and S phase of cell cycle, and their levels are dramatically reduced after mitosis (Klebig et al., 2009; Chen et al., 2012). Cell cycle delay and reduced number of proliferating cells can result in reduced mRNA in protein abundance for the mitosis- implicated targets.

5.6.2. Discrepancies between up-regulation of metabolism controllers and observed functional alterations in endothelial cells

A battery of targets, controlling different aspects of cell metabolism were up-regulated in response to 24-hour treatment with eluted proteins. Global alterations in expression of metabolic controllers (enzymes, receptors and transcription factors) are shown in Suppl. table 20.

Several targets, significantly up-regulated on mRNA level, also have demonstrated increased abundance on protein level when validated with immunoblot. Phosphoserine aminotransferase (PSAT1) is a cytosolic protein that catalyzes biosynthesis of L-serine from 3-phospho-D-glycerate (Luo, 2011, Fig. 45). Serine metabolism plays one of the key roles in multiple biosynthetic reactions as well as signaling in ECs. Serine is necessary for the biosynthesis of other AAs, sphingolipids and phosphatidylserine. It serves as a donor of one-carbon units for folate cycle and is a precursor for glycine and cysteine synthesis (Oberkersch & Santoro, 2019). Overexpression of this enzyme was shown to play a role in cancer, being

responsible for robust proliferation and angiogenesis in multiple cancer types (Vie et al., 2008; Gao et al., 2017; Mattaini et al., 2016). PSAT1 overexpression is related to poor response to chemotherapy and worse clinical prognosis in cancer patients (Liu et al., 2016; Liao et al., 2016; Dai et al., 2019; Qian et al., 2017). In ECs, enhanced serine biosynthesis is related to angiogenesis in cancer. Cancer ECs express considerably higher amounts of phosphoglycerate dehydrogenase (PHGDH) and PSAT1, contributing to biomass production, DNA biosynthesis, promoting proliferation and survival (Bierhausl et al., 2017; Vandekeere et al., 2018; Li et al., 2019). However, studies reporting the role of serine biosynthesis in maintenance of normal ECs function are scarce (de Bock et al., 2013).

Seryl-tRNA synthase (SARS) was also up-regulated according to the mRNA-array data (see suppl. table 15). This enzyme was shown to exhibit anti-angiogenic properties (Shi et al., 2014). SARS forms a complex with transcription factor Yin Yang 1 (YY1) and subsequently binds to the VEGFA-promoter in the cell nucleus. SARS-YY1 complex acts as an antagonist of transcription factor c-Myc, prohibiting VEGFA-mediated sprouting angiogenesis (Fu et al., 2017).

Other up-regulated amino-acyl tRNA synthetases: alanyl- (AARS), cysteinyl- (CARS), isoleucyl- (IARS) and glycyl- (GARS) (suppl. table 20) do not exhibit any anti-angiogenic properties and might reflect amino acid deficiency in response to treatment with eluted proteins. Together with up-regulation in mRNA levels of eukaryotic translation initiation factor 2A (EIF2A) this might be an evidence of amino acid response (AAR) activation with subsequent increase in expression of ATF4 and downstream metabolic regulators (ASNS, PSAT, MTHFD2, etc.), see Fig. 46.

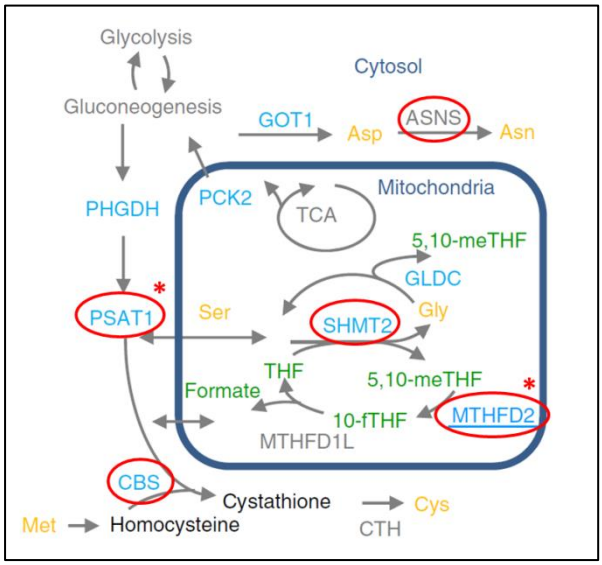

Figure 45: Metabolic crossroad between glycolysis, AA, nucleotide and fatty acid biosynthesis. Depicted enzymes regulate biosynthesis of serine (Ser), glycine (Gly), cysteine (Cys), methionine (Met), aspartate (Asp), asparagine (Asn) and inter-conversion of tetrahydrofolates (THF) in mitochondria. Image was adapted from Hitzel et al., 2018. Enzymes, up-regulated in the cells after 24 hour treatment with eluted protein fractions according to mRNA array data are highlighted with red frames; enzymes, proven to be up-regulated on protein level are marked with asterisk.
Abbreviations: 5,10-meTHF – 5,10-Methenyltetrahydrofolate, 10-fTHF – 10-formyltetrahydrofolate, ASNS – asparagine synthetase, CBS – cystathione-beta-synthase, GOT1 – glutamic-oxaloacetic transaminase 1, GLDC – glycine decarboxylase, MTHFD1L – methylentetrahydrofolate dehydrogenase 1-like, MTHFD2 – methylenetetrahydrofolate dehydrogenase, PCK2 – phosphoenolpyruvate carboxykinase 2, PHGDH – phosphoglycerate dehydrogenase, PSAT1 – pshosphoserine aminotransferase 1, SHMT2 – serine hydroxymethyltransferase 2, TCA – tricarboxylic acid cycle, THF – tetrahydrofolates.

Asparagine synthetase (ASNS) was another majorly up-regulated enzyme involved into amino acid metabolism (according to mRNA data, shown in suppl. tables 15 and 20). ASNS is a cytosolic ATP-dependent enzyme, converting aspartate and glutamine to asparagine and glutamate. It is expressed ubiquitously in multiple tissues. Expression of this enzyme is essential for cell growth and proliferation and is controlled by several activating transcription factors (ATF2, ATF3, ATF4, ATF5 and ATF6). Increased rates of ASNS expression

are observed in cancer cells due to intensive cell growth and proliferation under starvation conditions. In endothelial cells, asparagine metabolism and ASNS is particularly important for vessel sprouting and angiogenesis (Li et al., 2019). In non-cancer cells, ASNS gene transcription can be intensified as a response to limited amino acid consumption, amino acid response (AAR) or as a part of unfolded protein response (UPR) in endoplasmic reticulum (ER) due to ER-stress (Balasubramanian et al., 2013; Lomelino et al., 2017, Fig. 46).

MTHFD2 is a mitochondrial enzyme, mediating cross-talk between amino acid, folate metabolism and glycolysis (Fig. 45). MTHFD2 has low or undetectable expression levels in differentiated normal tissues, but is up-regulated in cancer, transformed cells, and developing embryos (Nilsson et al., 2014). Over-expression of MTHFD2 is fueling malignant cells with purine increasing cell survival and proliferation (Tedeshi et al., 2015; Konno et al., 2017; Lin et al., 2018; He et al., 2020). Several clinical studies have demonstrated that MTHFD2 might be predictor of poor outcome in cancer patients and is increasing the risk of metastasis and cancer recurrence (Liu et al., 2016; Nilsson et al., 2019).

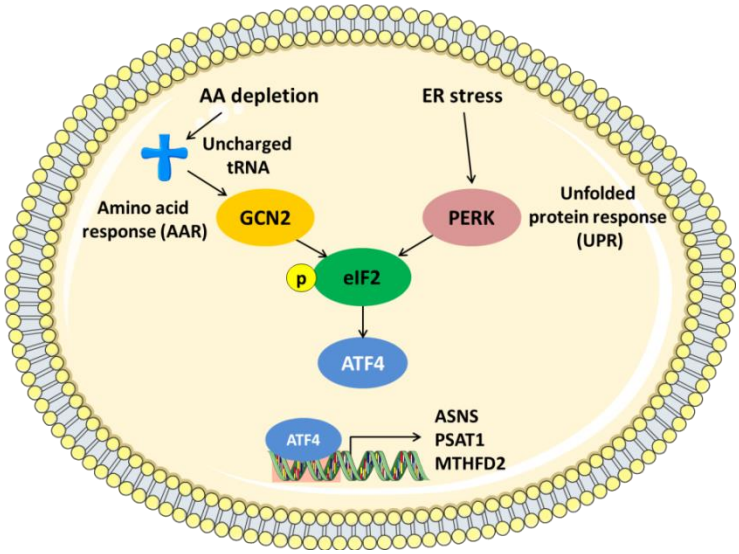

Figure 46: Pathways regulating ATF4-mediated gene expression. Depletion of amino acids increases the abundance of the corresponding uncharged tRNAs and subsequent activation of the GCN2 kinase. On the other hand, endoplasmic reticulum stress (ER stress) activates the UPR. Each stress condition increases phosphorylation of eIF2-kinase. Phosphorylation of eIF2 slows global protein synthesis, but paradoxically increases translation of a subset of mRNAs, including that for the transcription factor ATF4 that binds to gene promoters, inducing expression of ASNS, PSAT1 and MTHFD2 among others. Image is reproduced and adapted from Lomelino et al., 2017, using Servier Smart Art vector graphics, distributed under CC BY-NC 4.0 license.

Abbreviations: AA – amino acid, AAR – amino acid response, ASNS – asparagine synthetase, ATF4 – activating transcription factor 4, eIF2 - eukaryotic initiation factor 2, ER – endoplasmic reticulum, GCN2 – general control nonderepressible 2 serine/threonine-protein kinase, MTHFD2 – methylenetetrathydrofolatedehydrogenase 2, p-eIF2 – phosphorylated eukaryotic initiation factor 2, PERK - protein kinase RNA-like endoplasmic reticulum kinase, PSAT1 – phosphoserine aminotransferase 1, tRNA – transfer RNA, UPR – unfolded protein response.

In our experiments, protein abundance of MTHFD2 was increased by 1.5 times compared to untreated control, along with 3 times increase in protein abundance of PSAT1, and increased mRNA-levels of SHMT2 indicates towards increased activity of folate metabolism. These changes, combined with increased expression of multiple amino-acid metabolism controllers should result in enhanced proliferation, survival and migration (as in tumor endothelial cells, discussed *vide supra*). However, we did not observe any enhanced functionality of ECs (attachment, proliferation, migration etc.) due to several potential reasons. On one hand, metabolic changes might be compensatory due to activation of AAR and/or UPR in response to eluted proteins exposure. On the other hand, down-regulation of a massive battery of genes, responsible for cell cycle regulation might outweigh metabolic changes, causing

disproportional negative changes in the cells and leading to ultimate decline in viability, metabolism and migratory capacity.

5.6.3. Increased synthesis of pro-coagulant factors in endothelial cells

Both PAI-1 and tPA can be synthesized and secreted by ECs into circulation; these molecules are crucial for proper maintenance of physiological balance between coagulation and fibrinolysis (Fig. 47). ECs can produce an excessive amount of pro-coagulant, anti-fibrinolytic substances as a response to pro-inflammatory stimuli (e.g. cytokines, endotoxin). Tissue-type plasminogen activator (tPA) is a major activator of fibrinolysis, cleaving plasminogen to plasmin and is secreted by vascular endothelial cells (Urano et al., 2018). Plasminogen activator inhibitor-1 (PAI-1) is a serine-protease inhibitor secreted by a number of tissues (adipose tissue, endothelium, hepatocytes). It acts as an inhibitor of tPA, acting as a crucial negative regulator of fibrinolysis; PAI-1/tPA ratio represents the balance between endogenous systems of clotting and fibrinolysis (Chapin & Hajjar, 2015; Colman, 2006).
Increased circulating levels of PAI-1 and ratio between PAI-1 and tPA were widely discussed as potential tools to assess the risk of thrombotic vascular events and bleedings (Tofler et al., 2016; Ozolina et al., 2012). Recent systematic review and meta-analysis highlights the role of PAI-1 as potential predictor of disease severity and all-cause mortality in patients with sepsis (Tipoe et al., 2018). Increased production of PAI-1 can induce disseminated intravascular coagulation with subsequent tissue ischemia and organ dysfunction especially detrimental for septic patients. In patients undergoing cardiac surgery with CPB, PAI-1 levels were shown to predict postoperative atrial fibrillation (AF) (Fawzy et al., 2018; Pretorius et al., 2007). In post-operative settings, PAI-1 tends to increase (Colman, 2006), which together with CPB-induced endothelial dysfunction and enhanced endothelial production of PAI-1 can potentially result in thrombotic complications.

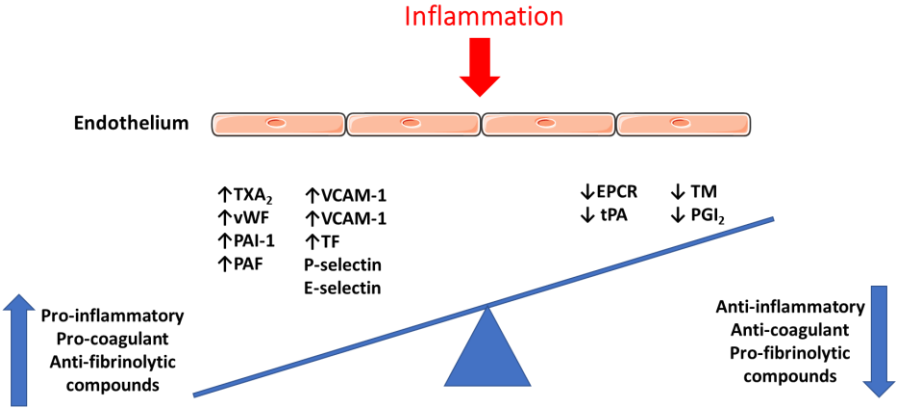

Figure 47: Secretion of pro-coagulant substances by ECs as a response to the inflammation (adaptation from Margetic, 2012). In response to pro-inflammatory stimuli, ECs produce pro-inflammatory, pro-coagulant and anti-fibrinolytic compounds, shifting the balance towards excessive coagulation and clot formation.

Abbreviations: ICAM-1 – intercellular adhesion molecule; PAI-1 – plasminogen activator inhibitor-1; PGI_2 - prostacyclin; TF – tissue factor; TM – thrombomodulin; tPA – tissue plasminogen activator; TXA_2 – thromboxane A2; VCAM-1 – vascular cell adhesion molecule; vWF – von Willebrand factor.

Inflammatory stimuli also increase biogenesis of specific granules in ECs – Weibel-Palade bodies (WPB) (Metcalf et al., 2008; Fig. 47). WPBs accumulate and release plethora of

biologically active molecules (monocyte chemoattractant protein-1, P-selectin, angiopoetin-2) along with von Willebrand factor (vWF) (McCormack et al., 2017; van Breevoort et al., 2012). VWF acts as an adhesive protein that mediates the recruitment of platelets to the endothelial surface and sub-endothelial matrix, facilitating formation of fibrin clot at the site of the injury (Schillemans et al., 2019; Springer, 2014). Clinical data suggests that concentration of vWF increases during CPB surgery as a result of endothelial activation (Tsang et al., 2008; Holdright et al., 1996; Valen et al., 1994). In patients undergoing mitral valve surgery, higher pre-operative plasma concentrations of vWF were associated with vasoplegia after valve surgery (Kortekaas et al., 2013). Study by Hernándes-Romero et al. (2016) indicates that there is a connection between the plasma vWF levels, tissue fibrosis and post-operative AF in ischemic patients (Hernándes-Romero et al., 2016).

Our findings together with *in vitro* observations (Poli et al., 2019), suggest that PAI-1 can be retained on the filter matrix (described in section 4.1.7). Plethora of pro-inflammatory factors also retained on the matrix (i.e. cytokines and CRP that can increase the production of PAI-1 and vWF in cultured endothelial cells). Therefore, the removal of these factors from circulation can be potentially beneficial in terms of prevention of endothelial dysfunction and concomitant thrombotic complications in post-operative period.

5.6.4. Limitations of the cell culture model

Considering the fact that we have applied a very complex protein mixture to the cultured endothelial cells, it remains elusive which proteins retained on the filter can produce such a tremendous outcome in terms of alterations in cell metabolism and viability, altering regenerative and proliferative potential of ECs. We cannot exclude that certain factors with high toxicity for the cells might be enriched on the filter, therefore treatment of ECs with elution does not accurately represent the situation in vivo, when susceptible endothelium is subjected to a number of pathophysiological assaults, pro-inflammatory plasma being just one of them. With our model we cannot explain the influence of other factors, attributing to endothelial damage during surgery with CPB, i.e. shear stress, hypoxia, hemodilution, aggregation and damage of blood cells (Gourlay & Gunaydin, 2012).

Use of serum control also imposes certain limitations for this model. Serum is a blood product obtained from the whole blood by coagulation with subsequent removal of fibrin clot. In comparison to plasma, some of the abundant coagulation factors (fibrinogen, high MW vWF) are depleted, certain proteins form complexes. During the coagulation process, blood cells can secrete a variety of factors into the serum (VEGF, chemokines MCP2, MCP3, MIP1β, MIP3α, PAI-1, MMP-9, and TIMP-1) (Ayache et al., 2006). Serum treatment can be more beneficial compared to elution due to the presence of erythrocyte- leukocyte- and platelet-derived factors. Differences in fibrinogen levels and other coagulation factors between serum and elution samples might explain why elution samples produce such profound functional alterations compared to serum control. Fibrinogen was among the most abundant proteins, identified universally in all of the elution samples (suppl. table 6). In cultured ECs, fibrinogen was shown to bind to ICAM-1 and integrin, causing phosphorylation of ERK and subsequent changes in cell morphology due to F-actin formation. These changes result in increased gaps between ECs and promote permeability of endothelial barrier (Tyagi et al., 2008). *In vitro* studies have shown that exposure of cultured ECs to fibrinogen results in ICAM-1 over-expression, thus mediating adhesion of leukocytes to endothelial surface

(Languino et al., 1993; Harley et al., 2000). Multiple studies emphasize that fibrinogen enhances endothelial migration and promotes angiogenesis (Dejana et al., 1985; Staton et al., 2005; Kaijzel et al., 2006; Kołodziejczyk et al., 2013). Therefore, changes in migratory capacity of ECs in our study cannot be attributed exclusively to presence of fibrinogen in the elutions.

Plasminogen was also eluted from all of the filters used for intraoperative HF. It is known that it binds to the surface of cultured ECs (Hajjar et al., 1986), being activated by secreted tPA and subsequently exerting fibrinolytic functions (Urano et al., 2002; Urano et al., 2018). Plasminogen can also be tethered to the endothelial surface by HRG, one of adapter proteins, identified in the elution (Jones et al., 2004; Fig. 44). When converted to plasmin, plasminogen might have deleterious effects on ECs. Exposure of cultured ECs to plasmin led to cell membrane damage and cell detachment (Okajima et al., 1995). Plasmin can activate ECs via annexin A2, followed by activation of Akt/NF-κB signaling, p38 and ERK1/2 phosphorylation, inducing the overexpression of ICAM-1 on endothelial surface (Dassah et al., 2009; Li et al., 2013).

Another limitation is related to the nature of cultured endothelial cells used for in vitro experiments with eluted proteins. HAECs are derived from aorta and are macrovascular endothelial cells, morphologically and physiologically different from the endothelium derived from microvascular beds (Brouillet et al., 2010). Sex- and age-dependent alterations in endothelial function (Hunter et al., 2019; Huxley et al., 2018; Brandes et al., 2005) could not be addressed in our experimental settings, using commercially available primary cells.

6. Conclusions and future directions

Polymer matrix of the CytoSorb devices binds multiple blood proteins during intraoperative hemofiltration. The majority of the proteins, which we could identify in the samples eluted from the filters used for intraoperative HF, had molecular weight below 60 kDa and were hydrophilic. Among all evaluated protein characteristics (molecular weight, protein length, isoelectric point, charge and hydrophobicity), only the protein length demonstrated significant correlation with relative protein abundance in the eluted protein fraction. Proteins, identified with LC-MS/MS, were mainly annotated as classic extracellular plasma proteins (enzyme inhibitors, enzymes, and transport molecules). Intracellular proteins accounted for 12.4% of all proteins identified on the filters used for intraoperative HF. Among small pro-inflammatory molecules with known in vitro binding to the polymer matrix, only PAI-1, S100A8, complement C3a and resistin were identified in the elutions with LC-MS/MS.

In our experimental settings we did not find convincing evidence of preferential binding of AGE-modified proteins to the polymer matrix. Further studies, employing LC-MS/MS with precise enrichment and/or labeling and quantification strategies are necessary to explore the modified protein binding in comparison to the unmodified counterparts.

Furthermore, we could detect measurable concentrations of CRP, IL-1β, IL-6, IL-8 and IL-10 in the eluted protein fractions with ELISA and CBA, IL-8 having the highest concentration among all cytokines. Patients with infective endocarditis tended to have higher levels of cytokines in the elution, however small number of patients and high inter-individual variability results in non-significant differences between the patient subgroups.

Our study was limited to the samples obtained from the patients undergoing valve surgery with CPB and HF, lacking samples from properly matched controls, undergoing the same type of intervention without HF. Taking into consideration this limitation, it is difficult to draw conclusion about significant contribution of HF into qualitative changes of plasma protein fractions. Changes in plasma samples, obtained from the patients, undergoing cardiac surgery with CPB can also occur due to hemodilution, surgical trauma and supplementation with donor FFP and other blood products.

In our functional analyses we found that endothelial cells, treated with plasma proteins, eluted from the polymer beads, demonstrate wide range of functional alterations, including impaired viability and metabolism, alteration in cell shape and attachment, as well as impaired lateral migration.

On mRNA level, down-regulation of a massive number of genes, involved in cell division happens within 24 hours of exposure with plasma proteins, derived from the filter matrix. These genes are mainly engaged in cytokinesis, formation of central spindle and mid-body. On protein level, significant reduction in relative abundance of kinesin superfamily protein 20A and mitotic checkpoint kinase BUB1 was confirmed.

Significant up-regulation of a cluster of genes, responsible for amino acid and mitochondrial one-carbon metabolism was observed on mRNA level and was verified with immunoblotting and immunocytochemistry. An increased expression of phosphoserine aminotransferase 1 and mitochondrial methyltetrahydrofolate reductase 2 does not translate into higher proliferation rates and better cell viability. Supported by the tendency towards increased ATF4 expression it indicates activation of unfolded protein response in the cell. In addition, the increased expression of metabolism enhancers is abolished by concomitant down-regulation of the plethora of other targets, crucial for survival and functional integrity of endothelium.

Proteins extracted from the filter matrix also contribute to endothelial activation by an increase in secretion of anti-fibrinolytic factor PAI-1. At the same time, secretion of tPA, possessing fibrinolytic properties, did not change significantly in our experiments. These alterations can cause changes in endothelial control of blood clotting and fibrinolysis, with a slant towards hyper-coagulation.

The results of our tests in cultured endothelial cells suggest that removal of a broad spectrum of plasma proteins via CytoSorb hemofiltration is potentially beneficial. It might exert protective properties by tackling an endothelial compound of systemic inflammatory dysregulation in patients with infective endocarditis undergoing valve surgery with CPB.

Inflammatory response starts after the initiation of surgery and extracorporeal circulation with inflammatory markers (interleukins, C-reactive protein, procalcitonin) peaking approximately by the end of first day post-operatively. Further studies are crucial to compare the spectrum and extent of adsorption of plasma proteins during intraoperative HF and HF in post-operative settings, performed in the ICU. Direct comparison of different polymer-bead-based filters is also an interesting avenue for research, crucially important for better understanding of HF and potential adverse events, associated with this type of treatment.

7. References

Achouiti, A; Vogl, T; van Till, JWO et al. (2013): S100A12 and Soluble Receptor for Advanced Glycation End Products Levels During Human Severe Sepsis. In *Shock* 40 (3), pp. 188–194. DOI: 10.1097/SHK.0b013e31829fbc38.

Aĝirbaşli, M; Nguyen, M-L; Win, K et al. (2010): Inflammatory and hemostatic response to cardiopulmonary bypass in pediatric population: feasibility of seriological testing of multiple biomarkers. In *Artificial organs* 34 (11), pp. 987–995. DOI: 10.1111/j.1525-1594.2010.01133.x.

Aird, WC. (2007): Phenotypic Heterogeneity of the Endothelium. In *Circulation Research* 100 (2), pp. 174–190. DOI: 10.1161/01.RES.0000255690.03436.ae.

Aird, WC. (2005): Spatial and temporal dynamics of the endothelium. In *Journal of Thrombosis and Haemostasis* 3 (7), pp. 1392–1406. DOI: 10.1111/j.1538-7836.2005.01328.x.

Aird, WC. (2003): The role of the endothelium in severe sepsis and multiple organ dysfunction syndrome. In *blood* 101 (10), pp. 3765–3777. DOI: 10.1182/blood-2002-06-1887.

Al-Fares, A; Pettenuzzo, T; Del Sorbo, L (2019): Extracorporeal life support and systemic inflammation. In *ICMx* 7 (S1), p. 246. DOI: 10.1186/s40635-019-0249-y.

Anderson, N L; Anderson, N G. (2002): The Human Plasma Proteome. In *Mol Cell Proteomics* 1 (11), p. 845. DOI: 10.1074/mcp.R200007-MCP200.

Andrades, M É; Lorenzi, R; Nagai, R et al. (2012): Plasma glycation levels are associated with severity in sepsis. In *European Journal of Clinical Investigation* 42 (10), pp. 1055–1060. DOI: 10.1111/j.1365-2362.2012.02694.x.

Anguizola, J; Matsuda, R; Barnaby, OS et al. (2013): Review: Glycation of human serum albumin. In *Clinica Chimica Acta* 425, pp. 64–76. DOI: 10.1016/j.cca.2013.07.013.

Ankawi, G; Xie, Y; Yang, B et al. (2019): What Have We Learned about the Use of Cytosorb Adsorption Columns? In *Blood Purif* 48 (3), pp. 196–202. DOI: 10.1159/000500013.

Apostolov, EO; Shah SV; Ray D; Basnakian A G. (2009): Scavenger Receptors of Endothelial Cells Mediate the Uptake and Cellular Proatherogenic Effects of Carbamylated LDL. In *Arteriosclerosis, Thrombosis, and Vascular Biology* 29 (10), pp. 1622–1630. DOI: 10.1161/ATVBAHA.109.189795.

Asai, A; Koseki, J; Konno, M et al. (2018): Drug discovery of anticancer drugs targeting methylenetetrahydrofolate dehydrogenase 2. In *Heliyon* 4 (12). DOI: 10.1016/j.heliyon.2018.e01021.

Ashburner, M.; Ball, C. A.; Blake, JA et al. (2000): Gene ontology: tool for the unification of biology. The Gene Ontology Consortium. In *Nat Genet* 25 (1), pp. 25–29. DOI: 10.1038/75556.

Asrar B M (2009): Targeting Endothelial Cell Surface Receptors: Novel Mechanisms of Microvascular Endothelial Barrier Transport. In *Journal of Medical Sciences* 2 (1), pp. 13–17.

Austin, R. C.; Lentz, S. R.; Werstuck, G. H. (2004): Role of hyperhomocysteinemia in endothelial dysfunction and atherothrombotic disease. In *Cell Death Differ* 11 (S1), pp. S56. DOI: 10.1038/sj.cdd.4401451.

Ayache, S; Panelli, M C.; Byrne, K M.; Slezak, S; Leitman, S F.; Marincola, F M.; Stroncek, D F. (2006). In *J Transl Med* 4 (1), p. 40. DOI: 10.1186/1479-5876-4-40.

Balasubramanian, M N.; Butterworth, E A.; Kilberg, M S. (2013): Asparagine synthetase: regulation by cell stress and involvement in tumor biology. In *Am J Physiol Endocrinol Metab* 304 (8), pp. E789.

Barbosa, M A.; Martins, MCL (Eds.) (2018): Peptides and Proteins as Biomaterials for Tissue Regeneration and Repair: Woodhead Publishing.

Baumann, A; Buchwald, D; Annecke, T et al. (2016): RECCAS - REmoval of Cytokines during CArdiac Surgery: study protocol for a randomised controlled trial. In *Trials* 17 (1), p. 137. DOI: 10.1186/s13063-016-1265-9.

Bejarano, E; Taylor, A (2019): Too sweet: Problems of protein glycation in the eye. In *Experimental Eye Research* 178, pp. 255–262. DOI: 10.1016/j.exer.2018.08.017.

Bernardi, MH.; Rinoesl, H; Dragosits, K et al. (2016): Effect of hemoadsorption during cardiopulmonary bypass surgery – a blinded, randomized, controlled pilot study using a novel adsorbent. In *Critical Care* 20 (1), p. 96.

Berridge, BR.; Van Vleet, JF.; Herman, E (2013): Chapter 46 - Cardiac, Vascular, and Skeletal Muscle Systems. In Wanda M. Haschek, Colin G. Rousseaux, Matthew A. Wallig (Eds.): Haschek and Rousseaux's Handbook of Toxicologic Pathology (Third Edition). Boston: Academic Press, pp. 1567–1665.

Bierhansl, L; Conradi, L-C; Treps, L et al. (2017): Central Role of Metabolism in Endothelial Cell Function and Vascular Disease. In *Physiology (Bethesda)* 32 (2), pp. 126–140. DOI: 10.1152/physiol.00031.2016.

Bierhaus, A.; Nawroth, P. P. (2009): Multiple levels of regulation determine the role of the receptor for AGE (RAGE) as common soil in inflammation, immune responses and diabetes mellitus and its complications. In *Diabetologia* 52 (11), pp. 2251–2263. DOI: 10.1007/s00125-009-1458-9.

Billings, FT; Ball, SK; Roberts, LJ; Pretorius, M (2011): Postoperative acute kidney injury is associated with hemoglobinemia and an enhanced oxidative stress response. In *Free Radic Biol Med* 50 (11), pp. 1480–1487.

Bito, R; Hino, S; Baba, A et al. (2005): Degradation of oxidative stress-induced denatured albumin in rat liver endothelial cells. In *American Journal of Physiology-Cell Physiology* 289 (3), pp. C531.

Boehne, M; Sasse, M; Karch, A et al. (2017): Systemic inflammatory response syndrome after pediatric congenital heart surgery: Incidence, risk factors, and clinical outcome. In *J Card Surg* 32 (2), pp. 116–125.

Boisrame-Helms J; Kremer H; Schini-Kerth V; Meziani F (2013): Endothelial Dysfunction in Sepsis. In *Current Vascular Pharmacology* 11, p. 150. Available online at https://doi.org/10.2174/1570161111311020005.

Bonavia, A.; Groff, A.; Karamchandani, K.; Singbartl, K. (2018): Clinical Utility of Extracorporeal Cytokine Hemoadsorption Therapy: A Literature Review. In *Blood Purif* 46 (4), pp. 337–349. DOI: 10.1159/000492379.

BRANDES, R.; FLEMING, I.; BUSSE, R. (2005): Endothelial aging. In *Cardiovascular Research* 66 (2), pp. 286–294.

Braun, I.; Deppe, A. C.; Weber, C.; Mihaylova, M.; Paunel-Görgülü, A.; Schlachtenberger, G. et al. (2018): Limitation of Circulating cfDNA Under the Use of a Cytokine Elimination Adsorber (CytoSorb) in Cardiac Surgery. In *Thorac cardiovasc Surg* 66 (S 01), pp. DGTHG-KV87. DOI: 10.1055/s-0038-1628092.

Brewster, L; Brey, E M.; Greisler, H P. (2014): Chapter 39 - Blood Vessels. In Robert Lanza, Robert Langer, Joseph Vacanti (Eds.): Principles of Tissue Engineering (Fourth Edition). Boston: Academic Press, pp. 793–812.

Brouillet, S; Hoffmann, P; Benharouga, M; Salomon, A; Schaal, J-P; Feige, J-J et al. (2010): Molecular Characterization of EG-VEGF-mediated Angiogenesis: Differential Effects on Microvascular and Macrovascular Endothelial Cells. In *MBoC* 21 (16), pp. 2832–2843. DOI: 10.1091/mbc.e10-01-0059.

Brouwer, WP; Duran, S; Kuijper, M; Ince, C (2019): Hemoadsorption with CytoSorb shows a decreased observed versus expected 28-day all-cause mortality in ICU patients with septic shock: a propensity-score-weighted retrospective study. In *Crit Care* 23 (1), p. 2095. DOI: 10.1186/s13054-019-2588-1.

Brown, DL. (Ed.) (2019): Cardiac Intensive Care (Third Edition). Philadelphia: Content Repository Only!

Bteich, M (2019): An overview of albumin and alpha-1-acid glycoprotein main characteristics: highlighting the roles of amino acids in binding kinetics and molecular interactions. In *Heliyon* 5 (11), pp. e02879.

Cahill, TJ.; Baddour, LM.; Habib, G et al. (2017): Challenges in Infective Endocarditis. In *Journal of the American College of Cardiology* 69 (3), pp. 325–344. DOI: 10.1016/j.jacc.2016.10.066.

Calabrò, MG; Febres, D; Recca, G et al. (2019): Blood Purification With CytoSorb in Critically Ill Patients: Single-Center Preliminary Experience. In *Artif Organs* 43 (2), pp. 189–194. DOI: 10.1111/aor.13327.

Chakraborty, A; Brooks, H; Zhang, P et al. (2007): Stanniocalcin-1 regulates endothelial gene expression and modulates transendothelial migration of leukocytes. In *Am J of Phys-Renal Physiology* 292 (2), pp. F895.

Chapin, JC; Hajjar, KA. (2015): Fibrinolysis and the control of blood coagulation. In *Blood Reviews* 29 (1), pp. 17–24. DOI: 10.1016/j.blre.2014.09.003.

Chapter 33 - Actin and Actin-Binding Proteins (2017). In Thomas D. Pollard, William C. Earnshaw, Jennifer Lippincott-Schwartz, Graham T. Johnson (Eds.): Cell Biology (Third Edition): Elsevier, pp. 575–591.

Chaudhuri, J; Bains, Y; Guha, S et al. (2018): The Role of Advanced Glycation End Products in Aging and Metabolic Diseases: Bridging Association and Causality. In *Cell Metabolism* 28 (3), pp. 337–352.

Chen C; Jamaluddin M; Yan S; Sheikh-Hamad D; Yao Q (2008): Human Stanniocalcin-1 Blocks TNF-α–Induced Monolayer Permeability in Human Coronary Artery Endothelial Cells. In *Arteriosclerosis, Thrombosis, and Vascular Biology* 28 (5), pp. 906–912. DOI: 10.1161/ATVBAHA.108.163667.

Chen, C-T; Hehnly, H; Doxsey, S J. (2012): Orchestrating vesicle transport, ESCRTs and kinase surveillance during abscission. In *Nature Reviews Molecular Cell Biology* 13 (8), pp. 483–488. DOI: 10.1038/nrm3395.

Chen, J; Han, W; Chen, J; Zong, W; Wang, W; Wang, Y et al. (2016): High performance of a unique mesoporous polystyrene-based adsorbent for blood purification. In *rb* 4 (1), pp. 31–37. DOI: 10.1093/rb/rbw038.

Chignalia, A Z.; Weinberg, G; Dull, R O. (2020): Norepinephrine Induces Lung Microvascular Endothelial Cell Death by NADPH Oxidase-Dependent Activation of Caspase-3. In *Oxidative Medicine and Cellular Longevity* 2020 (4), pp. 1–11. DOI: 10.1155/2020/2563764.

Chiu, WC; Lin, JY; Lee, TS et al. (2013): β2-Glycoprotein I inhibits VEGF-induced endothelial cell growth and migration via suppressing phosphorylation of VEGFR2, ERK1/2, and Akt. In *Mol Cell Biochem* 372 (1-2), pp. 9–15.

Chu, L-Y; Ramakrishnan, D P; Silverstein, R L. (2013): Thrombospondin-1 modulates VEGF signaling via CD36 by recruiting SHP-1 to VEGFR2 complex in microvascular endothelial cells. In *Blood* 122 (10), pp. 1822–1832. DOI: 10.1182/blood-2013-01-482315.

Chuah, Y K; Basir, R; Talib, H; Tie, T H; Nordin, N (2013): Receptor for Advanced Glycation End Products and Its Involvement in Inflammatory Diseases. In *International Journal of Inflammation* 2013, p. 15.

Chung, M J.; Brown, D L. (2019): 9 - Diagnosis of Acute Myocardial Infarction. In David L. Brown (Ed.): Cardiac Intensive Care (Third Edition). Philadelphia: pp. 91–98.e3.

Colman, R W. (2006): Hemostasis and thrombosis. Basic principles and clinical practice. 5th ed. Philadelphia: Lippincott Williams & Wilkins.

Cooper, J R., Giesecke, N. M (2015): Hemodilution and priming solutions. Fourth Edition: Wolters Kluwer Health (Cardiopulmonary Bypass and Mechanical Support: Principles and Practice).

Da Cruz, E M; Ivy, D; Jaggers, J (Eds.) (2014): Pediatric and Congenital Cardiology, Cardiac Surgery and Intensive Care. London: Springer London.

Däbritz, J; Langhorst, J; Lügering, A; Heidemann, J; Mohr, M; Wittkowski, H et al. (2013): Improving Relapse Prediction in Inflammatory Bowel Disease by Neutrophil-Derived S100A12. In *Inflammatory Bowel Diseases* 19 (6), pp. 1130–1138.

Dai, J; Wei, R; Zhang, P; Kong, B (2019): Overexpression of microRNA-195-5p reduces cisplatin resistance and angiogenesis in ovarian cancer by inhibiting the PSAT1-dependent GSK3β/β-catenin signaling pathway. In *J Transl Med* 17 (1), p. 190.

Dasgupta, A; Wahed, A (2014): Chapter 8 - Cardiac Markers. In Amitava Dasgupta, Amer Wahed (Eds.): Clinical Chemistry, Immunology and Laboratory Quality Control. San Diego: Elsevier, pp. 127–144.

Dasgupta, A; Wahed, A (Eds.) (2014): Clinical Chemistry, Immunology and Laboratory Quality Control. San Diego: Elsevier.

Dassah, M; Deora, A B.; He, K; Hajjar, K A. (2009): The endothelial cell annexin A2 system and vascular fibrinolysis. In *General physiology and biophysics* 28 Spec No Focus, pp. F20-8.

Datzmann, T; Träger, K (2017): Extracorporeal membrane oxygenation and cytokine adsorption. In *Journal of Thoracic Disease*, pp. S653-S660.

De Bock, K; Georgiadou, M; Carmeliet, P (2013): Role of Endothelial Cell Metabolism in Vessel Sprouting. In *Cell Metabolism* 18 (5), pp. 634–647. DOI: 10.1016/j.cmet.2013.08.001.

DeCicco-Skinner, K L.; Henry, G H.; Cataisson, C; Tabib, T; Gwilliam, J C; Watson, N J. et al. (2014): Endothelial cell tube formation assay for the in vitro study of angiogenesis. In *J Vis Exp* (91), pp. e51312. DOI: 10.3791/51312.

Dejana, E; Languino, LR.; Polentarutti, N et al. (1985): Interaction between fibrinogen and cultured endothelial cells. Induction of migration and specific binding. In *J. Clin. Invest.* 75 (1), pp. 11–18.

Denning, N-L; Aziz, M; Gurien, S D.; Wang, P (2019): DAMPs and NETs in Sepsis. In *Front. Immunol.* 10, pp. e187571. DOI: 10.3389/fimmu.2019.02536.

Devaraj, S; Xu, D Y; Jialal, I (2003): C-Reactive Protein Increases Plasminogen Activator Inhibitor-1 Expression and Activity in Human Aortic Endothelial Cells. In *Circulation* 107 (3), pp. 398–404.

Diab, M; Platzer, S; Guenther, A; Sponholz, C; Scherag, A; Lehmann, T et al. (2020): Assessing efficacy of CytoSorb haemoadsorber for prevention of organ dysfunction in cardiac surgery patients with infective endocarditis: REMOVE-protocol for randomised controlled trial. In *BMJ Open* 10 (3), pp. e031912.

Dieleman, J. M.; Peelen, L. M.; Coulson, T. G.; Tran, L.; Reid, C. M.; Smith, J. A. et al. (2017): Age and other perioperative risk factors for postoperative systemic inflammatory response syndrome after cardiac surgery. In *British Journal of Anaesthesia* 119 (4), pp. 637–644. DOI: 10.1093/bja/aex239.

Ding, Y; Kantarci, A; Hasturk, H et al. (2007): Activation of RAGE induces elevated O 2− generation by mononuclear phagocytes in diabetes. In *Journal of Leukocyte Biology* 81 (2), pp. 520–527.

Dubois, C; Marcé, D; Faivre, V et al. (2019): High plasma level of S100A8/S100A9 and S100A12 at admission indicates a higher risk of death in septic shock patients. In *Sci Rep* 9 (1), p. 801.

Esse, R; Barroso, M; Tavares de Almeida, I; Castro, R (2019): The Contribution of Homocysteine Metabolism Disruption to Endothelial Dysfunction: State-of-the-Art. In *IJMS* 20 (4), p. 867. DOI: 10.3390/ijms20040867.

Evora, Paulo Roberto Barbosa; Bottura, Camila; Arcêncio, Livia; Albuquerque, Agnes Afrodite Sumarelli; Évora, Patrícia Martinez; Rodrigues, Alfredo José (2016): Key Points for Curbing Cardiopulmonary Bypass Inflammation. In *Acta Cirurgica Brasileira* 31, pp. 45–52.

Fabian-Jessing, B K.; Massey, M J.; Filbin, M R.; Hou, P C.; Wang, H E.; Kirkegaard, H et al. (2018): In vivo quantification of rolling and adhered leukocytes in human sepsis. In *Crit Care* 22 (1), p. 240.

Fanali, G; Di Masi, A; Trezza, V; Marino, M; Fasano, M; Ascenzi, P (2012): Human serum albumin: From bench to bedside. In *Molecular Aspects of Medicine* 33 (3), pp. 209–290. DOI: 10.1016/j.mam.2011.12.002.

Fang, Y; Li, C; Shao, R; Yu, H; Zhang, Q (2018): The role of biomarkers of endothelial activation in predicting morbidity and mortality in patients with severe sepsis and septic shock in intensive care: A prospective observational study. In *Thrombosis Research* 171, pp. 149–154. DOI: 10.1016/j.thromres.2018.09.059.

Fawzy, S; Abdel AMF; El Badawy, MA; Mohamed, IH (2018): PAI-1 as a predictor after cardiopulmonary bypass for postoperative atrial fibrillation. In *Res Opin Anesth Intensive Care* 5 (1), p. 27.

Félétou M.: The Endothelium: Part 1: Multiple Functions of the Endothelial Cells—Focus on Endothelium-Derived Vasoactive Mediators. San Rafael (CA): Morgan & Claypool Life Sciences; 2011. Chapter 2, Multiple Functions of the Endothelial Cells.

Felgueiras, H. P.; Antunes, J. C.; Martins, M. C. L.; Barbosa, M. A. (2018): 1 - Fundamentals of protein and cell interactions in biomaterials. In Mário A. Barbosa, Martins, M. Cristina L (Eds.): Peptides and Proteins as Biomaterials for Tissue Regeneration and Repair: Woodhead Publishing, pp. 1–27.

Feri, M (2019): "In vitro comparison of the adsorption of inflammatory mediators by blood purification devices": a misleading article for clinical practice? In *Intensive Care Med Exp* 7 (1), p. 5.

Flier, S; Concepcion, AN.; Versteeg, D; Kappen, TH.; Hoefer, IE.; de Lange, D W et al. (2015): Monocyte hyporesponsiveness and Toll-like receptor expression profiles in coronary artery bypass grafting and its clinical implications for postoperative inflammatory response and pneumonia: An observational cohort study. In *European journal of anaesthesiology* 32 (3), pp. 177–188. DOI: 10.1097/EJA.0000000000000184.

Foell, Dirk; Wittkowski, Helmut; Vogl, Thomas; Roth, Johannes (2007): S100 proteins expressed in phagocytes: a novel group of damage-associated molecular pattern molecules. In *Journal of Leukocyte Biology* 81 (1), pp. 28–37. DOI: 10.1189/jlb.0306170.

Freise, Nicole; Burghard, Alina; Ortkras, Theresa; Daber, Niklas; Imam Chasan, Achmet; Jauch, Saskia-L. et al. (2019): Signaling mechanisms inducing hyporesponsiveness of phagocytes during systemic inflammation. In *blood* 134 (2), pp. 134–146. DOI: 10.1182/blood.2019000320.

Friesecke, S; Träger, K; Schittek, G A. et al. (2019): International registry on the use of the CytoSorb® adsorber in ICU patients. In *Medizinische Klinik - Intensivmedizin und Notfallmedizin* 114 (8), pp. 699–707. DOI: 10.1007/s00063-017-0342-5.

Frimat, M; Boudhabhay, I; Roumenina, L T. (2019): Hemolysis Derived Products Toxicity and Endothelium: Model of the Second Hit. In *Toxins* 11 (11), p. 660. DOI: 10.3390/toxins11110660.

Frommhold, D; Kamphues, A; Hepper, I et al. (2010): RAGE and ICAM-1 cooperate in mediating leukocyte recruitment during acute inflammation in vivo. In *Blood* 116 (5), pp. 841–849. DOI: 10.1182/blood-2009-09-244293.

Fu, C-Y; Wang, P-C; Tsai, H-J (2017): Competitive binding between Seryl-tRNA synthetase/YY1 complex and NFKB1 at the distal segment results in differential regulation of human vegfa promoter activity during angiogenesis. In *Nucleic Acids Research* 45 (5), pp. 2423–2437. DOI: 10.1093/nar/gkw1187.

Fu, Y. (2004): Norepinephrine induces apoptosis in neonatal rat endothelial cells via down-regulation of Bcl-2 and activation of β-adrenergic and caspase-2 pathways. In *Cardiovascular Research* 61 (1), pp. 143–151.

Fu, Y-C; Yin, S-C; Chi, C-S; Hwang, B; Hsu, S-L (2006): Norepinephrine induces apoptosis in neonatal rat endothelial cells via a ROS-dependent JNK activation pathway. In *Apoptosis* 11 (11), pp. 2053–2063. DOI: 10.1007/s10495-006-0192-8.

Fukuda, W; Daitoku, K; Minakawa, M; Fukui, K; Suzuki, Yi; Fukuda, I (2012): Infective endocarditis with cerebrovascular complications: timing of surgical intervention. In *Interact Cardiovasc Thorac Surg* 14 (1), pp. 26–30.

Fumagall, G; Panichi, V (2019): Chapter 151 - Biocompatibility of the Dialysis System. In Claudio Ronco, Rinaldo Bellomo, John A. Kellum, Zaccaria Ricci (Eds.): Critical Care Nephrology (Third Edition). Philadelphia. pp. 918–922.e2.

Gabay, C; Kushner, I (2001): Acute-phase Proteins (Major Reference Works). Available online at https://doi.org/10.1038/npg.els.0000497.

Gajahi S A; Catan, A; Giraud, P; Assouan K S; Guerin-Dubourg, A; Debussche, X et al. (2018): Glycation of human serum albumin impairs binding to the glucagon-like peptide-1 analogue liraglutide. In *J. Biol. Chem.* 293 (13), pp. 4778–4791. DOI: 10.1074/jbc.M117.815274.

Gao, S; Ge, A; Xu, S; You, Z; Ning, S; Zhao, Y; Pang, D (2017): PSAT1 is regulated by ATF4 and enhances cell proliferation via the GSK3β/β-catenin/cyclin D1 signaling pathway in ER-negative breast cancer. In *Journal of Experimental & Clinical Cancer Research* 36 (1), p. 179. DOI: 10.1186/s13046-017-0648-4.

Gavet, O; Pines, J (2010): Progressive Activation of CyclinB1-Cdk1 Coordinates Entry to Mitosis. In *Developmental Cell* 18 (4), pp. 533–543. DOI: 10.1016/j.devcel.2010.02.013.

Gemelli, C.; Cuoghi, A.; Magnani, S.; Atti, M.; Ricci, D.; Siniscalchi, A. et al. (2019): Removal of Bilirubin with a New Adsorbent System: In Vitro Kinetics. In *Blood Purif* 47 (1-3), pp. 10–15. DOI: 10.1159/000492378.

Georgiou, C; Irons, J; Ghosh, S; Falter, F; Perrino, Jr (2015): Priming solutions for cardiopulmonary bypass circuits. In Sunit Ghosh, Florian Falter, Jr Perrino (Eds.): Cardiopulmonary Bypass. Cambridge: Cambridge University Press, pp. 42–50.

Geyer, P E.; Voytik, E; Treit, P V.; Doll, S; Kleinhempel, A; Niu, L et al. (2019): Plasma Proteome Profiling to detect and avoid sample-related biases in biomarker studies. In *EMBO Mol Med* 11 (11), pp. e10427. DOI: 10.15252/emmm.201910427.

Ghosh, S; Falter, F; Perrino, Jr (Eds.) (2015): Cardiopulmonary Bypass. Cambridge: Cambridge University Press.

Gleason, TG.; Argenziano, M; Bavaria, JE et al. (2019): Hemoadsorption to Reduce Plasma-Free Hemoglobin During Cardiac Surgery: Results of REFRESH I Pilot Study. In *Seminars in Thoracic and Cardiovascular Surgery* 31 (4), pp. 783–793.

Granger DN, Senchenkova E. (2010): Leukocyte–Endothelial Cell Adhesion. San Rafael (CA): Morgan & Claypool Life Sciences (Inflammation and the Microcirculation).

Gravlee, G P.; Davis, R F.; Hammon, J W.; Kussman, B (2016): Cardiopulmonary bypass and mechanical support. Principles and practice. Fourth edition. Philadelphia: Wolters Kluwer.

Greco, V; Piras, C; Pieroni, L; Urbani, A (2017): Direct Assessment of Plasma/Serum Sample Quality for Proteomics Biomarker Investigation. In David W. Greening, Richard J. Simpson (Eds.): Serum/Plasma Proteomics: Methods and Protocols. New York, NY: Springer New York, pp. 3–21.

Greening, D W.; Simpson, R J. (Eds.) (2017): Serum/Plasma Proteomics: Methods and Protocols. New York, NY: Springer New York.

Gruda, MC; Ruggeberg, KG; O'Sullivan, P et al. (2018): Broad adsorption of sepsis-related PAMP and DAMP molecules, mycotoxins, and cytokines from whole blood using CytoSorb® sorbent porous polymer beads. In *PLOS ONE* 13 (1), pp. e0191676. DOI: 10.1371/journal.pone.0191676.

Guo, F; Li, Y; Wang, J; Li, Y; Li, Y; Li, G (2013): Stanniocalcin1 (STC1) Inhibits Cell Proliferation and Invasion of Cervical Cancer Cells. In *PLOS ONE* 8 (1), pp. e53989. DOI: 10.1371/journal.pone.0053989.

Haidari, Z; Wendt, D; Thielmann, M et al. (2020): Intraoperative Hemoadsorption in Patients With Native Mitral Valve Infective Endocarditis. In *The Annals of Thoracic Surgery. DOI:* 10.1016/j.athoracsur.2019.12.067.

Hajjar, K. A.; Harpel, P. C.; Jaffe, E. A.; Nachman, R. L. (1986): Binding of plasminogen to cultured human endothelial cells. In *The Journal of biological chemistry* 261 (25), pp. 11656–11662.

Hamasaki, M Y; Barbeiro, H V; Souza, H P; Machado, M C C; Silva, F P (2014): sRAGE in septic shock: a potential biomarker of mortality. In *Revista Brasileira de Terapia Intensiva* 26 (4). DOI: 10.5935/0103-507X.20140060.

Harley, S L.; Sturge, J; Powell, J T. (2000): Regulation by Fibrinogen and Its Products of Intercellular Adhesion Molecule-1 Expression in Human Saphenous Vein Endothelial Cells. In *Arterioscler Thromb Vasc Biol* 20 (3), pp. 652–658.

Harm, S.; Schildböck, C.; Hartmann, J. (2019): Cytokine Removal in Extracorporeal Blood Purification: An in vitro Study. In *Blood Purif. DOI:* 10.1159/000502680.

Haschek, W M.; Rousseaux, C G.; Wallig, M A. (Eds.) (2013): Haschek and Rousseaux's Handbook of Toxicologic Pathology (Third Edition). Boston: Academic Press.

Hassan, K; Kannmacher, J; Wohlmuth, P; Budde, U; Schmoeckel, M; Geidel, S (2019): Cytosorb Adsorption During Emergency Cardiac Operations in Patients at High Risk of Bleeding. In *The Annals of Thoracic Surgery* 108 (1), pp. 45–51.

Hawlik K.; Wild C.: Extracorporeal cytokine haemadsorption therapy in patients with sepsis or SIRS, Decision Support Document. Available online at http://eprints.hta.lbg.ac.at/1129/1/DSD_106.pdf.

He, H; Li, P-C; Jia, W; Hu, B; Ji, C-S (2020): High Expression of Methylenetetrahydrofolate Dehydrogenase 2 (MTHFD2) in Esophageal Squamous Cell Carcinoma and its Clinical Prognostic Significance. In *Med Sci Monit* 26. DOI: 10.12659/MSM.920259.

He, Y; Li, B; Luo, C; Shen, S; Chen, J; Xue, H et al. (2011): Asparagine synthetase is partially localized to the plasma membrane and upregulated by L-asparaginase in U937 cells. In *Journal of Huazhong University of Science and Technology [Medical Sciences]* 31 (2), pp. 159–163. DOI: 10.1007/s11596-011-0243-4.

Hendrickson, C M.; Matthay, M A. (2018): Endothelial biomarkers in human sepsis: pathogenesis and prognosis for ARDS. In *Pulm Circ* 8 (2), pp. 2045894018769876. DOI: 10.1177/2045894018769876.

Hernández-Romero, D; Lahoz, Á; Roldan, V et al. (2016): Von Willebrand factor is associated with atrial fibrillation development in ischaemic patients after cardiac surgery. In *Europace* 18 (9), pp. 1328–1334. DOI: 10.1093/europace/euv354.

Herwig, R; Hardt, C; Lienhard, M; Kamburov, A (2016): Analyzing and interpreting genome data at the network level with ConsensusPathDB. In *Nat Protoc* 11 (10), pp. 1889–1907. DOI: 10.1038/nprot.2016.117.

Hirsh, SL.; McKenzie, DR.; Nosworthy, NJ et al. (2013): The Vroman effect: Competitive protein exchange with dynamic multilayer protein aggregates. In *Colloids and Surfaces B: Biointerfaces* 103, pp. 395–404.

Hitzel, J; Lee, E; Zhang, Y et al. (2018): Oxidized phospholipids regulate amino acid metabolism through MTHFD2 to facilitate nucleotide release in endothelial cells. In *Nat Commun* 9 (1), p. 620. DOI: 10.1038/s41467-018-04602-0.

Hoen, B; Duval, X (2013): Infective Endocarditis. In *N Engl J Med* 368 (15), pp. 1425–1433. DOI: 10.1056/NEJMcp1206782.

Hofer, S; Uhle, F; Fleming, T; Hell, C; Schmoch, T; Bruckner, T et al. (2016): RAGE-mediated inflammation in patients with septic shock. In *Journal of Surgical Research* 202 (2), pp. 315–327. DOI: 10.1016/j.jss.2016.01.019.

Hoffmann J. (2013): Sepsistherapie. Berlin, Heidelberg: Springer-Verlag (Chirurgie Basisweiterbildung).

Hofmann Bowman, M. A.; Heydemann, A.; Gawdzik, J.; Shilling, R. A.; Camoretti-Mercado, B. (2011): Transgenic expression of human S100A12 induces structural airway abnormalities and limited lung inflammation in a mouse model of allergic inflammation. In *Clinical & Experimental Allergy* 41 (6), pp. 878–889.

Holdright, D; Hunt, B; Parrat R. et al. (1995): The effects of cardiopulmonary bypass on systemic and coronary levels of von Willebrand factor. In *European Journal of Cardio-Thoracic Surgery* 9 (1), pp. 18–21. DOI: 10.1016/s1010-7940(05)80043-0.

Holland, T L.; Baddour, L M.; Bayer, A S.; Hoen, B; Miro, J M.; Fowler, V G, (2016): Infective endocarditis. In *Nat Rev Dis Primers* 2, p. 16059. DOI: 10.1038/nrdp.2016.59.

Holubcova, Z; Kunes, P; Mandak, J et al. (2014): Could Pentraxin 3 Be a New Diagnostic Marker for Excessive Inflammatory Response in Cardiac Surgery? In *Thorac cardiovasc Surg* 62 (08), pp. 670-676.

Honore, P M.; Jacobs, R; Joannes-Boyau, O et al. (2013): Newly Designed CRRT Membranes for Sepsis and SIRS—A Pragmatic Approach for Bedside Intensivists Summarizing the More Recent Advances: A Systematic Structured Review. In *ASAIO Journal* 59 (2), pp. 99–106. DOI: 10.1097/MAT.0b013e3182816a75.

Hortin, GL.; Sviridov, D; Anderson, N. L (2008): High-Abundance Polypeptides of the Human Plasma Proteome Comprising the Top 4 Logs of Polypeptide Abundance. In *Clin. Chem.* 54 (10), p. 1608. DOI: 10.1373/clinchem.2008.108175.

Hou, P C.; Filbin, M R.; Wang, H et al. (2017): Endothelial Permeability and Hemostasis in Septic Shock: Results From the ProCESS Trial. In *Chest* 152 (1), pp. 22–31. DOI: 10.1016/j.chest.2017.01.010.

Houschyar, K S.; Pyles, M N.; Rein, S et al. (2017): Continuous Hemoadsorption with a Cytokine Adsorber during Sepsis – a Review of the Literature. In *Int J Artif Organs* 40 (5), pp. 205–211. DOI: 10.5301/ijao.5000591.

Huang, L; Belousova, T; Chen, M et al. (2012): Overexpression of stanniocalcin-1 inhibits reactive oxygen species and renal ischemia/reperfusion injury in mice. In *Kidney Int* 82 (8), pp. 867–877. DOI: 10.1038/ki.2012.223.

Huang, Z; Ung, T (2013): Effect of alpha-1-acid glycoprotein binding on pharmacokinetics and pharmacodynamics. In *Current drug metabolism* 14 (2), pp. 226–238.

Hudson, B I.; Lippman, M E. (2018): Targeting RAGE Signaling in Inflammatory Disease. In *Annu. Rev. Med.* 69 (1), pp. 349–364. DOI: 10.1146/annurev-med-041316-085215.

Humphrey, J. D. (2008): Vascular Adaptation and Mechanical Homeostasis at Tissue, Cellular, and Sub-cellular Levels. In *Cell Biochemistry and Biophysics* 50 (2), pp. 53–78. DOI: 10.1007/s12013-007-9002-3.

Hunter, L W.; Jayachandran, M; Miller, V M. (2019): Sex differences in the expression of cell adhesion molecules on microvesicles derived from cultured human brain microvascular endothelial cells treated with inflammatory and thrombotic stimuli. In *Biol Sex Differ* 10 (1), p. 22. DOI: 10.1186/s13293-019-0241-y.

Huxley, V H.; Kemp, S S.; Schramm, C; Sieveking, S; Bingaman, S; Yu, Y et al. (2018): Sex differences influencing micro- and macrovascular endothelial phenotype in vitro. In *J Physiol* 596 (17), pp. 3929–3949. DOI: 10.1113/JP276048.

Ignjatovic, V; Geyer, P E.; Palaniappan, K K.; Chaaban, J E.; Omenn, Gilbert S.; Baker, Mark S. et al. (2019): Mass Spectrometry-Based Plasma Proteomics: Considerations from Sample Collection to Achieving Translational Data. In *J. Proteome Res.* 18 (12), pp. 4085–4097. DOI: 10.1021/acs.jproteome.9b00503.

Ince, C; Mayeux, PR.; Nguyen, T et al. (2016): The endothelium in sepsis. In *Shock* 45 (3), pp. 259–270.

Israili, ZH.; Dayton, PG. (2001): HUMAN ALPHA-1-GLYCOPROTEIN AND ITS INTERACTIONS WITH DRUGS. In *Drug Metabolism Reviews* 33 (2), pp. 161–235. DOI: 10.1081/DMR-100104402.

Iurlaro, R; Muñoz-Pinedo, C (2016): Cell death induced by endoplasmic reticulum stress (283) (14).

Jaffer, U.; Wade, R. G.; Gourlay, T. (2010): Cytokines in the systemic inflammatory response syndrome: a review. In *HSR proceedings in intensive care & cardiovascular anesthesia* 2 (3), pp. 161–175.

Jawa, R S.; Anillo, S; Huntoon, K; Baumann, H; Kulaylat, M (2011): Interleukin-6 in surgery, trauma, and critical care part II: clinical implications. In *J Intensive Care Med* 26 (2), pp. 73–87. DOI: 10.1177/0885066610384188.

Jin, X; Yao, T; Zhou, Z; Zhu, J; Zhang, S; Hu, W; Shen, C (2015): Advanced Glycation End Products Enhance Macrophages Polarization into M1 Phenotype through Activating RAGE/NF- κ B Pathway. In *BioMed Research International* 2015 (5, article 579), pp. 1–12. DOI: 10.1155/2015/732450.

Jones, A L.; Hulett, MD.; Altin, J G.; Hogg, P; Parish, C R. (2004): Plasminogen Is Tethered with High Affinity to the Cell Surface by the Plasma Protein, Histidine-rich Glycoprotein. In *J. Biol. Chem.* 279 (37), pp. 38267–38276.

Kailzel EL; Koolwijk P; van Erck MGM et al. (2006): Molecular weight fibrinogen variants determine angiogenesis rate in a fibrin matrix in vitro and in vivo. In *J Thromb Haemost* 4 (9), pp. 1975–1981.

Kakhniashvili, D G.; Bulla, L A.; Goodman, S R. (2004): The Human Erythrocyte Proteome. In *Mol Cell Proteomics* 3 (5), pp. 501–509. DOI: 10.1074/mcp.M300132-MCP200.

Karamlou, T; Ungerleider, R M. (2014): Systemic Inflammatory Response to Cardiopulmonary Bypass in Pediatric Patients and Related Strategies for Prevention. In Da Cruz, Eduardo M, Dunbar Ivy, James Jaggers (Eds.): Pediatric and Congenital Cardiology, Cardiac Surgery and Intensive Care. London: Springer London, pp. 791–800. Available online at https://doi.org/10.1007/978-1-4471-4619-3_77.

Karas, P L.; Goh, S L.; Dhital, K (2015): Is low serum albumin associated with postoperative complications in patients undergoing cardiac surgery? In *icvts* 21 (6), pp. 777–786. DOI: 10.1093/icvts/ivv247.

Karkouti, K.; Beattie, W. S.; Wijeysundera, D. N.; Rao, V.; Chan, C.; Dattilo, K. M. et al. (2005): Hemodilution during cardiopulmonary bypass is an independent risk factor for acute renal failure in adult cardiac surgery. In *The Journal of Thoracic and Cardiovascular Surgery* 129 (2), pp. 391–400. DOI: 10.1016/j.jtcvs.2004.06.028.

Karsdal, M A. (Ed.) (2019): Biochemistry of Collagens, Laminins and Elastin (Second Edition): Academic Press.

Karu, I; Taal, G; Zilmer, K; Pruunsild, C; Starkopf, J; Zilmer, M (2010): Inflammatory/oxidative stress during the first week after different types of cardiac surgery. In *Scandinavian Cardiovascular Journal* 44 (2), pp. 119–124. DOI: 10.3109/14017430903490981.

Kerbaul, F; Bénard, F; Giorgi, R; Youlet, B; Carrega, L; Zouher, I et al. (2008): Adenosine A2A Receptor Hyperexpression in Patients With Severe SIRS After Cardiopulmonary Bypass. In *J Investig Med* 56 (6), p. 864. DOI: 10.2310/JIM.0b013e3181788d02.

Khakpour, S; Wilhelmsen, K; Hellman, J (2015): Vascular endothelial cell Toll-like receptor pathways in sepsis. In *Innate Immun* 21 (8), pp. 827–846. DOI: 10.1177/1753425915606525.

Khalid, I M.; Sharkh, SE. Abu; Samamarh, H et al. (2019): Spectroscopic Characterization of the Interaction between Dopamine and Human Serum Albumin. In *OJBIPHY* 09 (02), pp. 110–130.

Khan, T A; Saleemuddin, M; Naeem, A (2011): Partially Folded Glycated State of Human Serum Albumin Tends to Aggregate. In *Int J Pept Res Ther* 17 (4), pp. 271–279. DOI: 10.1007/s10989-011-9267-7.

Kierdorf, K; Fritz, G (2013): RAGE regulation and signaling in inflammation and beyond. In *Journal of Leukocyte Biology* 94 (1), pp. 55–68. DOI: 10.1189/jlb.1012519.

Klebig, C; Korinth, D; Meraldi, P (2009): Bub1 regulates chromosome segregation in a kinetochore-independent manner. In *J Cell Biol* 185 (5), pp. 841–858. DOI: 10.1083/jcb.200902128.

Klein, D; Demory, A; Peyre, F et al. (2009): Wnt2 acts as an angiogenic growth factor for non-sinusoidal endothelial cells and inhibits expression of stanniocalcin-1. In *Angiogenesis* 12 (3), pp. 251–265.

Klenotic, PA.; Page, RC.; Li, W et al. (2013): Molecular Basis of Antiangiogenic Thrombospondin-1 Type 1 Repeat Domain Interactions With CD36. In *Arterioscler Thromb Vasc Biol.* 33 (7), pp. 1655–1662.

Klont, F; Bras, L; Wolters, JC et al. (2018): Assessment of Sample Preparation Bias in Mass Spectrometry-Based Proteomics. In *Anal. Chem.* 90 (8), pp. 5405–5413. DOI: 10.1021/acs.analchem.8b00600.

Kogelmann, K; Jarczak, D Scheller, M; Drüner, M (2017): Hemoadsorption by CytoSorb in septic patients: a case series. In *Critical Care* 21 (1), p. 74. DOI: 10.1186/s13054-017-1662-9.

Kołodziejczyk, J; Ponczek, M B. (2013): Reviews The role of fibrinogen, fibrin and fibrin(ogen) degradation products (FDPs) in tumor progression. In *wo* 2, pp. 113–119. DOI: 10.5114/wo.2013.34611.

Konno, M; Asai, A; Kawamoto, K et al. (2017): The one-carbon metabolism pathway highlights therapeutic targets for gastrointestinal cancer. In *International Journal of Oncology* 50 (4), pp. 1057–1063.

Kortekaas, K A.; Lindeman, J HN.; Reinders, M E J.; Palmen, M; Klautz, R J M.; de Groot, P G.; Roest, M (2013): Pre-existing endothelial cell activation predicts vasoplegia after mitral valve surgery†. In *Interactive CardioVascular and Thoracic Surgery* 17 (3), pp. 523–530. DOI: 10.1093/icvts/ivt243.

Kraft, F; Schmidt, C; van Aken, H; Zarbock, A (2015): Inflammatory response and extracorporeal circulation. In *Developments in Extracorporeal Circulation* 29 (2), pp. 113–123. DOI: 10.1016/j.bpa.2015.03.001.

Kubbies M. (1992) High-Resolution Cell Cycle Analysis: The Flow Cytometric Bromodeoxyuridine-Hoechst Quenching Technique. In: Radbruch A. (eds) Flow Cytometry and Cell Sorting. Springer Laboratory. Springer, Berlin, Heidelberg. https://doi.org/10.1007/978-3-662-02785-1_10

Kumar, A; Anstey, C; Tesar, P; Shekar, K (2019): Risk Factors for Mortality in Patients Undergoing Cardiothoracic Surgery for Infective Endocarditis. In *The Annals of Thoracic Surgery* 108 (4), pp. 1101–1106.

Kuusela, P; Saraswat, M; Joenväärä, S et al. (2017): Changes in plasma protein levels as an early indication of a bloodstream infection. In *PLOS ONE* 12 (2), pp. e0172987. DOI: 10.1371/journal.pone.0172987.

Lai, W K C; Kan, M Y (2015): Homocysteine-Induced Endothelial Dysfunction. In *Ann Nutr Metab* 67 (1), pp. 1–12.

Landis, RC; Brown, JR; Fitzgerald, D et al. (2014): Attenuating the Systemic Inflammatory Response to Adult Cardiopulmonary Bypass. In *J Extra Corpor Technol* 46 (3), pp. 197–211.

Languino, LR.; Plescia, J; Duperray, A et al. (1993): Fibrinogen mediates leukocyte adhesion to vascular endothelium through an ICAM-1-dependent pathway. In *Cell* 73 (7), pp. 1423–1434.

Lanza, R; Langer, R; Vacanti, J (Eds.) (2014): Principles of Tissue Engineering (Fourth Edition). Boston: Academic Press.

Leaf, DE.; Rajapurkar, M; Lele, SS et al. (2015): Increased plasma catalytic iron in patients may mediate acute kidney injury and death following cardiac surgery. In *Kidney Int* 87 (5), pp. 1046–1054. DOI: 10.1038/ki.2014.374.

Lee, Jae-Eun; Kim, Shine Young; Shin, So-Youn (2015): Effect of Repeated Freezing and Thawing on Biomarker Stability in Plasma and Serum Samples. In *Osong Public Health and Research Perspectives* 6 (6), pp. 357–362. DOI: 10.1016/j.phrp.2015.11.005.

Lehman-McKeeman LD (2013): Casarett and Doull's Toxicology: The Basic Science of Poisons, 8e. Chapter 5: Absorption, Distribution, and Excretion of Toxicants. New York: United States: McGraw-Hill Education.

Leone, S.; Ravasio, V.; Durante-Mangoni, E. et al. (2012): Epidemiology, characteristics, and outcome of infective endocarditis in Italy. In *Infection* 40 (5), pp. 527–535. DOI: 10.1007/s15010-012-0285-y.

Levitt, D; Levitt, M (2016): Human serum albumin homeostasis: a new look at the roles of synthesis, catabolism, renal and gastrointestinal excretion, and the clinical value of serum albumin measurements. In *IJGM* Volume 9, pp. 229–255.

Li, L; Willard, B; Rachdaoui, N et al. (2012): Plasma Proteome Dynamics: Analysis of Lipoproteins and Acute Phase Response Proteins with Metabolic Labeling. In *Mol Cell Proteomics* 11 (7), pp. M111.014209.

Li, Q; Syrovets, T; Simmet, T et al. (2013): Plasmin induces ICAM 1 expression in human endothelial cells via NF-κB/mitogen-activated protein kinases-dependent pathways. In *Exp Biol Med* 238 (2), pp. 176–186.

Li, X; Kumar, A; Carmeliet, P (2019): Metabolic Pathways Fueling the Endothelial Cell Drive. In *Annu. Rev. Physiol.* 81 (1), pp. 483–503. DOI: 10.1146/annurev-physiol-020518-114731.

Li, X; Sun, X; Carmeliet, P (2019): Hallmarks of Endothelial Cell Metabolism in Health and Disease. In *Cell Metabolism* 30 (3), pp. 414–433. DOI: 10.1016/j.cmet.2019.08.011.

Liao, K-M; Chao, T-B; Tian, Y-F et al. (2016): Overexpression of the PSAT1 Gene in Nasopharyngeal Carcinoma Is an Indicator of Poor Prognosis. In *J Cancer* 7 (9), pp. 1088–1094. DOI: 10.7150/jca.15258.

Lin, H; Huang, B; Wang, H et al. (2018): MTHFD2 Overexpression Predicts Poor Prognosis in Renal Cell Carcinoma and is Associated with Cell Proliferation and Vimentin-Modulated Migration and Invasion. In *Cell Physiol Biochem* 51 (2), pp. 991–1000. DOI: 10.1159/000495402.

Lin, Li (2009): RAGE signaling in inflammation and arterial aging. In *Front Biosci* Volume (14), p. 1403. DOI: 10.2741/3315.

Liu, B; Jia, Y; Cao, Y et al. (2016): Overexpression of PSAT1 Predicts Poor Prognosis and Associates with Tumor Progression in Human Esophageal Squamous Cell Carcinoma. In *Cell Physiol Biochem* 39 (1), pp. 395–406. DOI: 10.1159/000445633.

Liu, C-W; Bramer, L; Webb-Robertson, B-J et al. (2018): Temporal expression profiling of plasma proteins reveals oxidative stress in early stages of Type 1 Diabetes progression. In *J Proteom* 172, pp. 100–110. DOI: 10.1016/j.jprot.2017.10.004.

Liu, X; Huang, Y; Jiang, C et al. (2016): Methylenetetrahydrofolate dehydrogenase 2 overexpression is associated with tumor aggressiveness and poor prognosis in hepatocellular carcinoma. In *Digestive and Liver Disease* 48 (8), pp. 953–960.

Liu, Y; Beyer, A; Aebersold, R (2016): On the Dependency of Cellular Protein Levels on mRNA Abundance. In *Cell* 165 (3), pp. 535–550. DOI: 10.1016/j.cell.2016.03.014.

Lomelino, C L.; Andring, J T.; McKenna, R; Kilberg, M S. (2017): Asparagine synthetase: Function, structure, and role in disease. In *J Biol Chem* 292 (49), pp. 19952–19958. DOI: 10.1074/jbc.R117.819060.

Lorenzi PL; Ryan MC; Ikediobi ON. ASNS (asparagine synthetase) (Atlas of Genetics and Cytogenetics in Oncology and Haematology). Available online at http://atlasgeneticsoncology.org/Genes/GC_ASNS.html, checked on 11/28/2019.

Luo, Ji (2011): Cancer's sweet tooth for serine. In *Breast Cancer Res* 13 (6), p. 317. DOI: 10.1186/bcr2932.

Luscinskas, Ph. D, Francis W.; Gimbrone, Michael A. (1996): ENDOTHELIAL-DEPENDENT MECHANISMS IN CHRONIC INFLAMMATORY LEUKOCYTE RECRUITMENT. In *Annu. Rev. Med.* 47 (1), pp. 413–421.

Malard, B; Lambert, C; Kellum, J A. (2018): In vitro comparison of the adsorption of inflammatory mediators by blood purification devices. In *Intensive Care Medicine Experimental* 6 (1), p. 12. DOI: 10.1186/s40635-018-0177-2.

Margetic, S (2012): Infl ammation and haemostasis. In *Biochemia Medica* 22 (1), pp. 49–62.

Matsuda, N (2016): Alert cell strategy in SIRS-induced vasculitis: sepsis and endothelial cells. In *J Intens Care* 4 (1), p. 21.

Mattaini, K R.; Sullivan, M R.; Vander H. (2016): The importance of serine metabolism in cancer. In *J Cell Biol* 214 (3), p. 249. DOI: 10.1083/jcb.201604085.

McCormack, J J.; Lopes da Silva, M; Ferraro, F; Patella, F; Cutler, D F. (2017): Weibel−Palade bodies at a glance. In *J Cell Sci* 130 (21), pp. 3611–3617. DOI: 10.1242/jcs.208033.

Meertens, JH.; Nienhuis, HL.; Lefrandt, JD et al. (2016): The Course of Skin and Serum Biomarkers of Advanced Glycation Endproducts and Its Association with Oxidative Stress, Inflammation, Disease Severity, and Mortality during ICU Admission in Critically Ill Patients: Results from a Prospective Pilot Study. In *PLoS ONE* 11 (8), pp. e0160893.

Merlot, Angelica M.; Kalinowski, Danuta S.; Des Richardson, R. (2014): Unraveling the mysteries of serum albumin—more than just a serum protein. In *Frontiers in Physiology* 5, p. 299. DOI: 10.3389/fphys.2014.00299.

Metcalf, DJ; Nightingale, TD; Zenner, HL et al. (2008): Formation and function of Weibel-Palade bodies. In *J Cell Science* 121 (1), pp. 19–27. DOI: 10.1242/jcs.03494.

Mi, H; Huang, X; Muruganujan, A et al. (2017): PANTHER version 11: expanded annotation data from Gene Ontology and Reactome pathways, and data analysis tool enhancements. In *Nucleic Acids Res* 45 (D1), pp. D183.

Michaelis, U. Ruth; Chavakis, Emmanouil; Kruse, Christoph; Jungblut, Benno; Kaluza, David; Wandzioch, Katalin et al. (2013): The Polarity Protein Scrib Is Essential for Directed Endothelial Cell Migration. In *Circ Res* 112 (6), pp. 924–934. DOI: 10.1161/CIRCRESAHA.112.300592.

Minimized Cardiopulmonary Bypass Techniques and Technologies (2012): Elsevier Science.

Mohammadipoor, A; Lee, R Hwa; Prockop, D J.; Bartosh, T J. (2016): Stanniocalcin-1 attenuates ischemic cardiac injury and response of differentiating monocytes/macrophages to inflammatory stimuli. In *Transl Res* 177, pp. 127–142. DOI: 10.1016/j.trsl.2016.06.011.

Moldogazieva, NT.; Mokhosoev, IM.; Mel'nikova, TI et al. (2019): Oxidative Stress and Advanced Lipoxidation and Glycation End Products (ALEs and AGEs) in Aging and Age-Related Diseases. In *Oxidative Medicine and Cellular Longevity* 2019 (10), pp. 1–14. DOI: 10.1155/2019/3085756.

Nambi, Vijay (Ed.) (2019): Biomarkers in Cardiovascular Disease: Elsevier.

Nandi, S K.; Nahomi, R B.; Rankenberg, J; Glomb, M A.; Nagaraj, R H. (2020): Glycation-mediated inter-protein cross-linking is promoted by chaperone–client complexes of α-crystallin: Implications for lens aging and presbyopia. In *J. Biol. Chem.* 295 (17), pp. 5701–5716. DOI: 10.1074/jbc.RA120.012604.

Nickel, T.; Deutschmann, A.; Hanssen, H.; Summo, C.; Wilbert-Lampen, U. (2009): Modification of endothelial biology by acute and chronic stress hormones. In *Microvascular Research* 78 (3), pp. 364–369. DOI: 10.1016/j.mvr.2009.07.008.

Nilsson, R.; Nicolaidou, V.; Koufaris, C. (2019): Mitochondrial MTHFD isozymes display distinct expression, regulation, and association with cancer. In *Gene* 716, p. 144032. DOI: 10.1016/j.gene.2019.144032.

Nilsson, R; Jain, M; Madhusudhan, N; Sheppard, N G; Strittmatter, L; Kampf, C et al. (2014): Metabolic enzyme expression highlights a key role for MTHFD2 and the mitochondrial folate pathway in cancer. In *Nat Commun* 5 (1), p. 1131. DOI: 10.1038/ncomms4128.

Nowotny, K; Jung, T; Grune, T; Höhn, A (2014): Accumulation of modified proteins and aggregate formation in aging. In *Experimental Gerontology* 57, pp. 122–131. DOI: 10.1016/j.exger.2014.05.016.

Nowotny, Kerstin; Schröter, David; Schreiner, Monika; Grune, Tilman (2018): Dietary advanced glycation end products and their relevance for human health. In *Ageing Research Reviews* 47, pp. 55–66. DOI: 10.1016/j.arr.2018.06.005.

Oberkersch, R E.; Santoro, M M. (2019): Role of amino acid metabolism in angiogenesis. In *Pioneering updates in vascular biology* 112, pp. 17–23. DOI: 10.1016/j.vph.2018.11.001.

Okajima, K; Abe, H; Binder, BR. (1995): Endothelial cell injury induced by plasmin in vitro. In *J Lab and Clin Med* 126 (4), pp. 377–384.

Olia, Salim E.; Maul, Timothy M.; Antaki, James F.; Kameneva, Marina V. (2016): Mechanical blood trauma in assisted circulation: sublethal RBC damage preceding hemolysis. In *Int J Artif Organs* 39 (4), pp. 150–159. DOI: 10.5301/ijao.5000478.

Oliveros, J. (2007-2015): Venny. An interactive tool for comparing lists with Venn's diagrams. Available online at https://bioinfogp.cnb.csic.es/tools/venny/index.htmlC.

Olmos, C; Vilacosta, I; Fernández, C; López, J; Sarriá, C; Ferrera, C et al. (2012): Contemporary epidemiology and prognosis of septic shock in infective endocarditis†. In *eurheartj* 34 (26), pp. 1999–2006. DOI: 10.1093/eurheartj/ehs336.

Ozolina, A; Strike, E; Jaunalksne, I; Krumina, A; Bjertnaes, L J.; Vanags, I (2012): PAI-1 and t-PA/PAI-1 complex potential markers of fibrinolytic bleeding after cardiac surgery employing cardiopulmonary bypass. In *BMC Anesthesiol* 12 (1), p. 17. DOI: 10.1186/1471-2253-12-27.

Paparella, D.; Yau, T. M.; Young, E. (2002): Cardiopulmonary bypass induced inflammation: pathophysiology and treatment. An update. In *ejcts* 21 (2), pp. 232–244. DOI: 10.1016/S1010-7940(01)01099-5.

Paradela-Dobarro, B; Bravo, S B.; Rozados-Luís, A; González-Peteiro, M; Varela-Román, A; González-Juanatey, J R et al. (2019): Inflammatory effects of in vivo glycated albumin from cardiovascular patients. In *Biomedicine & Pharmacotherapy* 113, p. 108763. DOI: 10.1016/j.biopha.2019.108763.

Passov, A; Petäjä, L; Pihlajoki, M et al. (2019): The origin of plasma neutrophil gelatinase-associated lipocalin in cardiac surgery. In *BMC Nephrology* 20 (1), p. 182. DOI: 10.1186/s12882-019-1380-4.

Pietzsch, J; Hoppmann, S (2009): Human S100A12: a novel key player in inflammation? In *Amino Acids* 36 (3), pp. 381–389. DOI: 10.1007/s00726-008-0097-7.

Piwowarczyk, P; Kutnik, P; Potręć-Studzińska, B; Sysiak-Sławecka, J; Rypulak, E; Borys, M; Czczuwar, M (2019): Hemoadsorption in isolated conjugated hyperbilirubinemia after extracorporeal membrane oxygenation support. Cholestasis of sepsis: A case report and review of the literature on differential causes of jaundice in ICU patient. In *Int J Artif Organs* 42 (5), pp. 263–268. DOI: 10.1177/0391398819834012.

Poli, E C.; Alberio, L; Bauer-Doerries, A; Marcucci, C; Roumy, A; Kirsch, M et al. (2019): Cytokine clearance with CytoSorb® during cardiac surgery: a pilot randomized controlled trial. In *Critical Care* 23 (1), p. 108. DOI: 10.1186/s13054-019-2399-4.

Poli, E C.; Rimmelé, T; Schneider, A G. (2019): Hemoadsorption with CytoSorb®. In *Intensive Care Medicine* 45 (2), pp. 236–239. DOI: 10.1007/s00134-018-5464-6.

Pollard, Thomas D.; Earnshaw, William C.; Lippincott-Schwartz, Jennifer; Johnson, Graham T. (Eds.) (2017): Cell Biology (Third Edition): Elsevier.

Poon, IKH; Patel, KK; Davis, DS et al. (2011): Histidine-rich glycoprotein: the Swiss Army knife of mammalian plasma. In *Blood* 117 (7), pp. 2093–2101. DOI: 10.1182/blood-2010-09-303842.

Posimo, JM; Unnithan, AS; Gleixner, AM et al. (2014): Viability assays for cells in culture. In *J Vis Exp* (83), pp. e50645. DOI: 10.3791/50645.

Potapova, T A.; Sivakumar, S; Flynn, JN et al. (2011): Mitotic progression becomes irreversible in prometaphase and collapses when Wee1 and Cdc25 are inhibited. In *MBoC* 22 (8), pp. 1191–1206. DOI: 10.1091/mbc.E10-07-0599.

Prasad, K; Mishra, M (2018): AGE–RAGE Stress, Stressors, and Antistressors in Health and Disease. In *Int J Angiol* 27 (01), pp. 1–12. DOI: 10.1055/s-0037-1613678.

Preedy, Victor R.; Patel, Vinood B. (Eds.): General Methods in Biomarker Research and their Applications (Biomarkers in Disease: Methods, Discoveries and Applications).

Pregernig, A; Müller, M; Held, U; Beck-Schimmer, B (2019): Prediction of mortality in adult patients with sepsis using six biomarkers: a systematic review and meta-analysis. In *Ann. Intensive Care* 9 (1), p. 414. DOI: 10.1186/s13613-019-0600-1.

Pretorius, M.; Donahue, BS.; Yu, C et al. (2007): PAI-1 as a Predictor of Postoperative Atrial Fibrillation After Cardiopulmonary Bypass. In *Circulation* 116 (11_suppl), pp. I-1. DOI: 10.1161/CIRCULATIONAHA.106.677906.

Proteins at Interfaces II (1995): American Chemical Society (ACS Symposium Series).

Punjabi, P P.; Taylor, K. M. (2013): The science and practice of cardiopulmonary bypass: From cross circulation to ECMO and SIRS. In *Global Cardiology Science and Practice* 2013 (3). DOI: 10.5339/gcsp.2013.32.

Pushpakumar, S; Kundu, S; Sen, U (2014): Endothelial Dysfunction: The Link Between Homocysteine and Hydrogen Sulfide. In *CMC* 21 (32), pp. 3662–3672. DOI: 10.2174/0929867321666140706142335.

Qian, C. (2017): Identification and validation of PSAT1 as a potential prognostic factor for predicting clinical outcomes in patients with colorectal carcinoma. In *Oncology Letters* 14, pp. 8014–8020.

Qin, P; Tang, X; Elloso, MM et al. (2006): Bile acids induce adhesion molecule expression in endothelial cells through activation of reactive oxygen species, NF-κB, and p38. In *Am J of Physiol* 291 (2), pp. H741. DOI: 10.1152/ajpheart.01182.2005.

Qiu, H; Jin, L; Chen, J et al. (2020): Comprehensive Glycomic Analysis Reveals That Human Serum Albumin Glycation Specifically Affects the Pharmacokinetics and Efficacy of Different Anticoagulant Drugs in Diabetes. In *Diabetes* 69 (4), pp. 760–770. DOI: 10.2337/db19-0738.

Rabbani, Naila; Ashour, Amal; Thornalley, Paul J. (2016): Mass spectrometric determination of early and advanced glycation in biology. In *Glycoconj J* 33 (4), pp. 553–568. DOI: 10.1007/s10719-016-9709-8.

Raynes, John G. (2015): Acute-Phase Proteins (Major Reference Works). Available online at https://doi.org/10.1002/9780470015902.a0000497.pub2.

Rodríguez-Nieto, S; Chavarría, T; Martínez-Poveda, B et al. (2002): Anti-angiogenic effects of homocysteine on cultured endothelial cells. In *Biochem and Biophys Res Comm* 293 (1), pp. 497–500. DOI: 10.1016/S0006-291X(02)00232-2.

Roh, J S; Sohn, D H (2018): Damage-Associated Molecular Patterns in Inflammatory Diseases. In *Immune Netw* 18 (4). Available online at https://doi.org/10.4110/in.2018.18.e27.

Ronco, Claudio; Bellomo, Rinaldo; Kellum, John A.; Ricci, Zaccaria (Eds.) (2019): Critical Care Nephrology (Third Edition). Philadelphia: Content Repository Only!

Sahni, A.; Sahni, S. K.; Simpson-Haidaris, P. J.; Francis, C. W. (2004): Fibrinogen binding potentiates FGF-2 but not VEGF induced expression of u-PA, u-PAR, and PAI-1 in endothelial cells. In *Journal of Thrombosis and Haemostasis* 2 (9), pp. 1629–1636. DOI: 10.1111/j.1538-7836.2004.00845.x.

Sahni, A; Francis, C W. (2000): Vascular endothelial growth factor binds to fibrinogen and fibrin and stimulates endothelial cell proliferation. In *Blood* 96 (12), pp. 3772–3778. DOI: 10.1182/blood.V96.12.3772.

Sahni, A; Sporn, L A; Francis, C W. (1999): Potentiation of Endothelial Cell Proliferation by Fibrin(ogen)-bound Fibroblast Growth Factor-2. In *J. Biol. Chem.* 274 (21), pp. 14936–14941. DOI: 10.1074/jbc.274.21.14936.

Sarkar, C; Ganju, R K.; Pompili, V J.; Chakroborty, D (2017): Enhanced peripheral dopamine impairs post-ischemic healing by suppressing angiotensin receptor type 1 expression in endothelial cells and inhibiting angiogenesis. In *Angiogenesis* 20 (1), pp. 97–107. DOI: 10.1007/s10456-016-9531-8.

Sato, H; Yamamoto, K; Kakinuma, A; Nakata, Y; Sawamura, S (2015): Accelerated activation of the coagulation pathway during cardiopulmonary bypass in aortic replacement surgery: a prospective observational study. In *J Cardiothorac Surg* 10, p. 84. DOI: 10.1186/s13019-015-0295-9.

Scarola C. (2010): Cardiopulmonary Bypass and Biocompatibility. In *J of Biomat Applic Revs* (4), p. 42.

Schädler, D; Pausch, C; Heise, D et al. (2017): The effect of a novel extracorporeal cytokine hemoadsorption device on IL-6 elimination in septic patients: A randomized controlled trial. In *PLOS ONE* 12 (10), pp. e0187015. DOI: 10.1371/journal.pone.0187015.

Schaer, C. A.; Deuel, J. W.; Bittermann, A. G. et al. (2013): Mechanisms of haptoglobin protection against hemoglobin peroxidation triggered endothelial damage. In *Cell Death Differ* 20 (11), pp. 1569–1579. DOI: 10.1038/cdd.2013.113.

Scheijen, J; Hanssen, N; van Greevenbroek, M M.; Van der Kallen, C J.; Feskens, E J M.; Stehouwer, C D A et al. (2018): Dietary intake of advanced glycation endproducts is associated with higher levels of advanced glycation endproducts in plasma and urine: The CODAM study. In *Clinical Nutrition* 37 (3), pp. 919–925. DOI: 10.1016/j.clnu.2017.03.019.

Schenk, H; Müller-Deile, J; Schmitt, R et al. (2017): Removal of focal segmental glomerulosclerosis (FSGS) factor suPAR using CytoSorb. In *J Clin Apher* 32 (6), pp. 444–452. DOI: 10.1002/jca.21538.

Schillemans, M.; Karampini, E.; Kat, M.; Bierings, R. (2019): Exocytosis of Weibel–Palade bodies: how to unpack a vascular emergency kit. In *J Thromb Haemost* 17 (1), pp. 6–18. DOI: 10.1111/jth.14322.

Schirone, L; Iaccarino, A; Saade, W et al. (2018): Cerebrovascular Complications and Infective Endocarditis: Impact of Available Evidence on Clinical Outcome. In *BioMed Research International* 2018, p. 6. DOI: 10.1155/2018/4109358.

Sekhon, Navdeep; Peacock, W. Frank (2019): Chapter 11 - Biomarkers to Assist in the Evaluation of Chest Pain: A Practical Guide. In Vijay Nambi (Ed.): Biomarkers in Cardiovascular Disease: Elsevier, pp. 115–128. Available online at http://www.sciencedirect.com/science/article/pii/B9780323548359000119.

Shcheglovitova, O. N.; Azizova, O. A.; Romanov, Yu. A. et al. (2006): Oxidized forms of fibrinogen induce expression of cell adhesion molecules by cultured endothelial cells from human blood vessels. In *Bull Exp Biol Med* 142 (3), pp. 308–312. DOI: 10.1007/s10517-006-0353-3.

Sheikh-Hamad, David (2010): Mammalian stanniocalcin-1 activates mitochondrial antioxidant pathways: new paradigms for regulation of macrophages and endothelium. In *Am J Physiol Renal Physiol* 298 (2), pp. F248. DOI: 10.1152/ajprenal.00260.2009.

Shi, Y; Xu, X; Zhang, Q et al. (2014): tRNA synthetase counteracts c-Myc to develop functional vasculature. In *eLife* 3, pp. M135.

Simoni, J (2019): Why do we need extracorporeal blood purification for sepsis and septic shock? In *Artif Organs* 43 (5), pp. 444–447. DOI: 10.1111/aor.13442.

Singer, M; Deutschman, C S.; Seymour, C W et al. (2016): The Third International Consensus Definitions for Sepsis and Septic Shock (Sepsis-3). In *JAMA* 315 (8), pp. 801–810. DOI: 10.1001/jama.2016.0287.

Singh, A; Mehta, Y; Trehan, N (2019): Bilirubin Removal Using CytoSorb Filter in a Cardiac Surgical Patient. In *Journal of Cardiothoracic and Vascular Anesthesia* 33 (3), pp. 881–883. DOI: 10.1053/j.jvca.2018.08.213.

Slack, S M.; Horbett, T A. (1995): The Vroman Effect. In : Proteins at Interfaces II, vol. 602: American Chemical Society (ACS Symposium Series), pp. 112-128.

Somer, F (2012): Recent advances in the comprehension and the management of perioperative systemic host response during cardiopulmonary bypass. In *Recent patents on cardiovascular drug discovery* 7 (3), pp. 180–185. DOI: 10.2174/157489012803832865.

Sparding, N.; Arvanitidis, A.; Karsdal, M. A. (2019): Chapter 28 - Type XXVIII collagen. In Morten A. Karsdal (Ed.): Biochemistry of Collagens, Laminins and Elastin (Second Edition): Academic Press, pp. 205–208.

Springer, T A. (2014): von Willebrand factor, Jedi knight of the bloodstream. In *Blood* 124 (9), pp. 1412–1425.

Squiccimarro, E; Labriola, C; Malvindi, P G et al. (2019): Prevalence and Clinical Impact of Systemic Inflammatory Reaction After Cardiac Surgery. In *Journal of Cardiothoracic and Vascular Anesthesia* 33 (6), pp. 1682–1690.

Staton, C A.; Brown, N J.; Lewis, C E. (2005): The role of fibrinogen and related fragments in tumour angiogenesis and metastasis. In *Expert Opinion on Biological Therapy* 3 (7), pp. 1105–1120.

Stenemo, M; Teleman, J; Sjöström, M; Grubb, G; Malmström, E; Malmström, J; Niméus, E (2016): Cancer associated proteins in blood plasma: Determining normal variation. In *Proteomics* 16 (13), pp. 1928–1937.

Szklarczyk, D; Gable, AL.; Lyon, D et al. (2019): STRING v11: protein-protein association networks with increased coverage, supporting functional discovery in genome-wide experimental datasets. In *Nucleic Acids Res* 47 (D1), pp. D607. DOI: 10.1093/nar/gky1131.

Taleska S, Sostaric M, Bozhinovska M; Rupert, Lea; Bosnic, Zoran; Jerin, Ales et al. (2020): Extracorporeal Hemadsorption versus Glucocorticoids during Cardiopulmonary Bypass: A Prospective, Randomized, Controlled Trial. In *Cardiovascular Therapeutics* 2020 (5), pp. 1–15. DOI: 10.1155/2020/7834173.

Tedeschi, P. M.; Vazquez, A.; Kerrigan, J. E.; Bertino, J. R. (2015): Mitochondrial Methylenetetrahydrofolate Dehydrogenase (MTHFD2) Overexpression Is Associated with Tumor Cell Proliferation and Is a Novel Target for Drug Development. In *Molecular Cancer Research* 13 (10), pp. 1361–1366.

The Gene Ontology Consortium (2018): The Gene Ontology Resource: 20 years and still GOing strong. In *nar* 47 (D1), pp. D330. DOI: 10.1093/nar/gky1055.

Thornalley, P J; Rabbani, N (2014): Detection of oxidized and glycated proteins in clinical samples using mass spectrometry — A user's perspective. In *Biochimica et Biophysica Acta (BBA) - General Subjects* 1840 (2), pp. 818–829. DOI: 10.1016/j.bbagen.2013.03.025.

Timmermans, K; Kox, M; Scheffer, G J; Pickkers, P (2016): DANGER IN THE INTENSIVE CARE UNIT: DAMPS IN CRITICALLY ILL PATIENTS. In *Shock (Augusta, Ga.)* 45 (2), pp. 108–116. DOI: 10.1097/SHK.0000000000000506.

Tobon-Velasco, J; Cuevas, E; Torres-Ramos, M (2014): Receptor for AGEs (RAGE) as Mediator of NF-kB Pathway Activation in Neuroinflammation and Oxidative Stress. In *CNSNDDT* 13 (9), pp. 1615–1626.

Tofler, G. H.; Massaro, J.; O'Donnell, C. J.; Wilson, P.W.F.; Vasan, R. S.; Sutherland, P. A. et al. (2016): Plasminogen activator inhibitor and the risk of cardiovascular disease: The Framingham Heart Study. In *Thrombosis Research* 140, pp. 30–35. DOI: 10.1016/j.thromres.2016.02.002.

Tsang, G; Allen, S; Pagano, D; Wong, C; Graham, T R.; Bonser, R S. (1998): von Willebrand factor and urinary albumin excretion are possible indicators of endothelial dysfunction in cardiopulmonary bypass. In *European Journal of Cardio-Thoracic Surgery* 13 (4), pp. 385–391. DOI: 10.1016/s1010-7940(98)00022-0.

Tsiatsiani, L; Heck, A. (2015): Proteomics beyond trypsin. In *FEBS J* 282 (14), pp. 2612–2626.

Tyagi, N; Roberts, AM.; Dean, WL.; Tyagi, SC.; Lominadze, D (2007): Fibrinogen induces endothelial cell permeability. In *Mol Cell Biochem* 307 (1-2), pp. 13–22. DOI: 10.1007/s11010-007-9579-2.

Urano, T; Castellino, FJ; Suzuki, Y (2018): Regulation of plasminogen activation on cell surfaces and fibrin. In *J Thromb Haemost* 16 (8), pp. 1487–1497. DOI: 10.1111/jth.14157.

Urano, T; Sator de Serrano, V; Gaffney, PJ; Castellino, FJ. (2002): Effectors of the activation of human [Glu1]plasminogen by human tissue plasminogen activator. In *Biochemistry* 27 (17), pp. 6522–6528.

Valen, G; Blombäck, M; Sellei, P; Lindblom, D; Vaage, J (1994): Release of von willebrand factor by cardiopulmonary bypass, but not by cardioplegia in open heart surgery. In *Thrombosis Research* 73 (1), pp. 21–29. DOI: 10.1016/0049-3848(94)90050-7.

Vallelian, F; Schaer, CA; Deuel, JW et al. (2018): Revisiting the putative role of heme as a trigger of inflammation. In *Pharmacol Res Perspect* 6 (2), pp. e00392. DOI: 10.1002/prp2.392.

van Beek, D; van der Horst, I; de Geus, AF et al. (2018): Albumin, a marker for post-operative myocardial damage in cardiac surgery. In *Journal of Critical Care* 47, pp. 55–60. DOI: 10.1016/j.jcrc.2018.06.009.

van Breevoort, D; van Agtmaal, EL; Dragt, BS et al. (2012): Proteomic Screen Identifies IGFBP7 as a Novel Component of Endothelial Cell-Specific Weibel-Palade Bodies. In *J. Proteome Res.* 11 (5), pp. 2925–2936.

Vandekeere, S; Dubois, C; Kalucka, J; Sullivan, M R.; García-Caballero, M; Goveia, J et al. (2018): Serine Synthesis via PHGDH Is Essential for Heme Production in Endothelial Cells. In *Cell Metabolism* 28 (4), pp. 573–587.e13.

Varshney, A; Sen, P; Ahmad, E; Rehan, M; Subbarao, N; Khan, R H (2010): Ligand binding strategies of human serum albumin: How can the cargo be utilized? In *Chirality* 22 (1), pp. 77–87. DOI: 10.1002/chir.20709.

Vénéreau, E; Ceriotti, C; Bianchi, ME (2015): DAMPs from Cell Death to New Life. In *Frontiers in Immunology* 6, p. 422. DOI: 10.3389/fimmu.2015.00422.

Vera, N; Cristófol, RM.; Rodríguez Farré, E. (1988): Protein binding and stability of norepinephrine in human blood plasma.-Involvement of prealbumin, ∝1-acid glycoprotein and albumin. In *Life Sciences* 43 (16), pp. 1277–1286. DOI: 10.1016/0024-3205(88)90582-6.

Vercaemst, L (2008): Hemolysis in cardiac surgery patients undergoing cardiopulmonary bypass: a review in search of a treatment algorithm. In *J Extra Corpor Technol* 40 (4), pp. 257–267.

Vermeulen W; Hanssen, S.; Buurman, W A.; Jacobs, Michael J. (2011): Cardiovascular surgery and organ damage: Time to reconsider the role of hemolysis. In *J of Thorac and Cardiovasc Surg* 142 (1), pp. 1–11.

Verrier, E D.; Morgan, E N. (1998): Endothelial response to cardiopulmonary bypass surgery. In *The Annals of Thoracic Surgery* 66 (5), pp. S17. DOI: 10.1016/S0003-4975(98)00965-5.

Vié, N; Copois, V; Bascoul-Mollevi, C; Denis, V; Bec, N; Robert, B et al. (2008): Overexpression of phosphoserine aminotransferase PSAT1 stimulates cell growth and increases chemoresistance of colon cancer cells. In *Molecular Cancer* 7 (1), p. 14. DOI: 10.1186/1476-4598-7-14.

Vinchi, F; Tolosano, E (2013): Therapeutic Approaches to Limit Hemolysis-Driven Endothelial Dysfunction: Scavenging Free Heme to Preserve Vasculature Homeostasis. In *Oxidative Medicine and Cellular Longevity* 2013 (11), pp. 1–11. DOI: 10.1155/2013/396527.

Wang, A; Gaca, J G.; Chu, V H. (2018): Management Considerations in Infective Endocarditis: A Review. In *JAMA* 320 (1), pp. 72–83. DOI: 10.1001/jama.2018.7596.

Wang, Y; Wang, H; Piper, M G.; McMaken, S; Mo, X; Opalek, J et al. (2010): sRAGE Induces Human Monocyte Survival and Differentiation. In *J.I.* 185 (3), pp. 1822–1835. DOI: 10.4049/jimmunol.0903398.

Warren, O J.; Smith, A J.; Alexiou, C; Rogers, P L B.; Jawad, Noorulhuda; Vincent, Charles et al. (2009): The Inflammatory Response to Cardiopulmonary Bypass: Part 1—Mechanisms of Pathogenesis. In *Journal of Cardiothoracic and Vascular Anesthesia* 23 (2), pp. 223–231. DOI: 10.1053/j.jvca.2008.08.007.

Werdan, K; Dietz, S; Löffler, B; Niemann, S; Bushnaq, H; Silber, R-E et al. (2014): Mechanisms of infective endocarditis: pathogen–host interaction and risk states. In *Nature Reviews Cardiology* 11 (1), pp. 35–50.

Wiegele, M; Krenn, C G. (2015): Cytosorb™ in a Patient with Legionella Pneumonia–Associated Rhabdomyolysis: A Case Report. In *ASAIO Journal* 61 (3), pp. e14-e16. DOI: 10.1097/MAT.0000000000000197.

Xia, C; Braunstein, Z; Toomey, A C.; Zhong, J; Rao, X (2018): S100 Proteins As an Important Regulator of Macrophage Inflammation. In *Front Immunol* 8, p. 1908. DOI: 10.3389/fimmu.2017.01908.

Xiao, L; Liu, Y; Wang, N (2013): New paradigms in inflammatory signaling in vascular endothelial cells. In *Am J of Physiol* 306 (3), pp. H317. DOI: 10.1152/ajpheart.00182.2013.

Yan, S F; Ramasamy, R; Schmidt, A M (2010): The RAGE Axis. In *Circulation Research* 106 (5), pp. 842–853.

Yano, K; Liaw, P C; Mullington, J M.; Shih, S C; Okada, H; Bodyak, N et al. (2006): Vascular endothelial growth factor is an important determinant of sepsis morbidity and mortality. In *J Exp Med* 203 (6), pp. 1447–1458.

Yeung, H Y.; Lai, K P.; Chan, H Y.; Mak, N K.; Wagner, G F.; Wong, Chris K. C. (2005): Hypoxia-Inducible Factor-1-Mediated Activation of Stanniocalcin-1 in Human Cancer Cells. In *endo* 146 (11), pp. 4951–4960.

Zakkar, M; Guida, G; Suleiman, M-S; Angelini, G D. (2015): Cardiopulmonary Bypass and Oxidative Stress. In *Oxidative Medicine and Cellular Longevity* 2015, p. 8. DOI: 10.1155/2015/189863.

Zhang, Y; Shan, P; Srivastava, A; Li, Z; Lee, P J. (2018): Endothelial Stanniocalcin 1 Maintains Mitochondrial Bioenergetics and Prevents Oxidant-Induced Lung Injury via Toll-Like Receptor 4. In *Antioxidants & Redox Signaling* 30 (15), pp. 1775–1796. DOI: 10.1089/ars.2018.7514.

Zhao, J (2014): Molecular mechanisms of AGE/RAGE-mediated fibrosis in the diabetic heart. In *WJD* 5 (6), p. 860.

Zhao, X; Liao, Y-N; Huang, Q (2018): The impact of RAGE inhibition in animal models of bacterial sepsis: a systematic review and meta-analysis. In *The Journal of international medical research* 46 (1), pp. 11–21.

8. Theses

1. CytoSorb hemofiltration, when applied intraoperatively removes a broad spectrum of proteins from blood. According to our data, the majority of proteins retained on the polymer matrix possess molecular weight below 60 kDa and hydrophilic properties.
2. Measurable concentrations of C-reactive protein and interleukins (IL-1β, IL-6, IL-8 and IL-10) were eluted form the filters. Concentration of IL-8 in the eluted material was the highest among all cytokines. Patients with infective endocarditis tended to have higher levels of cytokines in the eluted protein fractions.
3. Intraoperative hemofiltration with average time 145 min. did not result in significant reduction of cytokine concentration in plasma of patients.
4. In applied experimental settings there was no evidence of preferential binding of AGE-modified plasma proteins.
5. Material eluted from the CytoSorb matrix used for hemofiltration in patients with infective endocarditis causes dose-dependent and significant reduction in viability and functionality of cultured endothelial cells, altering cell attachment, migration and division.
6. Transcriptional changes, arising after 24-hour exposure of endothelial cells to the eluted material include significant up-regulation in gene clusters, controlling amino acid, nucleotide, folate and lipid metabolism, as well as massive down-regulation of the genes, responsible for cell division.
7. On protein level enzymes phosphoserine aminotransferase and mitochondrial methyltetrahydrofolate reductase 2 were significantly up-regulated.
8. Mitotic proteins kinesin superfamily protein 20A and mitotic checkpoint kinase (BUB1) were significantly down-regulated on the protein level.
9. Production of pro-coagulant factors tissue plasminogen activator and von-Willebrand factor by endothelial cells was significantly increased after exposure to the eluted protein mixture.
10. Hemofiltration can prevent systemic inflammatory response after valve surgery with cardiopulmonary bypass by removing blood proteins that facilitate endothelial activation.

9. Supplementary material

9.1. Supplementary tables

Supplementary table 1: Clinical trials, evaluating efficacy and safety of CytoSorb hemofiltration in patients undergoing heart surgery

Clinical Trial ID	Patient population	Brief summary, published results
NCT01879176	Elective CPB surgery	No reduction of inflammatory cytokines, no changes in perioperative course. Slower decrease of postoperative IL-10 (possible anti-inflammatory effect). Conclusion: HF during CPB was feasible (Bernardi et al., 2013).
NCT02566525 REFRESH	Elective cardiac surgery with CPB and anticipated duration above 180 min.	Intraoperative HF with CytoSorb was safe and feasible in this randomized, controlled pilot study during complex cardiac surgery. Treatment with CytoSorb resulted in significant reductions in pfHb during valve replacement surgery and reductions in C3a and C5a in the overall EFFICACY group (Gleason et al., 2019).
NCT03384875 REFRESHII-AKI	Incidence or severity of AKI in the first 48 hours after CPB	Suspended 27.11.2019 (DMC recommendation for collection of additional trial data).
NCT02666703 IMEECCACS	Patients undergoing complex cardiac surgery with CPB (eg: combined valve and coronary bypass grafting surgery, concomitant valve surgery, surgery of the ascending aorta and aortic arch, as well as re-operations of the same type)	CytoSorb HF was safe and well-tolerated in this study. Methylprednisolone was more effectively reducing inflammatory response after CPB surgery when compared to HF and standard care. HF was associuated with higher prolonged expression of CD64 on monocytes but short lasting expression of CD163 on granulocytes when compared to standard care (Taleska Stupica et al., 2020).
NCT03104179 REMOTE	Impact of intraoperative cytokine adsorption on postoperative patient course in patients undergoing cardiac surgery with CPB	Recruitment status is unknown (August 2020, last update in ClinicalTrial.gov database - 7.04.2017).
NCT02775123 CCCC	Myocardial ischemia, heart valve diseases, patients planned for elective cardiac surgery with CPB	CytoSorb® HA during CPB was not associated with an increased incidence of adverse event. The procedure did not result in significant coagulation factors' adsorption but only some signs of coagulation activation. However, the intervention was associated neither with a decrease in pro- or anti-inflammatory cytokine levels nor with any improvement in relevant clinical outcomes (Poli et al., 2019).
NCT02265419 CASHSP	Patients with multiple organ failure following heart surgery (treatment for 24 hours after operation)	Ongoing, study is still recruiting patients (August, 2020).

NCT02902939 **MyDeCCS**	Patients with ischemia heart disease and/or valvular heart disease, undergoing CABG and/or valve replacement/plastic procedures	Study is completed, results unpublished as of August, 2020.
NCT02297334	Coronary artery disease, heart valve disease (intraoperative hemofiltration)	Study is completed, results unpublished as of August, 2020.
DRKS00007928 **RECCAS**	Elective cardiac surgery requiring CPB and anticipated duration over 90 min.	Study completed, protocol published (Baumann et al., 2016), results unpublished as of August, 2020.
NCT02213939	On pump myocardial revascularization with the use of the cytokine adsorbing circuit	Study recruitment status is unknown as of August 2020.
NCT02312024	Sepsis, need of heart surgery	International registry, ongoing, primary results published (Friesecke et al., 2017).
NCT04157647 **IMHeS**	Patients with kidney failure, need of heart surgery with CPB	Aims to evaluate the relationship between intra- and postoperative HA and the post-surgical inflammatory response. Not yet recruiting as of August, 2020.
NCT03266302 **REMOVE**	Infective endocarditis, heart surgery with CPB	Completed, study protocoli s published (Diab et al., 2020), no results published as of August, 2020.
Effect of Cytosorb on Postoperative Sepsis in Cardiac Surgery	Patients with infective endocarditis of the native mitral valve undergoing surgery	Patients allocated to HA treatment during valve surgery had lower incidence of postoperative sepsis and sepsis-related death compared to control (Haidari et al., 2020)

Abbreviations: AKI – acute kidney injury; CABG – coronary artery bypass grafting surgery; CPB – cardiopulmonary bypass; DMC – data monitoring committee.

Supplementary table 2: Commonly used EC-certified adsorption cartridges, their properties and indications (adaptation from Ankawi et al., 2019)

	Cytosorb (CytoSorbents, USA)	**MG hemoperfusion cartridge (Biosky, China)**	**Oxiris (Baxter, France)**	**HA 330 (Jafron, China)**
Composition	Porous polymer beads	Macroporous polysterene resin beads	AN69-based membrane, surface treated with PEI and grafted with heparin	Styrene divinylbenzene copolymers
Indication	Severe sepsis and septic shock Cardiac surgery (intraoperative and postoperative) Poisoning	Severe sepsis and septic shock Cardiac surgery Kidney failure (adjuvant to HD) Poisoning	Severe sepsis and septic shock	Severe sepsis and septic shock Cardiac surgery (intraoperative and postoperative)
Toxins removed	Cytokines Chemokines Anaphylatoxins Myoglobin Free hemoglobin Bilirubin/bile acids Toxins/metals Drugs	Cytokines Chemokines Endotoxin Uremic toxins Drugs	Endotoxin Cytokines	Cytokines Complements Free hemoglobin
Prescription	Up to 24-h therapy daily for 2–7 consecutive days	120-150 minutes, frequency of the treatment depends on the indication	Prescribed dose > 35 ml/kg/h (60% convective). Filter replacement after 24 h or if there is no reduction in VP dose by 50%. Treatment should be stopped if VP are reduced by > 50% or after 3 days of treatment in case of no-response	2–6 h daily for 2 days
Blood flow rate (ml/min)	150–700	120-150	100–450	100–300
Anticoagulation	Heparin or citrate	Heparin	Heparin	Heparin or citrate
Additional features	Largest surface area		Adsorbs antithrombin-III from the blood	

Abbreviations: HD – hemodialysis; PEI – polyethyleneimine; SIRS – systemic inflammatory response syndrome; VP – vasopressors.

Supplementary table 3: Contaminant proteins identified in elution samples and excluded from further analysis

UniProt ID	Gene name	Protein name	Species	Potential source of contamination
P00761	N/A	Trypsin	Sus scrofa	Digestion enzyme
P02769	ALB	Serum albumin	Bos taurus	Laboratory contaminant, LC-MS/MS QC-peptide
P04264	KRT1	Keratin, type II cytoskeletal 1	Homo sapiens	Laboratory contaminant
P35908	KRT2	Keratin, type II cytoskeletal 2 epidermal	Homo sapiens	Laboratory contaminant
P35908	KRT79	Keratin, type II cytoskeletal 79	Homo sapiens	Laboratory contaminant
P35908	KRT77	Keratin, type II cytoskeletal 1b	Homo sapiens	Laboratory contaminant
P13645	KRT28	Keratin, type I cytoskeletal 28	Homo sapiens	Laboratory contaminant
P13645	KRT24	Keratin, type I cytoskeletal 24	Homo sapiens	Laboratory contaminant
P13645	KRT10	Keratin, type I cytoskeletal 10	Homo sapiens	Laboratory contaminant
P35527	KRT9	Keratin, type I cytoskeletal 9	Homo sapiens	Laboratory contaminant
P13647	KRT5	Keratin, type II cytoskeletal 5	Homo sapiens	Laboratory contaminant
P04259	KRT6B	Keratin, type II cytoskeletal 6B	Homo sapiens	Laboratory contaminant
P02533	KRT14	Keratin, type I cytoskeletal 14	Homo sapiens	Laboratory contaminant
P02533	KRT32	Keratin, type I cuticular Ha2	Homo sapiens	Laboratory contaminant
Q9NSB2	KRT84	Keratin, type II cuticular Hb4	Homo sapiens	Laboratory contaminant
P08779	KRT16	Keratin, type I cytoskeletal 16	Homo sapiens	Laboratory contaminant
P60985	KRTDAP	Keratinocyte differentiation-associated protein	Homo sapiens	Laboratory contaminant
Q04695	KRT17	Keratin, type I cytoskeletal 17	Homo sapiens	Laboratory contaminant
Q9BYQ8	KRTAP4-9	Keratin-associated protein 4-9	Homo sapiens	Laboratory contaminant
Q9BYQ6	KRTAP4-11	Keratin-associated protein 4-11	Homo sapiens	Laboratory contaminant
P02538	KRT6A	Keratin, type II cytoskeletal 6A	Homo sapiens	Laboratory contaminant
P35900	KRT20	Keratin, type I cytoskeletal 20	Homo sapiens	Laboratory contaminant
O43790	N/A	Keratin, type II microfibrillar, component 7C	Homo sapiens	Laboratory contaminant
O43790	KRT86	Keratin, type II cuticular Hb6	Homo sapiens	Laboratory contaminant
Q15323	N/A	Keratin, type I microfibrillar, 47.6 kDa	Homo sapiens	Laboratory contaminant
Q15323	KRT32	Keratin, type I cuticular Ha2	Homo sapiens	Laboratory contaminant
Q86Y46	KRT79	Keratin, type II cytoskeletal 79	Homo sapiens	Laboratory contaminant
Q86Y46	KRT74	Keratin, type II cytoskeletal 74	Homo sapiens	Laboratory contaminant
P08729	KRT7	Keratin, type II cytoskeletal 7	Homo sapiens	Laboratory contaminant

Supplementary table 4: Proteins, isolated exclusively in the elutions from filters applied during elective valve surgery (n=39)

UniProt ID	Gene name	Protein name	MW, kDa	Functions
P05164	MPO	Myeloperoxidase	83.9	Peroxidase activity
P01023	A2M	Alpha-2-macroglobulin	163.3	Binding
P08133	ANXA6	Annexin A6	75.9	Binding
P04083	ANXA1	Annexin A1	38.7	Binding
P30740	SERPINB1	Leukocyte elastase inhibitor	42.7	Peptidase inhibitor activity
P50995	ANXA11	Annexin A11	54.4	S100 protein binding
P32119	PRDX2	Peroxiredoxin-2	21.9	Antioxidant activity
P07237	P4HB	Protein disulfide-isomerase	57.1	Binding
Q8N6Q3	CD177	CD177 antigen	46.4	Binding
P32942	ICAM3	Intercellular adhesion molecule 3	59.5	Integrin binding, signaling receptor binding
Q93084	ATP2A3	Sarcoplasmic/endoplasmic reticulum calcium ATPase 3	114.0	Binding
Q9HDC9	APMAP	Adipocyte plasma membrane-associated protein	46.5	Arylesterase activity
P09917	ALOX5	Arachidonate 5-lipoxygenase	78.0	Arachidonate 5-lipoxygenase activity, iron binding
P30101	PDIA3	Protein disulfide-isomerase A3	56.8	Endopeptidase activity
P10643	C7	Complement component C7	93.5	Complement factor
Q9UGM5	FETUB	Fetuin-B	42.1	Cysteine-type endopeptidase inhibitor activity
P22894	MMP8	Neutrophil collagenase	53.4	Endopeptidase activity
P29622	SERPINA4	Kallistatin	48.5	Serine-type endopeptidase inhibitor activity
P02649	APOE	Apolipoprotein E	36.2	Amyloid-beta binding, antioxidant activity, cholesterol transfer activity
O75131	CPNE3	Copine-3	60.1	Calcium-dependent phospholipid binding
P23229	ITGA6	Integrin alpha-6	126.6	Cadherin binding
P09525	ANXA4	Annexin A4	35.9	Calcium-dependent phospholipid
Q96PD5	PGLYRP2	N-acetylmuramoyl-L-alanine amidase	62.2	N-acetylmuramoyl-L-alanine amidase activity
Q12907	LMAN2	Vesicular integral-membrane protein VIP36	40.2	Carbohydrate binding
Q10588	BST1	ADP-ribosyl cyclase/cyclic ADP-ribose hydrolase 2	35.7	ADP-ribosyl cyclase activity
O95197	RTN3	Reticulon-3	112.6	Neuroendocrine protein
P02766	TTR	Transthyretin	15.9	Hormone activity, identical protein binding
P63104	YWHAZ	14-3-3 protein zeta/delta	27.8	Cadherin binding
P07737	PFN1	Profilin-1	15.1	Actin binding
Q15828	CST6	Cystatin-M	16.5	Cysteine-type endopeptidase inhibitor

				activity
P39656	DDOST	Dolichyl-diphosphooligosaccharide--protein glycosyltransferase 48 kDa subunit	50.8	Neutrophil degranulation
P11142	HSPA8	Heat shock cognate 71 kDa protein	71.0	Protein folding chaperone
Q5SQ64	LY6G6F	Lymphocyte antigen 6 complex locus protein G6f	32.5	Platelet degranulation
P17301	ITGA2	Integrin alpha-2	129.3	Amyloid-beta binding, collagen binding
P51884	LUM	Lumican	38.4	Collagen binding, extracellular matrix structural constituent
P13671	C6	Complement component C6	104.8	Complement factor
Q96S97	MYADM	Myeloid-associated differentiation marker	35.3	Cell migration, adhesion regulator
O95498	VNN2	Vascular non-inflammatory molecule 2	58.5	Pantetheine hydrolase activity
P08709	F7	Coagulation factor VII	51.6	Calcium ion binding

Supplementary table 5: Proteins, isolated exclusively in the elutions from filters applied during infective endocarditis valve surgery, REMOVE-study (n=22)

UniProt ID	Gene name	Protein name	MW, kDa	Functions
Q14520	HABP2	Hyaluronan-binding protein 2	62.7	Glycocalyx component
P25311	AZGP1	Zinc-alpha-2-glycoprotein	34.3	Transmembrane transporter activity
P69905	HBA1	Hemoglobin subunit alpha	15.3	Heme binding, iron binding
P20160	AZU1	Azurocidin	26.9	Heparan sulfate proteoglycan binding
P27797	CALR	Calreticulin	48.1	Androgen receptor binding
Q12913	PTPRJ	Receptor-type tyrosine-protein phosphatase eta	145.9	Beta-catenin binding
P98160	HSPG2	Basement membrane-specific heparan sulfate proteoglycan core protein	468.8	Amyloid-beta binding, calcium ion binding, extracellular matrix structural constituent
P01019	AGT	Angiotensinogen	53.2	Growth factor activity, hormone activity
P02652	APOA2	Apolipoprotein A-II	11.2	Apolipoprotein receptor binding
P00995	SPINK1	Serine protease inhibitor Kazal-type 1	8.5	Endopeptidase inhibitor activity
Q9UBX5	FBLN5	Fibulin-5	50.2	Calcium ion binding
P0DOX8		Immunoglobulin lambda-1 light chain	22.8	Antigen binding
P16402	H1-3	Histone H1.3	22.4	Chromatin DNA binding
P07339	CTSD	Cathepsin D	44.6	Aspartic-type endopeptidase activity
P05155	SERPING1	Plasma protease C1 inhibitor	55.2	Serine-type endopeptidase inhibitor activity
P01619	IGKV3-20	Immunoglobulin kappa variable 3-20	12.6	Antigen binding
P08833	IGFBP1	Insulin-like growth factor-binding protein 1	27.9	Insulin-like growth factor binding
O75594	PGLYRP1	Peptidoglycan recognition protein 1	21.7	N-acetylmuramoyl-L-alanine amidase activity
P00740	F9	Coagulation factor IX	51.8	Calcium ion binding
P01700	IGLV1-47	Immunoglobulin lambda variable 1-47	12.3	Antigen binding
P13598	ICAM2	Intercellular adhesion molecule 2	30.7	Integrin binding
P01033	TIMP1	Metalloproteinase inhibitor 1	23.2	Cytokine activity, growth factor activity

Supplementary table 6: Proteins isolated in all 11 elution samples (n=127), their molecular weight and functional annotation

UniProt ID	Gene name	Protein name	MW, kDa	Functions
P02768	ALB	Serum albumin	69.4	Binding, transport
P21333	FLNA	Filamin-A	280.7	Binding, protein homodimerization activity
P01024	C3	Complement C3	187.1	Complement compound
P02788	LTF	Lactotransferrin (Lactoferrin)	78.2	Endopeptidase inhibitor, binding, transport
P02787	TF	Serotransferrin (Transferrin)	77.1	Iron transport
P02774	GC	Vitamin D-binding protein	52.9	Binding, transport
P00747	PLG	Plasminogen	90.6	Coagulation factor
P00450	CP	Ceruloplasmin	122.2	Binding, transport
P02751	FN1	Fibronectin	272.3	Binding, extracellular matrix structural constituent
P11215	ITGAM	Integrin alpha-M	127.2	Binding, protein heterodimerization activity
Q14624	ITIH4	Inter-alpha-trypsin inhibitor heavy chain H4	103.4	Endopeptidase inhibitor, acute phase reactant
P01042	KNG1	Kininogen-1	72	Endopeptidase inhibitor, coagulation factor
P01009	SERPINA1	Alpha-1-antitrypsin	46.7	Endopeptidase inhibitor, binding
P08603	CFH	Complement factor H	139.1	Complement compound
P06727	APOA4	Apolipoprotein A-IV	45.4	Lipid transport
P02749	APOH	Beta-2-glycoprotein 1	38.3	Anticoagulant, binds to heparin, phospholipids
P05107	ITGB2	Integrin beta-2	84.8	Binding, protein heterodimerization activity
P35579	MYH9	Myosin-9	226.5	Binding
P04196	HRG	Histidine-rich glycoprotein	59.6	Endopeptidase inhibitor activity, binding
P01011	SERPINA3	Alpha-1-antichymotrypsin	47.7	DNA binding, endopeptidase inhibitor activity
P10909	CLU	Clusterin	52.5	Extracellular chaperone
P05106	ITGB3	Integrin beta-3 (Platelet membrane glycoprotein IIIa)	87.1	Cell adhesion molecule binding, coreceptor activity, protein disulfide isomerase activity, vascular endothelial growth factor receptor 2 binding
P00751	CFB	Complement factor B	85.5	Complement factor
P02647	APOA1	Apolipoprotein A-I	30.8	Binding, transport
P08514	ITGA2B	Integrin alpha-IIb	113.4	Extracellular matrix binding fibrinogen
P02790	HPX	Hemopexin	51.7	Heme binding and transport
P14780	MMP9	Matrix metalloproteinase-9	78.5	Collagen binding, endopeptidase activity
P02671	FGA	Fibrinogen alpha chain	94.9	Extracellular matrix structural constituent, binding
P02675	FGB	Fibrinogen beta chain	55.9	Coagulation factor
P18206	VCL	Vinculin	123.8	Actin binding, structural molecule activity
P02753	RBP4	Retinol-binding protein 4	23.0	Retinol transmembrane transporter activity

P27105	STOM	Erythrocyte band 7 integral membrane protein	31.7	Protein heterodimerization activity, RNA polymerase binding
P02679	FGG	Fibrinogen gamma chain	51.5	Cell adhesion molecule binding, extracellular matrix structural constituent
P18065	IGFBP2	Insulin-like growth factor-binding protein 2	34.8	Insulin-like growth factor I binding
P02765	AHSG	Alpha-2-HS-glycoprotein	39.3	Endopeptidase inhibitor activity
P18428	LBP	Lipopolysaccharide-binding protein (LBP)	53.4	Lipoteichoic acid binding
P08697	SERPINF2	Alpha-2-antiplasmin	54.6	Plasmin and trypsin inhibitor
P01008	SERPINC1	Antithrombin-III	52.6	Binding, endopeptidase inhibitor activity
P08575	PTPRC	Receptor-type tyrosine-protein phosphatase C	147.5	Binding, protein homodimerization activity
P0DOX5	IGHG1	Immunoglobulin gamma-1 heavy chain	49.3	Antigen binding
P04217	A1BG	Alpha-1B-glycoprotein	54.3	Neutrophil and platelet degranulation
P00734	F2	Prothrombin	70.0	Binding, enzyme activator activity
P04004	VTN	Vitronectin	54.3	Extracellular matrix structural constituent, scavenger receptor activity
P80188	LCN2	Neutrophil gelatinase-associated lipocalin	22.6	Binding, protein homodimerization activity
P00738	HP	Haptoglobin	45.2	Antioxidant activity, hemoglobin binding
P43652	AFM	Afamin	69.1	Binding
P17213	BPI	Bactericidal permeability-increasing protein	53.9	Binding
P05160	F13B	Coagulation factor XIII	75.5	Coagulation factor
P03950	ANG	Angiogenin	16.6	Actin binding, protein homodimerization activity
P24158	PRTN3	Myeloblastin	27.8	Enzyme binding, endopeptidase activity
P02763	ORM1	Alpha-1-acid glycoprotein 1	23.5	Acute phase response protein
Q16610	ECM1	Extracellular matrix protein 1	60.7	Extracellular matrix structural constituent, binding
P01876	IGHA1	Immunoglobulin heavy constant alpha 1	37.7	Antigen binding
P61769	B2M	Beta-2-microglobulin	13.7	Binding, protein homodimerization activity
Q12805	EFEMP1	EGF-containing fibulin-like extracellular matrix protein 1	54.6	Binding, growth factor activity
P39060	COL18A1	Collagen alpha-1(XVIII) chain	178.2	Extracellular matrix structural constituent, binding
P01834	IGKC	Immunoglobulin kappa constant	11.8	Antigen binding
P05156	CFI	Complement factor I	65.8	Binding, scavenger receptor activity
P01859	IGHG2	Immunoglobulin heavy constant gamma 2	35.9	Antigen binding
P0DJI8	SAA1	Serum amyloid A-1 protein	13.5	Chemoattractant activity
P0DJI9	SAA2	Serum amyloid A-2 protein	13.5	Chemoattractant activity

P08246	ELANE	Neutrophil elastase	28.5	Binding, endopeptidase activity
P02775	PPBP	Platelet basic protein	13.9	Chemokine activity, transport
P16284	PECAM1	Platelet endothelial cell adhesion molecule	82.5	Protein homodimerization activity
P16671	CD36	Platelet glycoprotein 4	53.1	Toll-like receptor binding
P06396	GSN	Gelsolin	85.7	Binding
P22692	IGFBP4	Insulin-like growth factor-binding protein 4	27.9	Binding
P68871	HBB	Hemoglobin subunit beta	15.9	Binding, oxygen carrier
P11021	HSPA5	Endoplasmic reticulum chaperone BiP	72.3	ATPase activity, binding, chaperone
P00746	CFD	Complement factor D	27.0	Endopeptidase activity
P05556	ITGB1	Integrin beta-1	88.4	Binding
Q9Y490	TLN1	Talin-1	269.8	Binding, structural constituent of cytoskeleton
P05109	S100A8	Protein S100-A8	10.8	Binding, TLR-4 ligand
P19652	ORM2	Alpha-1-acid glycoprotein 2	23.6	Acute phase response protein
P60709	ACTB	Actin, cytoplasmic 1	41.7	ATP binding, cytoskeletal protein
P06702	S100A9	Protein S100-A9	13.2	Antioxidant activity, TLR-4 binding
P49913	CAMP	Cathelicidin antimicrobial peptide	19.3	Antimicrobial activity
P07996	THBS1	Thrombospondin-1	129.4	Binding
P01860	IGHG3	Immunoglobulin heavy constant gamma 3	41.3	Antigen binding
P61626	LYZ	Lysozyme C	16.5	Identical protein binding, antimicrobial activity
P34096	RNASE4	Ribonuclease 4	16.8	Nucleic acid binding, ribonuclease activity
P0DOY2	IGLC2	Immunoglobulin lambda constant 2	11.3	Antigen binding
P40199	CEACAM6	Carcinoembryonic antigen-related cell adhesion molecule 6	37.2	Identical protein binding, protein heterodimerization activity
P11279	LAMP1	Lysosome-associated membrane glycoprotein 1	44.9	Enzyme binding
Q9Y277	VDAC3	Voltage-dependent anion-selective channel protein 3	30.7	Nucleotide binding, porin activity
P31997	CEACAM8	Carcinoembryonic antigen-related cell adhesion molecule 8	38.2	Protein heterodimerization activity
P05452	CLEC3B	Tetranectin	22.5	Binding
P45880	VDAC2	Voltage-dependent anion-selective channel protein 2	31.6	Nucleotide binding, porin activity
P07359	GP1BA	Platelet glycoprotein Ib alpha chain	71.5	Thrombin-activated receptor activity
P05546	SERPIND1	Heparin cofactor 2	57.1	Endopeptidase inhibitor activity, binding
P01034	CST3	Cystatin-C	15.8	Binding, endopeptidase inhibitor activity
P01861	IGHG1	Immunoglobulin heavy constant	35.9	Antigen binding

		gamma 4		
P02760	AMBP	Protein AMBP	38.9	Calcium channel inhibitor activity, binding, endopeptidase inhibitor activity
P00748	F12	Coagulation factor XII	67.8	Calcium ion binding, misfolded protein binding, endopeptidase activity
P0C0L4	C4A	Complement C4-A	192.8	Complement component
P04839	CYBB	Cytochrome b-245 heavy chain	65.3	Binding, protein heterodimerization activity, superoxide-generating NADPH oxidase activity
P02748	C9	Complement component C9	63.2	Complement component
P0DOX7	IGKV1-5	Immunoglobulin kappa light chain	23.4	Antigen binding
P13498	CYBA	Cytochrome b-245 light chain	21.0	Electron transfer activity, binding, superoxide-generating NADPH oxidase activity
Q03591	CFHR1	Complement factor H-related protein 1	37.7	Protein heterodimerization activity, protein homodimerization activity
P16109	SELP	P-selectin	90.1	Protein binding, sialic acid binding
P21796	VDAC1	Voltage-dependent anion-selective channel protein 1	30.8	Ion channel binding, porin activity
P06681	C2	Complement C2	83.3	Metal ion binding, endopeptidase activity
P62979	UBA52	Ubiquitin-40S ribosomal protein S27a	17.9	Metal ion binding, RNA binding, structural constituent of ribosome
P04179	SOD2	Superoxide dismutase [Mn], mitochondrial	24.8	Identical protein binding, metal ion binding
P43304	GPD2	Glycerol-3-phosphate dehydrogenase, mitochondrial	80.9	Calcium ion binding, glycerol-3-phosphate dehydrogenase (quinone) activity
P02654	APOC1	Apolipoprotein C-I	9.3	Fatty acid binding
P02656	APOC3	Apolipoprotein C-III	10.9	Cholesterol binding
P59665	DEFA1	Neutrophil defensin 1	10.2	Antimicrobial protein
P27824	CANX	Calnexin	67.6	Binding
Q99969	RARRES2	Retinoic acid receptor responder protein 2	18.6	Signaling receptor binding
P24592	IGFBP6	Insulin-like growth factor-binding protein 6	25.3	Fibronectin binding, insulin-like growth factor binding
Q08722	CD47	Leukocyte surface antigen CD47	35.2	Cell-cell adhesion mediator activity, protein binding involved in heterotypic cell-cell adhesion
P21926	CD9	CD9 antigen	25.4	Integrin binding
P05090	APOD	Apolipoprotein D	21.3	Cholesterol binding, lipid transporter activity
Q16627	CCL14	C-C motif chemokine 14	10.7	CCR chemokine receptor binding, chemokine activity
Q9Y624	F11R	Junctional adhesion molecule A	32.6	Binding, protein homodimerization activity
P61224	RAP1B	Ras-related protein Rap-1b	20.8	GDP binding, GTPase activity
P13473	LAMP2	Lysosome-associated membrane	44.9	Enzyme binding

		glycoprotein 2		
P13224	GP1BB	Platelet glycoprotein Ib beta chain	21.7	Identical protein binding, transmembrane signaling receptor activity
O14773	TPP1	Tripeptidyl-peptidase 1	61.2	Endopeptidase activity, metal ion binding
P13796	LCP1	Plastin-2	70.3	Actin binding, integrin binding
P02042	HBD	Hemoglobin subunit delta	16.1	Binding, oxygen carrier
P30048	PRDX3	Thioredoxin-dependent peroxide reductase, mitochondrial	27.7	Alkyl hydroperoxide reductase activity
P55774	CCL18	C-C motif chemokine 18	9.8	Chemokine activity
P08571	CD14	Monocyte differentiation antigen CD14	40.1	Binding
P36980	CFHR2	Complement factor H-related protein 2	30.7	Protein hetero- and homodimerization

Supplementary table 7: Hydrophobic proteins isolated from the polymer matrix in all elution samples

UniProt ID	Protein name	Function	Subcellular localization
P68871	Hemoglobin subunit beta	Oxygen transport	Intracellular
P16671	Platelet glycoprotein 4	Receptor for a broad range of ligands	Membrane
P13498	Cytochrome b-245 light chain	Superoxide generation	Membrane
P27105	Erythrocyte band 7 integral membrane protein	Regulates ion channel activity and transmembrane ion transport	Membrane
P04839	Cytochrome b-245 heavy chain	Superoxide generation	Membrane
P18428	Lipopolysaccharide-binding protein	Binding of LPS	Secreted
P30048	Thioredoxin-dependent peroxide reductase, mitochondrial	Reduction of hydrogen peroxide	Mitochondria
P24158	Myeloblastin	Serine protease	Secreted
P08571	Monocyte differentiation antigen CD14	Innate immune response to bacterial LPS	Membrane
P55774	C-C motif chemokine 18	Chemokine	Secreted
P08246	Neutrophil elastase	Serine protease	Intracellular
P59665	Neutrophil defensin 1	Antibacterial, fungicide agent	Intracellular
P13224	Platelet glycoprotein Ib beta chain	Binding to von Willebrand factor	Membrane
P21926	CD9 antigen	Platelet activation and aggregation	Membrane
Q08722	Leukocyte surface antigen CD47	Cell adhesion	Membrane

Supplementary table 8: AGE-modifications identified on the proteins eluted from the CytoSorb filters

UniProt ID	Protein name	Identified modification, position			
		CML	CEL	MGH1	Arg-Pyr
P02768	Human serum albumin#	K36, K65, K75*, K88, K130*, K160, K257, K282, K286*, K305*, K310, K402*, K413*, K426, K437, K438*, K490, K524*, K543*, K549, K558, K588	K75*, K199, K257, K298, K402*, K413*, K426	R105*, R141, R361, R372, R434*, R452, R509*	R34
P02753	Retinol-binding protein 4#	K76	-	-	-
P02788	Lactotransferrin#	K282	-	-	-
P01834	Immunoglobulin kappa constant#	K62*	-	-	-
P04004	Vitronectin#	K117, K159, K131*	-	-	-
P02787	Serotransferrin#	K97*	-	-	-
P08514	Integrin alpha IIb#	K532*	-	-	-
P21333	Filamin-A#	K2240	-	-	-
P01857	Immunoglobulin heavy constant gamma 1	K96, K111	-	-	-
P02749	Beta-2-glycoprotein 1#	K25*, K221, K229*, K306	K25*	-	-
P36980	Complement factor H-related protein 2#	K40	-	-	-
P02679	Fibrinogen gamma chain#	K166*	-	-	-
P02790	Hemopexin#	K441	-	-	-
P02675	Fibrinogen beta chain#	K88, K178*	-	-	-
O60496	Docking protein 2		K21	-	-
P02763	Alpha-1-acid glycoprotein 1#	K138*	-	-	-
P02765	Alpha-2-HS-glycoprotein#	K68*	-	-	-
P02774	Vitamin D-binding protein#	K114	K394*, K402*	-	-
P01042	Kininogen-1#	K254	-	-	-
P59665	Neutrophil defensin 1#	-	-	R88	-
P01861	Immunoglobulin heavy constant gamma 1#	K197*	-	-	-
P13671	Complement component C6	K131*	-	-	-
P01859	Immunoglobulin heavy constant gamma 2#	-	K96, K196	-	-
O75182	Paired amphipathic helix protein Sin3b	-	-	-	R932, R935

Only non-contaminant proteins with PEP value < 0.05 were taken into consideration.

* Modification at this amino acid residue was identified in more than one elution sample.

Proteins isolated in all 11 samples eluted from the filters used for intraoperative hemofiltration.

Supplementary table 9: Proteins significantly up-regulated in the plasma samples after intraoperative HF in REMOVE-study subgroup

UniProt ID	Gene	Protein	Ratio	P-value	Q-value
P02144	MB	Myoglobin	5.84	2.56E-09	4.37E-09
P01040	CSTA	Cystatin-A	4.31	1.18E-09	2.05E-09
P31327	CPS1	Carbamoyl-phosphate synthase [ammonia], mitochondrial	4.22	0.05	0.03
P02788	LTF	Lactotransferrin	4.20	1.17E-18	3.57E-18
P32119	PRDX2	Peroxiredoxin-2	3.90	4.15E-57	4.38E-56
P30043	BLVRB	Flavin reductase (NADPH)	2.96	2.09E-19	7.13E-19
P04040	CAT	Catalase	2.77	3.57E-59	4.60E-58
P00915	CA1	Carbonic anhydrase 1	2.68	3.84E-89	7.42E-88
P15924	DSP	Desmoplakin	2.67	1.06E-05	1.21E-05
P14923	JUP	Junction plakoglobin	2.63	3.18E-05	3.34E-05
P68871	HBB	Hemoglobin subunit beta	2.39	2.99E-163	3.47E-161
P17174	GOT1	Aspartate aminotransferase, cytoplasmic	2.30	0.002	0.001
Q02818	NUCB1	Nucleobindin-1	2.24	2.36E-19	7.81E-19
P69891	HBG1	Hemoglobin subunit gamma-1	2.18	1.69E-07	2.46E-07
P80188	LCN2	Neutrophil gelatinase-associated lipocalin	2.17	2.44E-08	3.78E-08
Q9NZT1	CALML5	Calmodulin-like protein 5	2.16	8.99E-07	1.17E-06
P10599	TXN	Thioredoxin	2.10	1.94E-21	7.50E-21
Q6UWP8	SBSN	Suprabasin	2.08	0.0006	0.0005
Q06830	PRDX1	Peroxiredoxin-1	2.06	2.72E-15	6.72E-15
P31151	S100A7	Protein S100-A7	2.05	0.01	0.007
P00918	CA2	Carbonic anhydrase 2	1.99	5.05E-25	2.34E-24
P30041	PRDX6	Peroxiredoxin-6	1.93	3.29E-06	3.98E-06
P06702	S100A9	Protein S100-A9	1.91	4.42E-24	1.97E-23
Q14515	SPARCL1	SPARC-like protein 1	1.86	0.02	0.01
P00558	PGK1	Phosphoglycerate kinase 1	1.87	3.00E-06	3.67E-06
P04275	VWF	von Willebrand factor	1.86	1.18E-125	3.42E-124
P49913	CAMP	Cathelicidin antimicrobial peptide	1.83	1.99E-12	3.79E-12
P04070	PROC	Vitamin K-dependent protein C	1.78	2.36E-16	6.22E-16
P0CG47	UBB	Polyubiquitin-B	1.76	1.30E-12	2.51E-12
P81605	DCD	Dermcidin	1.69	4.17E-28	2.20E-27
P60174	TPI1	Triosephosphate isomerase	1.66	1.17E-06	1.49E-06
P00740	F9	Coagulation factor IX	1.62	5.08E-49	4.53E-48
P04406	GAPDH	Glyceraldehyde-3-phosphate dehydrogenase	1.61	1.04E-11	1.91E-11
P78417	GSTO1	Glutathione S-transferase omega-1	1.54	6.72E-09	1.11E-08
P00441	SOD1	Superoxide dismutase [Cu-Zn]	1.53	6.15E-07	8.20E-07
P05109	S100A8	Protein S100-A8	1.51	4.61E-35	2.81E-34

Supplementary table 10: Proteins significantly up-regulated in the plasma samples after intraoperative HF in elective AVR subgroup

UniProt ID	Gene	Protein	Ratio	P-value	Q-value
P14780	MMP9	Matrix metalloproteinase-9	16.02	0.0001	0.0001
P26038	MSN	Moesin	14.22	0.03	0.02
Q08554	DSC1	Desmocollin-1	8.75	4.44E-07	8.58E-07
Q00839	HNRNPU	Heterogeneous nuclear ribonucleoprotein U	7.13	0.02	0.01
P78417	GSTO1	Glutathione S-transferase omega-1	5.89	5.79E-06	1.02E-05
P31151	S100A7	Protein S100-A7	5.57	0.001	0.001
P68104	EEF1A1	Elongation factor 1-alpha 1	5.26	0.03	0.02
P60174	TPI1	Triosephosphate isomerase	4.12	0.0007	0.0008
P69891	HBG1	Hemoglobin subunit gamma-1	3.96	2.32E-05	3.74E-05
P30041	PRDX6	Peroxiredoxin-6	3.83	7.64E-11	1.97E-10
P02788	LTF	Lactotransferrin	3.49	0.0001	0.000156
P68871	HBB	Hemoglobin subunit beta	3.26	3.64E-95	2.11E-93
P06702	S100A9	Protein S100-A9	3.13	2.02E-61	5.85E-60
P32119	PRDX2	Peroxiredoxin-2	3.08	3.19E-26	1.76E-25
P04406	GAPDH	Glyceraldehyde-3-phosphate dehydrogenase	2.97	3.03E-13	9.25E-13
P04040	CAT	Catalase	2.93	2.59E-60	5.01E-59
P01040	CSTA	Cystatin-A	2.88	7.68E-05	0.000111
P0CG47	UBB	Polyubiquitin-B	2.76	2.47E-11	6.65E-11
P00915	CA1	Carbonic anhydrase 1	2.65	1.36E-37	1.57E-36
P02792	FTL	Ferritin light chain	2.58	0.006	0.005101
P02042	HBD	Hemoglobin subunit delta	2.54	5.87E-36	6.19E-35
P04075	ALDOA	Fructose-bisphosphate aldolase A	2.35	5.62E-05	8.69E-05
P08294	SOD3	Extracellular superoxide dismutase [Cu-Zn]	2.35	1.96E-20	7.84E-20
P07437	TUBB	Tubulin beta chain	2.33	0.0004	0.0005
P10599	TXN	Thioredoxin	2.16	5.65E-16	1.99E-15
P14618	PKM	Pyruvate kinase PKM	2.06	0.02	0.01
P00558	PGK1	Phosphoglycerate kinase 1	1.90	0.0002	0.0002
P07195	LDHB	L-lactate dehydrogenase B chain	1.83	6.26E-05	9.44E-05
P05109	S100A8	Protein S100-A8	1.78	1.98E-21	8.85E-21
P00740	F9	Coagulation factor IX	1.75	9.02E-26	4.55E-25
P08670	VIM	Vimentin	1.65	0.04	0.03
P04275	VWF	von Willebrand factor	1.63	9.13E-34	7.06E-33
P01602	IGKV1-5	Ig heavy chain V-I region 5	1.58	0.002	0.002
P03951	F11	Coagulation factor XI	1.57	0.0001	0.0001
P63104	YWHAZ	14-3-3 protein zeta/delta	1.55	6.70E-05	9.89E-05

Supplementary table 11: Proteins identified on the filter matrix, and down-regulated in plasma samples after the intervention in both patient subgroups (n=22)

UniProt ID	Gene name	Protein name	MW, kDa	Functions
P02787	TRF	Serotransferrin	77.1	Iron transport
P00747	PLG	Plasminogen	90.6	Anticoagulation factor
Q14624	ITIH4	Inter-alpha-trypsin inhibitor heavy chain H4	103.4	Endopeptidase inhibitor, acute phase reactant
P01042	KNG1	Kininogen-1	72.0	Endopeptidase inhibitor, coagulation factor
P01009	SERPINA1	Alpha-1-antitrypsin	46.7	Endopeptidase inhibitor, binding
P06727	APOA4	Apolipoprotein A-IV	45.4	Lipid transport
P02749	APOH	Beta-2-glycoprotein 1	38.3	Anticoagulant, binds to heparin, phospholipids
P04196	HRG	Histidine-rich glycoprotein	59,6	Endopeptidase inhibitor activity, binding
P10909	CLU	Clusterin	52.5	Extracellular chaperone
P00751	CFAB	Complement factor B	85.5	Complement factor
P02671	FGA	Fibrinogen alpha chain	94.9	Extracellular matrix structural constituent, binding
P02753	RBP4	Retinol-binding protein 4	23.0	Retinol transmembrane transporter activity
P08697	SERPINF2	Alpha-2-antiplasmin	54.6	Plasmin and trypsin inhibitor
P04004	VTN	Vitronectin	54.3	Extracellular matrix structural constituent, scavenger receptor activity
P0DJI9	SAA2	Serum amyloid A-2 protein	13.5	Chemoattractant activity
Q9Y490	TLN1	Talin-1	269.8	Binding, structural constituent of cytoskeleton
P19652	ORM2	Alpha-1-acid glycoprotein 2	23.6	Acute phase response protein
P01034	CST3	Cystatin-C	15.8	Endopeptidase inhibitor activity
P02654	APOC1	Apolipoprotein C-I	9.3	Fatty acid binding
P02656	APOC3	Apolipoprotein C-III	10.9	Cholesterol binding
P24592	IGFBP6	Insulin-like growth factor-binding protein 6	25.3	Fibronectin binding, insulin-like growth factor binding
P05090	APOD	Apolipoprotein D	21.3	Cholesterol binding, lipid transporter activity

Supplementary table 12: Proteins exclusively down-regulated in the plasma samples after CPB with HF in the subgroup of REMOVE-study participants (n=49)

UniProt ID	Gene name	Protein name	MW, kDa	Functions
P02750	LRG1	Leucine-rich alpha-2-glycoprotein	38.2	Neutrophil degranulation
P07357	C8A	Complement component C8 alpha chain	65.2	Complement component
P01871	IGHM	Immunoglobulin heavy constant mu	49.4	Antigen binding
O75882	ATRN	Attractin	158.5	Inflammatory response
P14618	PKM	Pyruvate kinase	57.9	Glycolytic enzyme
P12277	CKB	Creatine kinase B-type	42.6	Phosphocreatine metabolism
P01877	IGHA2	Immunoglobulin heavy constant alpha 2	36.6	Antigen binding
P19338	NCL	Nucleolin	76.6	Induction of chromatin decondensation
P06576	ATP5F1B	ATP synthase subunit beta, mitochondrial	56.6	ATP biosynthesis
P68104	EEF1A1	Elongation factor 1-alpha 1	50.1	GTP-dependent binding of aminoacyl-tRNA in ribosome
A6NIZ1	N/A	Ras-related protein Rap-1b-like protein	20.9	Cellular response to cAMP
P01598	IGKV1-5	Immunoglobulin kappa variable 1-5	12.8	Antigen binding
P01857	IGHG1	Immunoglobulin heavy constant gamma 1	36.1	Antigen binding
Q15485	FCN2	Ficolin-2	34.0	Activation of the lectin complement pathway
P01610	IGKV1-17	Immunoglobulin kappa variable 1-17	12.8	Antigen binding
P29401	TKT	Transketolase	67.9	Pentose-phosphate shunt enzyme
Q8WUM4	PDCD6IP	Programmed cell death 6-interacting protein	96.0	Endocytosis, multivesicular body biogenesis, membrane repair, cytokinesis, apoptosis
P01612	IGKV1-39	Immunoglobulin kappa variable 1-39	12.7	Antigen binding
P55072	VCP	Transitional endoplasmic reticulum ATPase	89.3	Fragmentation of Golgi stacks during mitosis
P30086	PEBP1	Phosphatidylethanolamine-binding protein 1	21.1	Negative regulation of MAPK cascade
O75400	PRPF40A	Pre-mRNA-processing factor 40 homolog A	108.8	Regulation of cell morphology and cytoskeletal organization
P01743	IGHV1-46	Immunoglobulin heavy variable 1-46	12.9	Antigen binding
P37802	TAGLN2	Transgelin-2	22.4	Platelet degranulation
P60660	MYL6	Myosin light polypeptide 6	16.9	Contractile muscle

				filament
O75369	FLNB	Filamin-B	278.2	Actin cytoskeleton organisation
P01617	IGKV2D-28	Immunoglobulin kappa variable 2D-28	13.0	Antigen binding
P61978	HNRNPK	Heterogeneous nuclear ribonucleoprotein K	51.0	pre-mRNA-binding
P80511	S100A12	Protein S100-A12	10.6	Regulation of inflammatory processes and immune response
O00410	IPO5	Importin-5	123.6	Nuclear transport receptor
P01761	IGHV1-69	Immunoglobulin heavy variable 1-69	12.7	Antigen binding
P04208	IGLV1-47	Immunoglobulin lambda variable 1-47	12.3	Antigen binding
P01714	IGLV3-19	Immunoglobulin lambda variable 3-19	12.0	Antigen binding
Q7L1Q6	BZW1	Basic leucine zipper and W2 domain-containing protein 1	48.0	Enhances histone H4 gene transcription
P80748	IGLV3-21	Immunoglobulin lambda variable 3-21	12.5	Antigen binding
B9A064	IGLL5	Immunoglobulin lambda-like polypeptide 5	23.1	Antigen binding
P01702	IGHV3-7	Immunoglobulin heavy variable 3-7	12.9	Antigen binding
P01781	IGHV1-2	Immunoglobulin heavy variable 1-2	13.1	Antigen binding
P02745	C1QA	Complement C1q subcomponent subunit A	26.0	Complement activation
P02745	PLEC	Plectin	531.8	Complement activation
A6NHG4	DDTL	D-dopachrome decarboxylase-like protein	14.2	Lyase
P22626	HNRNPA2B1	Heterogeneous nuclear ribonucleoproteins A2/B1	37.4	mRNA processing, regulation of transcription
Q12874	SF3A3	Splicing factor 3A subunit 3	58.9	pre-mRNA splicing
P01701	IGLV1-51	Immunoglobulin lambda variable 1-51	12.3	Antigen binding
P15880	RPS2	40S ribosomal protein S2	31.3	RNA processing
Q9NZP8	C1RL	Complement C1r subcomponent-like protein	53.5	Complement activation
P03951	F11	Coagulation factor XI	70.1	Coagulation factor
P38646	HSPA9	Stress-70 protein, mitochondrial	73.7	Mitochondrial chaperone protein
P04209	IGLV2-14	Immunoglobulin lambda variable 2-14	12.6	Antigen binding
P62841	RPS15	40S ribosomal protein S15	17.0	Ribosome small subunit assembly

Supplementary table 13: Proteins exclusively down-regulated in the plasma samples after CPB with HF in the subgroup of patients undergoing elective aortic valve surgery (n=13)

UniProt ID	Gene name	Protein name	MW, kDa	Functions
P49908	SELENOP	Selenoprotein P	43.2	Selenium binding
P07900	HSP90AA1	Heat shock protein HSP 90-alpha	84.7	Molecular chaperone
P08238	HSP90AB1	Heat shock protein HSP 90-beta	83.3	Molecular chaperone
P11597	CETP	Cholesteryl ester transfer protein	54.8	Cholesterol transport
P00739	HPR	Haptoglobin-related protein	39.0	Hemoglobin binding, acute inflammatory response
P14625	HSP90B1	Endoplasmin	92.5	Molecular chaperone
P33908	MAN1A1	Mannosyl-oligosaccharide 1,2-alpha-mannosidase IA	73.0	Protein glycosylation
P67936	TPM4	Tropomyosin alpha-4 chain	28.5	Ca^{2+}-dependent muscle contraction
P01712	IGLV2-11	Immunoglobulin lambda variable 2-11	12.6	Antigen binding
P22891	PROZ	Vitamin K-dependent protein Z	44.7	Blood coagulation
P02746	C1QB	Complement C1q subcomponent subunit B	26.7	Complement activation
P30043	BLVRB	Flavin reductase	22.1	Heme catabolism
P00918	CA2	Carbonic anhydrase 2	29.3	Bicarbonate transport

Supplementary table 14: Proteins down-regulated in plasma samples after CPB with HF in both patient subgroups (n=13)

UniProt ID	Gene name	Protein name	MW, kDa	Protein function
P02743	SAMP	Serum amyloid P-component	25.4	Acute phase response protein, complement activation
P02776	PF4	Platelet factor 4	10.9	Chemokine activity
P04180	LCAT	Phosphatidylcholine-sterol acyltransferase	49.6	Apolipoprotein A-I binding
P17936	IBP3	Insulin-like growth factor-binding protein 3	31.7	Fibronectin binding, insulin-like growth factor I binding
P43251	BTD	Biotinidase	61.1	Biotinidase activity
P02655	APOC2	Apolipoprotein C-II	11.3	Lipase inhibitor activity
P00325	ADH1B	All-trans-retinol dehydrogenase	39.9	Alcohol and retinol dehydrogenase activity
P06312	KV401	Immunoglobulin kappa variable 4-1	13.4	Antigen binding
P01764	HV323	Immunoglobulin heavy variable 3-23	12.6	Antigen binding
P41222	PTGDS	Prostaglandin-H2 D-isomerase	21.0	Fatty acid binding
P12814	ACTN1	Alpha-actinin-1	103.1	Actin filament and integrin binding
P10809	CH60	60 kDa heat shock protein, mitochondrial	61.1	Molecular chaperone
Q13790	APOF	Apolipoprotein F	35.4	Cholesterol binding

Supplementary table 15: Top-20 most significantly up-regulated genes in elution-treated HAECs (mRNA-array data, n=2)

Gene name	RefSeq ID	Protein name	Fold up-regulated	p-value
PSAT1	NM_021154	Phosphoserine aminotransferase 1	18.30	0.005
ASNS	NM_001178075	Asparagine synthetase (glutamine-hydrolyzing)	15.79	0.02
NUPR1	NM_001042483	Transcriptional regulator 1 (p8)	9.76	0.004
MTHFD2	NM_006636	Methylenetetrahydrofolate dehydrogenase (NADP+ dependent) 2	7.14	0.02
STC1	NM_003155	Stanniocalcin 1	6.47	0.04
DHCR7	NM_001163817	7-dehydrocholesterol reductase	6.31	0.002
SLC7A11	NM_014331	Solute carrier family 7	6.13	0.03
PTX3	NM_002852	Pentraxin 3, long	5.78	0.02
RAC2	NM_002872	Ras-related C3 botulinum toxin substrate 2	4.60	0.003
VEGFA	NM_001025366	Vascular endothelial growth factor A	4.57	0.03
SLC3A2	NM_001012662	Solute carrier family 3 (amino acid transporter heavy chain), member 2	4.49	0.003
ERRFI1	NM_018948	ERBB receptor feedback inhibitor 1	4.43	0.02
ANKRD20A3	NM_001012419	Ankyrin repeat domain 20 family, member A3	4.42	0.007
NOB1	NM_014062	NIN1/RPN12 binding protein 1 homolog	4.36	0.002
SARS	NM_006513	Seryl-tRNA synthetase	4.27	0.04
ZCCHC7	NM_001289119	Zinc finger, CCHC domain containing 7	4.22	0.04
STC2	NM_003714	Stanniocalcin 2	4.18	0.04
MYADM	NM_001020818	Myeloid-associated differentiation marker	4.14	0.002
ZBTB41	NM_194314	Zinc finger and BTB domain containing 41	4.00	0.04
TGFB1I1	NM_001042454	Transforming growth factor beta 1 induced transcript 1	4.00	0.002

Abbreviations: BTB - Broad-Complex, Tramtrack and Bric a brac; CCHC – CysCysHisCys domain; ERBB - Receptor tyrosine-protein kinase erbB-2; GTP – guanosintriphosphate; NADP+ - nicotinamide adenine dinucleotide phosphate; NIN1 - Neutral/alkaline invertase 1; Ras – rat sarcoma gene, encoding small G-protein; RPN12 - proteasome regulatory particle lid subunit; tRNA – transfer RNA.

Supplementary table 16: Top-20 most significantly down-regulated genes in elution-treated HAECs (mRNA-array data, n=2)

Gene name	RefSeq ID	Protein name	Fold down-regulated	p-value
KIF20A	NM_005733	Kinesin family member 20A	0.13	0.01
PBK	NM_001278945	PDZ binding kinase	0.15	0.01
FABP5	NM_001444	Fatty acid binding protein 5 (psoriasis-associated)	0.15	0.04
TXNIP	NM_006472	Thioredoxin interacting protein	0.16	0.01
CENPI	NM_006733	Centromere protein I	0.17	0.01
FOXM1	NM_001243088	Forkhead box M1	0.18	0.01
DLGAP5	NM_001146015	Discs, large (Drosophila) homolog-associated protein 5	0.18	0.04
PRC1	NM_001267580	Protein regulator of cytokinesis 1	0.19	0.04
GINS1	NM_021067	GINS complex subunit 1 (Psf1 homolog)	0.20	0.03
BUB1	NM_001278616	BUB1 mitotic checkpoint serine/threonine kinase	0.20	0.05
TPX2	NM_012112	TPX2, microtubule-associated	0.21	0.01
CCNB1	NM_031966	Cyclin B1	0.22	0.004
EFNB2	NM_004093	Ephrin-B2	0.23	0.004
FAM83D	NM_030919	Family with sequence similarity 83, member D	0.24	0.05
NDC80	NM_006101	NDC80 kinetochore complex component	0.24	0.04
ESCO2	NM_001017420	Establishment of sister chromatid cohesion N-acetyltransferase 2	0.24	0.03
PCDH10	NM_020815	Protocadherin 10	0.24	0.01
DIAPH3	NM_001042517	Diaphanous-related formin 3	0.25	0.04
MGP	NM_000900	Matrix Gla protein	0.25	0.04
ASPM	NM_001206846	Abnormal spindle microtubule assembly	0.25	0.02

Abbreviations: BUB1 - budding uninhibited by benzimidazoles 1; GINS - an acronym created from the first letters of the Japanese numbers 5-1-2-3 (***g****o*-***i****chi*-***n****i*-***s****an*) in a reference to the 4 protein subunits of the complex: Sld5, Psf1, Psf2, and Psf3; Gla - vitamin K-dependent carboxylation/gamma-carboxyglutamic domain; NDC80 - kinetochore complex component; PDZ (initialism) – protein domain common for post-synaptic density protein (**P**SD95), Drosophila disc large tumor suppressor (**D**lg1), and zonula occludens-1 protein (**z**o-1); Psf1 – protein of GINS-complex; TPX2 - microtubule nucleation factor.

Supplementary table 17: Pre- and postoperative plasma biomarkers of inflammatory response in patients undergoing valve surgery with CPB and HF

Patient number	C-reactive protein, mg/l		Procalcitonin, µg/l	
	Pre	Post	Pre	Post
1	80	64	3.83	0.42
2	54.9	37.4	8.53	92.9
3	166	51	0.12	0.71
4	6	49	0.03	8.06
5	41	71	1.14	1.82
6	48	29	0.5	1.76
7	34	92	n.a.	0.84
8	13	54	n.a.	1.8
9	2.3	101	n.a.	1.95
10	4.4	76.5	n.a.	0.51
11	5.7	48.7	n.a.	0.19
12	84	97	0.59	9.96

Supplementary table 18: Laboratory parameters of the blood in pre- and postoperative period

Patient number	Total plasma protein, g/l		Albumin, g/l		Fibrinogen, g/l		Hb, g/dL		Er, 10^{12}/l		HCT, l/l	
	Pre	Post	Pre	Post	Pre	Post	Pre	Post	Pre	Post	Pre	Post
1	n.a.	48	n.a.	27.1	4.31	3.9	4	5.1	2.52	3.08	0.19	0.24
2	78	61‡	27.8	7.8	3.41	2.28	7.2	6.7	4.59	4.13	0.36	0.32
3	67	28	28	11	3.59	3.04	5.8	5.4	4.2	3.2	0.32	0.23
4	62	49	35.6	26	4.53	4.09	8.7	7.7	4.46	3.19	0.40	0.35
5	58‡	56	22‡	20.6	n.a.	3.18	4.4	7.6	2.46	4.39	0.21	0.36
6	79‡	48	45.3‡	24,2	3.9	2.56	4.5	6.6	2.4	3.5	0.22	0.3
7	80	46	n.a.	29.5	5.99	3.41	7.4	5.9	3.63	3.04	0.34	0.27
8	79	45	n.a.	21.4	4.27	3.67	7.4	6.4	3.86	3.35	0.35	0.3
9	76	45	n.a.	34.9	3.25	3.41	9.6	6.9	5.1	3.67	0.43	0.31
10	58	37	36.6	29.5	4.4	3.77	8.6	5.3	4.87	2.96	0.42	0.26
11	76	51	n.a.	29.7	4.45	2.98	7	5.3	3.95	2.88	0.34	0.25
12	67	31	32	18	n.a.	4.82	5.7	7.5	3.5	4.38	0.28	0.35

Abbreviations: Hb – hemoglobin; Er – red blood cells; HCT – hematocrit.
n.a. – some of the parameters were not routinely measured in preoperative settings;
‡ – marked parameters were not measured directly in pre-operative settings.

Supplementary table 19: Duration of ICU stay, ventilation time, and perioperative vasopressor use (24 hours in ICU) in the study population

Patient number	Adrenalin, µg	Noradrenalin, µg	Duration of ICU stay, days	Ventilation time, hours/days
1	5568	2819	2	12 h
2	-	7680	8	8 d
3	95090	46160	52	52 d
4	14,4	1908	5	5 h
5	-	93960	39	35 d
6	-	4768	7	7 h
7	-	6962	7	10 h
8	15893	13570	6	24 h
9	-	1208	4	5 h
10	10	1800	9	12 h
11	-	672	3	10 h
12	-	35792	7*	7 d*

Abbreviations: ICU – intensive care unit.

* Patient was referred to another institution after 7 days of ICU-stay.

Supplementary table 20: Increased expression of metabolic regulators in response to treatment with eluted proteins (mRNA-array data)

Protein metabolism	Folate and nucleic acid metabolism	Energy metabolism	Lipid metabolism	Transcription factors
Amino acid synthetases: ASNS, CBS, PSAT, SHMT2	**Folate metabolism:** MTHFD2, MTHFD1L, SHMT2	**NAD/NADP+ metabolism:** TKT, PGD, H6PD, ME1, NDUFA10	**Cholesterol biosynthesis:** ACACA, ACAT2, CYP51A1, DHCR7, SDC, TM7SF2	ANKRD1, JUN, KLF11, NFE2L3, NFKBIZ, NR2F2, NUPR1, RORA, RGMB, ZFHX4
Amino-acyl tRNAs: AARS, CARS, GARS, IARS, SARS		**AMP biosynthesis:** ADSL, AK5	**Low-density lipoprotein receptor:** LDLR	
Transporters: SLC7A2, SLC1A5, SLC3A2, SLC7A11		**Biogenesis of mitochondria:** MTFR1L, OXA1L	**Cell membrane remodeling:** PLSCR4	
Control of translation: EEF2, EIF2A, EIF3D, EFTUD1, RPL7A, RPL13, RPL18A, OXA1L			**Prostaglandin biosynthesis:** PTGS1, PTGR1	

Abbreviations: AARS - aminoacyl-tRNA synthetase; ACACA - acetyl-CoA carboxylase alpha; ACAT2 - cytosolic acetoacetyl-CoA thiolase; ADSL - adenylosuccinate lyase; AK5 - adenylate kinase isoenzyme 5; ANKRD1 - ankyrin repeat domain 1; ASNS – asparagine synthetase (glutamine-hydrolyzing); CARS - cysteinyl-tRNA synthetase; CBS - cystathionine beta-synthase; CYP51A1 - lanosterol 14-alpha demethylase; DHCR7 - 7-dehydrocholesterol reductase; EEF2 - eukaryotic elongation factor 2; EIF2A - eukaryotic translation initiation factor 2A; EIF3D - eukaryotic translation initiation factor 3 subunit D; EFTUD1 - elongation factor Tu GTP-binding domain-containing protein 1 isoform 1; GARS - glycyl-tRNA synthetase 1; H6PD - hexose-6-phosphate dehydrogenase/glucose 1-dehydrogenase; IARS - isoleucyl-tRNA synthetase 1; JUN - jun proto-oncogene; KLF11 - Kruppel like factor 11; NDUFA10 - NADH:ubiquinone oxidoreductase subunit A10; LDLR - low-density lipoprotein receptor; MTHFD2 - methylenetetrahydrofolate dehydrogenase (NADP+ dependent) 2; MTHFD1L - methylenetetrahydrofolate dehydrogenase (NADP+ dependent) 1 like; MTFR1L - mitochondrial fission regulator 1 like; NFE2L3 - nuclear factor, erythroid 2 like 3; NFKBIZ - NFKB inhibitor zeta; NR2F2 - nuclear receptor subfamily 2 group F member 2; NUPR1 - nuclear protein 1, transcriptional regulator; OXA1L - mitochondrial inner membrane protein; PLSCR4 - phospholipid scramblase 4; PSAT - phosphoserine aminotransferase; PTGS1 - prostaglandin-endoperoxide synthase 1; PTGR1 - prostaglandin reductase 1; RPL7A - ribosomal protein L7a; RPL13 - ribosomal protein L13; RPL18A - ribosomal protein L18a; RORA - RAR related orphan receptor A; RGMB - repulsive guidance molecule B; SDC - syndecan 1; SHMT2 - serine hydroxymethyltransferase, mitochondrial; SLC7A2 - cationic amino acid transporter 2; SLC1A5 - sodium-dependent neutral amino acid transporter; SLC3A2 - solute carrier family 3 member 2; SLC7A11 - cystine/glutamate transporter; TKT – transketolase; TM7SF2 - transmembrane 7 superfamily member 2; ZFHX4 - zinc finger homeobox 4.

Supplementary table 21: Reagents, kits and antibodies used in experimental settings

Reagent / kit /antibody	Manufacturer	Ordering Nr
4–20% Criterion™ TGX™ Precast Midi Protein Gel	BioRad	#567-1093
4–20% Mini-PROTEAN® TGX™ Precast Protein Gel	BioRad	#456-1093
β-actin - 1°Ab	Cell Signalling Technology	#8457
β-actin - 1°Ab	Sigma Aldrich	A5441
Alexa Fluor 488 anti-mouse – 2°Ab	Dianova	715-546-150
ASNS - 1°Ab	Abcam	ab126254
ATF4 - 1°Ab	Abcam	ab184909
BCA Protein Assay Kit	Thermo Scientific	23225
Benzonase	Novagen	70664-10KUN
Bovine serum albumin	Applichem	A1391
BUB1 - 1°Ab	Abcam	ab195268
CBA Human Inflammatory Cytokine Kit	BD Biosciences	551811
CellTiter Blue Cell Viability Assay	Promega	G8081
Chloroform	Sigma Aldrich	32211-1L-M
COXIV - 1°Ab	Abcam	ab33985
Endothelial cell growth medium 2 (ECGM2)	Promocell	C-22011
Cy3 anti-rabbit - 2°Ab	Dianova	711-166-152
Cy3 anti-mouse - 2°Ab	Dianova	715-166-150
Goat anti-rabbit green	Li-Cor	926-32211
Fetal calf serum (FCS)	Zellbiologische Produkte	798586
Glycine	Roth	3187
Goat anti-mouse red	Li-Cor	926-68020
Histone H3 - 1°Ab	Cell Signaling	#14269
Human serum	Sigma	P2918
hs-CRP ELISA-kit	IBL International	EU59151
IL-6 ELISA kit	IBL International	BE58061
Isopropanol	Sigma Aldrich	33539-1L-M
KIF20A - 1°Ab	Abcam	ab70791
MTHFD2 - 1°Ab	Abcam	ab151447
PAI-1 - 1°Ab	Santa Cruz	sc-5297
PageRuler Prestained Protein Ladder	Thermo Scientific	26616
Penicillin-streptomycin	Sigma Aldrich	P4333
Phenylmethylsulfonylfluoride (PMSF)	Applichem	A0999
Phosphate-buffered saline pH 7.4 (1xPBS)	Gibco	10010-015
Phospho-KIF20A (Ser528) - 1°Ab	Invitrogen	#PA5-40224
Protease inhibitor cocktail (PIC)	Sigma-Aldrich	P8340
Protein transport inhibitor cocktail (PTIC)	Thermo Scientific	00-4980-03
PSAT1 - 1°Ab	Abcam	ab96136
RIPA buffer	Merck	20-188
RNeasy MinElute Cleanup Kit	Quiagen	74204
Roti-Stock, SDS 20% solution	Roth	1057
Roti fair TBS pH 7.6	Roth	1244
Sapphire700 Stain	Li-Cor	928-40022
Sodium orthovanadate	Sigma Aldrich	S6508
STC1 - 1°Ab	Abcam	ab83065
tPA - 1°Ab	Boster Immunnoleader	PB9345
Tris-hydrochloride	Boehringer Mannheim	812846
Trizma (Tris-base)	Sigma Aldrich	T1503
TRIzol Reagent	Life Technologies	15596018
Trypsin-EDTA	Life Technologies	15400-054
vWF - 1°Ab	Abcam	ab6994

1°Ab / 2°Ab – primary / secondary antibody

9.2. Supplementary figures

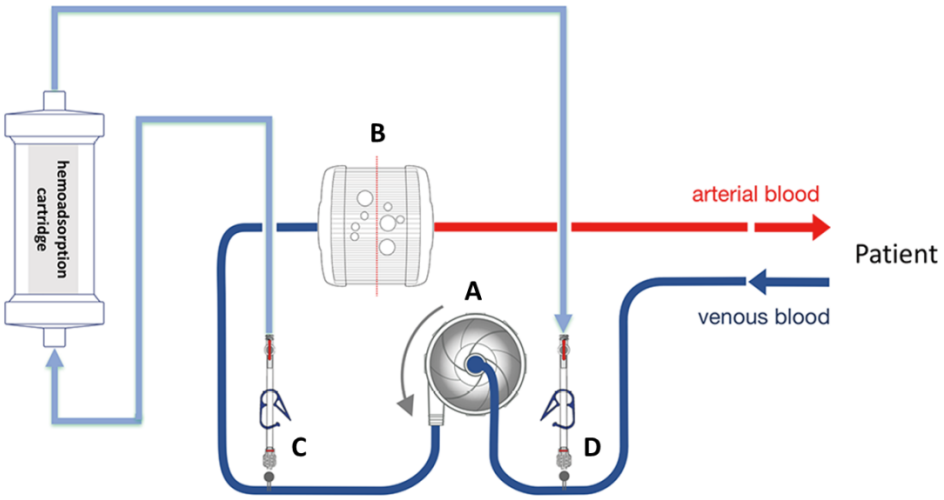

Supplementary figure 1: Application of hemofiltration cartridge in cardiopulmonary bypass. HF cartridge is integrated into extracorporeal circuit consisting of roller pump (A), membrane oxygenator (B), attached to the contour with adaptors (C, D). Figure from Datzmann & Träger, 2017.

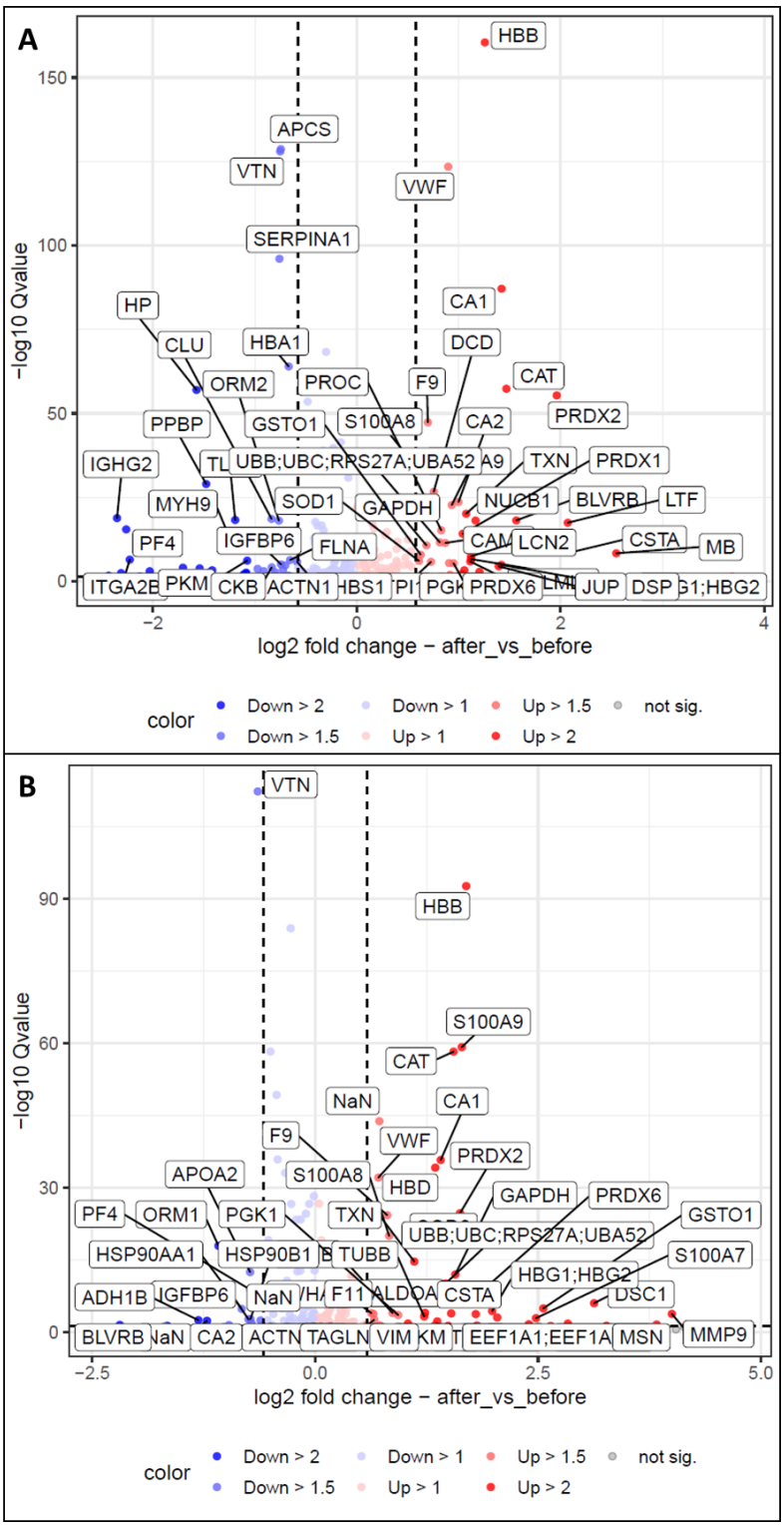

Supplementary figure 2: Volcano plot demonstrating significantly affected proteins in the plasma samples after intraoperative HF. Up-regulated proteins (compared to the plasma sample before surgery with CPB and HF) are shown in red, down-regulated in blue. Only proteins with q-value below 0.05 are shown in color. Protein abundance was altered in a reproducible way; however, there were certain differences between samples from (A) REMOVE-study participants and (B) patients, undergoing elective surgery, especially in the down-regulated proteins.

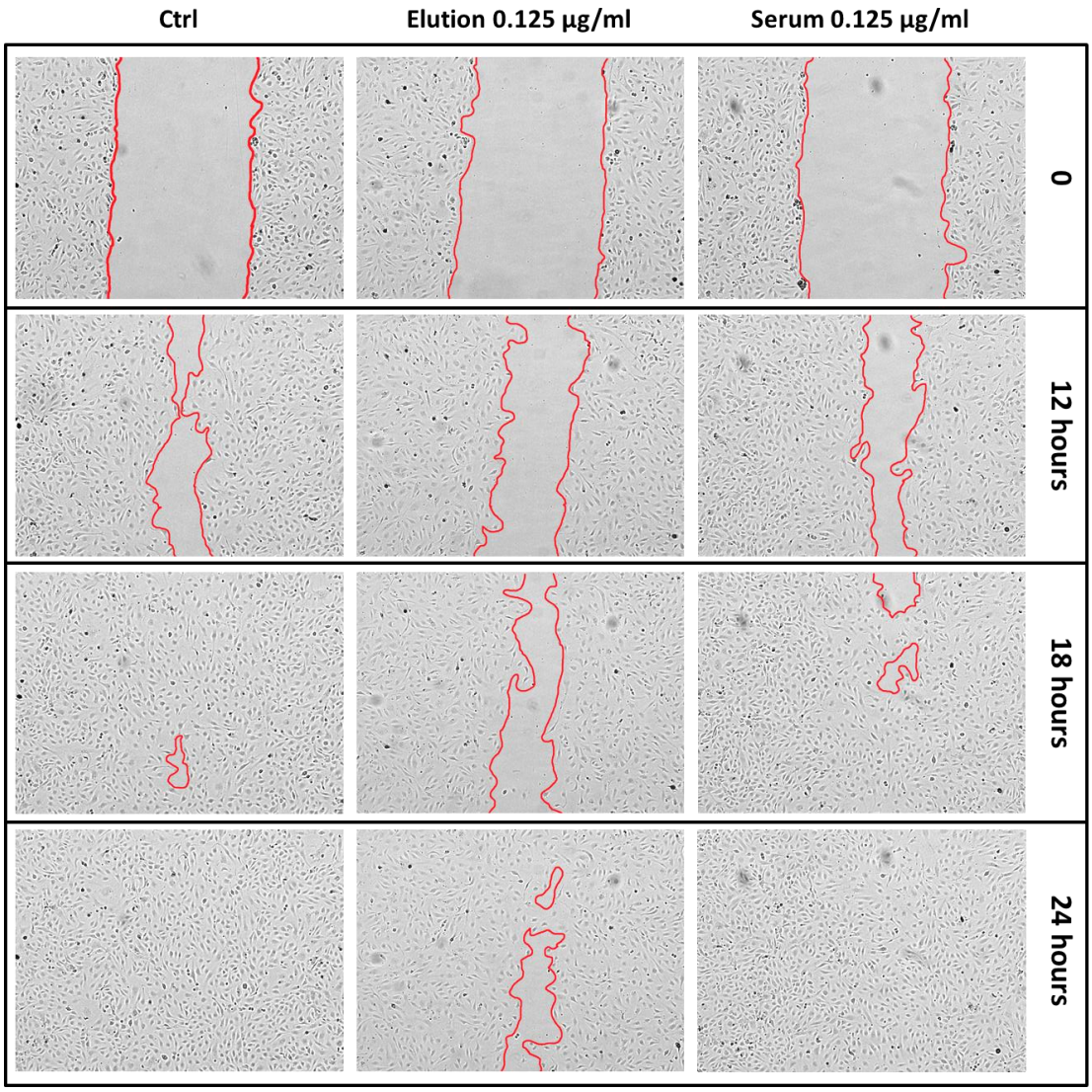

Supplementary figure 3: Representative microphotographs of the HAECs at different time points after scratch. Scratch borders are delineated in red; all microphotographs are taken with 4×magnification.

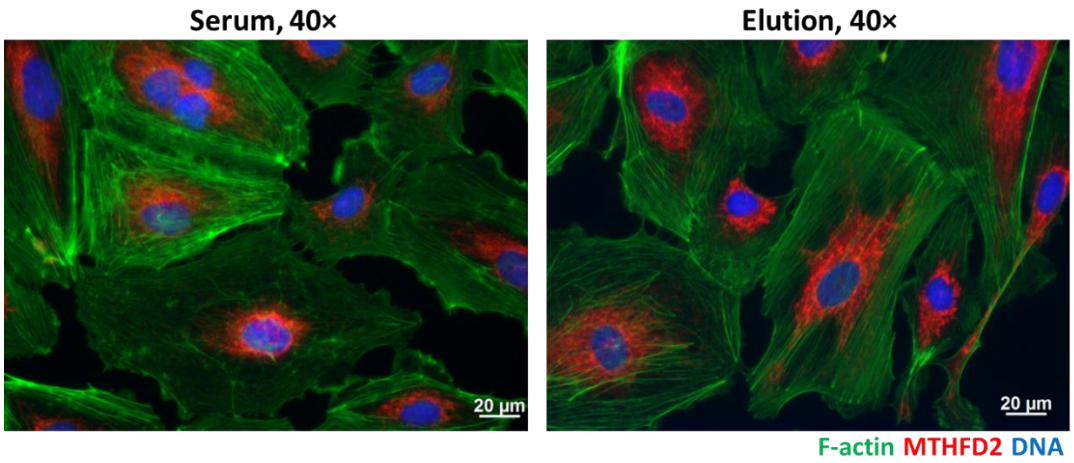

Supplementary figure 4: ICC-detection of MTHFD2 treated HAECs. Cytoplasmic perinuclear localization of MTHFD2 (red) in HAECs, treated with 0.125 µg/ml of eluted proteins and HAECs treated with corresponding amount of serum, 40 × magnification. DAPI was used to stain the nuclei and Phalloidin Alexa Fluor 488 was used for F-actin staining.

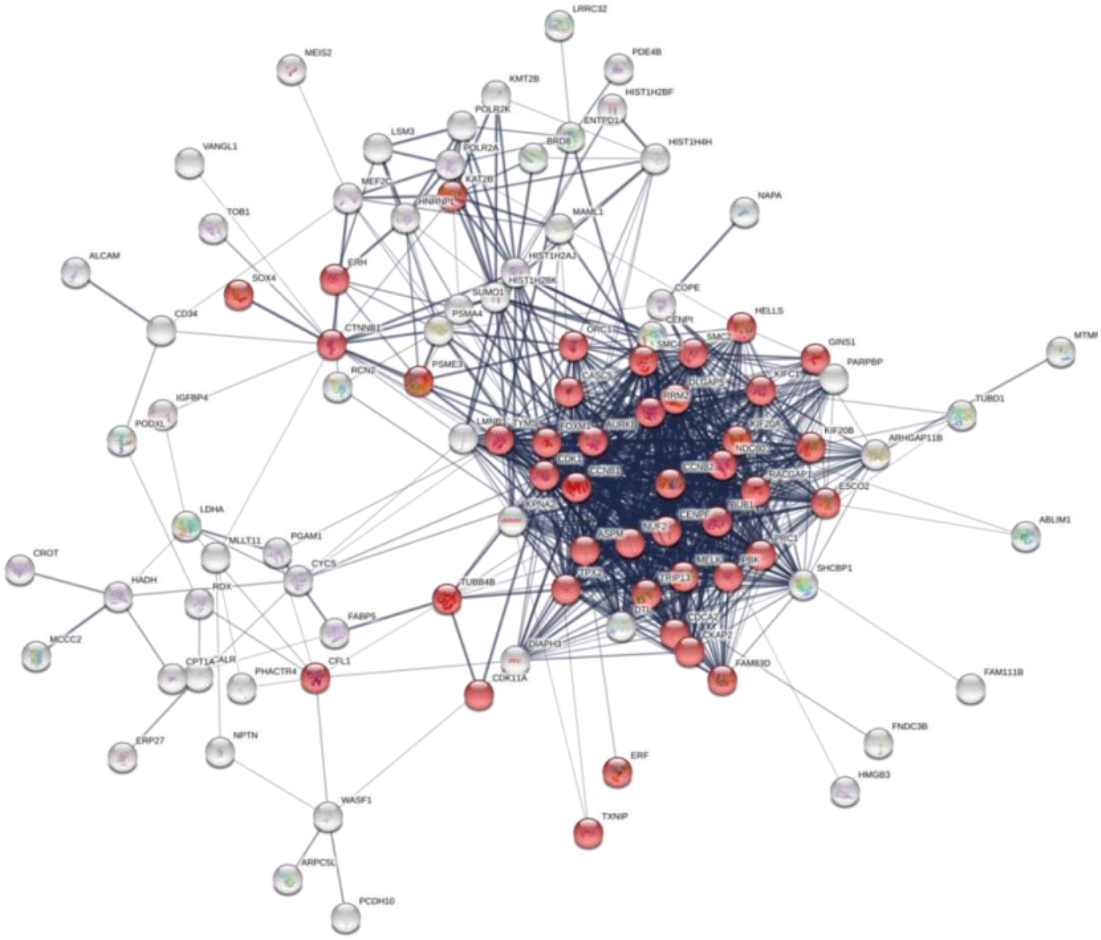

Supplementary figure 5: Biological network analysis for the down-regulated genes (n=119). All genes, involved into cell cycle regulation are highlighted in red. Down-regulated genes were mainly involved into regulation of the cell cycle and cell division, including formation of spindle and other morphological controllers of duplication and cell cycle.

Declarations

(1) I declare that I have not completed or initiated a doctorate procedure at any other university.

(2) Declaration concerning the truth of information given. I declare that all information given is accurate and complete. The thesis has not been used previously at this or any other university in order to achieve an academic degree.

(3) Declaration under Oath. I declare under oath that this thesis is my own work entirely and has been written without any help from other people. I met all regulations of good scientific practice and I used only the sources mentioned and included all the citations correctly both in word or content.

Veronika Piskovatska

Halle, September 2020

Acknowledgements

I sincerely appreciate time, effort and expertise of everyone who contributed to this work with their advice or constructive critique. Special thanks to the thesis committee mambers, who helped me throughout the whole project with advice: Prof. Dr. Andreas Simm, Prof. Dr. Regine Heller, Prof. Dr. Marcus Glomb.

This work would probably be impossible without active contributors and advisors in the HCH lab and ZMG: Dr. Kristin Wächter, Dr. Patrick Winterhalter, Dr. Anne Großkopf, Dr. Jette Rahn, and Dr. Vesselin Kristov.

Collaborators from Mass-spectrometry Core Facilities: Dr. Matt Fuzsard (Halle), Dr. Alessandro Ori, Dr. Joanna M. Kirkpatrick (FLI, Jena).

Collaborators in the clinic of Heart Surgery: Dr. Britt Hoffmann, Dr. Edina Korca, Ltd. Kardiotechnicker Marcus Stiller.

Fellow ProMoAge students and collaborators: Georgiana Toma, Arina Urazova, Katrin Kalies, Christoph Hochmann.

Technical assistants: Nicole Glaubitz, Frances Schmidt, Annika Küttner, Pascal Rudewig.

Special thanks to Dr. Nancy Zimmermann, Daniela Weiß and Anja Kirschner for their help in navigating through paperwork and bureaucratical matters.

I am immensely grateful to Dr. Alexander Navarrete Santos, Dr. Kristin Wächter and Nicole Glaubitz for their everyday help in form of theoretical and practical advice, active troubleshooting in the lab and incredible kindness. Without any doubt, I owe all my knowledge and skills in the field of protein biochemistry to Dr. Alexander Navarrete Santos.

Special thanks to Prof. Dr. Susanna Tykhonova who massively contributed to my theoretical knowledge and skills.

This work would be impossible without my strong foundation – my family. I am especially grateful to my mother, grandmother and aunt, whose intelligence, incredible sense of purpose and professionalism have always been my best example in life. Thanks for supporting my aspirations and being always there for me.